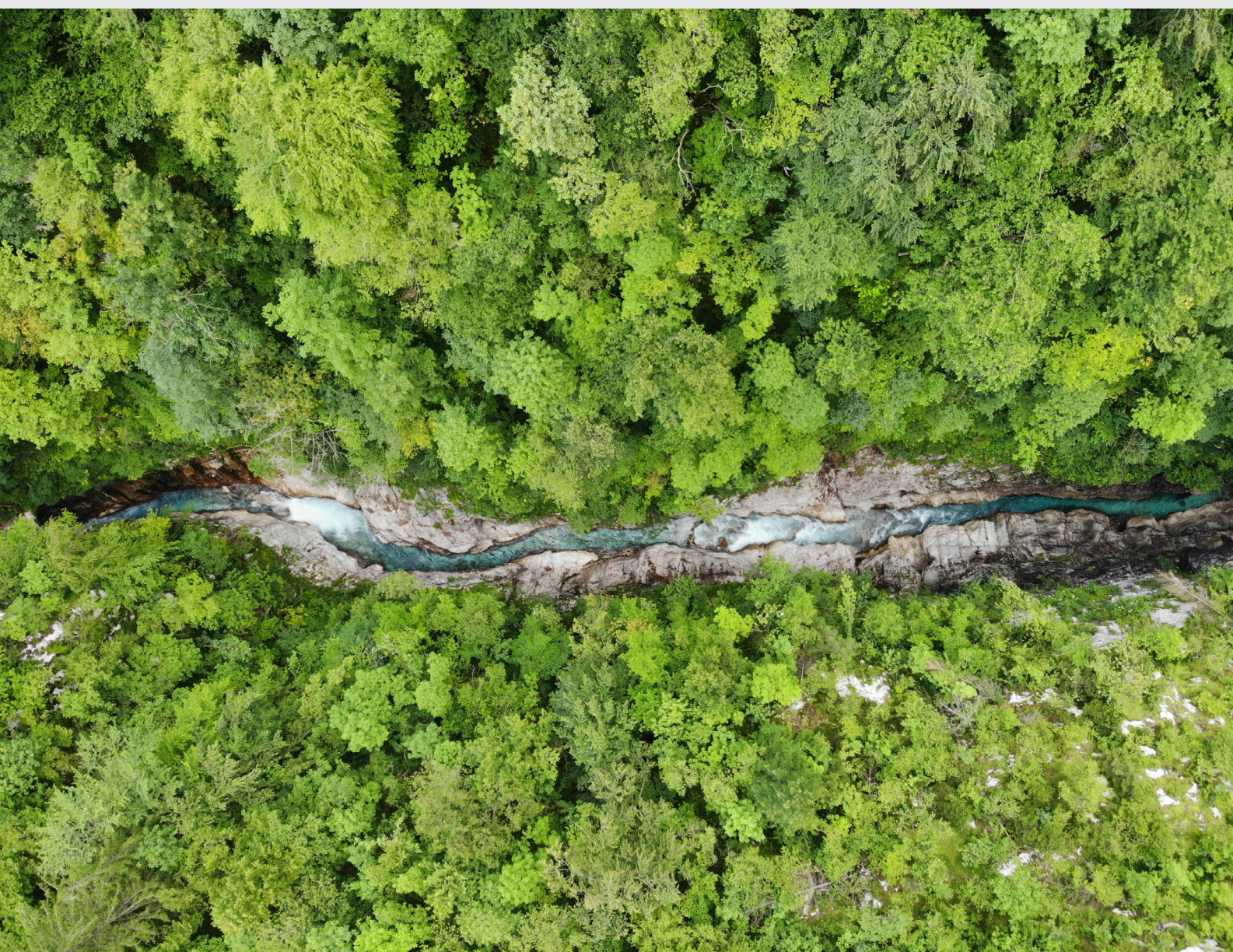


GEOLOGIJA

2022 | št.: **65/2**



ISSN

Tiskana izdaja / Print edition: 0016-7789
Spletna izdaja / Online edition: 1854-620X

GEOLOGIJA

65/2 – 2022



GEOLOGIJA	2022	65/2	125-260	Ljubljana
------------------	-------------	-------------	----------------	------------------



Izdajatelj: Geološki zavod Slovenije, zanj direktor MILOŠ BAVEC
Publisher: Geological Survey of Slovenia, represented by Director MILOŠ BAVEC
Financirata Javna agencija za raziskovalno dejavnost Republike Slovenije in Geološki zavod Slovenije
Financed by the Slovenian Research Agency and the Geological Survey of Slovenia

Glavna in odgovorna urednica / Editor-in-Chief: MATEJA GOSAR

Tehnična urednica / Technical Editor: BERNARDA BOLE

Uredniški odbor / Editorial Board

DUNJA ALJINOVIC
Rudarsko-geološki naftni fakultet, Zagreb
MARIA JOÃO BATISTA
National Laboratory of Energy and Geology, Lisbona
MILOŠ BAVEC
Geološki zavod Slovenije, Ljubljana
MIHAEL BRENCIĆ
Naravoslovnotehniška fakulteta, Univerza v Ljubljani
GIOVANNI B. CARULLI
Dip. di Sci. Geol., Amb. e Marine, Università di Trieste
KATICA DROBNE
Znanstvenoraziskovalni center SAZU, Ljubljana
JADRAN FAGANELI
Nacionalni inštitut za biologijo, MBP, Piran
JANOS HAAS
Etvös Lorand University, Budapest
BOGDAN JURKOVŠEK
Geološki zavod Slovenije, Ljubljana
ROMAN KOCH
Institut für Paläontologie, Universität Erlangen-Nürnberg

MARKO KOMAC
Poslovno svetovanje s.p., Ljubljana
HARALD LOBITZER
Geologische Bundesanstalt, Wien
MILOŠ MILER
Geološki zavod Slovenije, Ljubljana
RINALDO NICOLICH
Università di Trieste, Dip. di Ingegneria Civile
SIMON PIRC
Naravoslovnotehniška fakulteta, Univerza v Ljubljani
MIHAEL RIBIČIĆ
Naravoslovnotehniška fakulteta, Univerza v Ljubljani
NINA RMAN
Geološki zavod Slovenije, Ljubljana
MILAN SUDAR
Faculty of Mining and Geology, Belgrade
SAŠO ŠTURM
Institut »Jožef Stefan«, Ljubljana
MIRAN VESELIĆ
Fakulteta za gradbeništvo in geodezijo, Univerza v Ljubljani

Naslov uredništva / Editorial Office: GEOLOGIJA Geološki zavod Slovenije / Geological Survey of Slovenia
Dimičeva ulica 14, SI-1000 Ljubljana, Slovenija
Tel.: +386 (01) 2809-700, Fax: +386 (01) 2809-753, e-mail: urednik@geologija-revija.si
URL: <http://www.geologija-revija.si/>

GEOLOGIJA izhaja dvakrat letno. / GEOLOGIJA is published two times a year.
GEOLOGIJA je na voljo tudi preko medknjižnične izmenjave publikacij. /
GEOLOGIJA is available also on exchange basis.



Izjava o etičnosti

Izdajatelj revije Geologija se zavedamo dejstva, da so se z naglim naraščanjem števila objav v svetovni znanstveni literaturi razmahnil tudi poskusi plagiatorstva, zlorab in prevar. Menimo, da je naša naloga, da se po svojih močeh borimo proti tem pojavom, zato v celoti sledimo etičnim smernicam in standardom, ki jih je razvil odbor COPE (Committee for Publication Ethics).

Publication Ethics Statement

As the publisher of Geologija, we are aware of the fact that with growing number of published titles also the problem of plagiarism, fraud and misconduct is becoming more severe in scientific publishing. We have, therefore, committed to support ethical publication and have fully endorsed the guidelines and standards developed by COPE (Committee on Publication Ethics).

Baze, v katerih je Geologija indeksirana / Indexation bases of Geologija: Scopus, Directory of Open Access Journals, GeoRef, Zoological Record, Geoscience e- Journals, EBSCOhost

Cena / Price

Posamezni izvod / Single Issue

Posameznik / Individual: 15 €

Institucija / Institutional: 25 €

Letna naročnina / Annual Subscription

Posameznik / Individual: 25 €

Institucija / Institutional: 40 €

Tisk / Printed by: TISKARNA JANUŠ d.o.o.

Slika na naslovni strani: Korita pri Klužah. Zmagovalna fotografija na fotografskem natečaju »Geopestrost pred domačim pragom« v okviru 6. slovenskega geološkega kongresa v Rogaški Slatini. Avtor: Borut Stojilkovič.

Cover page: The Kluže Gorge. The winning photo in a photo competition »Geodiversity at our doorstep» in the scope at 6th Slovenian Geological Congress in Rogaška Slatina. Author: Borut Stojilkovič.

VSEBINA – CONTENTS

<i>Bračič Železnik, B. & Rman, N.</i> Uvodnik.....	129
<i>Peternel, T., Šegina, E., Jež, J., Jemec Auflič, M., Janža, M., Logar, J., Mikoš, M. & Bavec, M.</i> Review of the research and evolution of landslides in the hinterland of Koroška Bela settlement (NW Slovenia)..... Pregled raziskav in nastanek plazov v zaledju naselja Koroška Bela (SZ Slovenija)	131
<i>Fifer Bizjak, K. & Vezočnik, R.</i> Prediction of the peak shear strength of the rock joints with artificial neural networks Napoved vrhunske strižne trdnosti po razpoki v kamnini z nevronskimi mrežami	151
<i>Šegina, E., Jemec Auflič, M., Zupan, M., Jež, J. & Peternel, T.</i> Composite landslide in the dynamic alpine conditions: a case study of Urbas landslide Sestavljeni plaz v dinamičnih alpiskih razmerah: primer plazu Urbas	161
<i>Rožič, B., Gale, L., Oprčkal, P., Švara, A., Popit, T., Kunst, L., †Turnšek, D., Kolar-Jurkovšek, T., Šmuc, A., Ivekovič, A., Udovč, J. & Gerčar, D.</i> A glimpse of the lost Upper Triassic to Middle Jurassic architecture of the Dinaric Carbonate Platform margin and slope Pogled v izgubljeno zgornjetriasno in spodnjejursko arhitekturo pobočja in roba Dinarske karbonatne platforme	177
<i>Križnar, M.</i> Lower Permian (Artinskian) chondrichthyan tooth remains (Petalodontidae) from Dovje (Karavanke Mts., NW Slovenia) Spodnjeperski (artinskijski) ostanki zob morskih psov (Petalodontidae) iz Dovjega (Karavanke, SZ Slovenija)av	217
<i>Jarc, S.</i> Statistical approach to interpretation of geochemical data of stream sediment in Pleše mining area Statistični pristop k interpretaciji geokemičnih podatkov potočnega sedimenta na območju rudišča Pleše	225
<i>Miklavc, P. & †Celarc, B.</i> Depositional environment of the Middle Triassic Strelovec Formation on Mt. Raduha, Kamnik-Savinja Alps, northern Slovenia Sedimentacijsko okolje srednjetriasne Strelovske formacije na Raduhi v Kamniško-Savinjskih Alpah, severna Slovenija	237
Poročila in ostalo - Reports and More	
<i>Bračič Železnik, B.</i> : Poročilo o aktivnostih Slovenskega geološkega društva v letu 2021	251
<i>Bedjanič, M.</i> : Nova razstava: Dihanje Zemlje – mofete v Slovenskih Goricah	256
<i>Martínez-Pérez, C.</i> : Tea Kolar-Jurkovšek's Pander Medal.....	258
Navodila avtorjem.....	259
Instructions for authors	260



Uvodnik

»Vedeti (ne)vidno – vloga geologije v naši družbi« je bil slogan 6. slovenskega geološkega kongresa, ki je potekal od 3. do 5. oktobra 2022. Osrednji strokovni dogodek, na katerem se vsaka štiri leta srečajo geologi, je letos potekal v Rogaški Slatini, saj je razvoj kraja neposredno povezan z izviri mineralne vode, ki so posledica geoloških struktur in procesov. Tudi grafična podoba kongresa je bila sestavljena iz delčkov, ki ponazarjajo posamezne veje geologije in združeni v celoto dajo celovito sliko okolja, v katerem živimo, tako tisto na površju, ki jo vidimo, kakor tisto pod površjem, ki nam je skrita.

Pri organizaciji 6. slovenskega geološkega kongresa sta moči združila Slovensko geološko društvo in Društvo slovenski komite mednarodnega združenja hidrogeologov. Kongresa se je udeležilo 115 udeležencev, ki so svoje dosežke, raziskave in aktivnosti predstavili v 63 predavanjih in 25 posterjih. Predstavitve so potekale v 10 sekcijah, ki so pokrivalo področja regionalne, strukturne in sedimentarne geologije, mineralnih surovin in geoenergije, paleontologije, kraških pojavov, hidrogeologije, inženirske geologije, digitalizacije v geologiji, mineralogije in petrologije, geokemije, raziskovanja geogenih in antropogenih vplivov na okolje, varovanja geološke dediščine in vključevanja geoloških vsebin na področju vzgoje in izobraževanja.

Če je bil na predhodnih kongresih opazen osip udeležbe geologov, ki svoja znanja uporabljajo pri aplikativnem delu, je bila udeležba teh strokovnjakov na 6. slovenskem geološkem kongresu zelo vzpodbudna, saj je bilo predstavljenih kar 22 predavanj.

6. slovenski geološki kongres smo pričeli z vabljenim predavanjem Martine Stupar, ki je predstavila geopestrost v Sloveniji ter vrednotenje in varstvo geološke dediščine, saj je bil 6. oktober 2022 prvi mednarodni dan geopestrosti.

Sledilo je vabljenemu predavanju, ki je bilo posvečeno strukturno-geološko in geodinamsko razgibanemu širšemu območju Rogaške Slatine. Jure Atanackov je v predavanju »Problematika Šoštanjskega in Labotskega preloma na širšem območju Rogaške Slatine« predstavil trenutne izzive interpretacije razvoja ozemlja. Dobro poznavanje razvoja ozemlja bi morda omogočilo uspešno pridobivanje novih virov mineralne vode.

V Sloveniji se v letu 2022 izvajata dva velika gradbena projekta, drugi tir železniške proge Divača–Koper in vzhodna cev Karavanškega predora, kjer je prisotnost geološke stroke zelo pomembna. Ta tema je bila predstavljena v vabljenem predavanju Andreja Ločniškarja drugi dan kongresa.

Vabljenemu predavanju je zaokročilo predavanje Miha Jerška o značilnostih mineralov iz Haloz. Predstavil je morfološke značilnosti kristalov kremenca in kalcita, ki jih najdemo v bližnjih Halozah in so odraz razmer pri njihovem nastanku.

V okviru kongresa je potekala okrogla miza »Vedeti (ne)vidno – vloga geologije v naši družbi«, na kateri smo opozorili na aktualne družbene izzive, kot so ekstremni vremenski dogodki, varnostni konflikti, samooskrba, odpornost, zeleni prehod, krožno gospodarstvo, geo- in biodiverziteteta, aktiven snovni krog in kako lahko geologi pripomoremo k rešitvi trenutne krize in izoblikujemo optimistično vizijo za prihodnost. Šest panelistov je najprej izpostavilo aktualne izzive, nato pa skušalo poiskati rešitve in sinergije med različnimi aktivnostmi, potrebami in stališči.

Najbolj izstopajoč obkongresni dogodek je bila fotorazstava »Geopestrost pred domačim pragom«, ki je bila namenjena promociji in počastitvi prvega mednarodnega dneva geopestrosti. Na natečaj je prispelo 37 fotografij 9 avtorjev. Prvo nagrado je dobila fotografija Boruta Stojilkovića »Korita pri Klužah« in krasi tudi naslovnico tokratne številke Geologije. Navdušila je z barvno in oblikovno dovršenostjo ter pogledom iz perspektive, običajno skrite človeškim očem. Razkriva lepoto moči in povezanosti hidroloških in geomorfoloških pojavov, ki so objeti v bujno zelenilo žive narave. Zanimiva centralna kompozicija, prevladujoča zelena barva in nenavaden pogled, na poznan motiv, naredijo to fotografijo izstopajočo.

Kongres se je zaključil s strokovnimi ekskurzijami, ki so udeležence kongresa popeljale na različne konce Slovenije in jih seznanile z aktualnimi geološkimi problematikami. Pohorje je bilo predstavljeno z novega vidika – kot ekstenzijski kompleks, ki pripada najzahodnejšemu delu Panonskega bazena. Obiskali smo litostratigrafske formacije med Rogaško Slatino in Bočem ter geološko pot v Kozjanskem krajinskem parku, ogledali smo si gradnjo vzhodne cevi Karavanškega cestnega predora in se seznanili z upravljanjem ranljivih teles podzemne vode na Dravskem polju.

6. slovenski geološki kongres ni bil le strokovni dogodek, ampak predvsem priložnost za druženje, obuditev starih znanstev in spletnje novih poznanstev. To nam je odlično uspelo.

Podrobnosti o kongresu in spremljajočih dogodkih, spletno obliko kongresnih povzetkov in opis ekskurzij najdete na spletni strani [6. slovenski geološki kongres 2022 \(geo-zs.si\)](http://6.slovenski-geološki-kongres-2022.geo-zs.si). Vabljeni k ogledu.

Za konec naj se zahvalimo vsem sponzorjem za finančno in materialno podporo, udeležencem kongresa za strokovni prispevek ter celotni ekipi, ki je v organizacijo dogodka vložila številne ure svojega prostega časa in neizmerljivo količino dela.

Srečno in na snidenje na 7. slovenskem geološkem kongresu v Lipici.

Branka Bračič Železnik in Nina Rman



Review of the research and evolution of landslides in the hinterland of Koroška Bela settlement (NW Slovenia)

Pregled raziskav in nastanek plazov v zaledju naselja Koroška Bela (SZ Slovenija)

Tina PETERNEL¹, Ela ŠEGINA¹, Jernej JEŽ¹, Mateja JEMEC AUFLIČ¹, Mitja JANŽA¹,
Janko LOGAR², Matjaz MIKOŠ³ & Miloš BAVEC¹

¹Geological Survey of Slovenia, Dimičeva ulica 14, SI-1000 Ljubljana, Slovenia; e-mails: tina.peternel@geo-zs.si, jernej.jez@geo-zs.si, mateja.jemec@geo-zs.si, mitja.janza@geo-zs.si, milos.bavec@geo-zs.si

²Chair of Geotechnical Engineering, Faculty of Civil and Geodetic Engineering, University of Ljubljana, Ljubljana, Slovenia; e-mail: janko.logar@fgg.uni-lj.si

³Chair of Hydrology and Hydraulic Engineering, Faculty of Civil and Geodetic Engineering, University of Ljubljana, Ljubljana, Slovenia; e-mail: matjaz.mikos@fgg.uni-lj.si

Prejeto / Received 30. 5. 2022; Sprejeto / Accepted 22. 9. 2022; Objavljeno na spletu / Published online 30. 9. 2022

Key words: landslide, debris flow, research, monitoring, landslide evolution, Koroška Bela

Ključne besede: plaz, drobirski tok, raziskava, monitoring, nastanek plazov, Koroška Bela

Abstract

This paper gives an overview of landslide research and the activity of landslides located above the Koroška Bela settlement in Northwest Slovenia. There are several landslides in this area and they pose a direct threat to the settlement below. The settlement is very densely populated (about 2,100 inhabitants) and has well-developed industry and infrastructure. It is built on deposits from past debris flows, indicating that large slope mass movements have occurred in the past. In this regard, the hinterland of Koroška Bela has been investigated since 2006, within the framework of various research, technical and European projects. The most extensive geological and geotechnical investigations were carried out after April 2017, when part of the Čikla landslide collapsed and mobilised into a debris flow. All of the investigations which have been carried out over the years revealed that the hinterland of Koroška Bela is characterised by high landslide activity due to geological, hydrogeological and tectonic conditions. In order to protect people and their property, it is essential to implement a holistic mitigation measure which includes remediation works (drainage works, debris flow breaker, etc.) and non-structural measures (monitoring system, early warning system, risk management, etc.). Regular and continuous monitoring of all landslides is also crucial to observe the landslide dynamics and evaluate the effectiveness of structural mitigation measures.

Izveček

Članek predstavlja pregled raziskav in aktivnosti plazov, ki se nahajajo nad naseljem Koroška Bela v severozahodni Sloveniji. Obravnavano območje je podvrženo plazovom, ki predstavljajo neposredno nevarnost za spodaj ležeče naselje. Naselje je gosto poseljeno (s približno 2.100 prebivalci) in ima dobro razvito industrijo ter infrastrukturo. Zgrajeno je na sedimentih preteklih drobirskih tokov, kar tudi dokazuje, da so se obsežni pobočni masni premiki prožili tudi v preteklosti. Zaradi naštetih dejstev na tem območju potekajo raziskave že od leta 2006, ki so se izvajale v okviru različnih raziskovalnih, tehničnih in evropskih projektov. Najobsežnejše geološke in geotehnične preiskave so bile izvedene po aprilu 2017, in sicer po sprožitvi manjšega drobirskega toka na Čikli. Vse raziskave in študije, ki so bile izvedene v vseh teh letih, so pokazale, da je zaledje Koroške Bele podvrženo aktivnim plazovom, ki so se formirali predvsem zaradi danih geoloških, hidrogeoloških in tektonskih razmer. Za zaščito ljudi in njihovega imetja je nujna celostna izvedba varovalnih ukrepov, ki bodo vključevali tako preventivne (npr. sistem za opazovanje, opozorilni sistem, načrt obvladovanja ogroženosti, itd.), kot tudi gradbene ukrepe (npr. drenažni sistem, pregrade, itd.). Prav tako je nujno izvajanje rednega in kontinuiranega spremljanja vseh aktivnih plazov v zaledju, ki bo omogočal prepoznavanje dinamike plazov in meril učinkovitost izvedenih gradbenih ukrepov.

Introduction

Catastrophic landslides are usually the result of rapid collapse of soil, rock, and fluids triggered by heavy rainfall, snowmelt, earthquakes, or anthropogenic activities (Gariano & Guzzetti, 2016; Lacroix et al., 2020). In Slovenia, landslides are fairly common and are related to active tectonics, diverse geological settings and climatic conditions. Landslides frequently occur in clastic rocks located under steep slopes composed of highly permeable carbonate rocks (Jemec Auflič et al., 2017a). An example of this is the slope morphology of the Vipava Valley, which is primarily influenced by the different lithology of the thrust units and is characterised by steep carbonate cliffs and gentle lower slopes formed in the underlying flysch (Verbovšek et al., 2017; Popit et al., 2022).

In recent decades, four major landslides have occurred in Slovenia, with a volume of approximately $1 \times 10^6 \text{ m}^3$. In November 2002, the Stože debris flow formed in the catchment area above the village of Log pod Mangartom. The debris flow caused seven casualties and destroyed residential and farm buildings (Mikoš, 2020). In the same period, reactivation of the Slano Blato landslide occurred above the village of Lokavec (Fifer Bizjak & Zupančič, 2009; Mikoš et al., 2009; Maček et al., 2016) and, one year later (2001), the Strug landslide occurred above the village of Koseč (Mikoš et al., 2006). A large landslide area is also located in Rebernice in the Vipava valley, where deep-seated landslides have formed in complex

geological settings (Popit et al., 2014; Popit, 2017). This area is crossed by a motorway, where investigations and remediation works are constantly carried out due to road subsidence.

These events, and the fact that alpine and perialpine regions are highly susceptible to landslides, have revealed that, on the whole, Slovenia needs to pay more attention to landslide prevention measures, to reduce the impact of landslide activity and to protect people and infrastructure (Mikoš, 2021).

This paper focuses on historical, as well as current, landslide activity on the mountain slopes above the settlement of Koroška Bela in Northwest Slovenia (Fig. 1). This territory is one of the most active landslide-prone areas in Slovenia. It attracts additional attention due to historical evidence of past debris flows in recent geological history. The first registered event occurred in the 18th century and it caused partial or complete destruction of more than 40 buildings and devastated cultivated areas in the village of Koroška Bela (Lavtižar, 1897; Zupan, 1937). The most recent event occurred in April 2017, when part of the Čikla landslide collapsed and turned into a debris flow (Jež et al., 2019a). Even though this particular debris flow did not reach the settlement, it was perceived to be an additional warning sign that slope mass movements in the hinterland of Koroška Bela are still a source of potential debris flows. The area of interest is also prone to other types of landslides, such as slides, flows, falls, and combinations thereof.



Fig. 1. Location of Koroška Bela and the extent of the landslide-prone area.

Koroška Bela is a densely populated urban settlement in the alpine Upper Sava River valley. It is built on a typical torrential fan with an estimated area of 1.02 km², formed by past debris flows. Currently, it has about 2,100 inhabitants, a well-developed steel works and an important infrastructure connection between the capital of Slovenia and Northwest Slovenia.

In this respect, the landslide-prone area in the hinterland of Koroška Bela has been under investigation since 2006. The research started within the framework of various national and international projects (Fig. 2; Table 1). All of the investigations can be roughly divided into two stages: before and after the Čikla debris flow in April 2017. The first set of studies, carried out before April 2017, was primarily scientific. Their main objective was to identify and understand the characteristics and kinematics of landslides. Studies carried out after April 2017 were primarily conducted with the goal of developing and implementing mitigation measures (Fig. 2; Table 1).

Morphological and geological settings

The hilly and mountainous hinterland of Koroška Bela is a part of the Belščica slope (Karavanke mountain ridge). It covers an area of approximately 6 km² and extends from 520 to 2,100 m a.s.l. It is characterised by medium to steep slopes, sloping to the southwest. Since the slopes are exposed to the sun, they experience relatively large temperature oscillations. The area is characterised by very rugged terrain, dominated by concave slopes. The prevalence of concave slopes may have an indirect influence on the potential occurrence of landslides since, in these areas, the velocity of water flow usually decreases, resulting in water accumulation that increases soil water saturation and slope instability (Hengl & Reuter (2009) cited in Romer & Ferentinou (2016)). Komac (2005) also observed that a greater number of landslides in Slovenia occur in concave areas. The land use map shows that the Koroška Bela hinterland is almost completely

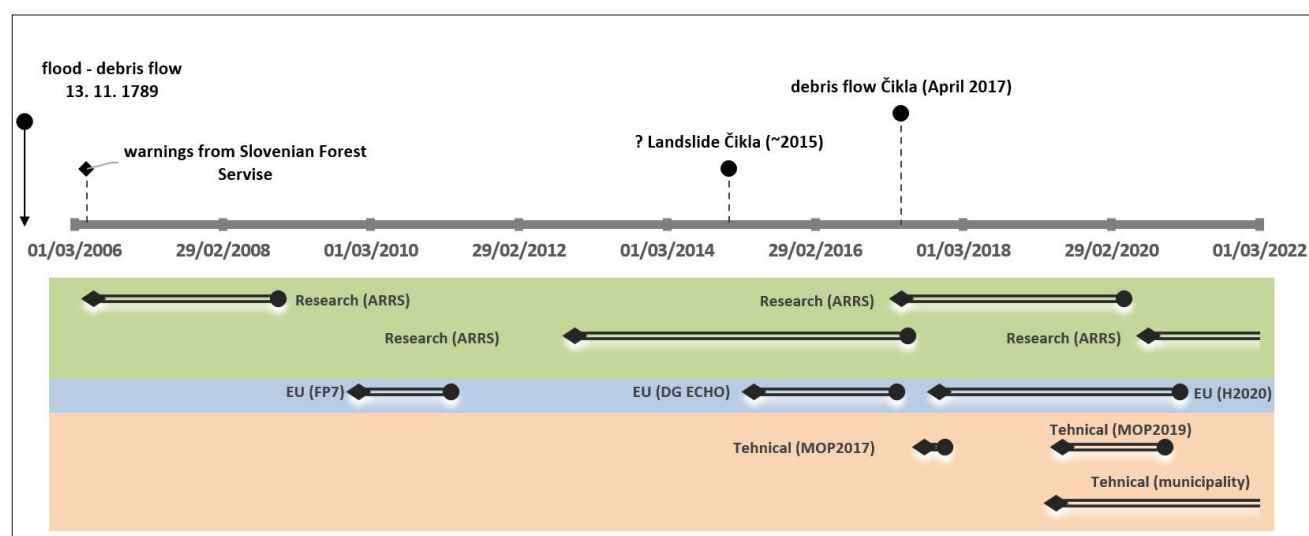


Fig. 2. Timeline of landslide activity and research since 1789. The coloured background defines the type of project (green – research projects funded by Slovenian Research Agency; blue – projects cofunded by EU Programmes; orange – technical projects funded by the Ministry of the Environment and Spatial Planning and the Municipality of Jesenice).

This paper gives an overview of landslide research above the Koroška Bela settlement. The first part consists of a detailed description of the study area, the investigations conducted and their main outcomes. The second part deals with the evaluation of recent landslide activity using multitemporal digital orthophoto imagery and digital elevation models (DEMs).

This paper summarises the extensive successive research carried out in the Koroška Bela landslide area and provides an example of good practice in landslide risk management.

vegetated and covered with forest (MKGP, 2016; Peternel, 2017). In this case, it is assumed that the forest has a rather limited protective function against slope instabilities, since most of the forest consists of larch and spruce, which are characterised by shallow root systems. Conversely, large unstable trees on steep slopes can increase the risk of triggering landslides, as windstorms may cause uprooting, toppling and falling of trees and accelerate the weathering and erosion of slopes (Jakša & Kolšek, 2009). In addition, fallen trees and other vegetation accumulate in the

Bela stream as additional unstable material that could be mobilised during torrential floods.

The Koroška Bela hinterland is defined by complex geological and tectonic conditions. For geological maps and detailed geological descriptions of the Koroška Bela hinterland, the reader is referred to previous studies (Jež et al., 2008; Peternel et al., 2017, 2018). A general, geological description of the wider Koroška Bela area has been presented by Buser (1978), Buser (1980) and Jež et al. (2008). The study area mainly consists of Upper Carboniferous and Permian clastic rocks – Permian carbonates and Triassic to Lower Jurassic carbonate rocks (Jež et al., 2008). The main slope instabilities are related to tectonic contacts between the clastic Upper Carboniferous to Permian rocks (claystone, siltstone, sandstone and conglomerate) and various Permian and Triassic carbonate and clastic rocks. (Jež et al., 2008).

Tectonically, the area belongs to the Southern Alps (Placer, 2008). It is a part of the Košuta fault zone and is dissected by numerous NW-SE faults connecting two major fault zones (the Sava and Periadriatic fault zones) (Jež et al., 2008). The rocks are heavily deformed and, therefore, very prone to rapid and deep weathering. Carbonate rocks in the uppermost parts of the Belščica slope are also subject to intense physical and chemical weathering, resulting in large quantities of talus and scree material.

Prominent morphological features in the study area are relatively long ridges interrupted by long, deep, narrow and irregular mountain watercourses (Brenčič & Poltnig, 2008; Janža et al., 2018). In general, three types of aquifers characterise the regional hydrogeological settings, which are determined by geological conditions: intergranular aquifers in clayey carbonate gravels, karst-fissured aquifers in carbonate rocks and small local aquifers, typically occurring in clastic rocks.

The morphology of the slopes, unfavourable geological and tectonic conditions, and climatic diversity contribute to the fact that the region above Koroška Bela is prone to landslides and torrents and represents the source of potential debris flows that could pose a threat to the densely populated settlement below. Landslide activity is evidenced by an irregular and hummocky terrain comprised of protrusions and depressions of various sizes, curved trees, tension cracks, erosion slumps and wetlands on the surface, as well as widespread subsidence of local roads.

The first warnings of landslide activity in the area, that attracted the attention of our research

group, were reports of sliding by the Slovenian Forest Service. They reported the subsidence of a local road, the presence of curved trees and erosion flanks in the wider catchment area of the Urbas water reservoir (Fig. 2).

Climatic conditions

The study area is characterised by an alpine climate, ranging from a low mountain to a high mountain climate (Brenčič & Poltnig, 2008). The climate is highly variable due to the effects of alternating high and low atmospheric pressure and alternating atmospheric fronts. The variable climatic conditions are also related to the great differences in altitude, the rugged terrain with deep and narrow valleys, and the slope orientation (Rakovec et al., 2000). It is typical for this part of the Karavanke Mountains that the mean annual precipitation ranges from 1,600 to 2,000 mm, while the maximum 24-hour precipitation with a 100-year return period is estimated between 180 and 210 mm (Internet 1). There are two annual precipitation peaks, with the main precipitation peak in autumn and the second in spring.

An overview of past research

An overview of all the implemented investigations is listed in Table 1. The first research started within the Target Research Project (TRP): Debris flow risk assessment in Slovenia. Within the TRP project, geological mapping of the Koroška Bela hinterland, a study of alluvial fan deposits, and modelling of debris flows using a Flo-2D model were carried out. The project results showed that the alluvial fan of Koroška Bela consists of a sequence of depositional layers related to several historic debris flows (Jež et al., 2008; Mikoš et al., 2008). Based on detailed engineering mapping of this area, the Urbas landslide was identified (for the first time), named and described as the Potoška planina landslide (Jež et al., 2008). Furthermore, the estimated magnitudes of debris flows for the Bela torrential watershed were calculated by Sodnik and Mikoš (2006), using various morphological parameters. By applying different empirical equations for the determination of the design discharge and flood volume with a 100-year return period, different debris flow magnitudes were calculated, ranging from 19,687 m³ to 93,231 m³ (Sodnik & Mikoš, 2006). The Bela torrential fan was classified as a transitional fan, where debris flows are possible. For debris flow modelling, a Flo 2-dimensional model was used

with different numerical square grids generated from digital elevation models (Sodnik et al., 2009, 2012, 2013; Sodnik & Mikoš, 2018; Bezak et al., 2020). The calculated results showed that the estimated inundated area ranges between 118 and 145 m² and the average maximum flow depth ranges from 0.6 to 1.2 m, depending on the square grid applied.

The first monitoring at the Urbas landslide was established using a novel motion detection device that was developed within the EU funded project “Integrated Interferometry and GNSS for Precision Survey (I2GPS)” founded by the Seventh Framework Programme (FP7-GALILEO-2008-GSA-1). The device integrated interferometric synthetic aperture radar (InSAR) and global navigation satellite system (GNSS) technologies. Two compact active transponder (CAT) units (InSAR data) and a combined CAT and GNSS unit (providing 3D displacement assessments) were installed to monitor the surface displacements of the landslide and its vicinity (Komac et al., 2015). The InSAR and GNSS results showed relatively large (up to 32 mm horizontal and up to 15 mm vertical) displacements during a relatively short monitoring period (02/2011 – 08/2011), indicating a displacement of the central-upper and south-eastern parts of the landslide body (Komac et al., 2015, 2018). The Urbas landslide was further investigated and monitored within the framework of a PhD thesis (Peternel, 2017). To evaluate the kinematics of the Urbas landslide, understand the characteristics of the sliding process and assess the surface displacement rates and changes in surface topography, periodical monitoring was conducted using a variety of remote sensing and in-situ geodetic techniques (unmanned aerial vehicle (UAV) photogrammetry, terrestrial laser scanning (TLS), and tachymetric surveys) (Peternel et al., 2015, 2017a; Peternel, 2017; Peternel & Komac, 2017). The surveys revealed that the Urbas landslide is a composite landslide (Cruden & Varnes, 1996) consisting of rock falls (upper part), deep-seated landslides (main body) and debris flow source areas (lower part) (Peternel, 2017; Peternel et al., 2017a). The long-term activity of the Urbas landslide over the past 138 years has also been reconstructed using the dendrogeomorphological analysis of bent trees (Oven et al., 2019). Dendrogeomorphology has proven to be a highly useful method in the study of past slope mass movements and has recently been applied to the analysis of the debris flood magnitude in the Planica valley (Novak et al., 2020). The estimated risk and visible activi-

ty of landslides have increasingly attracted the attention of the inhabitants of Koroška Bela and the Civil protection service. For this purpose, the socio-economic impact was assessed within the framework of the EU-funded project “RECALL Resilient European Communities Against Local Landslides”. In addition, a cooperative team of decision-makers, response authorities, technical experts and other stakeholders was formed to increase awareness and understanding of landslide risk in the community (Jemec Auflič et al., 2017b, 2017c, 2019). In-depth research continued within the research project “Studying landslide movements from source areas to zone of deposition using a deterministic approach (ARRS J1-8153)”. As a part of the project, two additional research trenches, with depths between 3.00 and 3.95 m, were excavated on the alluvial fan where the Koroška Bela settlement has been developed; 11 samples of organic material were collected for radiocarbon dating. The main sedimentological units of the research trenches are layers of debris flow deposits interbedded with thick silty and sandy lenses, fluvial (fine-grained) deposits and flood/mudflow deposits (Jež et al., 2019b), suggesting several past depositional events. Age dating of the organic sediments revealed that most of the sediment was deposited during the Last Glacial Maximum (LGM), while two or three debris layers were found in the upper part of the fluvial succession, and these were deposited during the Holocene. The youngest deposits were attributed to the debris flow which occurred in 1789 (Jež et al., 2019b). In addition, Sodnik et al. (2017) upgraded their models by modelling debris flow source areas with a multi-model approach using field data, susceptibility and trigger modelling, implemented using LS-Rapid (Loi et al., 2020). This research project was granted as a strategically important project in the category of International Programme on Landslides (IPL) in 2017-2020.

A very important milestone, which gave additional impetus to the study of landslide areas, occurred in April 2017, when part of the Čikla landslide collapsed and mobilised as a mass flow with a significant amount of talus material and vegetation. The debris flow had an estimated volume of 5,000 m³ and was triggered by heavy rainfall, with 200 mm of precipitation falling in 48 hours (Jež et al., 2019a; Peternel et al., 2022a). This event was one of the triggers for the intensification of detailed geological, geotechnical and hydrogeological investigations of landslides in the hinterland of Koroška Bela in 2017 (Table 1). For the spatial distribution of the applied

methods and the description of the engineering geological and hydrogeological results of the Urbas and Čikla landslides, the reader is referred to previous studies (Peternel et al., 2017b, 2018; Janža et al., 2018). The initial investigations were limited and provided only a rough insight into the geological and hydrogeological conditions of the observed landslides. The main outcomes were (Peternel et al., 2017b, 2018, 2019; Janža et al., 2018):

- In the hinterland of Koroška Bela there are more than 20 landslides, five of which have an area of more than 8,000 m²: the Urbas, Čikla, Potoška planina, Malnež and Obešnik landslides. Among these, Urbas and Čikla are considered the most active.
- Landsliding mechanisms are defined by the complex lithological composition, intensive tectonic deformation and hydrogeological conditions. The rocks and sediments in the study area are heavily deformed and prone to weathering, which results in weak geomechanical properties of the bedrock.
- In the Urbas and Čikla landslides, hydrogeological conditions are very heterogeneous and cannot be characterised uniformly due to complex geological and tectonic conditions. The groundwater is recharging by a combination of infiltration of precipitation and subsurface inflow from the carbonate hinterland. In the upper parts of the landslides, groundwater occurs at the contact between slope deposits and weathered clastic rocks.
- Preliminary 3D reconstructions of the landslide body showed that the calculated volumes of the Urbas and Čikla landslides are 895,000 m³ and 141,000 m³, respectively. For landslide volume calculation, the GOCAD-SKUA software was used.
- The modelling results showed that the estimated potential debris flows would have catastrophic consequences in the Koroška Bela settlement. In some densely populated parts, the simulated depth of the potential debris flow exceeds 5 m, which indicates that the application of mitigation measures is inevitable.
- The results of the preliminary investigations also revealed the need for continuous near-real and real-time monitoring and additional geological (hydrogeological, geophysical), geodetic and geotechnical investigations to obtain a basis for mitigation and remediation measures.

Based on these results and the historical facts, the Municipality of Jesenice recognised the high risk and established a monitoring system for the Urbas and Čikla landslides. The monitoring network consists of extensometers, rain-gauges, piezometers, inclinometers and motion detection cameras. All the electronic geotechnical sensors are wired and powered through the base station, which also serves as an automated data logger. To store and access all measured monitoring data, the eTeren platform (<https://eteren.geo-zs.si/home>) was developed in 2021.

In 2019, additional geological, geotechnical and geodetic investigations were carried out in the frame of the project funded by the Ministry of the Environment and Spatial Planning. The main purposes of this project were the engineering, geological and hydrogeological characterisation of landslides and the implementation of the stability analyses and feasibility studies of mitigation and remediation measures (Table 1). The Geological Survey of Slovenia (GeoZS), which led the project, also involved the Faculty of Civil and Geodetic Engineering (University of Ljubljana) and experts from the Italian Geological Survey (ISPRA) were called in as external consultants. Within the framework of the project, the following main outcomes were drawn (Bezák et al., 2020, 2021; Peternel et al., 2020a, 2020b, 2022a):

- The preliminary results of real-time landslide monitoring showed that the dynamics of the Urbas and Čikla landslides represent a combination of steadily sliding mass behaviour as well as episodic, rapid displacements corresponding to increased rainfall.
- Improved 3D reconstruction of the landslides resulted in the following estimated volumes: Urbas: 1,578,700 m³, Čikla: 330,500 m³, Malnež: 173,750 m³, Obešnik: 301,780 m³. For landslide volume calculation, the GOCAD-SKUA software was used.
- The study confirmed that the Urbas and Čikla landslides are a source area for debris flows and pose a direct risk to the settlement of Koroška Bela.
- Observations of the Malnež, Obešnik and Potoška planina landslides, which were first identified in 2017, showed that their current state and dynamics pose a significantly lower direct risk to the settlement. Nevertheless, monitoring should be continued and improved.
- The field investigation of the Bela stream and its tributaries revealed that more than

Table 1. An overview of past landslide risk research projects in the Koroška Bela area. The coloured background is defined by the type of project (green – research projects funded by the Slovenian Research Agency; blue – projects cofunded by EU Programmes; orange – technical projects funded by the Ministry of the Environment and Spatial Planning/Municipality of Jesenice).

	Duration	Type of project	Project	Type of research	Location	Research papers
1.	01/06/2006 30/11/2008	ARRS	Debris flow risk assessment in Slovenia	- trench (Koroška Bela): 2 - geological map of the hinterland of KB - debris flow modelling using the Flo-2D	Hinterland of Koroška Bela; alluvial fan	Sodnik & Mikoš, 2006; Mikoš et al., 2008; Jež et al., 2008
2.	01/01/2010 31/03/2011	EU: FP7	I2GPS – Integrated Interferometry and GNSS for Precision Survey	- 1st monitoring of surface displacements using InSAR and GNSS	Urbas	Komac et al., 2012a; 2012b; 2015; 2018
3.	01/12/2012 31/05/2017	ARRS	Dynamics of the slope mass movements in the Potoška planina with analyses of results of remote sensing and terrestrial surveys techniques and in-situ measurements	Lower part: - Tachymetric m.: 7 - UAV photogrammetry: 7 Upper part: - TLS: 2 - UAV photogrammetry: 2	Urbas	Peternel et al., 2015; 2017a; Peternel & Komac, 2017; Peternel, 2017
4.	04/05/2015 04/04/2017	EU: DG ECHO	RECALL Resilient European Communities Against Local Landslides	Cooperative team Monitoring using crackmeter method	Urbas	Jemec Aulič et al., 2017b; 2017c; 2019
5.	01/05/2017 30/04/2020	ARRS	Studying landslide movements from source areas to zone of deposition using a deterministic approach.	trench (Koroška Bela): 2 Geophysical m.: vertical electrical sounding (VES)	Urbas, Čikla, Koroška Bela	Sodnik et al., 2017; Jež et al., 2019a; 2019b
6.	21/08/2017 30/11/2017	MOP2017	Implementation of urgent engineering geological, hydrogeological, geophysical, geomechanical and geodetic surveys to determine the objective degree of risk to the population from slope mass movements in the Potoška Planina area and prepare expert documentation proposing mitigation measures.	- geological mapping of the hinterland of Koroška Bela; - engineering-geological (EG) mapping of landslides Urbas and Čikla; - hydrogeological (HG) mapping + in-situ investigations; - 9 boreholes (2 inclinometers; 2 piezometers); - 2 trenches (1 Urbas, 1 Čikla); - seismic Refraction Tomography (SRT): 4 cross-sections (3 Urbas, 1 Čikla); - electrical resistivity tomography (ERT): 4 cross-sections (3 Urbas, 1 Čikla); - light detection and ranging (LiDAR)	Urbas, Čikla	Peternel et al., 2017b; Peternel et al., 2018; Janžić et al., 2018
7.	04/07/2019 20/11/2020	MOP2019	Detailed geological-geotechnical and hydrogeological characterization of large landslides in the hinterland of Koroška Bela settlement for the stability analyses and for a feasibility study of mitigation measures	- update EG map; - EG mapping: Malnež, Obešnik; - mapping of Bela stream; - 17 boreholes (9 inclinometers; 8 piezometers); - in-situ geotechnical investigations (presiometer: 26; SPT: 4) - in-situ HG investigations (slug t.: 1; pumping t.: 11; tracking t.: 2) - geophysical m. (SRT: 1.200 m; ERT: 2.400 m; GPR: 270 m); - inclinometric m.: 0 + 4/6 measurements - tachymetric m.: 4 (dec/19; apr/20; sept/20; jun/21) - UAV photogrammetry (Urbas): 2 (sept/19; avg/20) - trenches (Koroška Bela): 2	Urbas, PP, Čikla, Malnež, Obešnik:	Peternel et al., 2020a; 2020b; 2022 Bezjak et al., 2020; 2021; Koren et al., 2022
8.	01/09/2020 31/08/2022	ARRS	Deep-seated landslide prediction modelling based on a combination of physical modelling and a data-driven approach	- continues monitoring; - landslide dynamic modelling; - landslide prediction modelling.	Urbas, Čikla	Peternel et al., 2020; 2022a; 2022b
9.	01/11/2017 31/01/2021	EU: H2020	GIMS: Geodetic Integrated Monitoring System	GNSS antenna: 7	Urbas	Šegina et al., 2020
10.	02/06/2019 ongoing	municipality Jesenice	Establishment and maintenance of monitoring system at Urbas and Čikla landslides	- raingauges - ekstenziometers - web camera - motion detection camera	Urbas, Čikla	reports (GeoZS archive)

15,000 m³ of material was deposited in the Bela and Čikla watercourses as a result of previous debris flow events. Potential torrential floods could mobilise the debris material deposited along the Čikla and Bela streams.

- The existing check dams do not have sufficient capacity to fulfil the sediment and debris flow management needed in the area.
- It is essential to implement holistic remediation measures to protect the population and infrastructure. Primarily, remediation measures must be taken on the Čikla and Urbas landslides and the torrents below.
- In the future, periodic and continuous monitoring of all landslides is essential in order to observe landslide dynamics and to verify the effectiveness of potential remediation measures.
- Future impacts of climate change should also be considered when designing mitigation measures. The analysis of the impact of future climate change shows that the negative impact of total and effective rainfall, air temperature, evapotranspiration and runoff from the Bela stream catchment is expected to increase, compared to the previous period.

In parallel, near real-time monitoring of the Urbas landslide was improved with the GNSS system developed in the frame of EU project GIMS: Geodetic Integrated Monitoring System (No. 776335). The system provides a continuous, simultaneous and accurate monitoring of surface displacement at multiple locations across the Urbas landslide (Šegina et al., 2020; Peternel et al., 2022b). The availability of the remote data and the ease of installation of the GNSS units proved that the system is very suitable for

monitoring landslide areas that are difficult to access. For this reason, the Čikla landslide was also equipped with the GNSS unit to monitor the displacement of a large boulder located in the active part of the Čikla landslide.

Currently, the main ongoing activities are carried out within the Postdoctoral Research Project (ARRS, Z1-2638). The main objective of the project is to investigate landslide triggering parameters (rainfall, groundwater level, etc.) and to develop a landslide prediction model based on quantitative methods using data collected through continuous monitoring of landslide displacements. The results of the study, carried out on the Urbas landslide, showed that the dynamics of a landslide vary, depending on local geological and hydrogeological conditions. Consequently, certain parts of the landslide are at different evolutionary states and respond differently to the same external triggers (Peternel et al., 2022b).

Long term evaluation of landslide activity using orthophotos and LiDAR-derived DEMs

Since the in-situ landslide monitoring provides spatially limited information, remote sensing data, such as digital orthophotography and laser scanning data, have been used to provide an overview of landslide activity across the entire area. The landslide activity was estimated through analysis/review of orthorectified aerial photography (digital orthophotos or DOFs) with a resolution 0.50 m, taken between 1994 and 2020, and digital elevation models (DEMs) with a resolution of 1 m, taken in 2014 and 2017. An overview of the spatial data used is presented in Table 2. The analysis provided the first information on landslide activity in the entire Koroška Bela hinterland, which encompasses a total area

Table 2. An overview of orthophotos used and DEMs derived from LiDAR.

Type of spatial data	Number of the acquisition	Date of acquisition	Resolution	Availability
DOF	1	27. 7. 1994 (C26) 12. 9. 1999 (D26)	0.5	Public
	2	22. 7. 2006 (C26) 20. 7. 2006 (D26)	0.5	Public
	3	11. 8. 2011	0.5	Public
	4	5. 7. 2015	0.5	Public
	5	24. 8. 2017	0.5	Public
	6	28. 7. 2020	0.5	Public
DEMs	1	2014	1.0	Public
	2	14. 11. 2017	1.0	Upon request

of 7 km². It also enabled the evaluation of the kinematics of landslides for the period when the monitoring system was not yet in place.

First, a visual interpretation of six DOFs was used to obtain information on visible landslide changes over time. Particular attention was paid to changes that might indicate landslide activity, such as disturbed or absent vegetation cover, deformation of the local roads and a growing erosion surface. The observed features were manually digitised and compared to all available orthophotos. Based on this comparison, the intensity of change was classified into three classes: low, medium and high change intensity (Fig. 3). Then, all observed changes were characterised by the type of phenomenon (landslide or deforestation), and verified by field investigations. The field in-

In addition to DOF analysis, elevation and volumetric changes resulting from landslide activity have also been estimated by comparing two successive DEMs. Elevations from the earlier DEM were subtracted from the latter on a cell-by-cell basis, at 1 m resolution. Decreases in elevation represent erosion zones (red colour), while increases in elevation indicate accumulation zones (Fig. 4). It should be noted that this method only indicates changes in surface elevation and volume and does not provide any insight into the overall mass balance of the area.

The elevation difference calculated for the entire Koroška Bela hinterland between 2014 and 2017 shows that 43,616 m³ of material accumulated and 107,283 m³ eroded during this period, indicating that the Koroška Bela hinterland is a

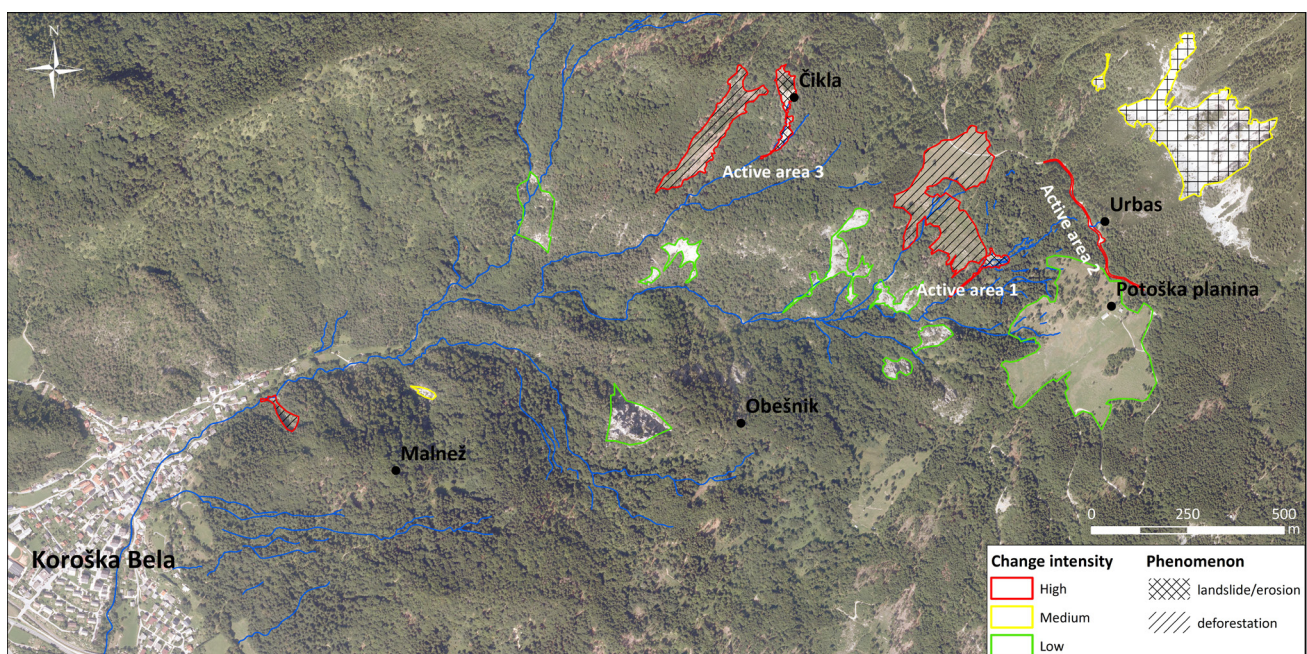


Fig. 3. Assessment of change intensity by visual interpretation and comparison of multitemporal orthophotos. The highest change intensity due to landslides was observed in the areas crossed by the Bela stream and its tributaries.

vestigations revealed that some large areas were the result of deforestation and were excluded from further analysis.

Based on the results of the change intensity assessment and field investigations, we identified three landslide active areas that have been analysed in more detail (Fig. 3):

- Active area 1: The lower part of the Urbas landslide, which has the potential to mobilise into a debris flow (see section 2.1).
- Active area 2: Local road crossing the main body of the Urbas landslide (see section 2.2).
- Active area 3: Pre and post-Čikla debris flow (see section 2.3).

predominantly erosive area. The erosion is mostly limited to the carbonate slopes, while accumulation occurs in the form of scree deposits under steep slopes. Carbonates on the Belščica slope are prone to extensive planar erosion, which is mainly concentrated in gullies, indicating most of the torrential transport and removal of the available, mechanically weathered top layer of rock. Similar processes are anticipated on carbonate slopes of the Alničje ridge. The most intensive erosion and accumulation of material occurred in the Čikla landslide, where a typical sequence of downslope erosion, followed by accumulation (at the foot of the landslide) can be observed.

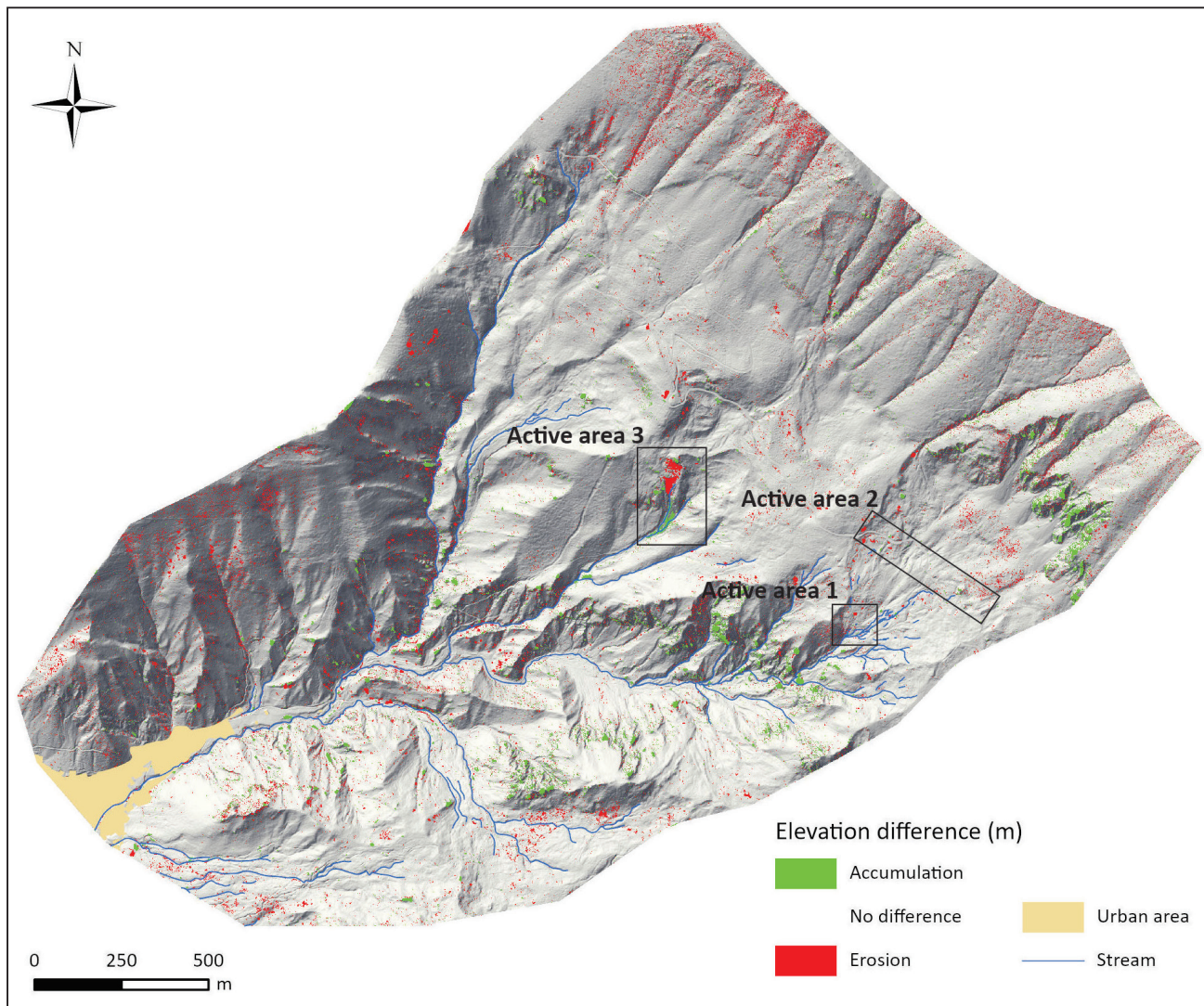


Fig. 4. Spatial extent and temporal change of elevation changes of active areas based on the series of DEM analyses.

Active area 1: Čikla landslide

Čikla landslide activity can already be seen by comparing the 2011 and 2015 DOFs (Fig. 5A and 5B), which shows that part of the Čikla landslide collapsed before 2017. Although the exact date and trigger mechanism of this event are unknown, the erosion of about 1,200 m² can be seen from the 2015 DOF.

Another event occurred on the night of April 28–29, 2017, when part of the Čikla landslide body collapsed and mobilised a large amount of debris and vegetation into a mass flow. The sliding material flowed several hundred metres along the Čikla stream. The triggering of this event was attributed to heavy rainfall. The nearby meteorological station (Javorniški Rovt) measured 204 mm of precipitation in 48 hours.

DOF analysis indicates that about 5,500 m² of the area was affected by debris flow, representing 21 % of the total Čikla landslide area, determined by detailed engineering geological mapping (Peternel et al., 2020). DEMs analysis indicates that approximately 1,214 m² was affected by significant erosion. The volume of eroded surface material was approximately 4,700 m³ and the surface had subsided an average of 2 m (up to 6 m in peak areas) (Fig. 6, area 1). The lower part of the Čikla landslide is characterised by an accumulation of material, with an average increase of 2.0 m and a maximum increase of 2.5 m. The estimated volume of accumulated material is about 1,700 m³ (Fig. 6, area 2). The deficit of material was either deposited further down the slope outside the observed area or it was removed by the torrent.

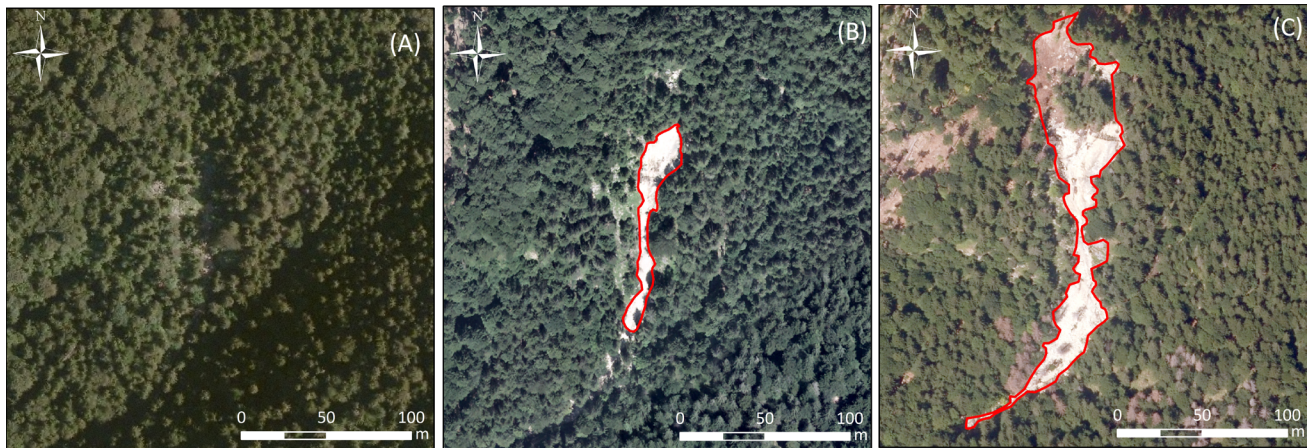


Fig. 5. Digital orthophotos of the Čikla landslide from 2011 (A), 2015 (B) and 2017 (C). Red line represents the manually digitised boundary of the Čikla debris flow.

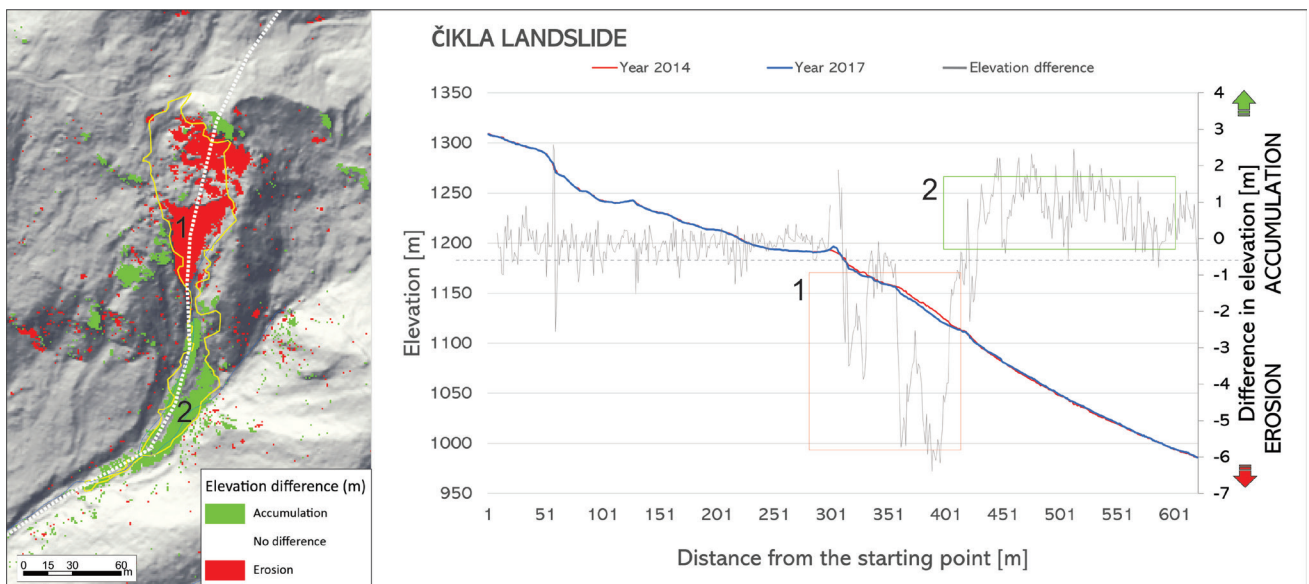


Fig. 6. Surface elevation difference (z-axis) between two LiDAR-derived DEMs from 2014 and 2017. Cross-section shows elevation differences along the Čikla landslide. The yellow line indicates Čikla debris flow (Fig. 5C).

Active area 2: The lower part of the Urbas landslide

Based on previous research (Peternel, 2017; Peternel et al., 2017a; Šegina et al., 2020) and field investigations, the lower part of the Urbas landslide is considered the most active landslide in the area of concern. It is crossed by the Bela stream, which has formed gully-type morphology. The sliding mass consists of tectonically deformed and weathered clastic rocks, covered by a relatively thick cover of carbonate gravel and boulders. The Bela stream causes significant erosion and increases the possibility of downstream mobilisation of the sliding mass. The area is characterised by bare, rugged ground with fallen trees, strong gully erosion and flank ridges.

The DOF analysis clearly indicates that erosion progressively increases during the year. The estimated extent of this area was determined by manual digitalisation of the available DOFs and is represented in Table 3 and Figure 7. No erosion was observed in the 1999 DOF, while the 2020 DOF was overexposed in this area, so digitisation was not possible.

Most activity was observed between 2015 and 2017, when the extent of the erosion area increased by about 1,200 m² (or 400 m² per year) which is twice as large as in previous years. The DOF analysis also shows that, after this event, the Bela torrent channel became enlarged due to the active erosion of the Bela stream. The wider area was also subjected to deforestation of its slopes, which could also increase erosion.

Table 3. Estimated extent of the lower part of the Urbas landslide.

Orthophoto	1999	2006	2011	2015	2017	2020
Area (m ²)	no evidenced activity	90	320	1,060	2,300	no data – overexposed image

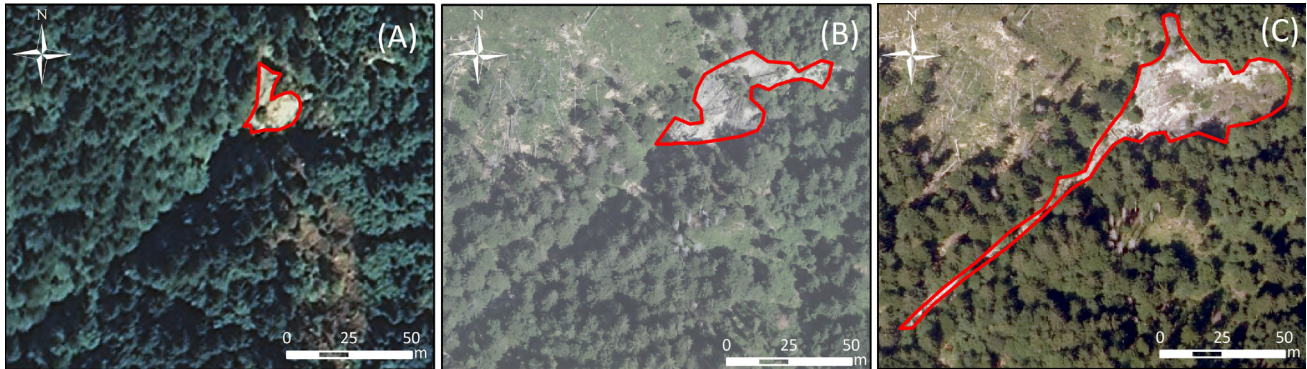


Fig. 7. Digital orthophotos of the lower part of the Urbas landslide from 2006 (A), 2015 (B) and 2017 (C). Red line represents the manually digitalised boundary of the Cikla debris flow.

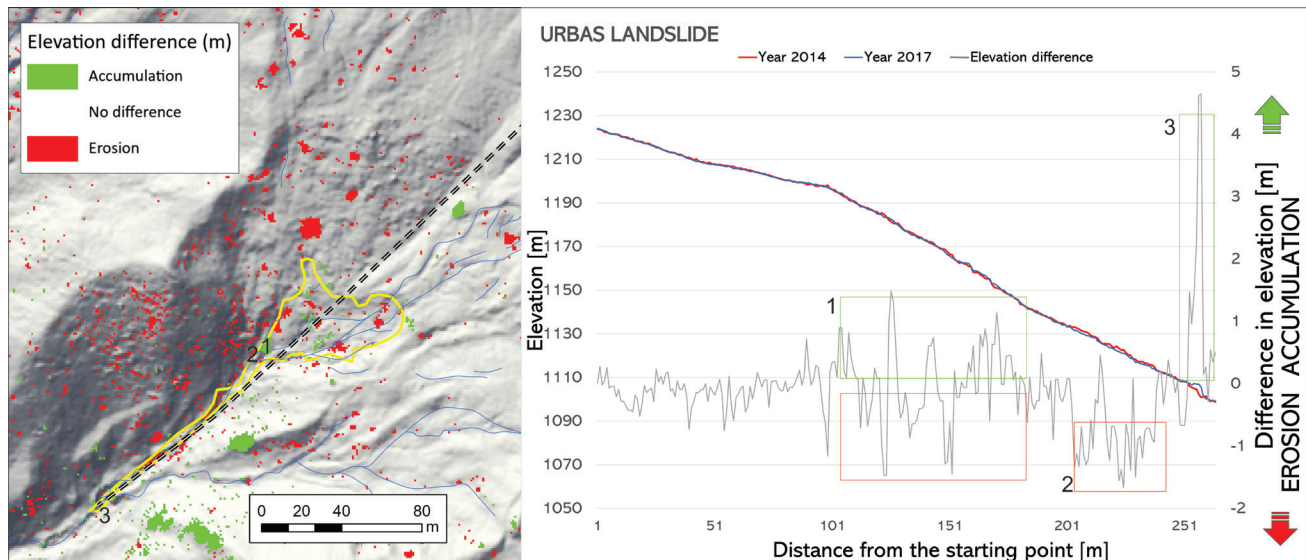


Fig. 8. Surface elevation difference (z-axis) between two LiDAR-derived DEMs from 2014 and 2017. The cross-section shows elevation differences along the Urbas landslide. The yellow line indicates the lower part of Urbas (Fig. 7C).

DEMs analysis shows that approximately 87 m² of the lower part of the Urbas landslide has been affected by erosion, while 12 m² was characterised by accumulation. The volume of eroded surface material was approximately 273 m³ and the surface had subsided between 2 and 5 m (Fig. 8, area 1 and area 2). The Bela torrent channel is characterised by an accumulation of material, with a maximum increase of 2 m. The estimated volume of accumulated material is about 24 m³ (Fig. 8, area 3). The deficit of material was either deposited further down the slope, outside the analysed area, or had been transported away by the torrent.

Active area 3: Subsidence of the local road

The strong landslide activity also affects the local road that crosses the main body of the Urbas landslide, which consists of decomposed siltstone and claystone. Above the road, near the Urbas spring, a minor scarp was formed (Fig. 9). Manual measurements of the minor scarp indicate that it has been opening at a rate of 0.5 to 0.8 m per year. This area consists of clastic rocks with very low permeability, which is reflected in the occurrence of springs charged from the carbonate hinterland. The Urbas spring is partly captured and used to supply water to nearby mountain huts but the rest of the surface water flows uncontrolled

along the landslide and across the road. Local geological and hydrogeological conditions are reflected in continuous subsidence and occasional road collapses. The increased water flow causes intense road erosion and often makes it impassable, particularly during periods of intense or prolonged rainfall.

For this reason, the road has been reconstructed several times by adjusting the road level to the terrain, which can be observed on cross sections in Figure 10. Cross section 3 also indicates strong

subsidence of the road level, ranging from 0.7 m (for the period from 1999 to 2017) to 11.0 m (for the period from 1999 to 2017) (Fig. 10). Road reconstruction was carried out by backfilling with gravel material and log cribs. Backfilling material represents an additional weight that accelerates sliding. Due to subsidence, the road level was later relocated by cutting into the slope. No appropriate drainage system has ever been implemented.

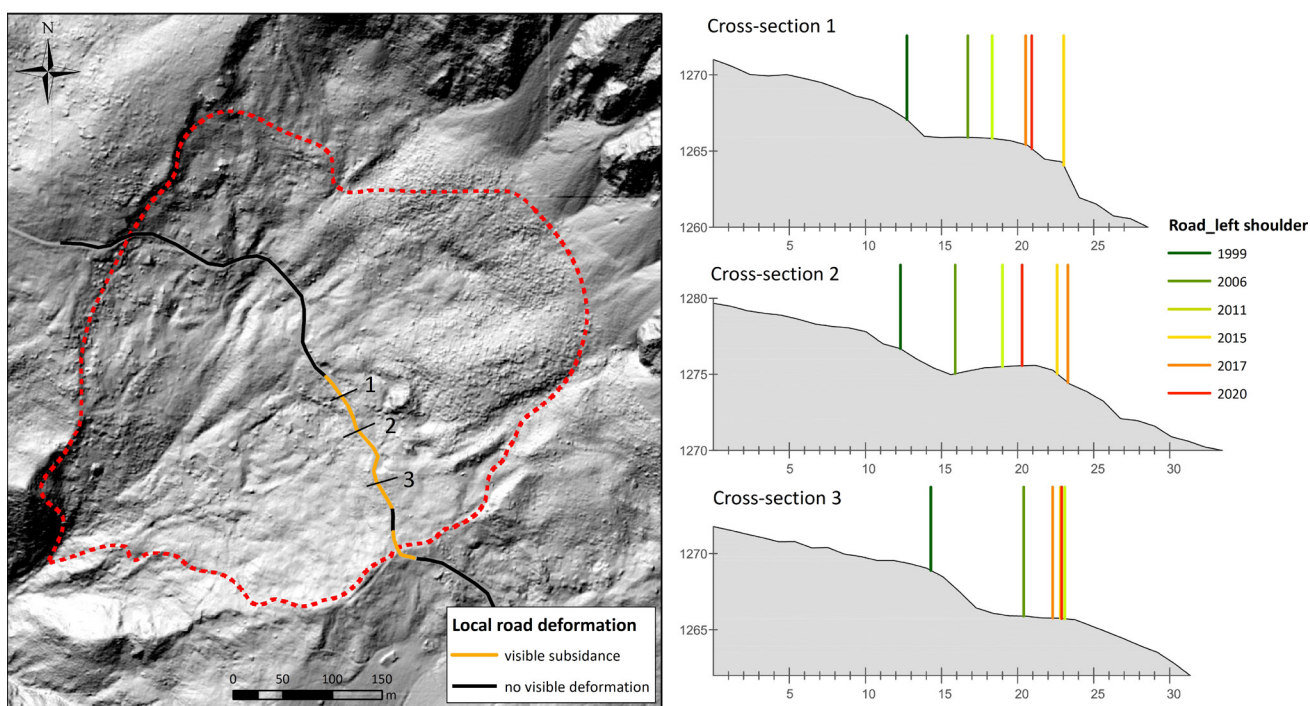


Fig. 9. Longitudinal tension crack above the local road representing a minor scarp.



Fig. 10. Position of local road that crosses the Urbas landslide. Cross-sections represent the position of the road's left shoulder, which has been manually digitalised in orthophotos.

Discussion

Archival DOFs and LiDAR-derived DEMs were used to show the long-term evolution of landslide activity. This approach has been successfully applied in landslide mapping and characterisation by several researchers (Prokešova et al., 2010; Jaboyedoff et al., 2012; Bühler et al., 2012; Kenner et al., 2014; Popit et al., 2014; Đomlija et al., 2019; Görüm, 2019).

Our case review of the available archival data enabled the observation of landslide activity, even for the period when no monitoring system had been established. This approach turned out to be very useful when observing landslide activity for the entire hinterland of Koroška Bela, especially for the remote areas that have not yet been investigated in detail. The results were further validated using the data from the existing monitoring system.

Analysis of the changes of the Čikla landslide surface provides us with useful information about the extent and volume assessment of the debris flow that occurred in April 2017. At that time, no detailed investigations had been conducted and there was no monitoring system for the Čikla landslide. The detailed geological and hydrogeological investigations conducted after April 2017 showed that the Čikla landslide covers an area of 26,000 m² and its volume was estimated to be about 330,500 m³ (Peternel et al., 2017b, 2018, 2020a, 2022a). To date, the Čikla landslide has also been investigated by drilling five boreholes. Two were installed with piezometers and three with inclinometers. The depth of the boreholes was about 40 m. Boreholes and inclinometers indicate that the maximum shear surface occurs at a depth of 28 m, while the average sliding surface is about 23 m deep (Peternel et al. 2018, 2020a). Groundwater level appears at the contact between the debris deposits and the weathered bedrock. The 2017 debris flow occurred in the central part of the Čikla landslide, beneath a large carbonate block that is tectonically deformed and structurally lies within the clastic Carboniferous rocks (Fig. 6, zone 2).

In contrast to Čikla, the Urbas landslide has been the subject of several studies in the past (Jež et al., 2008; Komac et al., 2015; Auflič et al., 2017; Peternel, 2017; Peternel et al., 2017a). For example, the lower part of the Urbas landslide was investigated in detail between December 2012 and April 2016, using UAV photogrammetry and tachymetric measurements. Comparisons of the national orthophotos allows the calculation of the extent of erosion over a long period

of time, while the high-resolution DOFs and the DEMs derived from UAV photogrammetry provide accurate displacement vectors and elevation changes. Surface displacement patterns for the entire monitoring period (December 2012 to April 2016) were analysed based on the sum of displacement vectors for all observation periods. The determined displacements ranged from 0.9 to 19.0 m, with a clear SW directional orientation (Peternel 2017, Peternel et al. 2017a). No geotechnical in-situ investigations (inclinometers or piezometers) were conducted in the lower part of the Urbas landslide due to difficult access and rugged morphology. Although these results only indicate changes at the surface and do not provide information on the depth of sliding surface, they contribute to a better understanding of landslide behaviour and kinematics.

Reviewing the available archival orthophotos, we also observed the deformation of the local road that crosses the main body of the Urbas landslide. Digitised road shoulders provided information about the continuous subsidence and collapse of the road. Nearby boreholes along the road indicated that the road crosses the landslide area with a depth of sliding surface ranging between 8 and 15 m (Peternel et al., 2018). Monitoring of the surface displacements using GNSS also indicates the constant displacements of the landslide main body. The GNSS antenna located below the road, and measuring the surface displacements in real-time, showed displacements of 37 mm over a period of one year (Šegina et al., 2020).

Conclusions

In this paper we summarise all conducted and on-going research and the main findings related to the landslide prone areas above the settlement of Koroška Bela. For the first time, we have also revealed the evolution of landslide activity over the last 25 years. According to investigations so far, the following main outcomes are defined:

- The main landslides detected in the Koroška Bela hinterland are the Čikla, Urbas, Potoška Planina, Malnež and Obešnik landslides. All landslides are characterised by high activity due to intense rainfall events, long-term precipitation and/or groundwater table change. In addition, the moderate-high seismicity of the area could be another predisposing factor contributing to the occurrence of threatening landslides.

- Under the above conditions, the potential risk induced by the mass movements on the town of Koroška Bela can be generally assessed as follows:
 - very high risk due to the occurrence of fast-moving landslides (i.e. debris flows) that have already affected the urban area in the past and might happen in the future;
 - moderate to high risk derived by the slow-moving landslides detected in the slopes up-hill of Koroška Bela, some of them (i.e. the Malnež landslide) potentially threatening the eastern part of the town.
- Even though a lot of knowledge and information has been gained, there are still unknowns that need to be resolved and improvements that have to be implemented. There is still a need for further geological and geotechnical investigations for: i) the improvement of the geological model of the study area, ii) integration with the equipment already installed and, iii) set-up of an integrated monitoring system for the control of slope deformations acting in the landslide areas in the Karavanke mountains.
- Implementation of direct and indirect feasible, effective and sustainable landslide mitigation strategies aimed at reducing the landslide risk in the Koroška Bela settlement.
- Due to the estimated risk, there was a need to set up a continuous and flexible monitoring system that could serve as a basis for a local landslide warning system. With the aid of landslide monitoring, early landslide activity can be detected and landslide impacts can be reduced. In this stage we set up customised dashboards that allowed access to all real-time monitoring sensors. In this way, GeoZS emergency services and stakeholders can access daily updated data, presented on a webpage, at any time. In future, we plan to upgrade the local warning system with email alerts sent to registered users when determined threshold values are exceeded.
- This study is a step forward in landslide management in Slovenia. Several activities that have been implemented within the framework of different projects have enabled the establishment of connections between national and local authorities, scientific and technical experts, and Civil Protection and residents of Koroška Bela.

Acknowledgements

This research was funded by the Slovenian Research Agency through grants Z1-2638, J1-8153, P1-0419, P1-0011, P1-0020 and P2-0180. Additional financial support was provided by the Ministry of the Environment and Spatial Planning, and the Municipality of Jesenice.

The authors would also like to thank the reviewers and the editor for their constructive comments, which helped to improve the manuscript.

References

- Bezák, N., Peternel, T., Medved, A. & Mikoš, M. 2021: Climate Change Impact Evaluation on the Water Balance of the Koroška Bela Area, NW Slovenia. In: Vilímek, V., Wang, F., Strom, A., Sassa, K., Bobrowsky, P.T. & Takara, K. (eds.): *Understanding and Reducing Landslide Disaster Risk* (WLF 2020), 221–228. https://doi.org/10.1007/978-3-030-60319-9_25
- Bezák, N., Sodnik, J., Maček, M., Jurček, T., Jež, J., Peternel, T. & Mikoš, M. 2021: Investigation of potential debris flows above the Koroška Bela settlement, NW Slovenia, from hydro-technical and conceptual design perspectives. *Landslides*, 18: 3891–3906. <https://doi.org/10.1007/s10346-021-01774-7>
- Brenčič, M. & Poltnig, W. 2008: Podzemne vode Karavank: skrito bogastvo = Grundwasser der Karawanken: versteckter Schatz. Ljubljana, Graz, Geološki zavod Slovenije, Joanneum Research Forschungsgesellschaft m.b.H.: 143 p.
- Buser, S. 1978: Osnovna geološka karta SFRJ. List Celovec (Klagenfurt) 1:100.000. Zvezni geološki zavod Beograd.
- Buser, S. 1980: Osnovna geološka karta SFRJ 1:100.000. Tolmač lista Celovec (Klagenfurt). Zvezni geološki zavod, Beograd: 62 p.
- Bühler, Y., Marty, M. & Ginzler, C. 2012: High resolution DEM generation in high-alpine terrain using airborne remote sensing techniques. *Trans. GIS* 16/5: 635–647. <https://doi.org/10.1111/j.1467-9671.2012.01331.x>
- Cruden, D. M. & Varnes, D. J. 1996: *Landslide Types and Processes*. Landslides: investigation and mitigation (Special Report). National Research Council, Transportation Research Board, 247: 36–75.
- Đomlija, P., Bernat Gazibara, S., Arbanas, Ž. & Mihalić Arbanas, S. 2019: Identification and Mapping of Soil Erosion Processes Using the Visual Interpretation of LiDAR Imagery.

- ISPRS Int. J. Geo-Inf., 8: 438. <https://doi.org/10.3390/ijgi8100438>
- Fifer Bizjak, K. & Zupančič Valant, A. 2009: Site and laboratory investigation of the Slano blato landslide. *Eng. Geol.*, 105/3–4: 171–185. <https://doi.org/10.1016/j.enggeo.2009.01.006>
- Gariano, S. L. & Guzzetti, F. 2016: Landslides in a changing climate. *Earth. Sci. Rev.*, 162: 227–252. <https://doi.org/10.1016/j.earscirev.2016.08.011>
- Görüm, T. 2019: Landslide recognition and mapping in a mixed forest environment from airborne LiDAR data. *Eng. Geol.*, 258. <https://doi.org/10.1016/j.enggeo.2019.105155>
- Jaboyedoff, M., Oppikofer, T., Abellán, A., Derron M.H., Loye, A., Metzger, R. & Pedrazzini, A. 2012: Use of LIDAR in landslide investigations: a review. *Nat Hazards* 61: 5–28. <https://doi.org/10.1007/s11069-010-9634-2>
- Jakša, J. & Kolšek, M. 2009: Naravne ujme v slovenskih gozdovih = Natural disasters in Slovenian forests. *Ujma*, 23: 72–81.
- Janža, M., Serianz, L., Šram, D. & Klasinc, M. 2018: Hydrogeological investigation of landslides Urbas and Čikla above the settlement of Koroška Bela (NW Slovenia). *Geologija*, 61/2: 191–203. <https://doi.org/10.5474/geologija.2018.013>
- Jemec Auflič, M., Jež, J., Popit, T., Košir, A., Maček, M., Logar, J., Petkovšek, A., Mikoš, M., Calligaris, C. & Boccali, C. 2017a: The variety of landslide forms in Slovenia and its immediate NW surroundings. *Landslides* 14: 1537–1546. <https://doi.org/10.1007/s10346-017-0848-1>
- Jemec Auflič, M., Kumelj, Š., Peternel, T., Milanič, B. & Jež, J. 2017b: Projekt RECALL: odpornost evropskih skupnosti ob lokalnih zemeljskih plazovih = Project RECALL: resilient European communities against local landslides. *Ujma*, 31: 181–186.
- Jemec Auflič, M., Peternel, T., Kumelj, Š., Jež, J., Milanič, B., Dolžan, E. & Brunelli, G. 2017c: RECALL project: toward resilient European communities against local landslides. In: Mikoš, M., Arbanas, Ž., Yin, Y. & Sassa, K. (eds.): *Advancing Culture of Living with Landslides*. WLF 2017. Springer, Cham: 405–412. https://doi.org/10.1007/978-3-319-53487-9_47
- Jemec Auflič, M., Kumelj, Š., Peternel, T. & Jež, J. 2019: Understanding of landslide risk through learning by doing: case study of Koroška Bela community, Slovenia. *Landslides*, 16/9: 1681–1690. <https://doi.org/10.1007/s10346-018-1110-1>
- Jež, J., Mikoš, M., Trajanova, M., Kumelj, Š., Budkovič, T. & Bavec, M. 2008: Vršaj Koroška Bela - Rezultat katastrofičnih pobočnih dogodkov = Koroška Bela alluvial fan - The result of the catastrophic slope events; Karavanke Mountains, NW Slovenia. *Geologija*, 51/2: 219–227. <https://doi.org/10.5474/geologija.2008.022>
- Jež, J., Peternel, T., Milanič, B., Markelj, A., Novak, M., Celarc, B., Janža, M. & Jemec Auflič, M. 2019a: Čikla landslide in Karavanke Mts. (NW Slovenia). In: Uljarevič, M., Zekan, S., Salković, S. & Ibrahimović, D. (eds.): *Proceedings of the 4th Regional Symposium on Landslides in the Adriatic - Balkan Region*. Geotechnical Society of Bosnia and Herzegovina, Sarajevo: 239–242.
- Jež, J., Markelj, A., Milanič, B., Mencin Gale, E., Atanackov, J., Mechernich, S., Peternel, T. & Jemec Auflič, M. 2019b: Preliminarni rezultati o starosti vršaja Bele v Koroški Beli. In: Rožič, B. (ed.): *24. posvetovanje slovenskih geologov = 24th Meeting of Slovenian Geologists*. Univerza v Ljubljani, Naravoslovnotehniška fakulteta, Oddelek za geologijo, Ljubljana: 49–51.
- Kenner, R., Bühler, Y., Delaloye, R., Ginzler, C. & Phillips, M. 2014: Monitoring of high alpine mass movements combining laser scanning with digital airborne photogrammetry. *Geomorphology*, 206: 492–504. <https://doi.org/10.1016/j.geomorph.2013.10.020>
- Komac, M. 2005: Napoved verjetnosti pojavljanja plazov z analizo satelitskih in drugih prostorskih podatkov. *Geološki zavod Slovenije*, Ljubljana: 284 p.
- Komac, M., Milanič, B., Jež, J., Bavec, M., Holly, R., Mahapatra, P., Hanssen, R., Van der Marel, H., & Fromberg, A. 2012a: Opazovanje plazenja s kombinacijo metod radarske interferometrije in GPS. *Ujma*, 26: 175–182.
- Komac, M., Jež, J., Celarc, B., Milanič, B. & Bavec, M. 2012b: Prvi rezultati merjenja premikov površja na območju Jesenic in Potoške planine s kombinacijo InSAR in GPS meritev. In: Ciglič, R., Perko, D., Zorn, M. (eds.): *Geografski informacijski sistemi v Sloveniji 2011–2012*. Založba ZRC, Ljubljana: 25–31.
- Komac, M., Holley, R., Mahapatra, P., Van Der Marel, H. & Bavec, M. 2015: Coupling of GPS/GNSS and radar interferometric data for a 3D surface displacement monitoring of landslides. *Landslides*, 12/2: 241–257. <https://doi.org/10.1007/s10346-014-0482-0>
- Komac, M., Peternel, T. & Auflič, M. J. 2018: TXT-tool 2.386-2.1: SAR Interferometry as

- a Tool for Detection of Landslides in Early Phases. In: *Landslide dynamics: ISDR-ICL landslide interactive teaching tools*. Springer, Cham: 275–285. https://doi.org/10.1007/978-3-319-57774-6_19
- Koren, K., Serianz, L. & Janža, M. 2022: Characterizing the Groundwater Flow Regime in a Landslide Recharge Area Using Stable Isotopes: A Case Study of the Urbas Landslide Area in NW Slovenia. *Water*, 14: 912. <https://doi.org/10.3390/w14060912>
- Lacroix, P., Handwerger, A. L. & Bièvre, G. 2020: Life and death of slow-moving landslides. *Nat. Rev. Earth Environ.*, 1/8: 404–419. <https://doi.org/10.1038/s43017-020-0072-8>
- Lavtižar, J. 1897: *Zgodovina župnij in zvonovi v dekaniji Radolica*. 148 p.
- Loi, D. H., Sassa, K., Dang, K. & Le Luong, H. 2020: Landslide Hazard Zoning Based on the Integrated Simulation Model (LS-Rapid). In: *Workshop on World Landslide Forum*. Kyoto, Springer.
- Maček, M., Majes, B. & Petkovšek, A. 2016: Lessons learned from 6 years of suction monitoring of the Slano blato landslide. *Riv. Ital. di Geotec.*, 1: 21–31.
- Mikoš, M., Fazarinc, R. & Ribičič, M. 2006: Sediment production and delivery from recent large landslides and earthquake-induced rock falls in the Upper Soča River Valley, Slovenia. *Eng. Geol.*, 86/2–3: 198–210. <https://doi.org/10.1016/j.enggeo.2006.02.015>
- Mikoš, M., Bavec, M., Budkovič, T., Durjava, D., Hribernik, K., Jež, J., Klabus, A., Komac, M., Krivic, M., Kumelj, Š., Maček, M., Mahne, M., Novak, M., Otrin, J., Petje, U., Petkovšek, A., Ribičič, M., Sodnik, J., Šinigoj, J. & Trajanova, M. 2008: Ocena ogroženosti zaradi delovanja drobirskih tokov. Ciljni raziskovalni projekt: Znanje za varnost in mir 2006–2010. Ljubljana, Univerza v Ljubljani, Fakulteta za gradbeništvo in geodezijo, Geološki zavod Slovenije: 224 p.
- Mikoš, M., Petkovšek, A. & Majes, B. 2009: Mechanism of landslides in over-consolidated clays and flysch. *Landslides*, 6: 367–371. <https://doi.org/10.1007/s10346-009-0171-6>
- Mikoš, M. 2020: After 2000 Stože Landslide: Part I–Development in landslide research in Slovenia. *Acta Hydrotech.*, 33/59: 129–153. <https://doi.org/10.15292/acta.hydro.2020.09>
- Mikoš, M. 2021: After 2000 Stože Landslide: Part II–Development of landslide disaster risk reduction policy in Slovenia. *Acta Hydrotech.*, 34/60: 39–59. <https://doi.org/10.15292/acta.hydro.2021.04>
- Ministrstvo za kmetijstvo, gozdarstvo in prehrano Republike Slovenije, 2016: Javno dostopni podatki. Grafični podatki GERK za celo Slovenijo. <http://rkg.gov.si/GERK/> (Pridobljeno 30. 4. 2022).
- Novak, A., Popit, T., Levanič, T., Šmuc, A. & Kaczka, R. J. 2020: Debris flooding magnitude estimation based on relation between dendrogeomorphological and meteorological records. *Geomorphology*, 367: 107303. <https://doi.org/10.1016/j.geomorph.2020.107303>
- Oven, D., Levanič, T., Jež, J. & Kobal, M. 2019: Reconstruction of landslide activity using dendrogeomorphological analysis in the Karavanke mountains in NW Slovenia. *Forests*, 10/11: 1009. <https://doi.org/10.3390/f10111009>
- Peternel, T., Komac, M. & Oštir, K. 2015: Monitoring of Potoška planina landslide (Karavanke Mountains, NW Slovenia). In: Abolmasov, B., Marjanović, M. & Đurić, U. (eds.): *Proceedings of the 2nd Regional Symposium on Landslides in the Adriatic-Balkan Region*. University of Belgrade, Faculty of Mining and Geology, Belgrade: 49–54.
- Peternel, T. 2017: Dinamika pobočnih masnih premikov na območju Potoške planine z uporabo rezultatov daljinskih in terestričnih geodetskih opazovanj ter in-situ meritev: doktorska disertacija. Ljubljana, Univerza v Ljubljani, Naravoslovnotehniška fakulteta: 183 p.
- Peternel, T., Kumelj, Š., Oštir, K. & Komac, M. 2017a: Monitoring the Potoška planina landslide (NW Slovenia) using UAV photogrammetry and tachymetric measurements. *Landslides*, 14/1: 395–406. <https://doi.org/10.1007/s10346-016-0759-6>
- Peternel, T., Jež, J., Milanič, B., Markelj, A., Jemec Auflič, M., Kumelj, Š., Celarc, B., Novak, M., Janža, M., Šram, D., Serianz, L., Bole, Z., Demšar, M., Klasinc, M. & Sodnik, J. 2017b: Izvedba najnужnejših inženirskogeoloških, hidrogeoloških, geofizikalnih in geomehaniških ter geodetskih raziskav za ugotovitev objektivne stopnje tveganja za prebivalstvo zaradi masnih premikov na območju Potoške planine in izdelava strokovnih podlag s predlogi zaščitnih ukrepov: izdelava celovitih geoloških strokovnih podlag in izdelava modela monitoringa za oceno ogroženosti naselja Koroška Bela s pojavi pobočnega masnega premikanja. Geološki zavod Slovenije, Ljubljana: 129 p.

- Pernel, T. & Komac, M. 2017: Observing surface movement patterns of the Potoška planina landslide using geodetic techniques. In: Jemec Auflič, M., Mikoš, M. & Verbovšek, T. (eds.): *Advances in landslide research: proceedings of the 3rd Regional Symposium on Landslides in the Adriatic Balkan Region*. Geological Survey of Slovenia, Ljubljana: 77–81.
- Pernel, T., Jež, J., Milanič, B., Markelj, A. & Jemec Auflič, M. 2018: Engineering-geological conditions of landslides above the settlement of Koroška Bela (NW Slovenia). *Geologija*, 61/2: 177–189. <https://doi.org/10.5474/geologija.2018.012>
- Pernel, T., Jež, J., Milanič, B., Markelj, A., Sodnik, J., Maček, M. & Jemec Auflič, M. 2019: Implementation of multidisciplinary approach for determination of landslide hazard. In: Mikoš, M. & Bezak, N. (eds.): *Buildings and infrastructure resilience: WCF2019 book of abstracts with programme*. Univerza v Ljubljani, Fakulteta za gradbeništvo in geodezijo, Ljubljana :124 p.
- Pernel, T., Jež, J., Janža, M., Zupan, M., Markelj, A., Maček, M., Logar, J., Smolar, J., Mikoš, M., Bezak, N., Sodnik, J., Serianz, L., Klančič, K., Šram, D., Jemec Auflič, M., Novak, A., Šegina, E., Oblak, A., Adrinek, S., Koren, K., Milanič, B., Zajc, M., Hrovat, M., Jurček, T., Kuder, S., Petrovič, D., Grigillo, D., Urbančič, T. & Kozmus Trajkovski, K. 2020a: Podrobna geološka-geotehnična in hidrogeološka karakterizacija velikih plazov v zaledju naselja Koroška Bela za potrebe izdelave stabilnostnih analiz in študijo izvedljivosti sanacijskih rešitev: krovno poročilo. Geološki zavod Slovenije, Fakulteta za gradbeništvo in geodezijo, Ljubljana: 218 p.
- Pernel, T., Šegina, E., Zupan, M., Auflič, M. J. & Jež, J. 2020b: Preliminary Result of Real-Time Landslide Monitoring in the Case of the Hinterland of Koroška Bela, NW Slovenia. In: Tiwari, B., Sassa, K., Bobrowsky, P.T. & Takara, K. (eds.): *Understanding and Reducing Landslide Disaster Risk*. WLF 2020. Springer, Cham: 459–464. https://doi.org/10.1007/978-3-030-60706-7_49
- Pernel, T., Jež, J., Janža, M., Šegina, E., Zupan, M., Markelj, A., Novak, A., Jemec Auflič, M., Logar, J., Maček, M., Bezak, N., Sodnik, J. & Mikoš, M. 2022a: Mountain slopes above Koroška Bela (NW Slovenia) – a landslide prone area. In: Peranić, J., Vivoda Prodan, M., Bernat Gazibara, S., Krkač, M., Mihalić Arbanas, S., Arbanas, Ž. (eds.): *Landslide Modelling & Applications: Proceedings of the 5th Regional Symposium on Landslides in the Adriatic-Balkan Region*. University of Rijeka, Faculty of Civil Engineering, Faculty of Mining; University of Zagreb, Geology and Petroleum Engineering, Rijeka: 13–18.
- Pernel, T., Janža, M., Šegina, E., Bezak, N. & Maček, M. 2022b: Recognition of Landslide Triggering Mechanisms and Dynamics Using GNSS, UAV Photogrammetry and In Situ Monitoring Data. *Remote Sensing*, 14/14: 3277. <https://doi.org/10.3390/rs14143277>
- Placer, L. 2008: Principles of the tectonic subdivision of Slovenia. *Geologija*, 51/2: 205–217. <https://doi.org/10.5474/geologija.2008.021>
- Popit, T., Rožič, B., Šmuc, A., Kokalj, Ž., Verbovšek, T. & Košir, A. 2014: A LIDAR, GIS and basic spatial statistic application for the study of ravine and palaeo-ravine evolution in the upper Vipava valley, SW Slovenia. *Geomorphology*, 204: 638–645. <https://doi.org/10.1016/j.geomorph.2013.09.010>
- Popit, T. 2017: Origin of planation surfaces in the hinterland of Šumljak sedimentary bodies in Rebrnice (Upper Vipava Valley, SW Slovenia). *Geologija*, 60/2: 297–307. <https://doi.org/10.5474/geologija.2017.021>
- Popit, T., Rožič, B., Šmuc, A., Novak, A. & Verbovšek, T. 2022: Using a Lidar-Based Height Variability Method for Recognizing and Analyzing Fault Displacement and Related Fossil Mass Movement in the Vipava Valley, SW Slovenia. *Remote Sens.*, 14/9: 2016. <https://doi.org/10.3390/rs14092016>
- Prokešová, R., Kardoš, M. & Medvedová, A. 2010: Landslide dynamics from high-resolution aerial photographs: A case study from the Western Carpathians, Slovakia. *Geomorphology*, 115: 90–101. <https://doi.org/10.1016/j.geomorph.2009.09.033>
- Rakovec, J., Vrhovec, T. & Gregorič, G. 2000: *Osnove meteorologije za naravoslovce in tehnike*. Društvo matematikov, fizikov in astronomov Slovenije, Ljubljana: 239 p.
- Romer, C. & Ferentinou, M. 2016: Shallow landslide susceptibility assessment in a semi-arid environment – A Quaternary catchment of KwaZulu-Natal, South Africa. *Eng. Geol.*, 201: 29–44. <https://doi.org/10.1016/j.enggeo.2015.12.013>
- Šegina, E., Pernel, T., Urbančič, T., Realini, E., Zupan, M., Jež, J., Caldera, S., Gatti, A., Tagliaferro, G. & Consoli, A. 2020: Monitoring Surface Displacement of a Deep-Seated Landslide by a Low-Cost and near Real-Time

- GNSS System. Remote Sensing, 12/20: 3375. <https://doi.org/10.3390/rs12203375>
- Sodnik, J. & Mikoš, M. 2006: Estimation of magnitudes of debris flows in selected torrential watersheds in Slovenia. *Acta Geogr. Slov.*, 46/1: 93–123. <https://doi.org/10.3986/AGS46104>
- Sodnik, J., Kumelj, Š., Peternel, T., Jež, J. & Maček, M. 2017: Identification of Landslides as Debris Flow Sources Using a Multi-model Approach Based on a Field Survey–Koroška Bela, Slovenia. Workshop on World Landslide Forum, Springer.
- Sodnik, J., Petje, U. & Mikoš, M. 2009: Terrain topography and debris flow modelling. *Geod. Vestn.*, 53/2: 305–318.
- Sodnik, J., Vrečko, A., Podobnikar, T. & Mikoš, M. 2012: Digital terrain models and mathematical modelling of debris flows. *Geod. Vestn.*, 56/4: 826–837.
- Sodnik, J., Podobnikar, T., Petje, U. & Mikoš, M. 2013: Topographic data and numerical debris flow modeling. *Landslide Science and Practice*. Claudio, M., Stefano, C. & Sassa, K. Berlin, Springer 1: 573–578. <https://doi.org/573-578>. [10.1007/978-3-642-31325-7_75](https://doi.org/10.1007/978-3-642-31325-7_75)
- Sodnik, J., Kumelj, Š., Peternel, T., Jež, J. & Maček, M. 2017: Identification of landslides as debris flow sources using a multi-model approach based on a field survey - Koroška Bela, Slovenia. In: Mikos, M., Tiwari, B., Yin, Y. & Sassa, K. (eds.): *Advancing Culture of Living with Landslides*. WLF 2017. Springer, Cham: 1119–1126. https://doi.org/10.1007/978-3-319-53498-5_127
- Sodnik, J. & Mikoš, M. 2018: Two-dimensional debris flow modelling and topographic data: TXT-tool 3.386-1.1. *Landslide dynamics: ISDR-ICL landslide interactive teaching tools*, 2: 235–250. https://doi.org/10.1007/978-3-319-57777-7_11
- Verbovšek, T., Košir, A., Teran, M., Zajc, M. & Popit, T. 2017: Volume determination of the Selo landslide complex (SW Slovenia): integrating field mapping, ground penetrating radar and GIS approaches. *Landslides* 14, 1265–1274. <https://link.springer.com/article/10.1007/s10346-017-0815-x>
- Wheaton, J.M., Brasington, J., Darby, S.E. & Sear, D.A. 2010: Accounting for uncertainty in DEMs from repeat topographic surveys: improved sediment budgets. *Earth Surf. Process. Landf.*, 35: 136–156. <https://doi.org/10.1002/esp.1886>
- Williams, R.D. 2012: DEMs of difference. In: *Geomorphological Techniques*. British Society for Geomorphology: 17 p.
- Zupan, G. 1937: *Krajevni leksikon Dravske banovine*. Ljubljana, Uprava Krajevnega leksikona dravske banovine Ljubljana.
- Internet sources:
Internet 1: http://meteo.arso.gov.si/uploads/probase/www/climate/image/sl/by_variable/precipitation/mean-annual-measured-precipitation_81-10.png (30. 4. 2022)



Prediction of the peak shear strength of the rock joints with artificial neural networks

Napoved vrhunske strižne trdnosti po razpoki v kamnini z nevronskimi mrežami

Karmen FIFER BIZJAK & Rok VEZOČNIK

Slovenian National Building and Civil Engineering Institute, Dimičeva ul. 12, SI-1000 Ljubljana, Slovenia;
e-mail: karmen.fifer@zag.si, rok.vezocnik@zag.si

Prejeto / Received 4. 5. 2022; Sprejeto / Accepted 7. 10. 2022; Objavljeno na spletu / Published online 18. 11. 2022

Key words: artificial neural network, camera-type 3D scanner, rock mechanics, rock joint, joint roughness

Ključne besede: nevronska mreža, 3D skener s kamero, mehanika kamnin, razpoke, hrapavost razpok

Abstract

With the development of computer technology, artificial neural networks are becoming increasingly useful in the field of engineering geology and geotechnics. With artificial neural networks, the geomechanical properties of rocks or their behaviour could be predicted under different stress conditions. Slope failures or underground excavations in rocks mostly occurred through joints, which are essential for the stability of geotechnical structures. This is why the peak shear strength of a rock joint is the most important parameter for a rock mass stability. Testing of the shear characteristics of joints is often time consuming and suitable specimens for testing are difficult to obtain during the research phase. The roughness of the joint surface, tensile strength and vertical load have a great influence on the peak shear strength of the rock joint. In the presented paper, the surface roughness of joints was measured with a photogrammetric scanner, and the peak shear strength was determined by the Robertson direct shear test. Based on six input characteristics of the rock joints, the artificial neural network, using a backpropagation learning algorithm, successfully learned to predict the peak shear strength of the rock joint. The trained artificial neural network predicted the peak shear strength for similar lithological and geological conditions with average estimation error of 6 %. The results of the calculation with artificial neural networks were compared with the Grasselli experimental model, which showed a higher error in comparison with the artificial neural network model.

Izvleček

Nevronske mreže postajajo z razvojem računalniške tehnologije vedno bolj uporabne tudi na področju inženirske geologije in geotehnike. Z nevronskimi mrežami lahko na osnovi večjega števila podatkov napovemo geomehanske lastnosti kamnine ali njihovo obnašanje v različnih napetostnih pogojih. Porušitve brežin ali podzemnih prostorov v kamninskem masivu se večinoma pojavijo po razpokah, zato so strižne lastnosti v razpokah ali prelomih bistvene za stabilnost geotehničnih objektov. Preiskave strižnih lastnosti so večinoma dolgotrajne, prav tako pa je pri vrtnanju v fazi raziskav težko pridobiti primerne vzorce. Velik vpliv na velikost vrhunske strižne trdnosti ima hrapavost površine razpoke, natezna trdnost in vertikalna obremenitev. V predstavljenem članku je hrapavost površine razpok izmerjena s fotogrametričnim skenerjem, vrhunska strižna trdnost pa je določena z Robertsonovo direktno strižno preiskavo. Na osnovi šestih vhodnih karakteristik razpok in kamnine ter izmerjene strižne trdnosti z Robertsonovo preiskavo, lahko z naučeno nevronske mreže uspešno napovemo vrhunske strižne trdnosti po razpokah. Tako naučena nevronska mreža lahko dovolj natančno napove vrhunske strižne trdnosti za podobne litološke razmere in geološke pogoje, z upoštevanjem dokaj nizke napake, to je 6 %. Rezultate izračuna z nevronskimi mrežami smo primerjali z eksperimentalnim modelom, ki je v primerjavi z nevronskimi mrežami pokazal višjo napako napovedi vrhunske strižne trdnosti.

Introduction

The idea for artificial neural networks (ANN) is in the functioning of the human brain. The human brain is the central system of the human nervous system, composed from almost 10 billion biological neurons that are interconnected by synapses. The cellular body of a neuron receives input signals from many synapses with different electrical activity (Flood & Kartam, 1994, Bishop, 1995, Lopez et. al., 2022).

Scientists were therefore drawn to the idea of making a device that mimics the brain. These are made up of a huge number of cells interconnected by thin “threads”. These cells are called neurons, and their connections or “threads” are called synapses. Neurons send electrical stimuli to each other through synapses. Synapses are characterized by differences in electrical conductivity, which changes during learning. Thus, the knowledge acquired during learning is accumulated in synapses or in their conductivity. If the sum of the signals arriving at an individual neuron via synapses is large enough, the ignition of an individual neuron occurs. This means that this neuron sends a signal to its output, which is transmitted through the synapses to other neurons (Jain et al., 1996, Maio & Santillo, 2020).

The ANN tries to simulate the human brain activity and until now several applications are already known in rock mechanics field (Lawal & Kwon, 2021; Abdalla et al., 2015; Armaghani, 2015; Hussain et al., 2019; Sarkar et al., 2010).

The shear behaviour of a jointed rock masses depends on the shear characteristics of the discontinuities in the rock mass. To determine the shear strength in rock mass discontinuities many researchers developed experimental relationships between the roughness of the discontinuities and the peak shear strength (Barton, 1973; 1976; Barton and Choubey, 1977; Hoek and Brown, 1980; Hoek and Bray, 1981; Hoek, 2000; Huang et al., 1992; Patton, 1966; Pellet et al., 2013).

Recently, scanners have been used as a non-destructive method to measure and characterise the joint surface in three dimensions. The roughness metric based on the three-dimensional morphology was proposed by Grasselli (2001, 2002). An ATOS scanner was used for the accurate measurement of the joint roughness. Details of the scanner characteristics are summarized in Table 1. Several empirical relations were developed for determining the geometry of the joint surface, such as contact area A^0 , roughness parameter C and maximum dip angle θ^*_{max} (Grasselli & Egger, 2003).

ANNs have already been used for prediction of the shear characteristics of rock samples in published papers. The shear strength of shale rock samples was predicted based on the minimum and intermediate strength using a triaxial test (Moshrefi et al., 2018). Back propagation multi-layer perceptron was used for learning. Influence of heterogeneity on rock strength at different strain rates was predicted with an ANN, as well as parameters of crack inclination, distance, filling and strain rate (Jiang et al., 2021). Shear behaviour of clean rock discontinuities was studied including normal stress, dilation, horizontal displacement, asperity angle, amplitude, joint rock compressive strength and friction angle of an intact sample. The ANN model fitted the measuring results better than some analytical models. Shear strength parameters were obtained using shale samples, sheared in a triaxial cell. The input parameters were point load index, Brazilian tensile strength, ultrasonic velocity, Schmidt hammer test and friction angle as an output parameter (Armaghani et al., 2014).

Drilling data and well logs were used for the uniaxial compressive strength prediction with ANN (Asadi, 2017). Porosity, density, penetration rate and P wave velocity were used to predict the uniaxial strength of rock between wells that are close to each other. For limestone the uniaxial strength was compared with the results of the ANN and regression analysis (Khanlari & Abdilor, 2011).

Table 1. Characteristics of the scanner with camera (ATOS I).
Tabela 1. 3D skener s kamero (ATOS I).

Item	Value
Measured Points	800.000
Measurement Time (seconds)	0.8
Measuring Area (mm ²)	125 × 100 - 1000 × 800
Point Spacing (mm)	0.13-1.00
Measuring volume (mm ³)	125 × 100 × 90 to 1000 × 800 × 800
Measuring points per individual scan	1032 × 776 pixels

In the presented paper, the ANN was used for the peak shear strength prediction of the rock joints. The input parameters were tensile strength, basic shear angle and the morphologic parameters of the rock joints obtained from the 3D scanner measurements. Results were compared with the Robertson direct shear test for different rock samples.

Methods

Artificial Neural network model

The model of the ANN tries to simulate the behaviour of the human brain and nervous system by its architecture. A detailed description of the ANNs is beyond the scope of this paper and can be found in many publications (Masters, 1993; Jain et al., 1996; Almeida, 2002; Shahin et al., 2002).

ANNs learn from the presented data and use these data to adjust their weights in an attempt to minimise the model input variables and the corresponding outputs. The advantage of ANNs is that they do not need any prior knowledge about the relationship between the input-output variables. This is a benefit in comparison with most of the empirical and statistical methods.

The basic unit of ANN is a neuron or node (Fig. 1). It receives input signals ($x_1 .. x_n$) and a bias value, which is always 1. In the neuron input, signals are multiplied with their weight values ($w_1 .. w_n$). The bias assures that even if all input signals are zero, there is activation in the neuron. The activation function ($G(I)$) is used for introducing the non-linearity to the ANN.

$$I = w_0 + w_1y_1 + w_2y_2 \dots + w_ny_n \quad (1)$$

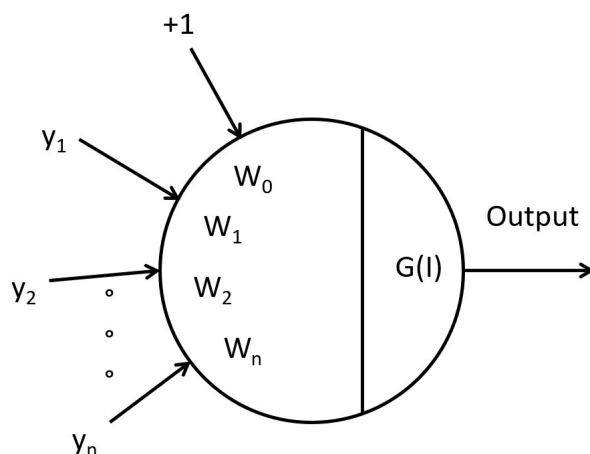


Fig. 1. Typical neuron in ANN.
Sl. 1. Značilen nevron v ANN.

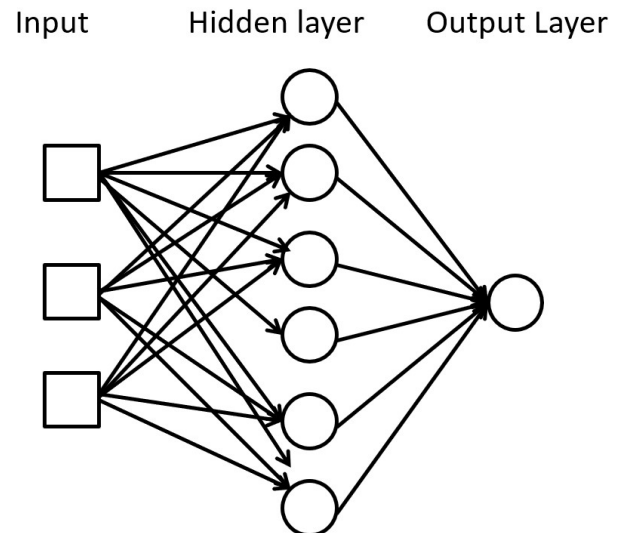


Fig. 2. Structure of the BP artificial neural network.
Sl. 2. Struktura povratne nevronske mreže.

A typical ANN is composed of three different layers of neurons; one input layer, one or multiple hidden layers and one output layer. The simplified model is presented in Figure 2.

The input layer consists of neurons which receive information from input data. The number of neurons in the input layer depends on input data sources. For presented application the input neurons were; σ_t (tensile strength), φ_b (basic friction angle) and scanning parameters A_0 (maximum contact area), C (roughness parameter) and θ_{max}^* (maximum apparent dip angle).

The hidden layer contains a different number of neurons and is connected with the input and output layer with a linear or non-linear transfer function (Rashidian et al., 2013). The hidden layer processes the information received from the input neurons, and passes it to the output layer.

The output layer produces an appropriate response to the given input. For presented ANN there is a single output neuron; measured shear peak stress (τ_p).

The propagation of information in ANNs starts at the input layer where the network is presented with a historical set of input data and the corresponding (desired) outputs. The back-propagation algorithm, used in this paper, is the most widespread because it has a simple structure and clear mathematical meaning (Cybenko, 1989). It consists of two phases: forward and backward. In the forward phase, the training data set was introduced to the network and fed forward until a prediction was calculated. The final output is then compared to the target value and the error signal is calculated. In the backward phase, the error signal is back propagated in the network from the output layer to the input layer and the

appropriate weight changes are calculated using a mathematical criterion that minimizes the errors (Jain et al., 1996; Khandelwal et al., 2004).

Using these errors and a learning rule, the network adjusts its weights until it can find a set of weights that calculate an input/output pair with the smallest error. This phase is called “learning” or “training”. Once the training phase of the model has been successfully finished, the performance of the trained model has to be validated using an independent validation set of data.

For the presented application 70 % of the data were used for a training set and the rest for the testing. The test set measured how well the model learned based on the data from the learning phase. For validation, data are usually taken from the whole set when there are not enough additional data for this procedure.

Use of a 3D Scanner

For measuring rock joint surface roughness, an Advanced Topometric Sensor (ATOS I) was used (Fig. 3) which operates by combining measuring principles of optical triangulation, photogrammetry and fringe projection (Keller & Mendricky, 2015). With the help of a projector, different light-dark fringe patterns are produced by the measuring part.

The ATOS system consists of three separate components: the fringe digital projector and two CCD cameras. The two cameras, separated by a fixed distance, operate on the basis of known relative orientation thus forming the basis for triangulation. The fringe digital projector, located midway between both cameras, projects a structured light pattern onto the object to be scanned. During the scanning process, the coded fringe pattern undergoes a phase shift which means the pattern rapidly changes and is therefore nearly invisible to the human visual perception abilities. This pattern alteration process is recorded by the two CCD sensors with 3D coordinates calculated for each camera pixel by applying optical transformation equations. The resulting highly-detailed image consists of millions of measuring 3D points which are acquired within a very short time (few seconds) without physically contacting the scanned surface. In the final step, the accompanying sensor software automatically generates a high-resolution point cloud which represents a precise 3D image of the scanned surface. Optionally, this point cloud can be further transformed into a surface model (using typical triangular or square grid templates (Fig. 4). In the figure the

roughness of the rock joint surface measured from the share plane is presented.

The quality of surface measurements is obviously very important for the estimation of surface roughness. The quality of the morphological model depends on the density of the measuring points, the measuring resolution and the precision with which these points can be located in space. The measuring area of the ATOS I system ranges from $125 \times 100 \text{ mm}^2$ to $1000 \times 800 \text{ mm}^2$ and the number of measuring points per individual scan reaching up to 1032×776 pixels.

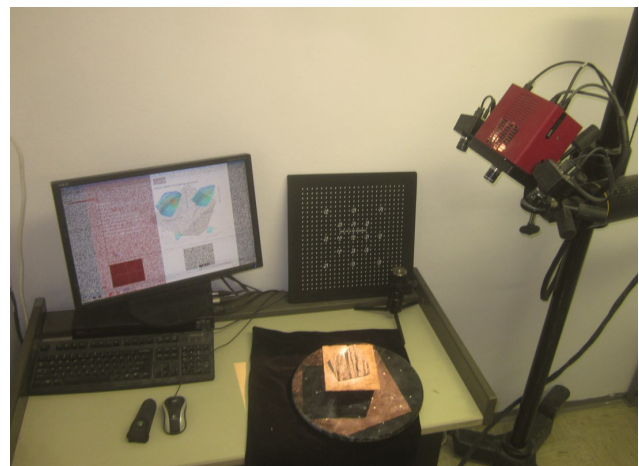


Fig. 3. The ATOS I 3D scanner and the sample.
Sl. 3. Skenirani ATOS I 3D in skenirani vzorec.

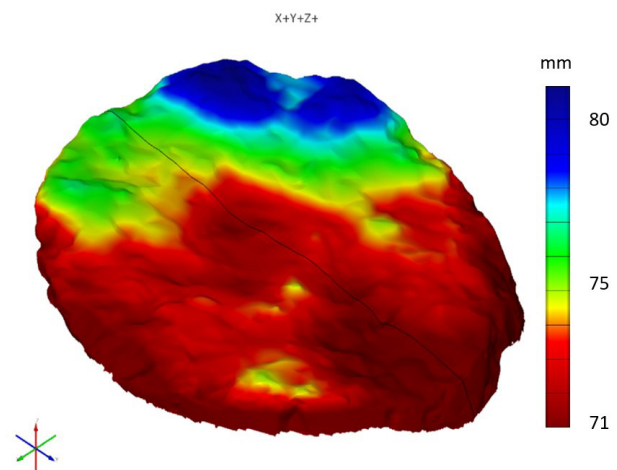


Fig. 4. Surface model of the rock joint.
Sl. 4. Skenirana površina razpoke.

Calculation methods of Grasselli model for the peak shear stress calculation

Morphological parameters were calculated from scanning samples according to the Grasselli (2001) procedure (G01). The apparent dip angle was used to calculate the three-dimensional morphology parameters (Fig. 5). The procedure is presented in equations 2 to 6.

Table 2. Input data for the peak shear strength calculation

Tabela 2. Vhodni podatki za izračun vrhunske strižne trdnosti

No	Lithology	σ_t (MPa)	σ_n (MPa)	A_0 (-)	C (-)	θ^*_{max} (°)	ϕ_b (°)
1	limestone	1.99	0.1	0.4147	17.03	86.86	24
2	limestone	1.99	0.3	0.5791	16.99	89.69	24
3	limestone	1.99	0.4	0.5499	28.75	75.55	24
4	limestone	1.99	0.4	0.1773	12.87	86.2	24
5	limestone	1.99	0.4	0.4859	20.87	82.807	24
6	limestone	1.99	0.3	0.4015	11.82	89.86	24
7	limestone	1.99	0.2	0.3953	27.92	86.95	24
8	limestone	1.99	0.4	0.4535	12.2	51.89	24
9	dolomite	2.17	0.15	0.3410	11.9	90	25
0	shale	0.3	0.4	0.5420	15.04	86.21	24
11	shale	0.3	0.2	0.4720	9.22	42.93	24
12	siltstone	2	0.1	0.4606	6.26	73.33	26
13	siltstone	2	0.4	0.2000	11.61	87.28	26
14	siltstone	2	0.4	0.3037	13.88	89.12	26
15	claystone	0.3	0.2	0.1200	19.98	84.74	20
16	claystone	0.3	0.2	0.4707	24.69	87.1	20
17	claystone	0.3	0.1	0.3459	13.27	89.9	20
18	sandstone	1	0.4	0.4613	11	79.25	30
19	claystone	0.3	0.1	0.4999	6.69	89.7	20
20	claystone	0.3	0.4	0.5020	9.4	84.24	24
21	siltstone /claystone	1	0.4	0.3655	28.62	89.9	24
22	claystone	0.3	0.4	0.3953	24.4	79.72	24
23	siltstone/ claystone	0.3	0.2	0.5105	9.25	89.05	24
24	siltstone	7.37	0.4	0.4238	15.05	89.71	30
25	dolomite	3.02	0.1	0.5829	6.46	79.12	30
26	dolomite	3.02	0.3	0.4821	7.21	82.08	30
27	siltstone	2	0.3	0.5153	12.46	84.87	30
28	dolomite	3.02	0.3	0.4821	7.21	82.09	30
29	dolomite	2.49	0.25	0.4126	6.06	90	28
30	claystone	0.3	0.4	0.4824	15.59	85.47	20

The prediction of peak shear stress (τ_p) with ANN and G01 model was performed in the next step. For both calculations the same input parameters were used (σ_n , σ_t , A_0 , C , θ^*_{max} , φ_b).

Results of the ANN model

Several ANN structures were used for the τ_p prediction, with a different number of neurons in the input layer, but the best results were achieved with the next structure:

Input layer; 6 neurons (σ_n , σ_t , A_0 , C , θ^*_{max} , φ_b)
 Hidden layer, 29 neurons
 Output layer, one neuron (τ_p)

For example, if we added residual shear angle (φ_r) and type of lithology to the presented 6 input neurons, the calculation made by the ANN did not converge to the minimum error.

A hyperbolic tangent transfer function was used as the activation function. We also used an sigmoidal function, but the average estimation error (E_{av}) was almost the same. The trained ANN predicted the peak shear strength with quite a small average estimation error; $E_{av} = 6\%$ (Table 2). A comparison between the predicted peak shear strength with the ANN and with the results from the laboratory Robertson test is presented in Figure 6.

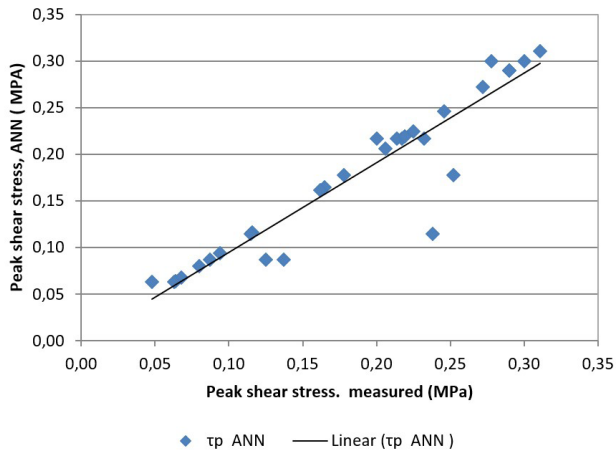


Fig. 6. Measured peak shear stress vs ANN predicted.
Sl. 6. Primerjava izmerjene vrhunske strižne trdnosti in izračunane z ANN.

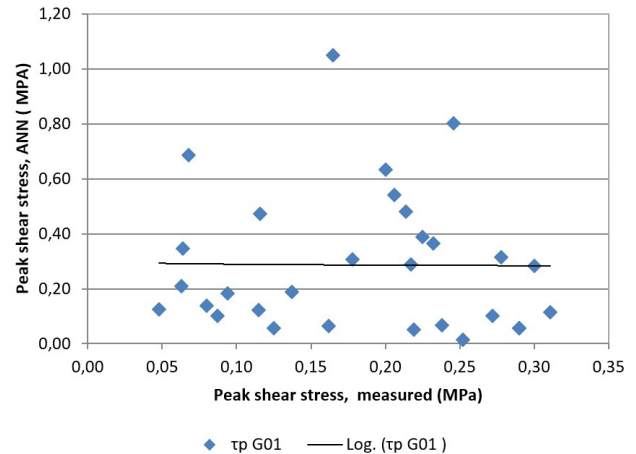


Fig. 7. Measured peak shear stress vs G01 model.
Sl. 7. Primerjava izmerjene vrhunske strižne trdnosti in izračunane z G01 modelom.

Result of G01 model

Next calculation was done based on the G01 model (eq. 8) and compared with the results obtained from laboratory Robertson tests. The average estimation error between the Robertson tests and calculation with G01 model was much higher, $E_{av} = 28 \%$ (Table 3).

The comparison between the calculated peak shear strength with the G01 model and with the results from the laboratory Robertson test is presented in Figure 7.

Discussion

The presented calculation was demonstrated by analysing 30 samples of jointed rock. The input parameters for the Grasselli calculation (G01) and the ANN were the same. The peak shear stress depends on the normal stress under which the shear test is performed and because of this, the normal stress (σ_n) is one of the most important parameters. Grasselli (2001) showed that A_0 , C and θ^*_{max} , are the most important morphological parameters and tensile strength (σ_t) and basic friction angle ϕ_b are the most important strength characteristics of the rock.

Table 3. Results of peak shear strength calculation for ANN and G01 model.

Tabela 3. Rezultati izračuna vrhunske strižne trdnosti izračunani z ANN in G01 modelom.

No	τ_p meas. (MPa)	τ_p ANN (MPa)	τ_p G01 (MPa)	No	τ_p meas. (MPa)	τ_p ANN (MPa)	τ_p G01 (MPa)
1	0.06	0.06	0.35	16	0.07	0.07	0.68
2	0.25	0.18	0.01	17	0.05	0.06	0.13
3	0.17	0.17	1.05	18	0.31	0.31	0.11
4	0.21	0.21	0.54	19	0.06	0.06	0.21
5	0.20	0.22	0.63	20	0.28	0.30	0.31
6	0.18	0.18	0.31	21	0.27	0.27	0.10
7	0.12	0.12	0.47	22	0.22	0.22	0.05
8	0.23	0.22	0.36	23	0.14	0.09	0.19
9	0.12	0.12	0.12	24	0.25	0.25	0.80
10	0.30	0.30	0.28	25	0.09	0.09	0.18
11	0.13	0.09	0.06	26	0.29	0.29	0.06
12	0.08	0.08	0.14	27	0.23	0.23	0.39
13	0.22	0.22	0.29	28	0.29	0.29	0.06
14	0.21	0.22	0.48	29	0.24	0.12	0.07
15	0.09	0.09	0.10	30	0.16	0.16	0.07
					E_{ave}	6%	28%

The peak shear stress of the rock joints was measured in laboratory and then predicted with the ANN and with the G01 model. The results of both calculations are presented in Figure 8. Prediction of peak shear stress with the ANN is very close to the measured results, while the calculations with the Grasselli model were much higher in comparison to the measured results for at least for 30 % of samples.

Samples used in a comparable study (Grasselli, 2001) have larger dimensions, at least 200 mm x 100 mm x 100 mm and were consolidated under a normal load higher than 1 MPa. In our case, samples were tested under the normal loads between 0.1 and 0.4 MPa. The use of smaller samples and lower vertical load are probably a reason for the higher average estimation error obtained with the G01 model. Such large samples are often difficult to obtain for testing. Samples are usually taken from boreholes and they have a maximal diameter of 10 cm and in this case the Robertson shear test is much more convenient. The result of the Robertson test was peak shear stress which was then calculated with the ANN and Grasselli model.

The calculation with the ANN reaches very good results; E_{ave} was 6 %. The calculated Pearson coefficient was 0.93, which confirms a very high correlation between the measured peak shear stress and the predicted peak shear stress with ANN. The comparison between the calculated and measured peak shear strength is presented in Figure 8.

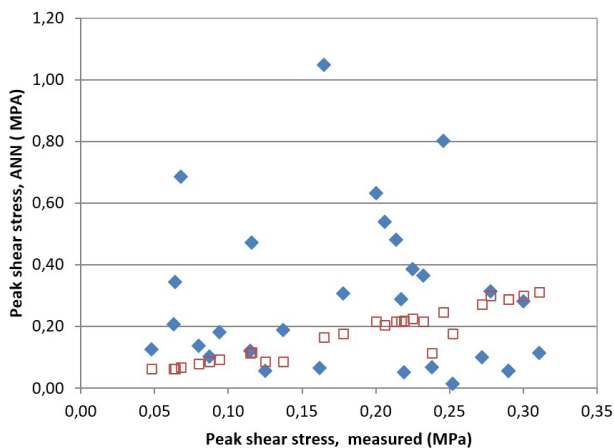


Fig. 8. Peak shear stress; measured, predicted with ANN and calculated with G01 model.

Sl. 3. Vrhunska strižna trdnost, napovedana z ANN in izračunana z G01.

Results of more tests with different rock lithology have to be included in to the ANN in the future. Given the diverse lithological composition in Slovenia, it is necessary to include samples of metamorphic and igneous rocks. Also, the number of samples of soft rock has to be increased, because the main geotechnical problems usually occurred in soft rocks like shale or claystone.

Higher number of samples could assure that the trained ANN would be a useful tool in engineering practice.

Conclusions

Shear geomechanical characteristic are the most important factor in the stability of the jointed rock mass. Usually the failure occurs along a fissure or a joint. Peak shear stress is the main parameter for a slope design, foundations or tunnel excavations. If it is exceeded, the failure could cause large damage to geotechnical structures. In the paper the technology of rock joint scanning was used for determining the morphological parameters of the joint roughness. Additional parameters were obtained from the Robertson direct shear test and tensile strength from the Brazilian test. Results showed that the ANN could successfully predict the peak shear with quite small error. The future research will be focused on analysing more samples with different

lithology, especially soft rock, to make the ANN usable for wider engineering practice.

References

- Abdalla J.A., Attom M.F. & Hawileh R. 2015: Prediction of minimum factor of safety against slope failure in clayey soils using artificial neural network. *Environmental Earth Science*, 73/9: 5463–5477. <https://doi.org/10.1007/s12665-014-3800-x>
- Ak, H. & Konuk, A. 2008: The effect of discontinuity frequency on ground vibrations produced from bench blasting: a case study. *Soil Dynamics and Earthquake Engineering*, 28/9: 686–694. <https://doi.org/10.1016/j.soildyn.2007.11.006>
- Almeida, J.S. 2002: Predictive non-linear modeling of complex data by artificial neural networks. *Current Opinion in Biotechnology*, 13/1: 72–76. [https://doi.org/10.1016/s0958-1669\(02\)00288-4](https://doi.org/10.1016/s0958-1669(02)00288-4)
- ASTM – 16 2017: Standard Test Method for Performing Laboratory Direct Shear Strength Tests of Rock Specimens Under Constant Normal Force. ASTM International.
- Asadi, A. 2017: Application of artificial neural networks and prediction of uniaxial compressive strength of rock using well logs and drilling data. *Procedia Engineering* 191: 279–286. <https://doi.org/10.1016/j.proeng.2017.05.182>
- Armaghani, D.J., Hajihassani M., Bejarbaneh B., Y., Marto A. & Mohamad, E.T. 2014: Indirect measure of shale shear strength parameters by means of rock index tests through an optimised artificial neural network. *Measurement*, 55: 487–498.
- Armaghani, J.D., Momeni E., Khalil, A.S. & Khandelwal, M. 2015: Feasibility of ANFIS model for prediction of ground vibrations resulting from quarry blasting. *Environmental Earth Sciences*, 74: 2845–2860. <https://doi.org/10.1007/s12665-015-4305-y>
- Barton, N. 1973: Review of a new shear-strength criterion for rock joints. *Eng. Geol.*, 7/4: 287–332. [https://doi.org/10.1016/0013-7952\(73\)90013-6](https://doi.org/10.1016/0013-7952(73)90013-6)
- Barton, N. 1976: The shear strength of rock and rock joints. *Int. J. Rock. Mech. and Min. Sci. & Geomech. Abstr.*, 13/97: 255–279. [https://doi.org/10.1016/0148-9062\(76\)90003-6](https://doi.org/10.1016/0148-9062(76)90003-6)
- Barton, N. & Choubey, V. 1977: The shear strength of rock joints in theory and practice. *Rock Mechanics*, 10:1–54. <https://doi.org/10.1007/BF01261801>

- Bishop, C.M. 1995: Neural network for pattern recognition (1st ed). Oxford University Press.
- Cybenko, G. 1989. Approximation by superpositions of a sigmoidal function. *Math. Control Signals Systems*, 2: 303-314. <https://doi.org/10.1007/BF02551274>
- Flood, I. & Kartam, N. 1994. Neural networks in civil engineering. I: principles and understanding. *Journal of Computing in Civil Engineering*, 8/2: 131-148.
- Grasselli, G. 2001: Shear strength of rock joints based on quantified surface description. (Dissertation). Ecole Polytechnique Federale de Lausanne, Lausanne.
- Grasselli, G., Wirth, J. & Egger, P. 2002: Quantitative three-dimensional description of a rough surface and parameter evolution with shearing. *International Journal of Rock Mechanics and Mining Sciences*, 39: 789-800.
- Grasselli, G. & Egger, P. 2003: Constitutive law for the shear strength of rock joints based on three-dimensional surface parameters. *International Journal of Rock Mechanics and Mining Sciences*, 40: 25-40.
- Hoek, E. & Bray, J. W. 1981: Rock slope engineering. Vancouver, CRC Press.
- Hoek, E. & Brown, E. T. 1980: Empirical strength criterion for rock masses. *Journal of Geotechnical and Geoenvironmental Engineering*, 106: 1013-1035.
- Hoek, E. 2000: Shear strength of discontinuities. *Rock engineering*, 61-72. <https://www.rocscience.com/assets/resources/learning/hoek/Practical-Rock-Engineering-Full-Text.pdf>
- Huang, S. L., Oelfke, S. M. & Speck, R. C. 1992: Applicability of fractal characterization and modelling to rock joint profiles. *International Journal of Rock Mechanics and Mining Sciences & Geomechanics Abstracts*, 29: 89-98.
- Hussain, A., Surendar, A., Clementking, A., Kanagarajan, S. & Ilyashenko, L.K. 2019: Rock brittleness prediction through two optimization algorithms namely particle swarm optimization and imperialism competitive algorithm. *Engineering with Computers*, 35/3: 1027-1035. <https://doi.org/10.1007/s00366-018-0648-9>
- Jain, A.K., Mao, J. & Mohiuddin, K.M. 1996: Artificial neural networks - a tutorial. *Computer*, 29/3: 31-44.
- Jiang S., Sharafisafafa, M. & Shen, L. 2021: Using Artificial neural networks to predict influence of heterogeneity on rock strength at different strain rates. *Materials*, 14/11: 3042. <https://doi.org/10.3390/ma14113042>
- Keller, P. & Mendricky, R. 2015: Parameters influencing the precision of slm production. *MM Science Journal*, October 2015.
- Khanlari, G. & Abdilor, Y. 2011: Estimation of strength parameters of limestone using artificial neural network and regression analysis. *Australian Journal of basic and Applied Science*, 5/11: 1049-1053.
- Kulatilake, P. H. S. W., Shou, G., Huang, T. H. & Morgan, R. M. 1995: New peak shear strength criteria for anisotropic rock joints. *International Journal of Rock Mechanics and Mining Sciences & Geomechanics Abstracts*, 32/7: 673-697.
- Khandelwal, M., Roy, M.P. & Singh, P.K. 2004: Application of artificial neural network in mining industry. *Indian Mining Engineering Journal*, 43: 19-23.
- Lawal, A.I. & Kwon, S. 2021: Application of artificial intelligence to rock mechanics: An overview. *Journal of Rock Mechanics and Geotechnical Engineering*, 13/1: 248-266.
- Lopez, O.A.M., Lopez, A.M. & Crossa, J. 2022: Fundamentals of Artificial Neural Networks and Deep Learning. *Multivariate Statistical Machine Learning Methods for Genomic Prediction*: 379-425. Springer, Cham. https://doi.org/10.1007/978-3-030-89010-0_10
- Maio, V.D. & Santillo, S. 2020: Information Processing and Synaptic Transmission. *Advances in Neural Signal Processing*. <https://doi.org/10.5772/intechopen.88405>
- Masters, T. 1993: Practical network recipes in C++. Academic Press, San Diego, California, USA.
- Moshrefi, S., Shahriar, K., Ramezanzadeh, A. & Goshtasbi, K. 2018: Prediction of ultimate strength of shale using artificial neural network. *Journal of mining & Environment*, 9/1: 91-105. <https://doi.org/10.22044/jme.2017.5790.1390>
- Patton, F.D. 1966: Multiple modes of shear failure in rock. In: *Proceedings of the 1st congress of International Society for Rock Mechanics*, 1: 509-513.
- Pellet, F. L., Keshavarz, M. & Boulon, M. 2013: Influence of humidity conditions on shear strength of clay rock discontinuities. *Engineering Geology*, 157: 33-38.
- Rashidian, V. & Hassanlourad, M. 2013: Application of Artificial Neural Network for Modeling the Mechanical Behavior of Carbonate Soils. *International Journal of Geomechanics*, (ASCE) GM.1943-5622.0000299.

Sarkar, K., Tiwary, A. & Singh, T.N. 2010: Estimation of strength parameters of rock using artificial neural networks. *Bulletin of Engineering Geology and the Environment*, 69: 599–606.

Shahin, M.A., Jaksa, M.B. & Maier H.R. 2001: Artificial neural network-based Settlement Prediction Formula for Shallow Foundations on Granular Soils, *Australian Geomechanics*.



Composite landslide in the dynamic alpine conditions: a case study of Urbas landslide

Sestavljeni plaz v dinamičnih alpskih razmerah: primer plazu Urbas

Ela ŠEGINA, Mateja JEMEC AUFLIČ, Matija ZUPAN, Jernej JEŽ & Tina PETERNEL

Geological Survey of Slovenia, Dimičeva ulica 14, SI-1000 Ljubljana, Slovenia; e-mail: ela.segina@geo-zs.si, mateja.jemec@geo-zs.si, matija.zupan@geo-zs.si, jernej.jez@geo-zs.si, tina.peternel@geo-zs.si

Prejeto / Received 27. 5. 2022; Sprejeto / Accepted 12. 10. 2022; Objavljeno na spletu / Published online 12. 12. 2022

Key words: composite landslide, alpine conditions, kinematics, monitoring, sediment discharge

Ključne besede: sestavljeni plaz, alpske razmere, kinematika, monitoring, prehajanje sedimenta

Abstract

The alpine environment is characterized by complex geology, high-energy terrain, deeply incised river valleys with high erosional potential, extreme weather conditions and dynamic geomorphic processes. Such settings provide favourable conditions for the formation of composite landslides rather than individual slope mass movement phenomena. As an example, we present the kinematics of the composite landslide Urbas in the North of Slovenia which developed in the complex geological and morphological settings characteristic of the alpine environment. The research combines several monitoring techniques and involves the integration of both surface and subsurface displacements measured in the landslide area. The results indicate that the composite sliding process consists of several simultaneous and interrelated types of movements occurring in different segments of the unstable mass that are governed by different mechanisms of displacements, such as rockfall, sliding and debris flow. The kinematic characteristics of a deep-seated landslide that formed in such conditions vary spatially, but is rather homogenous vertically, indicating translational type of movement. Spatial kinematic heterogeneity is primarily related to the diverse terrain topography, reflecting in different displacement trends. Based on the revealed kinematic properties of the sliding material, the sediment discharge illustrates the sliding material balance which estimates the volume of the retaining material that represents the potential for slope mass movement events of larger scales.

Izveček

Za alpsko okolje so značilni kompleksna geologija, razčlenjeno površje, globoko vrezane rečne doline z visokim erozijskim potencialom, ekstremne vremenske razmere in dinamični geomorfni procesi. Takšne razmere so, bolj kakor za nastanek posameznih pojavov pobočnih premikov, prikladne za razvoj sestavljenih plazov. Kot primer takšnega pojava predstavljamo primer sestavljenega plazu Urbas, ki se nahaja v severnem delu Slovenije in je nastal v zapletenih geoloških in morfoloških razmerah značilnih za alpsko okolje. V raziskavi združujemo več tehnik spremljanja plazov in povežujemo izmerjene površinske premike in premike na območju drsne ploskve. Rezultati kažejo, da proces sestavljenega plazenja vključuje več medsebojno povezanih tipov premikov, ki se, z različnimi mehanizmi premikanja (podor, plazenje, drobirski tok), istočasno odvijajo v različnih delih premikajoče se gmote. Kinematične značilnosti globokega plazu, ki je nastal v takšnih razmerah, se spreminjajo prostorsko, po globini pa so precej homogene, kar nakazuje na translacijski tip premikanja plazu. Prostorska kinematična heterogenost pa je v prvi vrsti posledica oblikovanosti površja, ki se odraža v različnih hitrostih premikov. Na podlagi ugotovljenih kinematičnih lastnosti plazečega materiala smo s pomočjo računanja prehajanja sedimenta ponazorili bilanco plazeče se mase in ocenili prostornino materiala, ki zastaja na območju plazu in ki predstavlja potencial za pojav pobočnih masnih premikov večjih razsežnosti.

Introduction

The alpine environment is generally characterized by complex geology, high-energy terrain, steep rocky slopes, deeply incised river valleys with high erosional potential, extreme weather conditions and dynamic geomorphic processes. Such conditions are favourable for the formation of slope mass movements of different types and sizes, from large-scale deep-seated rotational and translational slides to shallow landslides, slumps and sediment gravity flows in the form of debris flows or mudflows. Rather than individual slope mass movements, such complex conditions commonly result in the formation of landslides, characterized by several types of movements that act simultaneously in different parts of the sliding mass.

While complex landslides are slope mass movements with a combination of two or more principal types of movement in a sequence (Varnes, 1978), the composite landslides exhibit at least two types of movements simultaneously in different segments of the failing mass (Cruden & Varnes, 1993).

The main challenge in investigating the composite landslides is in capturing the complete landslide area, which may consist of several different geomorphological features and could be driven by different geomorphic processes. For example, steep rocky mountain peaks with rockfall areas in the hinterland of the deep-seated landslide could provide supplementary input material and impact the main sliding process along the sliding surface with an additional load. Also, the sliding material originating from the deep-seated landslide could supply the debris-flow channel. Different processes involved in the composite landslides demand different monitoring techniques that considerably worsen the data comparison. Heterogeneous geomechanical characteristics of the sliding material, common for composite landslides in complex geological conditions, also need to be considered as an important factor. For this reason, landslide body kinematics needs to be analysed in three dimensions, as surface displacements may not adequately represent the displacements occurring at depth.

Landslide kinematics is a common topic in the modern landslide research (Baum et al., 1993; Coe et al., Brückl et al., 2006; Baldi et al., 2008; Mackey et al., 2009; Uzielli et al., 2015; Schlögel et al., 2015b; Gullà et al., 2016; Schulz et al., 2012, 2017; Frattini et al., 2018; Crippa & Agliardi, 2021). Also, several landslides in the alpine environment have already been analysed and presented from

different perspectives (Crosta et al., 2004; Mikoš et al., 2006; Boniello et al., 2010; Barth 2013; Husain et al., 2015; Schlögel et al., 2015a; Viganò et al., 2021; Jemec Auflič et al., 2017; Mikoš 2020, 2021 etc.). Although natural conditions are rather commonly characterized by complex geological and morphological settings, the kinematic or other analysis of composed landslides remains a rare topic in landslide research (Stumvoll et al., 2022).

The contribution of the present paper to the scientific community is to expose the phenomenon of composite land sliding, present the applicable methodological approaches and give an example of the composite landslide kinematics that develops in the complex alpine conditions.

Study area

The composite landslide Urbas is located in the Karawanks mountain ridge in the eastern part of the Alps (Fig. 1) and extends between the elevations of 1150 m at the toe and 1350 m at the crown. The area is under the influence of the alpine climate, characterized by an annual precipitations between 2000 and 2600 mm with the primary precipitation peak in autumn and secondary in the spring, and usually 150–200 days of snow cover per year (Slovenian Environment Agency).

In the last decades, several site investigations and monitoring projects have been carried out in the wider landslide-prone area (Mikoš et al., 2008; Jež et al., 2008; Komac et al., 2014; Oven et al., 2019; Peternel et al., 2018; Janža et al., 2018; Jemec Auflič et al., 2019; Šegina et al., 2020). For a detailed overview of the investigations see Peternel et al. (2022). Several landslide bodies were identified, among which the composite landslide Urbas is the largest phenomenon in the area (Peternel et al., 2018) (Fig. 1). It covers an area of about 1 km². Like some other slope instabilities in the area (Peternel et al., 2018), its occurrence is tightly connected to the complex geological settings of the Karawanks system (Fodor et al., 1998; Jež et al., 2008).

Spatially limited deep-seated sliding formed within the Košuta fault zone in a several hundred meters wide area of soft, tectonically deformed Palaeozoic clastic rocks with low permeability (siltstone and claystone predominate, while sandstone and conglomerate appear in subordinate quantities) that stretches along the Karawanks in the central part of the slope (Fig. 2a). An estimated volume of the deep-seated landslide body is 1.578.700 m³. A sliding surface was determined at the depth of down to 29.9 m (Fig. 2b).

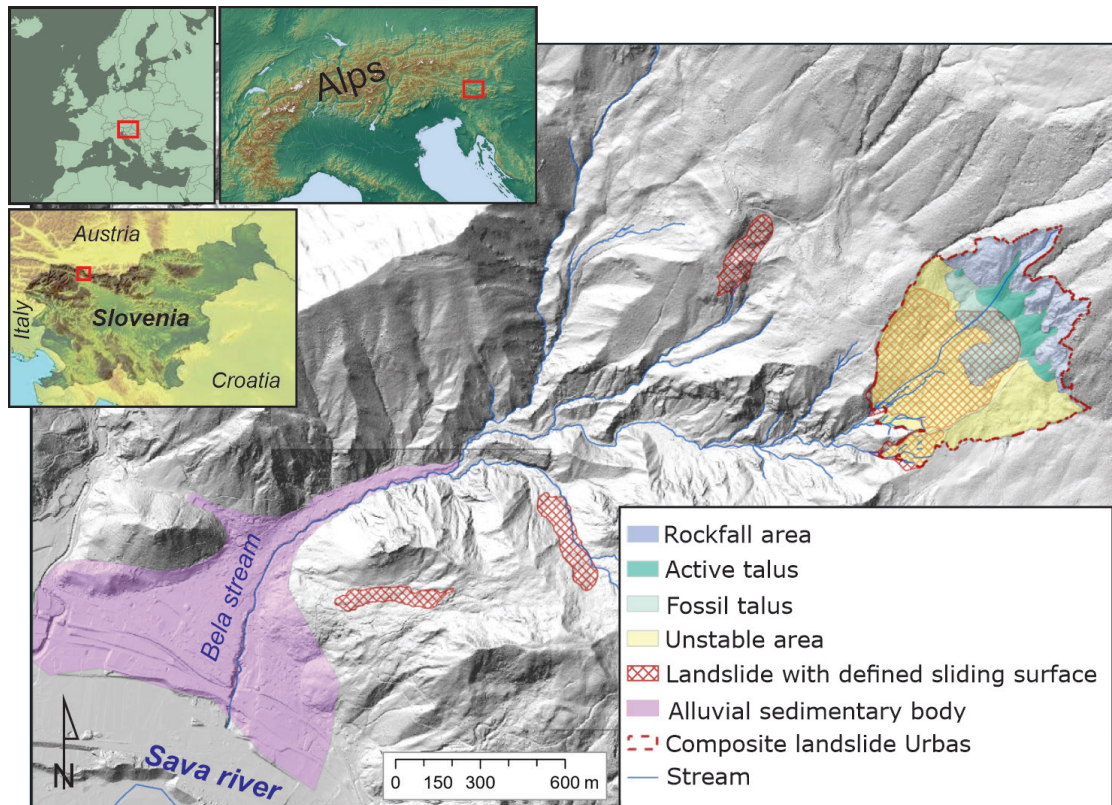


Fig 1. Location and main elements of the composite landslide Urbas.

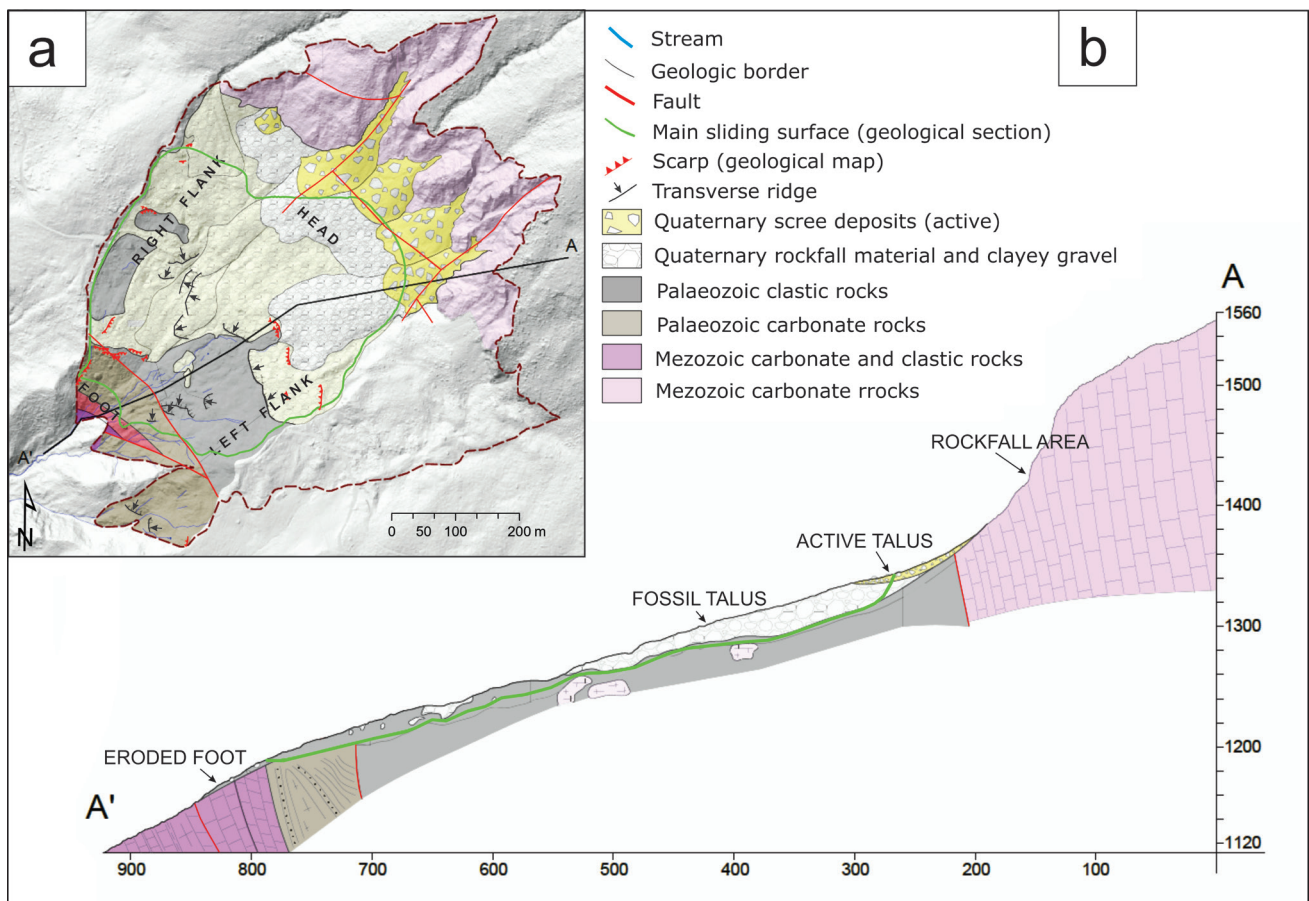


Fig. 2. a – Geological settings of the Urbas landslide, b – Geological section of the Urbas landslide (modified after Šegina et al., 2020). The SKUA-GOCAD software was used to obtain the main sliding surface.

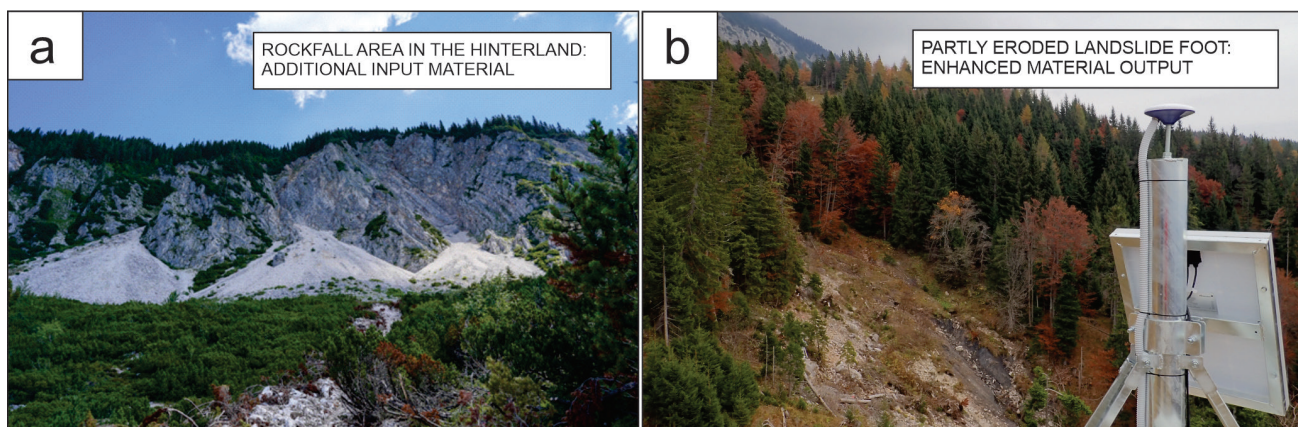


Fig. 3. Field view of specific elements of the composed landslide in the dynamic alpine conditions, an example of Urbas landslide. a – The rockfall input area provides a supplementary sliding material. Past rockfall events that are already vegetated are visible in the front, b – Fluvially eroded landslide foot.

Above the deep-seated landslide body, the area is bounded by the rocky mountain ridge composed of the Triassic and Jurassic limestone. A wide rockfall zone indicates locally tectonized and mechanically weak rocks that with different processes such as rockfalls, rockslides and toppling of boulders, provide a continuous supply of the slope material to the surface of the deep-seated landslide body. The material accumulates under the steep rocky cliffs in a form of several accumulation fans that cover the landslide crown so that the main scarp remains buried underneath, invisible to the naked eye. Traces of inactive, partly vegetated talus cones extending further downslope indicate more intensive rockfall activity in the past (Fig. 3a).

Downslope, the deep-seated landslide body is limited by the geologic contact between weath-

ered clastic and considerably more compact Palaeozoic and Triassic carbonate rocks. There, the two ridges composed of relatively more stable bedrock force the sliding mass accumulating from a 500 m wide area to move through the narrow, 100 m wide debris flow channel (Fig. 3b). The channel was incised by the Bela stream that collects surface waters from the main landslide body characterized by the low permeability of clastic rocks. While the soft clastic rocks are mostly washed out by the Bela stream in a suspension, fragments of different sizes originating from the rockfall zone in the hinterland of the landslide body are gradually, but constantly transported down the Bela stream towards the distant Sava valley. Such topography disables the deposition of a typical landslide foot. Instead, several paleo alluvial sedimentary bodies evidenced in over

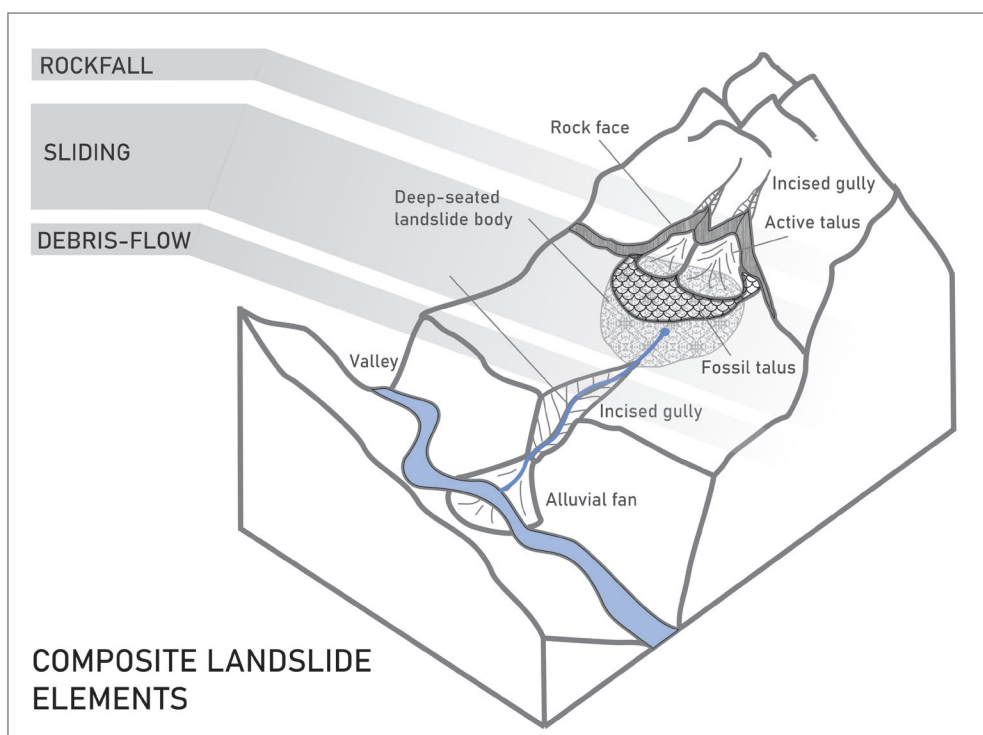


Fig. 4. Composite landslide elements as evidenced in the case study of the Urbas landslide.

2 km distant Sava valley indicate that the material originating from the landslides in the area mobilized into the debris flows during the several massive, instantaneous events (Jež et al., 2008; Jež et al., 2019) (Fig. 1).

Investigations revealed that the Urbas landslide is composite landslide (Cruden & Varnes, 1996) consisting of three elements characterized by different types of movements:

- rockfall area located in the upper part,
- deep-seated landslide defined by the sliding surface, and
- debris-flow source area located in the lower part of the composite landslide (Peternel et al., 2017; Peternel, 2017) (Fig. 4).

For a complete understanding of geomorphological processes operating within the composite landslide, we considered not only the deep-seat-

ed landslide defined by its sliding surface but the entire area of the composite landslide phenomena including an active rockfall zone, main deep-seated landslide body, talus accumulation area, the zone of the debris flow channel and surrounding unstable or potentially unstable areas that exhibit shallow surface displacements visible on the digital elevation model (Fig. 2).

Materials and methods

Monitoring techniques

Inaccessibility, lack of electric power, irregular topography, steep slopes, specific slope aspect, extreme weather conditions, dense vegetation, as well as nature protected areas (Natura 2000 etc.) represent common limitations in monitoring complex environments such as the alpine. Such

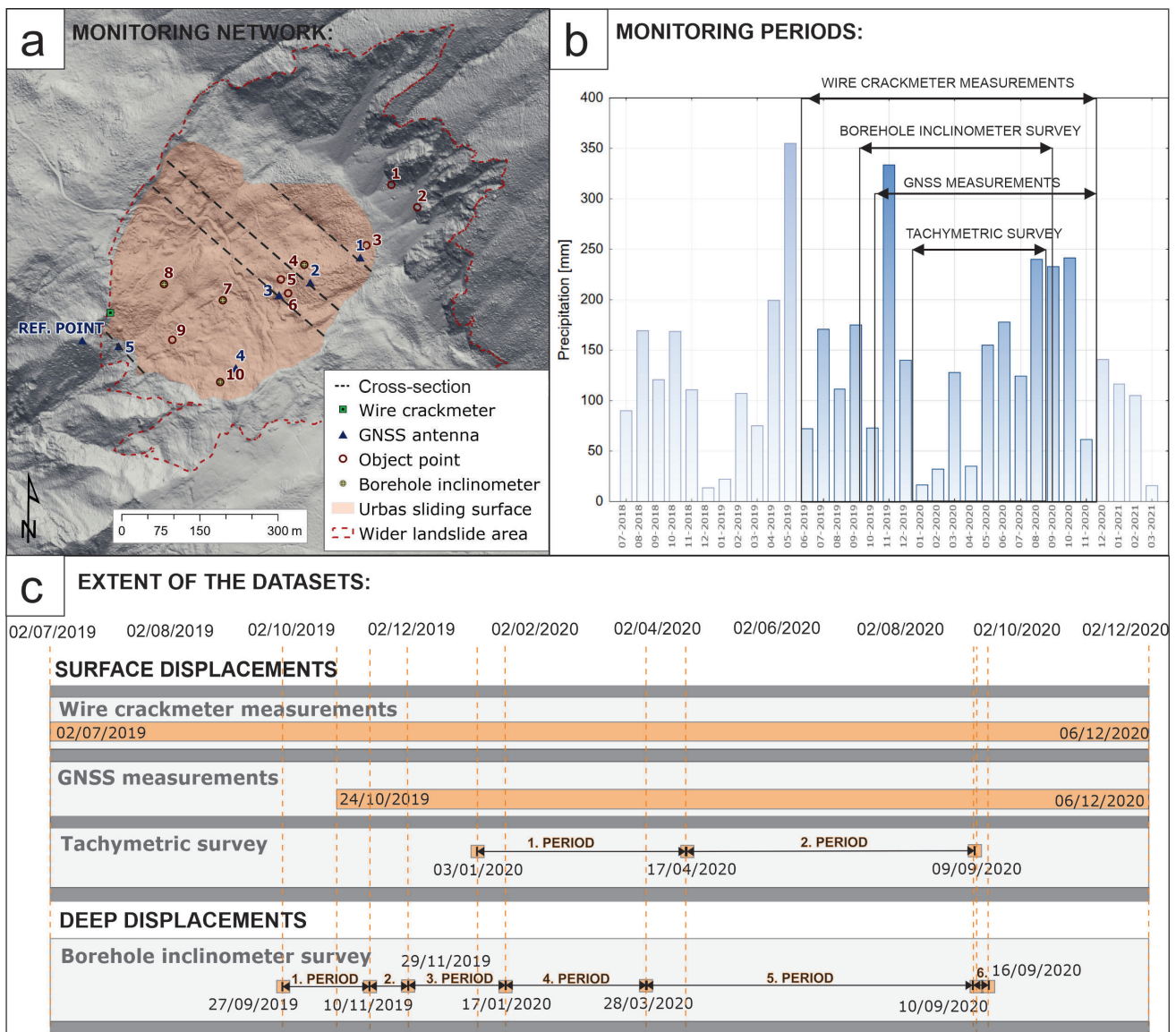


Fig. 5. a – Monitoring network, b – Monthly precipitation values during the monitoring, c – The extent of the integrated datasets.

limitations prevent some monitoring techniques from acquiring satisfactory results, for example, the InSAR. Considering all the constraints, the Urbas landslide was simultaneously monitored with four different monitoring techniques which were considered to deliver the most useful results and were integrated to obtain the complete kinematics of the landslide (Fig. 5a, c). They include two continuous (wire crackmeter and GNSS), and two periodic monitoring techniques (in situ geodetic field campaigns using tachymetric measurements and borehole inclinometer surveys) (Fig. 5a, c).

Wire crackmeter measurements

A wire crackmeter consists of a transducer box which includes the rotary electronic sensor with a wire tensioning device. The target is an eyebolt expansion anchor (Fig. 6a). The wire crackmeter is located at the right flank in the lower part of the Urbas landslide (Fig. 5a). It continuously monitors the opening of the right flank by providing measurements at 15 min intervals. It measures the absolute length of the wire installed across the crack, presuming that the carbonate ridge at the outer side of the scarp is stable. The stability of the ridge was approved by the geological-geomorphological field examination (Peternel et al., 2018). The accuracy of the wire crackmeter measurements is estimated to be 1 mm. The extent of the dataset is 1.5 years (Fig. 5c).

GNSS measurements

GNSS stations monitor the displacements occurring at the surface of the landslide (Fig. 6b). Covering the entire landslide body, the GNSS monitoring network aims to reveal spatial differences in landslide kinematics. GNSS monitoring network consists of 6 GNSS stations, with one representing the local reference point (Fig. 5a). Its stability was determined by computing its position over the whole monitoring period by the absolute positioning (PPP) considering the EU plate motion. Based on this, GNSS position calculation daily provides the coordinates (X, Y and Z) of 5 antennae of interest. Technical specifications of the GNSS monitoring system are presented in Šegina et al. (2020). GNSS method provides continuous data with a daily interval with the accuracy of 1 mm for the horizontal component (X, Y) and 2 mm for the vertical component of the displacement (Z). For the scope of this research, the coordinates displacements were presented as a 3D displacement [mm]. Over a one-year-long dataset was available (Fig. 5c).

Tachymetric surveys using a total station

Tachymetric surveys measured accurate surface displacements. Permanent topographic prisms were installed on the concrete plates that surround the piezometers and inclinometers caps (Fig. 6c). The measurements were taken with the Leica Nova MS50 (angular accuracy 1", distance accuracy 1 mm + 1.5 ppm) and Leica GPH1P

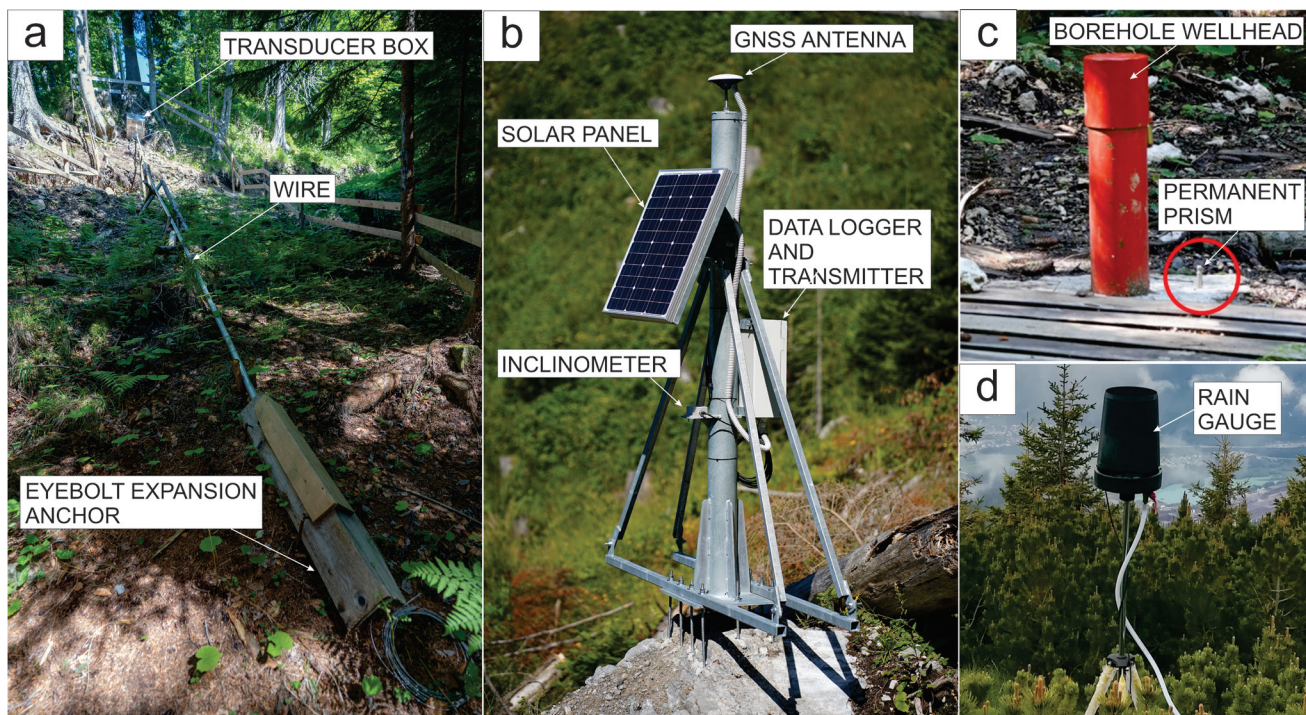


Fig. 6. a – Wire crackmeter, b – GNSS station, c – Location of permanent prisms for a tachymetric survey, d – Rain gauge.

precision prisms (centring accuracy of 0.3 mm). Vertical and horizontal displacements were determined for 8 checkpoints. We established 4 reference points on a supposedly stable terrain (stations 1, 2, 11, and 12 in Fig. 5a). Reference points 11 and 12 are located on the carbonate ridge, which divides the deep-seated landslide body and unstable area on the SE. The displacement were presented as 3D displacements [mm]. Three geodetic field campaigns were carried out in the year 2020 (Fig. 5c).

Borehole inclinometer survey

The borehole inclinometer survey provides unique information on the subsurface landslide displacements down to its sliding surface. A total of four boreholes were drilled and equipped with inclinometer casings with a diameter of 60 mm to define the depth of the sliding surface and to enable monitoring of the displacements of the entire landslide body at various locations. The boreholes were drilled at least 2 m into the stable bedrock to ensure reliable measurements. The measurements were performed down to 34.5 m (Inclinometer 4), 23.5 m (Inclinometer 7), 27.5 m (Inclinometer 8) and 27 m (Inclinometer 10). The horizontal displacements was derived from the tilt of the probe that is measured bottom-up in the borehole with a uniaxial technique and at an interval of 0.5 m. When the probe was unable to pass through the casing, measurements of the absolute shear displacement became impossible (marked with “sheared”). Periodic inclinometer surveys in the boreholes started in September 2019. Seven consecutive borehole inclinometer field measurements were carried out during the years 2019 and 2020 (Fig. 5c).

Precipitation measurements

Rain gauge provides a continuous dataset on the amount of the precipitations with an hourly interval and an accuracy of 0.2 mm. It is located in the central part of the composite landslide area (Fig. 5a and Fig. 6d).

Monitoring data integration

First, we analysed surface and subsurface displacements separately. Subsurface displacements were acquired only with a borehole inclinometer survey. Surface displacements were monitored by three different techniques that were integrated to provide information on the spatial kinematic characteristics of the landslide surface. We integrated two continuous datasets, namely GNSS and wire crackmeter data, with the periodic

tachymetric measurements. The integration of continuous and periodic measurements includes the following steps: i) definition of the periods when periodic measurements were acquired, ii) selection of the same periods in the continuous datasets, iii) calculation of absolute displacement that occurred within the defined periods for both datasets and iv) correlation and analysis of the data.

In the next step, we integrated surface and subsurface displacements to analyse landslide kinematic characteristics with depth. We considered surface displacements acquired with a tachymetric survey, wire crackmeter and GNSS methods and subsurface displacements acquired by inclinometer surveys. The integration was carried out following the presented integration method. The displacements data are presented as absolute measured values [mm]. In some cases, the results are presented as average monthly rate [mm/month] to enable the comparison of data in monitoring periods of different duration.

Sediment discharge

Sediment discharge as an indicator of sliding material balance (Guerriero et al., 2017; Mackey et al., 2009) was employed to analyse the interrelationship between the three different elements of the composite landslide. It reveals the potential retention of the material in the area of the deep-seated landslide. The Urbas landslide body is considerably narrowing from the landslide head to the landslide foot due to relatively more stable bedrock that limits the sliding surface from the sides. 500 m wide landslide's head reduces to around 100 m wide valley at the landslide foot (Fig. 2a). To reveal the effect of a decreasing landslide cross-section on the displacement rate of the sliding material, we observed the total volume of the displaced material that moved through the sectors of the landslide. Based on the defined sliding surface (Fig. 2b) and the available digital terrain model with 1 m resolution (Slovenian Environmental Agency), we extracted the cross-sections across the landslide at the locations of four GNSS monitoring points (GNSS 1, 2, 3 and 5) that are rather evenly distributed along the profile of the landslide (Fig. 5a).

We calculated the difference between the volume of the material that entered and the volume of the material that left the particular sector (sectors are shown in Fig. 11) between the adjacent GNSS points during the entire GNSS monitoring period (24/10/2019–06/12/2020), assuming that on the cross-section, the landslide moves perpendicular

to it and with same rate as measured with the GNSS method:

$$\Delta V = (A_2 \times d_2) - (A_1 \times d_1) \quad (1)$$

A_1 = area of the upper cross-section [m^2]

A_2 = area of the lower cross-section [m^2]

d_1 = measured displacement at the upper cross-section [m]

d_2 = measured displacement at the lower cross-section [m]

Results and discussion

Surface displacements

Surface displacements were analysed during the period between 03/01/2020–09/09/2020 (251 days). They combined the data acquired with GNSS stations, wire crackmeter and tachymetric surveys (Table 1). To align with tachymetric field campaigns, we isolated two periods, namely the first between 03/01/2020–17/04/2020 (106 days) and the second between 17/04/2020–09/09/2020 (145 days) (Table 1).

Object points 1 and 2 are located on the bedrock that is considered stable. The surface morphology indicates that the left flank of the landslide is not entirely stable, but during the monitoring period, the displacement was small (18.71 mm) (Object point 10), or even under the detectability of the method (GNSS 4). Small displacements were also detected by the wire crackmeter at the right flank of the landslide (23.91 mm). Medium displacements occurred at the landslide head (36.17–46.69 mm) (Object points 3–6 and GNSS 1–3). Similar displacements were observed at Object point 8. Higher activity was observed at the central part of the landslide (Object points 7 and GNSS 5). During the monitoring period, this part moved for approximately 150 mm.

Figure 7a shows a spatial distribution of surface displacements. The most complete dataset shows the displacements measured during the second monitoring period. It visualizes spatial heterogeneity in the kinematics of landslide surface material. At the surface, the central part of the landslide moves considerably faster than on the edges and at the head of the landslide.

Table 1. Measured displacements of the surface material.

PERIOD	03/01/2020 17/04/2020	18/04/2020 09/09/2020	03/01/2020 09/09/2020
DURATION [number of days]	106	146	252
SURFACE DISPLACEMENT [mm]	DISPLACEMENT IN PERIOD 1 [mm]	DISPLACEMENT IN PERIOD 2 [mm]	CUMULATIVE DISPLACEMENT [mm]
Object point 1	0.00	0.00	0.00
Object point 2	0.00	0.00	0.00
Object point 3	15.58	21.51	37.09
Object point 4	19.66	24.42	44.08
Object point 5	21.24	25.45	46.69
Object point 6	17.06	23.86	40.91
Object point 7	69.35	86.17	155.52
Object point 8	19.88	27.52	47.40
Object point 9		73.23	
Object point 10	13.93	4.79	18.71
GNSS 1	13.90	25.82	39.52
GNSS 2	16.29	27.77	43.90
GNSS 3	13.20	23.09	36.17
GNSS 4	under detectability	under detectability	under detectability
GNSS 5	47.96	97.66	145.58
Reference point	0.00	0.00	0.00
Wire crackmeter	9.54	14.37	23.91

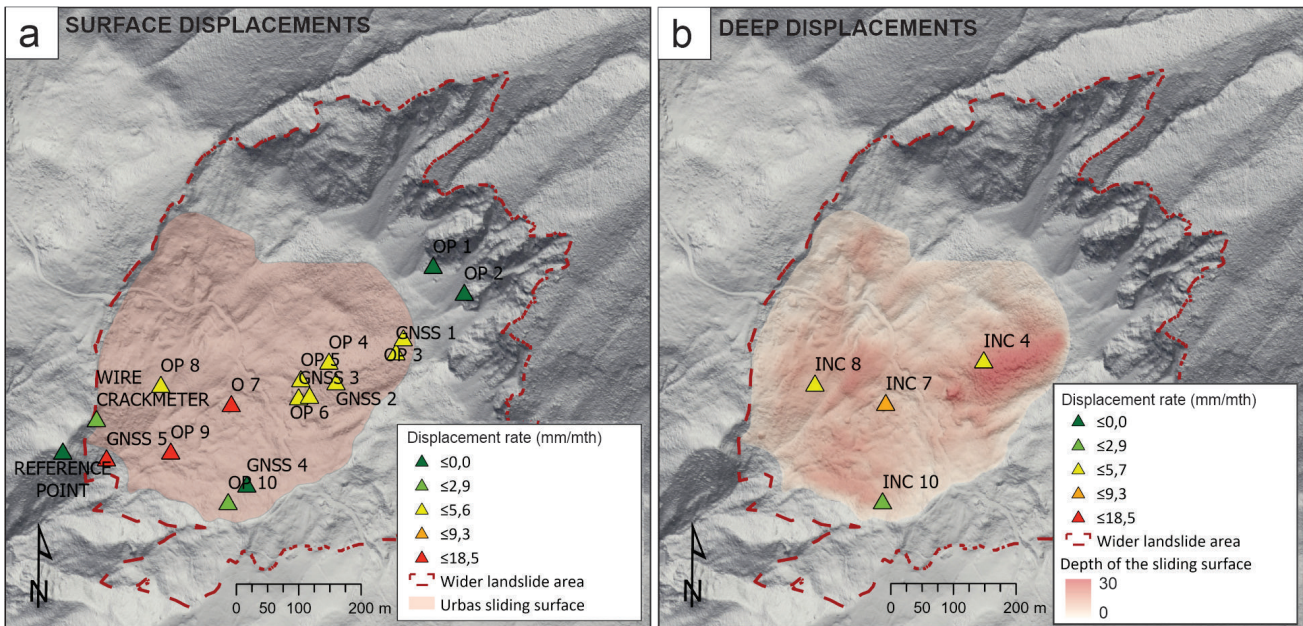


Fig. 7. a – Surface displacement rate measured in the second monitoring period. b – Subsurface displacement rate at the sliding surface and the depth of the sliding surface. Scales are comparable.

Subsurface displacements

The borehole inclinometer survey indicates a variable depth of the sliding surface of the deep-seated landslide body. It occurs down to the depth of 20 m in the central part and at the head of the landslide, at 11.5 m at the right and 3.5 m at the left flank of the landslide. Based on other borehole drillings and geophysical surveys carried out during the investigation of the Urbas landslide, the sliding surface is the deepest at the head of the landslide due to thick deposits of the slope talus, followed by the central part of the landslide (Fig. 7b).

Subsurface displacements were measured in four boreholes during the period between 27/09/2019-16/09/2020 (356 days) (Fig. 5c). Seven borehole inclinometer surveys were carried out during this time. They defined six monitoring periods (Table 2, Table 3). We present results of displacements measured at the depth of 1 and 10 m,

respectively. At the depth of 20 m, no displacement occurred in any borehole.

The same spatial heterogeneity of the displacement trends detected at the surface was observed also in the depth of the landslide body (Fig. 7a, b). Generally, similar spatial relationships were observed: the largest subsurface displacement was measured in the central part, medium in the head and minimal at the left flank of the landslide area (Table 2, Table 3, Fig. 7b).

Vertically, the observed displacements indicate various types of movements in different parts of the deep-seated landslide body. Some parts move as a compact sliding mass while some developed several sliding surfaces or exhibit a gradual vertical change in sliding velocity. Such behaviour is related to the geomechanical characteristics of the sliding material and the topography of the sliding surface. At the head of the landslide (Inclinometer 4) and at the right flank

Table 2. Measured displacements at the depth of 1 m.

PERIOD	27/09/2019 10/11/2019	11/11/2019 29/11/2019	30/11/2019 17/01/2020	18/01/2020 28/03/2020	29/03/2020 10/09/2020	11/09/2020 16/09/2020	27/09/2019 16/09/2020
DURATION [number of days]	45	19	49	72	167	6	356
SUBSURFACE DISPLACEMENTS (at -1 m) [mm]	PERIOD 1 [mm]	PERIOD 2 [mm]	PERIOD 3 [mm]	PERIOD 4 [mm]	PERIOD 5 [mm]	PERIOD 6 [mm]	CUM. DISPL. [mm]
Inclinometer 4		15.3		10.3	26.4		52.0
Inclinometer 7			47.8	9.3 sheared			57.1
Inclinometer 8	7.6	1.9	11.0	14.0	24.9		59.4
Inclinometer 10		2.6		0.0	0.6		3.2

Table 3. Measured displacements at the depth of 10 m.

PERIOD	27/09/2019 10/11/2019	11/11/2019 29/11/2019	30/11/2019 17/01/2020	18/01/2020 28/03/2020	29/03/2020 10/09/2020	11/09/2020 16/09/2020	27/09/2019 16/09/2020
DURATION [number of days]	45	19	49	72	167	6	356
SUBSURFACE DISPLACEMENTS (at -10 m) [mm]	PERIOD 1 [mm]	PERIOD 2 [mm]	PERIOD 3 [mm]	PERIOD 4 [mm]	PERIOD 5 [mm]	PERIOD 6 [mm]	CUM. DISPL. [mm]
Inclinometer 4		16.6		11.3	25.8		53.7
Inclinometer 7			0.00*	sheared			
Inclinometer 8	7.6	2.4	10.7	13.0	24.8		58.5
Inclinometer 10		0.0		0.6	0.2		0.8

* The displacement is not captured because the sliding surface occurs at 9 m.

(Inclinometer 8), the landslide body moved rather homogeneously from the sliding surface up to the topographical surface as a thick layer of gravel (or clayey gravel) slides on tectonically weakened mudstone (Fig. 8). On the opposite, the left flank of the landslide moved heterogeneously, forming two sliding surfaces at 4 and 11.5 m depth respectively (Inclinometer 10) (Fig. 8). The displacements recorded shallower with respect to the sliding surface at -3 m are of anthropogenous nature. The landslide body moved heterogeneously in the central part as well (Inclinometer 7). In this sector, the rate of displacement with depth gradually decreases due to heterogeneity of the sliding material and irregular basement morphology that cause the material to slow down (Fig. 8). In the 2. period, the inclinometer

was sheared due to active sliding processes and further displacement monitoring was impossible (see Table 3). The nature of displacements along the landslide profiles as indicated by the inclinometer measurements indicates translational type of landslide movement.

The interaction of surface and subsurface displacements

We integrated surface displacements acquired with a tachymetric survey at inclinometers caps and subsurface displacements derived from inclinometer measurements. We compared the 1. period of a tachymetric survey (03/01/2020-17/04/2020) with the 4. period of borehole inclinometer survey (17/01/2020-28/03/2020) (common

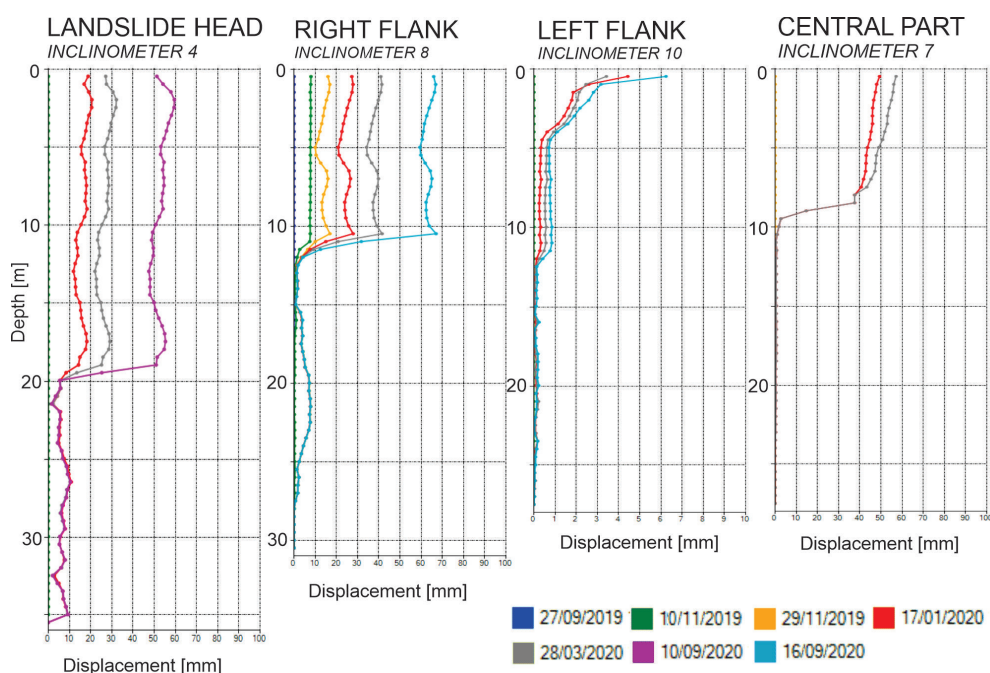


Fig. 8. The characteristics of subsurface displacement: A – at the landslide head (Inclinometer 4), B – at the right flank of the landslide (Inclinometer 8), C – at the left flank of the landslide (Inclinometer 10) and D – in the central part of the landslide (Inclinometer 7).

period 1) and the 2. period of the tachymetric survey (17/04/2020-09/09/2020) with the 5. period of the borehole inclinometer survey (28/03/2020-10/09/2020) (common period 2) (see Fig. 5c). The discrepancy of surface displacements obtained by tachymetric survey in comparison to 1 m and 10 m deep displacements obtained by inclinometer measurements are presumed to be related

to a weak temporal overlapping of the observed periods (common period 1: 34 days longer observation period for tachymetric measurements; common period 2: 21 days longer observation for inclinometer measurements) (Fig. 9). Considering this, the surface and deep displacements seem to be relatively homogeneous and the landslide movement can be considered as translational.

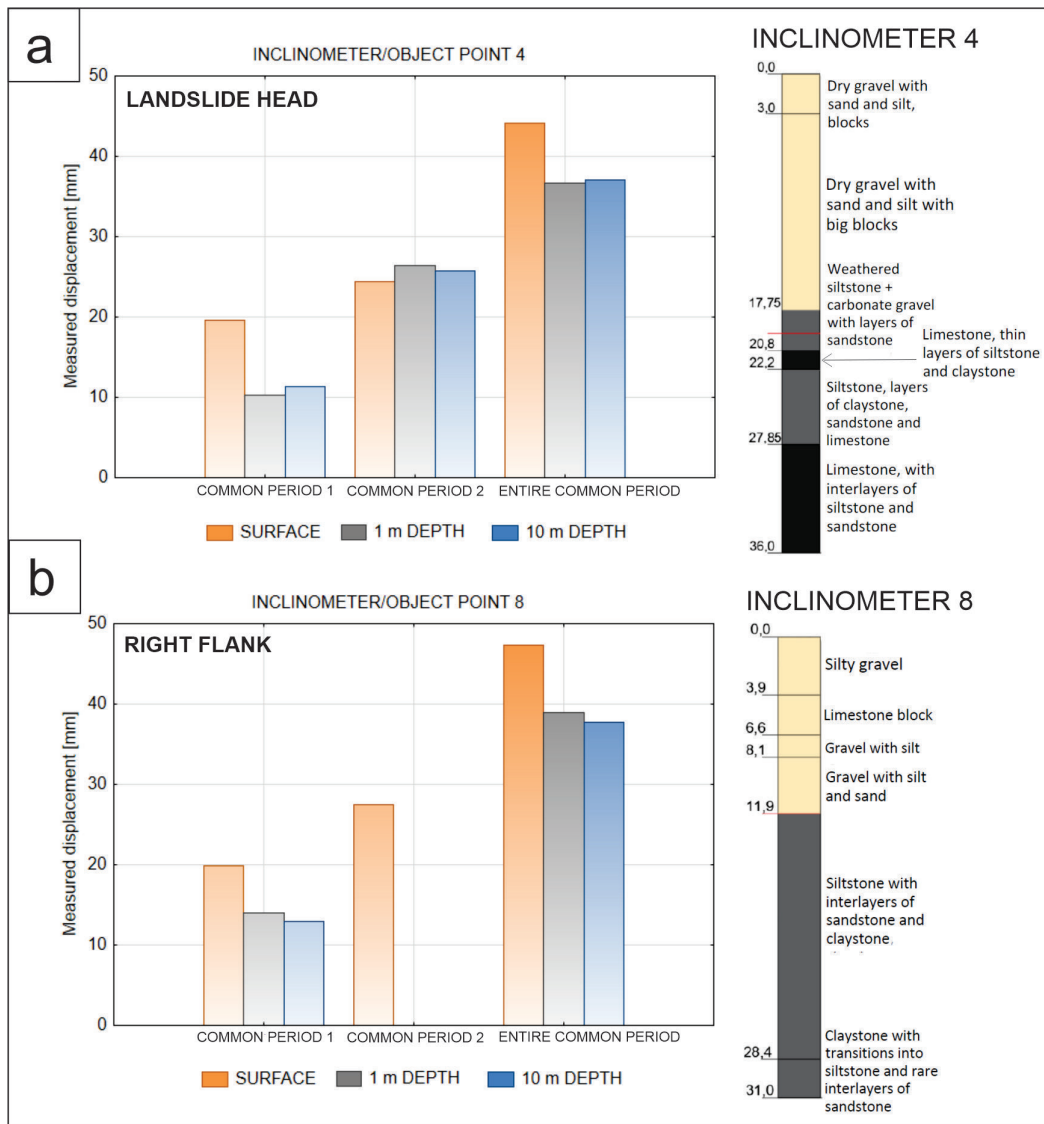


Fig. 9. Combined data on surface and subsurface displacements at the Inclinerometers / Object points 4 and 8.

Table 4. Sliding material balance. Sectors are shown in Figure 5 and Figure 10.

SECTOR	Area of cross-section - IN [m ²]	Measured displacement - IN [m]	Area of cross-section - OUT [m ²]	Measured displacement - OUT [m]	V of displaced material - IN [m ³]	V of displaced material - OUT [m ³]	ΔV [m ³]
UPPER	2417	0.072	4273	0.079	174	338	-164
MIDDLE	4273	0.079	3862	0.069	338	267	71
LOWER	3826	0.069	119	0.570	267	68	199

Sliding material balance

Referring to the vertical kinematic homogeneity, surface displacements obtained by the GNSS method were considered in the calculation of the sliding material balance.

Calculation showed that 164 m^3 more material left the upper sector than entered it (Fig. 10). Several explanations are possible: i) we underestimated the extent of the sliding surface in the upper (northern) part of the landslide, ii) the upper part of the landslide is emptying (no morphological signs visible to confirm this option), iii) the upper part of the landslide moves irregularly in time so that the complete kinematic characteristics of the sliding was not captured. Based on the data from the GNSS station recently located in the northern part of the landslide, the sliding surface must have been underestimated in this area.

In the middle and lower sectors, 71 and 199 m^3 less material left the areas than entered them respectively, indicating the minor retention of the material in both sectors. The amounts of the retained material are relatively small, but only over a year-long monitoring period has been considered.

Bottom line, 270 m^3 of the sliding material retained in the middle and lower sectors of the landslide. More reasonably, monitoring at the landslide foot does not entirely capture the displacement of the output material, as soft rocks are washed out in a suspension and unconsolidated scree material of small dimensions probably moves faster than fragments of a size of a boulder on which GNSS 5 is installed. Thus, the actual volume that retained on the landslide is presumably considerably smaller than calculated. Also, the calculations consider rather a short monitoring period (one year and 2 months) which

might not be enough to reveal the complete sliding material balance.

Kinematics of the composite landslide Urbas

A deep-seated landslide body moves rather homogeneously, indicating the translational type of the landslide movement. Current data suggest that the displacement at the sliding surface is induced by the scree accumulation which poses an additional load on the uppermost part of the deep-seated landslide body. However, an additional hydrological analysis will give a clearer insight into the triggering factors of the displacement mechanisms in the head of the deep-seated landslide.

Sediment discharge indicates no substantial accumulation of the material in the area of the landslide. At present conditions, the composite landslide Urbas is a rather balanced geomorphic system, where the supplementary input of the material from the rockfall zone is rather successfully compensated with the enhanced erosion of the material in the debris-flow channel at the landslide foot. The increased displacement rate evidenced in the area of eroded landslide foot mainly reflects the topographical narrowing of the space available for the transport of the material through the debris-flow channel rather than increased activity of the sliding in this part. The localised erosion in this part of the composite landslide is particularly effective due to the low permeability of the bedrock in the main landslide body that provides temporary and permanent streams. However, the evidence of past events indicates that, in particular weather conditions, the occasional extreme debris-flow events are capable of reaching the bottom of the valley (Jež et al., 2008).

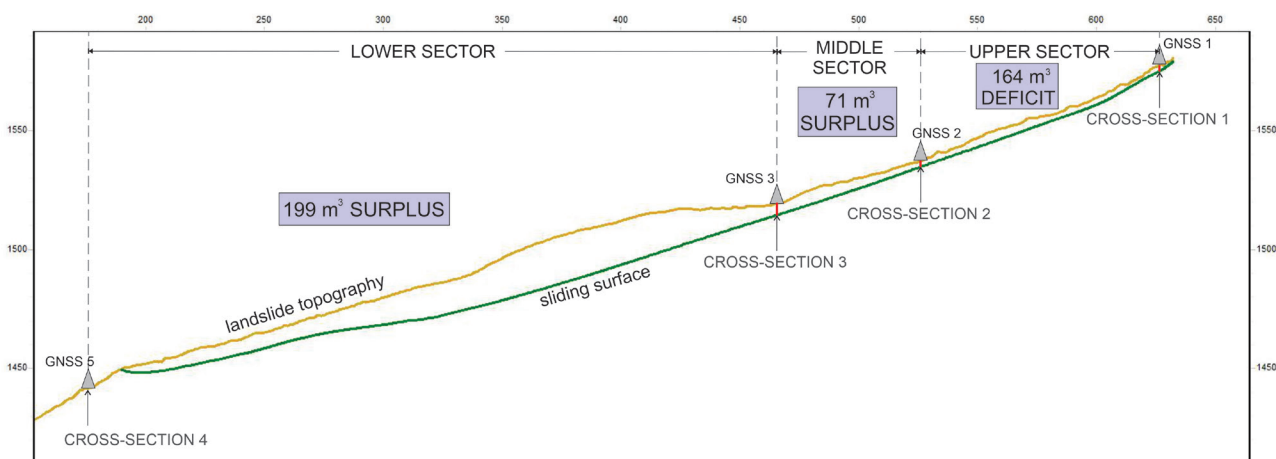


Fig. 10. Sliding material balance along the longitudinal profile of the landslide. The SKUA-GOCAD software was used to obtain the main sliding surface.

Conclusions

Due to complex geology and terrain topography, the alpine areas are common environments for landslide formation. This research shows that rather than simple sliding, specific environmental settings induce the formation of composite landslides characterized by several simultaneous and interacting types of movements. Understanding such landslide kinematics requires a comprehensive approach including the following elements:

- the definition of the complete landslide area that includes, together with the landslide body defined by its sliding surface, also the potential material supply and erosion zones,
- extended monitoring network capable of capturing the spatial differences of the displacement trends,
- consideration of both surface and subsurface displacements,
- consideration of the dynamic sliding system: a constant supply of the additional material from the rockfall areas in the hinterland, representing continuous additional material input, and erosion of the landslide's foot, representing enhanced material output,
- influence of complex geology and topography characteristic for compressional orogens, on landslide kinematics
- estimation of the sliding material balance based on the sediment discharge which considers the topographic aspect of the sliding surface and estimates the potential retention of the material on the landslide area that may represent the potential risk for the occurrence of mass movement events of larger scales.

Acknowledgements

The research was funded by the Slovenian Research Agency (Research Program P1-0419, J1-8153 project; Z1-2638 project, Research Project J1-3024), the Ministry of Environment and Spatial Planning, and the Municipality of Jesenice. We also thank the GIMS project (the European GNSS Agency under the European Union's Horizon 2020 research and innovation programme under grant agreement No. 776335).

References

- Baldi, P., Cenni, N., Fabris, M. & Zanutta, A. 2008: Kinematics of a landslide derived from archival photogrammetry and GPS data. *Geomorphology*, 102:435-444. <https://doi.org/doi.org/10.1016/j.geomorph.2008.04.027>
- Barth, N. 2013: The Cascade rock avalanche: Implications of a very large Alpine Fault-triggered failure, New Zealand. *Landslides*, 11. <https://doi.org/10.1007/s10346-013-0389-1>
- Baum, R.L., Fleming, R.W. & Johnson, A.M. 1993: Kinematics of the Aspen Grove landslide, Ephraim Canyon, Central Utah. *U.S. Geological Survey Bulletin*, 1842-F.
- Boniello, M. A., Calligaris, C., Lapasin, R. & Zini, L. 2010: Rheological investigation and simulation of a debris-flow event in the Fella watershed. *Nat. hazards earth syst. sci.*, 10/5: 989-997. <https://doi.org/10.5194/nhess-10-989-2010>
- Brückl, E., Brunner, F.K. & Kraus, K. 2006: Kinematics of a deep-seated landslide derived from photogrammetric, GPS and geophysical data. *Eng. Geol.*, 88: 149-159. <https://doi.org/10.1016/j.enggeo.2006.09.004>
- Coe, J.A., Ellis, W.L., Godt, J.W., Savage, W.Z., Savage, J.E., Michael, J.A., Kibler, J.D., Powers, P.S., Lidke, D.J. & Debray, S. 2003: Seasonal movement of the Slumgullion landslide determined from Global Positioning System surveys and field instrumentation, July 1998-March 2002. *Eng. Geol.*, 68: 67-101. [https://doi.org/10.1016/S0013-7952\(02\)00199-0](https://doi.org/10.1016/S0013-7952(02)00199-0)
- Crippa, C. & Agliardi, F. 2021: Practical Estimation of Landslide Kinematics Using PSI Data. *Geosciences*, 11/ 214. <https://doi.org/10.3390/geosciences11050214>
- Crosta, G., Chen, H. & Lee, C. F. 2004: Replay of the 1987 Val Pola Landslide, Italian Alps. *Geomorphology*, 60: 127-146. <https://doi.org/10.1016/j.geomorph.2003.07.015>
- Cruden, D. & Varnes, D. 1996: Landslides: investigation and mitigation. Chapter 3 - Landslide types and processes. *Transportation Research Board Special Report, National Agency of Sciences, Special Report*, 247: 36-75.
- Fodor L., Jelen M., Márton E., Skaberne D., Čar J. & Vrabec, M. 1998: Miocene-Pliocene tectonic evolution of the Periadriatic line in Slovenia – implications for Alpine-Carpathian extrusion models. *Tectonics* 17: 690-709.
- Frattini, P., Crosta, G.B., Rossini, M. & Allievi, J. 2018: Activity and kinematic behaviour of deep-seated landslides from PS-InSAR displacement rate measurements. *Landslides*, 15:1053-1070. <https://doi.org/10.1007/s10346-017-0940-6>
- Giordan, D., Allasia, P., Manconi, A., Baldo, M., Satangelo, M., Cardinali, M., Corazza,

- A., Albanese, V., Lollino, G. & Guzzetti, F. 2013: Morphological and kinematic evolution of a large earthflow: the Montaguto landslide, southern Italy. *Geomorphology*, 187: 61–79. <https://doi.org/10.1016/j.geomorph.2012.12.035>
- Gullà, G., Peduto, D., Borrelli, L., Antronico, L. & Fornaro, G. 2016: Geometric and kinematic characterization of landslides affecting urban areas: the Lungro case study (Calabria, Southern Italy). *Landslides*, 14. <https://doi.org/10.1007/s10346-015-0676-0>
- Guerriero, L., Coe, J. A., Revellino, P., Grelle, G., Pinto, F. & Guadagno, F.M. 2014: Influence of slip-surface geometry on earth-flow deformation, Montaguto earth flow, southern Italy. *Geomorphology*, 219: 285–305. <https://doi.org/10.1016/j.geomorph.2014.04.039>
- Handwerker, A.L., Roering, J.J., Schmidt, D.A. & Rempel, A.W. 2015: Kinematics of earthflows in the Northern California Coast Ranges using satellite interferometry. *Geomorphology*, 246: 321–333. <https://doi.org/10.1016/j.geomorph.2015.06.003>
- Hussin, H.Y., Ciurean, R., Frigerio, S., Marcato, G., Calligaris, C., Reichenbach, P., Van Westen, C.J. & Glade, T. 2015: Assessing the effect of mitigation measures on landslide hazard using 2D numerical runout modeling. *Landslide Science for a safer geoenvironment*, 2: 679–684.
- Janža, M., Serianz, L., Šram, D. & Klasinc, M. 2018: Hydrogeological Investigation of Landslides Urbas and Čikla Above the Settlement of Koroška Bela. *Geologija*, 61/2:191–203. <https://doi.org/10.5474/geologija.2018.013>
- Jemec Auflič, M., Jež, J., Popit, T., Košir, A., Maček, M., Logar, J., Petkovšek, A., Mikoš M., Calligaris, C., Boccali, C., Zini, L., Reitner, J. & Verbovšek, T. 2017: The variety of landslide forms in Slovenia and its immediate NW surroundings. *Landslides*, 14. <https://doi.org/10.1007/s10346-017-0848-1>
- Jež, J., Mikoš, M., Trajanova, M., Kumelj, Š., Budkovič, T. & Bavec, M. 2008: Vršaj Koroška Bela - rezultat katastrofičnih pobočnih dogodkov = Koroška Bela alluvial fan - the result of the catastrophic slope events (Karavanke Mountains, NW Slovenia). *Geologija*, 51/2: 219–227. <https://doi.org/10.5474/geologija.2008.022>
- Jež, J., Peternel, T., Milanič, B., Markelj, A., Novak, M., Celarc, B., Janža, M. & Jemec Auflič, M. 2019: Čikla landslide in Karavanke Mts. (NW Slovenia). In: Uljarevič, M., Zekan, S. Salković, S. & Ibrahimović, D. (eds.): *Proceedings of the 4th Regional Symposium on Landslides in the Adriatic - Balkan Region*. 23–25 October 2019, Sarajevo: Geotechnical Society of Bosnia and Herzegovina: 239–242.
- Komac, M., Holley, R., Mahapatra, P., Van Der Marel, H. & Bavec, M. 2014: Coupling of GPS/GNSS and Radar Interferometric Data for a 3D Surface Displacement Monitoring of Landslides. *Landslides*, 12: 241–257. <https://doi.org/10.1007/s10346-014-0482-0>
- Mackey, B. & Roering, J. 2009: Long-term kinematics and sediment flux of an active earthflow, Eel River, California. *Geology*, 37: 803–806. <https://doi.org/10.1130/G30136A.1>
- Mikoš, M., Bavec, M., Budkovič, T., Durjava, D., Hribernik, K., Jež, J., Klabus, A., Komac, M., Krivic, M., Kumelj, Š., Maček, M., Mahne, M., Novak, M., Otrin, J., Petje, U., Petkovšek, A., Ribičič, M., Sodnik, J., Šinigoj, J. & Trajanova, M. 2008: Ocena ogroženosti zaradi delovanja drobirskih tokov: končno poročilo: (ciljni raziskovalni projekt: znanje za varnost in mir 2006–2010). Fakulteta za gradbeništvo in geodezijo in Geološki zavod Slovenije, Ljubljana: 224 p.
- Mikoš, M. 2020: After 2000 Stože landslide: part I - development in landslide research in Slovenia. *Acta hydrotechnical*, 33/59: 129–153. <https://doi.org/10.15292/acta.hydro.2020.09>
- Mikoš, M. 2021: After 2000 Stože landslide: part II - development of landslide disaster risk reduction policy in Slovenia. *Acta hydrotechnical*, 34/60: 39–59. <https://doi.org/10.15292/acta.hydro.2021.04>
- Mikoš, M., Brilly, M., Fazarinc, R. & Ribičič, M. 2006: Strug landslide in W Slovenia: A complex multi-process phenomenon. *Engineering Geology*, 83/1–3: 22–35. <https://doi.org/10.1016/j.enggeo.2005.06.037>
- Oven, D., Levanič, T., Jež, J. & Kobal, M. 2019: Reconstruction of landslide activity using dendrogeomorphological analysis in the Karavanke mountains in NW Slovenia. *Forests*, 10/11: article 1009. <https://doi.org/10.3390/f10111009>
- Peternel, T., Jež, J., Milanič, B., Markelj, A. & Auflič, M.J. 2018: Engineering-Geological Conditions of Landslides Above the Settlement of Koroška Bela. *Geologija*, 61/2:177–189. <https://doi.org/10.5474/geologija.2018.012>
- Peternel, T. 2017: Dinamika pobočnih masnih premikov na območju Potoške planine z uporabo rezultatov daljinskih in terestričnih geodetskih opazovanj ter in-situ meritev.

- Dissertation. Univerza v Ljubljani, Ljubljana: 183 p.
- Peternel, T., Jež, J., Milanič, B., Markelj, A., Jemec Auflič, M., Kumelj, Š., Celarc, B., Novak, M., Janža, M. & Šram, D. 2017: Izvedba najnужnejših inženirskogeoloških, hidrogeoloških, geofizikalnih in geomehanskih ter geodetskih raziskav za ugotovitev objektivne stopnje tveganja za prebivalstvo zaradi masnih premikov na območju Potoške planine in izdelava strokovnih podlag s predlogi zaščitnih ukrepov. Geološki zavod Slovenije.
- Peternel, T., Šegina, E., Jež, J., Jemec Auflič, M., Janža, M., Logar, J., Mikoš, M. & Bavec, M. 2022: Review of research and evolution of landslides in the hinterland of Koroška Bela settlement in NW Slovenia. *Geologija*, 62/2: 129–147. <https://doi.org/10.5474/geologija.2022.008>
- Schlögel, R., Malet, J.P., Remaître, A., Reichenbach, P. & Doubre, C. 2015a: Analysis of a landslide multi-date inventory in a complex mountain landscape: The Ubaye valley case study. *Natural Hazards and Earth System Sciences Discussions*, 3: 2051–2098. <https://doi.org/10.5194/nhessd-3-2051-2015>
- Schlögel, R., Malet, J.P., Doubre, C. & Lebourg, T. 2015b: Structural control on the kinematics of the deep-seated La Clapière landslide revealed by L-band InSAR observations. *Landslides*, 13. <https://doi.org/10.1007/s10346-015-0623-0>
- Schulz, W.H., Coe, J.A., Shurtleff, B.L., Panosky, J., Farina, P., Ricci, P.P. & Barsacchi, G. 2012: Kinematics of the Slumgullion landslide revealed by ground-based InSAR surveys. In: Eberhardt, E., Froese, C., Turner, A.K. & Leroueil, S. (eds.): *Landslides and Engineered Slopes, Protecting Society Through Improved Understanding*. 2. Taylor & Francis Group, London, 1273–1279.
- Schulz, W. H., Coe, J. A., Ricci, P. P., Smoczyk, G. M., Shurtleff, B. L. & Panosky, J. 2017: Landslide kinematics and their potential controls from hourly to decadal timescales: Insights from integrating ground-based InSAR measurements with structural maps and long-term monitoring data. *Geomorphology*, 285: 121–136. <https://doi.org/10.1016/j.geomorph.2017.02.011>
- Šegina, E., Peternel, T., Urbančič, T., Realini, E., Zupan, M., Jež, J., Caldera, S., Gatti, A., Tagliaferro, G., Consoli, A., González, J. & Jemec Auflič, M. 2020: Monitoring Surface Displacement of a Deep-Seated Landslide by a Low-Cost and near Real-Time GNSS System. *Remote Sensing*, 12/20: 3375. <https://doi.org/10.3390/rs12203375>
- Uzielli, M., Catani, F., Tofani, V. & Casagli, N. 2015: Risk analysis for the Ancona landslide - I: characterization of landslide kinematics. *Landslides* 12: 69–82. <https://doi.org/10.1007/s10346-014-0474-0>
- Varnes, D. 1978: Slope movement types and processes. Transportation Research Board Special Report.
- Viganò, A., Rossato, S., Martin, S., Ivy-Ochs, S., Zampieri, D., Rigo, M. & Monegato, G. 2021: Large landslides in the Alpine valleys of the Giudicarie and Schio-Vicenza tectonic domains (NE Italy). *Journal of Maps*, 17/3: 197–208. <https://doi.org/10.1080/17445647.2021.1880979>



A glimpse of the lost Upper Triassic to Middle Jurassic architecture of the Dinaric Carbonate Platform margin and slope

Pogled v izgubljeno zgornjetriasno in spodnjejursko arhitekturo pobočja in roba Dinarske karbonatne platforme

Boštjan ROŽIČ¹, Luka GALE^{1,2}, Primož OPRČKAL³, Astrid ŠVARA⁴, Tomislav POPIT¹, Lara KUNST⁶, [†]Dragica TURNŠEK³, Tea KOLAR-JURKOVŠEK², Andrej ŠMUC¹, Aljaž IVEKOVIČ⁷, Jan UDOVČ² & David GERČAR¹

¹University of Ljubljana, Faculty of Natural Sciences and Engineering, Department of Geology, Aškerčeva 12, SI-1000 Ljubljana, Slovenia; e-mail: bostjan.rozic@ntf.uni-lj.si

²Geological Survey of Slovenia, Dimičeva ulica 14, SI-1000 Ljubljana, Slovenia

³Slovenian National Building and Civil Engineering Institute, Dimičeva ulica 12, SI-1000 Ljubljana, Slovenia

⁴Karst Research Institute, ZRC-SAZU, Titov trg 2, SI-6230 Postojna, Slovenia

⁵Ivan Rakovec Institute of Paleontology, ZRC-SAZU, Novi trg 2, SI-1000 Ljubljana, Slovenia

⁶ZOO Ljubljana, Večna pot 70, SI-1000 Ljubljana, Slovenia

⁷Odsek za nanostrukturne materiale, IJS, Jamova c. 39, 1000 Ljubljana, Slovenia

Prejeto / Received 20. 4. 2022; Sprejeto / Accepted 19. 10. 2022; Objavljeno na spletu / Published online 21. 12. 2022

Key words: Slovenian Basin, Dinaric Carbonate Platform, Middle Jurassic, limestone breccia, debris-flow, Stratigraphy, Ponikve Breccia

Ključne besede: Slovenski bazen, Dinarska karbonatna platforma, srednja jura, apnenčaste breče, drobirski tok, stratigrafija, Ponikvanska breča

Abstract

In the southernmost outcrops of the Slovenian Basin the Middle Jurassic coarse-grained limestone breccia (mega)beds are interstratified within a succession that is otherwise dominated by hemipelagites and distal turbidites. In this paper, these beds are described as the Ponikve Breccia Member of the Tolmin Formation. We provide descriptions of the studied sections with detailed geological maps and analysis of the breccia lithoclasts. From the latter, a non-outcropping margin of the Dinaric Carbonate Platform is reconstructed. In the Late Triassic the platform margin was characterized by a Dachstein-type marginal reef. After the end-Triassic extinction event, the platform architecture remained, but the reefs were replaced by sand shoals characterized by ooids. In the late Early Jurassic and/or early Middle Jurassic a slope area might have been dissected by normal faults and a step-like paleotopography was formed. In the Bajocian, during a period of major regional geodynamic perturbations, extensional or transtensional tectonic activity intensified and triggered the large-scale collapses of the Dinaric Carbonate Platform margin producing the limestone breccias described herein. This may in turn have caused a backstepping of the platform margin, as is evident from the occurrence of Late Jurassic marginal reefs that are installed directly above the Upper Triassic and Lower Jurassic inner platform successions.

Izvleček

V najjužnejših izdankih Slovenskega bazena se znotraj zaporedja, v katerem sicer prevladujejo hemipelagične kamnine in distalni turbiditi, pojavljajo (vele)plasti srednjejurske debelozrnate apnenčeve breče. V prispevku so te plasti opisane kot Ponikvanska breča in sicer kot člen Tolminske formacije. V opisu podajamo podroben opis proučenih profilov, vključujoč detajlne geološke karte in analizo litoklastov v breči. Iz slednjega je bilo možno rekonstruirati danes nerazgaljeni rob Dinarske karbonatne platforme. V poznem triasu je bil zanj značilen dachsteinski tip obrobne grebene. Po triasno-jurskem izumrtju je arhitektura platforme sicer ostala enaka, vendar so grebene nadomestile peščene plitvine, za katere so značilni ooidi. V pozni spodnji juri in/ali zgodnji srednji juri je bilo območje pobočja razčlenjeno najverjetneje z normalnimi prelomi in nastala je stopničasta paleotopografija. V bajociju se je v času velikih regionalnih geodinamskih sprememb okrepila ekstenzijska ali transtenzijska tektonska aktivnost, ki je sprožila obsežne porušitve robnega dela Dinarske karbonatne platforme in nastale so tukaj opisane apnenčaste breče. To bi lahko povzročilo umik roba platforme, kar je razvidno iz pozicije zgornjejurskih obrobnih grebenov, ki se pojavljajo neposredno nad zgornjetriasnim in spodnjejurskim zaporedjem notranjega dela platforme.

Introduction

The present-day geological structure of the territory of Slovenia is largely the result of the Late Cretaceous and post-Cretaceous tectonic shortening of the continental crust stemming from the Alpine orogenesis (Placer, 1999; Vrabc & Fodor, 2006). The nappe structure is especially evident in western Slovenia, where successions of three large Mesozoic paleogeographic units meet at the thrust faults (Fig. 1). Successions of the Triassic–Early Jurassic Julian Carbonate Platform (JCP hereinafter) and of the Early Jurassic–Late Cretaceous Julian High are preserved in the Krn Nappe, which forms most of the Julian Alps and the Kamnik–Savinja Alps (Placer, 1999). The Krn Nappe is in thrust-tectonic contact with the Tolmin Nappe to the south. The latter is characterised by deeper-marine successions deposited in the Slovenian Basin (SB hereinafter). Further south, the Tolmin Nappe is in turn thrust over the Trnovo and Hrušica Nappes of the External Dinarides, consisting largely of shallow-marine

carbonates of the Dinaric Carbonate Platform (DCP hereinafter) (Placer, 1999). According to Vlahović et al. (2005), the latter is a local synonym for the northern sector of the Southern Tethyan Megaplatfrom (Middle Triassic–Toarcian), and of the Adriatic Carbonate Platform (Toarcian–end of Cretaceous).

The central unit of the Mesozoic topography is the SB, which lies between the Julian and Dinaric Carbonate platforms, which separates them but also provides a common sedimentary basin, acting as a sink for carbonate resediments shed from either of them. From the Early Jurassic to the beginning of Toarcian, the main source of carbonate shed into the SB was the JCP (Rožič, 2006, 2009). However, a dramatic decline in the proportion of resedimented limestone was recorded during and after the Pliensbachian, when the JCP tectonically disintegrated and carbonate production ceased (Šmuc, 2005; Šmuc & Goričan, 2005; Rožič et al., 2014a).

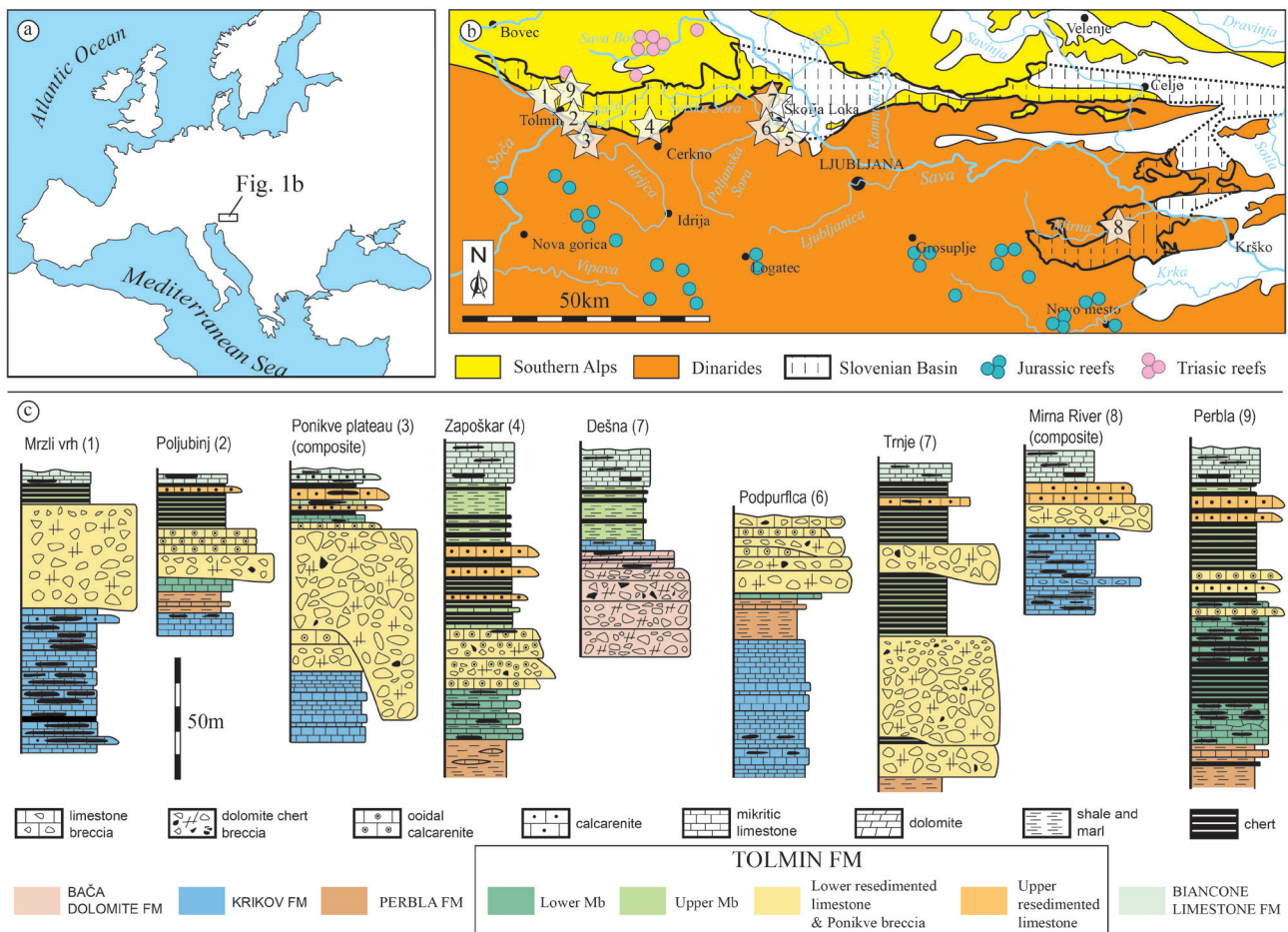


Fig. 1. a) Position of the studied area within the Europe; b) Present day distribution of three major Mesozoic paleogeographic units of the Southalpine-Dinaric transition: Julian Carbonate Platform (yellow without stripes), Dinaric Carbonate Platform (orange without stripes) and Slovenian Basin (areas with stripes). Upper Triassic (pink circles) and Upper Jurassic (blue circles) locations of marginal reefs are marked (compiled from Turnšek, 1997, Placer, 1999 and Rožič, 2016); c) Schematic sections of the Ponikve Breccia Member and Perbla section as a type locality of the Tolmin Formation (section localities are marked on Fig. 1b).

Younger, Toarcian to end-Jurassic deposits from the SB are instead dominated by hemipelagic sediments (Rožič, 2009). In the southern parts of the SB, however, sporadic resedimented limestones occur also in the Middle and Upper Jurassic, mainly in the form of calciturbidites less than a meter thick interbedded within radiolarite. They are interstratified in two distinct levels dated to Bajocian–Callovian and Kimmeridgian–lower Tithonian, respectively (Rožič & Popit, 2006; Rožič, 2009; Goričan et al., 2012). Instead of being derived from the “north”, these carbonate resediments originated in the “southerly” lying DCP. The extensive research of the southernmost outcrops of the SB showed that the lower (Bajocian–Callovian) resedimented limestones laterally pass into successions of limestone megabreccias and subordinate calciturbidites up to 80 m thick (Fig. 1c). These resediments likely record the collapse of the DCP margin (Rožič et al., 2019).

The composition of the resediments and their regional significance were recently presented by Rožič et al. (2019), but a more detailed analysis of the “lost” margin of the DCP was not included in such. The aims of this paper are thus: 1) to formalize breccia megabeds as a member of the Tolmin Formation and to describe its lateral occurrences by contributing supplementary data on the local geological settings of the studied section, 2) to present a detailed clast analysis (microfacies, biostratigraphy, paleoenvironment) of the recently studied sections (Rožič et al., 2019) and the Poljubinj and Zapoškar sections from older studies (Rožič, 2009), and 3) to reconstruct the Norian–Rhaetian, Lower Jurassic, and early Middle Jurassic margin stratigraphy of the DCP on the basis of clasts from megabreccias.

Clast analysis also aims to answer two prominent regional questions. The first is the question of the structure and composition of the non-preserved Norian–Rhaetian marginal reefs on the south-lying DCP. To the contrary, however, the Upper Jurassic marginal reefs of the DCP are well documented, but they are positioned far towards the inner parts of the platform. Our study at least partially answers the second question; namely, it elucidates the causes for the back-steeping of the DCP margin.

Geological setting

The SB is a large-scale (at least several tens of kilometres wide and extending W-E across the entire territory of present-day Slovenia) intraplateau basin that shows continuous Ladinian to Maastrichtian deeper-marine sedimenta-

tion that was bordered by the DCP to the “south” and the JCP to the “north” (present-day directions). The latter disintegrated in the Pliensbachian and by the Bajocian turned into the submarine plateau called the Julian High (Buser, 1996; Šmuc, 2005; Šmuc & Rožič, 2010). The most continuous succession of the SB is preserved in the Tolmin Nappe, which is the lowermost nappe of the eastern Southern Alps (Placer, 1999, 2008). In the eastern part of Slovenia, the equivalent deeper-marine successions are also found within the so-called Transition Zone between the Internal and the External Dinarides, where they form nappes covering the shallow-marine successions of the DCP (Buser, 1996, 2010; Rožič, 2016). All of the studied sections represent the southernmost outcrops of the SB, distributed from the town of Tolmin in the west to the Mirna River Valley near the town of Sevnica in the east. Further to the east, the Mesozoic rocks are covered by the Neogene sediments of the Central Paratethys (Buser, 2010).

The Ladinian succession of the SB is dominated by Pseudozilian beds, by volcanoclastic, clastic, and less frequently carbonate sediments. A similar succession is observed also in the Carnian Amficlina beds, but with fewer volcanoclastics (Buser, 1989, 1996). In the southern part of the SB a large-scale platform collapse was documented within the Carnian strata (Gale et al., 2016). After the reestablishment of continuous carbonate production on the DCP in the Norian, the SB became dominated by carbonates, mostly by Norian–Rhaetian Bača Dolomite (Buser, 1996), and locally limestones of the Slatnik Formation (Rožič et al., 2009; Gale et al., 2012).

The Jurassic succession of the SB begins with the Hettangian–Pliensbachian Krikov Formation, which is characterized by alternating hemipelagic and resedimented limestones. The latter dominate in the northern part of the SB, suggesting that the JCP was the main source of the resediments (Rožič, 2006, 2009). After the disintegration of the JCP, the SB became starved of (resedimented) carbonate, resulting in the deposition of the Toarcian marlstone-dominated Perbla Formation and Aalenian–lower Tithonian chert-dominated Tolmin Formation (Rožič, 2009; Goričan et al., 2012). Two levels of resediments occur within the Tolmin Formation in the southern and central parts of the SB, both shed from the DCP (Rožič & Popit, 2006; Rožič, 2009). The lower level, Bajocian–Bathonian (?Callovian) in age, is a distal equivalent of the limestone megabreccias analysed herein (Rožič et al., 2019).

The Jurassic–Cretaceous transition is marked by a sharp turn to the calcareous hemipelagic sedimentation, and Upper Tithonian–Berriassian Biancone-type limestone was deposited. Above, a poorly understood Valanginian–Barremian stratigraphic gap is present (Buser, 1996; Rožič et al., 2014a). Until the end of the Cretaceous the SB continuously received resedimented limestones from the DCP, but the nature of the hemipelagic sedimentation was changing. During the Aptian–Lower Cenomanian it was marl dominated (Lower Flyschoid formation). The Upper Cenomanian–Turonian succession was characterized by globotruncana-rich marly, varicoloured limestone (included in Lower Flyschoid formation by Cousin, 1981; also in our maps). Coniacian to Campanian is represented by Scaglia-type Volče Limestone, composed of gray hemipelagic limestones with cherts. The Maastrichtian Upper Flyschoid formation is again marlstone dominated. It records a gradual transition to syn-orogen flysch sedimentation (Cousin, 1981; Buser, 1989, 1996).

Methods

A detailed geological mapping (scale 1: 5000) was performed in all investigated areas. Sedimentological sections were logged at 1: 100 or 1: 50 scales. Sections were sampled in dense intervals. Microfacies, corals, and foraminifera from the matrix and clasts of breccias were determined for more than 300 thin sections using an optical polarizing microscope. Approximately 1500 clasts were analysed and divided into 25 groups according to their age and microfacies characteristics. Each group was compared with the Standard Microfacies Types (after Wilson, 1975; revised in Flügel, 2004). Classification of carbonates follows Dunham (1962), with modifications by Embry and Klovan (1971). In the Lovriš section, several samples of conodonts were taken from bigger clasts. A standard technique to recover conodonts was applied using diluted acetic acid followed by heavy liquid separation. One sample was positive. In the Mrzli vrh, Lovriš, and Trnje sections cherts above, within, and below the limestone megabreccia unit were treated (with diluted 9 % hydrofluoric acid) for radiolarians but yielded no results.

Formalization of the Ponikve Breccia Member of the Tolmin Formation

Short description of the Tolmin Formation: The Tolmin Formation was defined by Rožič (2009) as an Aalenian–lower Tithonian unit composed of siliceous hemipelagites (for Perbla type sec-

tion see Fig. 1c). It was divided into two members. The lower member, Aalenian–middle Bajocian in age, is composed of dark siliceous limestone and chert. The upper member (middle Bajocian–lower Tithonian) comprises varicoloured radiolarite. Calciturbidites are interstratified within the pelagites in the southern and central parts of the SB in two levels. The lower level lies at the boundary between the lower and the upper member of the formation. These calciturbidites were approximately dated to the Bajocian–Bathonian (?Callovian) and named Lower resedimented limestones. The upper level occurs in the uppermost part of the formation. It was dated to the upper Kimmeridgian–lower Tithonian and named the Upper resedimented limestones. Herein, we formalize the limestone breccia megabeds as a new member of the Tolmin Formation, and represents the lateral, proximal variability of the Lower resedimented limestones.

Name: Ponikve Breccia Member – It is thickest and best studied near the Ponikve Village on the Šentviška planota plateau. A similar term is also used for the Ponikve Klippe (that geologically comprises the Šentviška planota plateau), which is considered to represent the southernmost outcrops of the SB in western Slovenia.

Previous work: The Ponikve Breccia Member is characteristic for the southernmost sections of the SB succession. Breccias belonging to this member were previously mentioned by Cousin (1981) from localities near Tolmin, and by Ogorelec and Dozet (1997) from the vicinity of the town of Boštanj near the valley of the Mirna River. Breccias from the Poljubinj and Zapoškar sections were previously described in Rožič and Popit (2006), and Rožič (2009). Middle Jurassic Limestone breccia beds are reported from the Železniki area by Demšar (2016). A first detailed description of the unit was given by Rožič et al. (2019).

Short definition: The Ponikve Breccia Member is usually several tens of meters thick. It can consist of a single or multiple, often amalgamated breccia beds. The member lies with a sharp erosional contact on older basinal formations, most often on the Hettangian–Pliensbachian Krikov Formation dominated by hemipelagic limestone with chert. At the top, the Ponikve Breccia member is conformably overlain by radiolarite or hemipelagic limestone with chert of the Tolmin Formation (Rožič, 2009; Rožič et al., 2014a). In some locations, the upper boundary is marked by a disconformity and younger formations (e.g. Lower Flyschoid formation) are overlain.

The thickness of the limestone breccia beds varies from meter-scale up to almost 80 m. Breccia is coarse grained and often contains meter-sized boulders. It consists of the Upper Triassic to Middle Jurassic basin, slope, and platform margin carbonate lithoclasts. Clasts are embedded in a micrite matrix with ooids and bioclasts (thin-shelled bivalves, crinoids). Breccia beds can be associated with calciturbidites, namely graded microbreccia and calcarenite. Exceptionally, hemipelagic sediments can be interstratified between thick breccia beds. Towards the central part of the basin this member laterally passes into the Lower resedimented limestones of the Tolmin Formation.

Description of the type locality: The type locality of the Ponikve Breccia Member is the Podbrdo section (Fig. 2), located on the SW slopes of the Šentviška planota plateau (N46°08'06", E13°47'50"), near the village of Ponikve. The section is named after the local name for a gorge and is not to be mistaken for the town of Podbrdo that lies in the Bača Valley.

In this section, the Ponikve Breccia Member lies unconformably on the Krikov Formation dominated by hemipelagic limestone. It is 57.5 m thick and composed of amalgamated limestone breccia and subordinate calcarenitic beds. It begins with three limestone breccia beds (0.6, 2.3 and 8.4 m thick) that contain cm-sized lithoclasts. The succession continues with an interval almost 5 m thick dominated by fine-grained limestone breccia, often matrix supported (pebbly calcarenite). Beds at the base of this interval are several tens of centimetres thick and become less expressed upwards. The thickest and coarsest bed follows, which reaches 37 meters and contains lithoclasts up to 10 m in size. The Ponikve Breccia Member ends with two graded fine-grained limestone breccia beds (1.3 m and 2.5 m thick, respectively) followed by three thin packstone beds.

The Ponikve Breccia Member is overlain by siliceous limestones and cherts of the Tolmin Formation (for details see Rožič et al., 2014a). Two supplementary sections were logged in the vicinity of the type section (see below).

Lateral variability: geological maps of the studied areas and description of the studied sections

The Ponikve Breccia Mb is characteristic for the SB's southernmost (most marginal) sections. So far, it is documented in areas of the sections presented herein. Additionally, Middle Jurassic

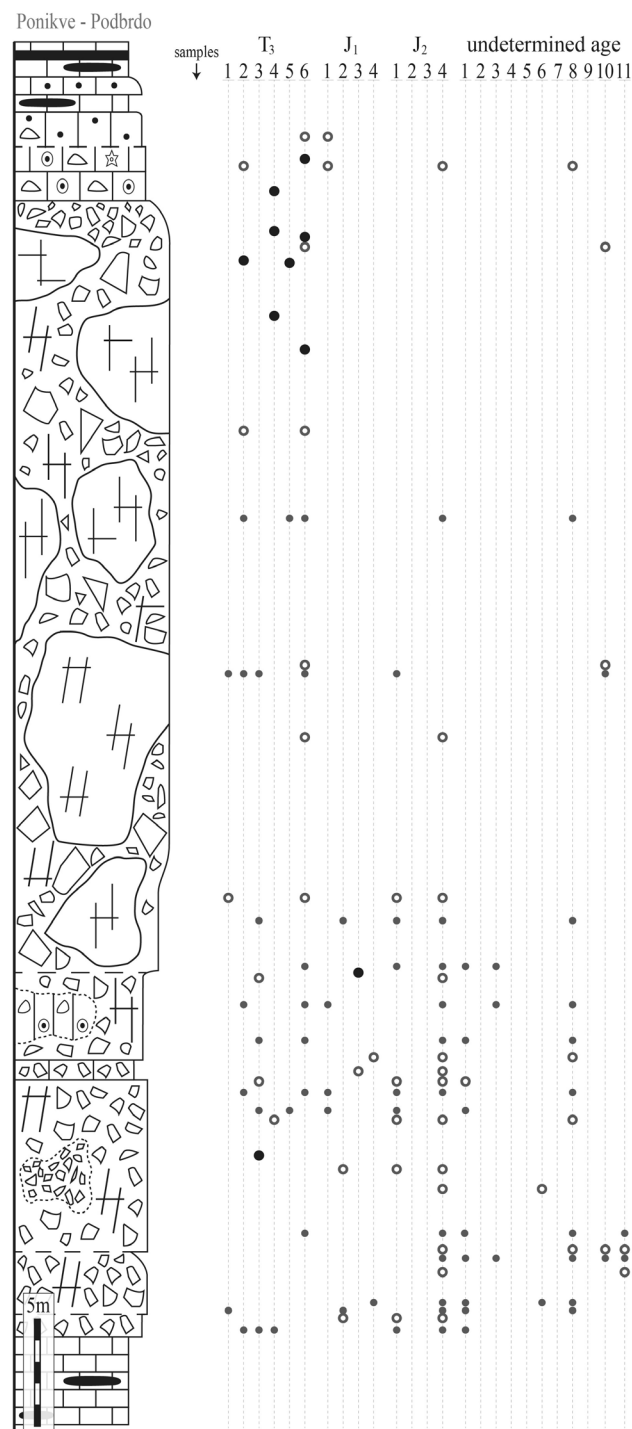


Fig. 2. Detailed stratigraphic log of the Podbrdo section (type locality of the Ponikve Breccia Member) with positions of specific lithoclast types (for legend see Fig. 7).

breccia beds are mapped in the SB outcrops near the town of Železniki (Demšar, 2016) which is located between the Zapoškar and Škofja Loka sections, and near the town of Boštanj (Ogorelec & Dozet, 1997), close to the Mirna sections and the town of Celje (Sherman et al., 2022). The areas of the studied sections are described in a west-to-east direction.

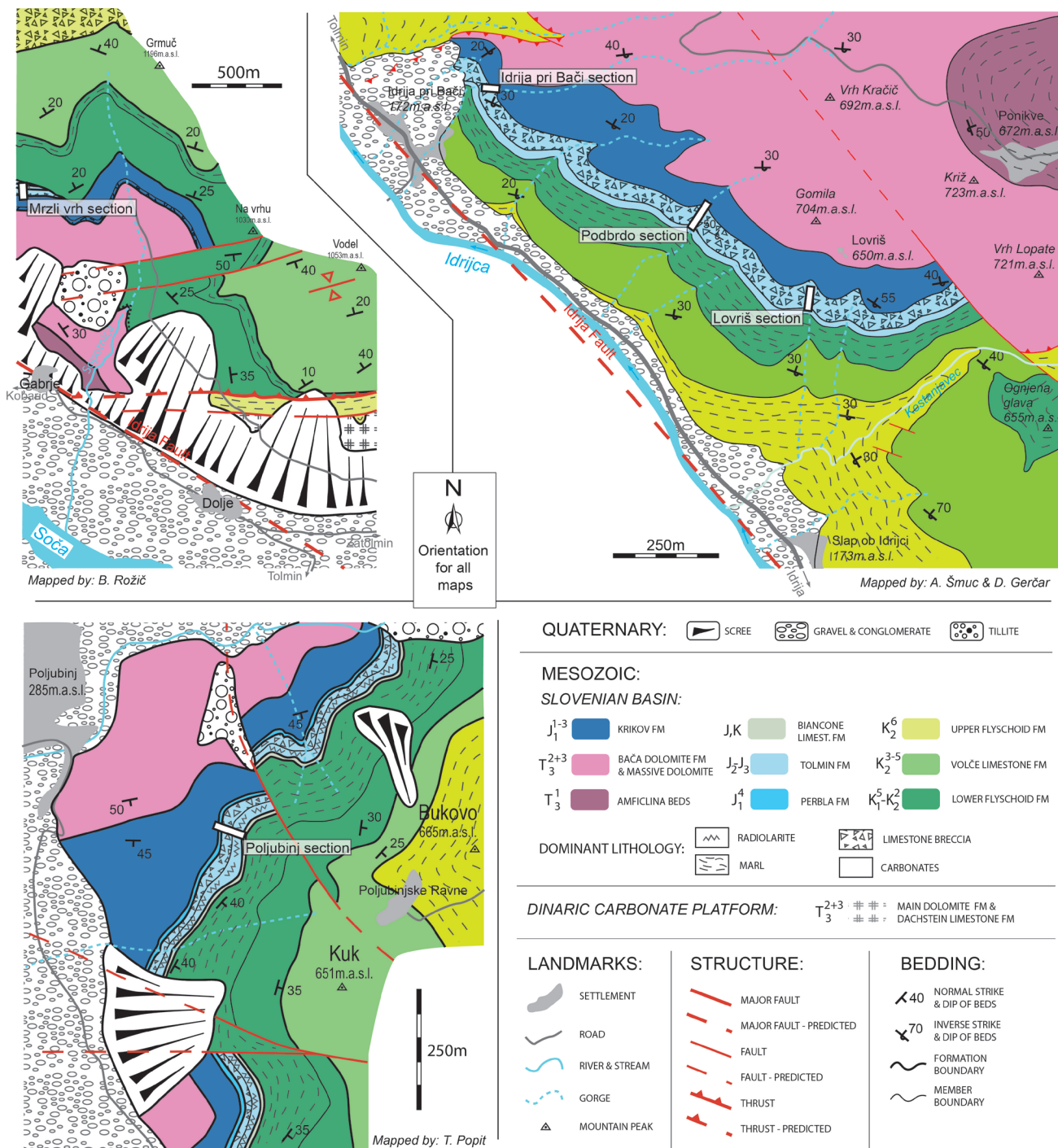


Fig. 3. Geological maps of the Mrzli vrh, Poljubinj and Ponikve Plateau areas with locations of the studied sections.

Mt. Mrzli vrh section

The Mt. Mrzli vrh section was logged 3.5 km NW of the town of Tolmin where the westernmost outcrops of the SB are preserved (Fig. 3). The succession is generally equal to the one described above in the Geological Setting chapter, but the Norian–Rhaetian is dominated by massive dolomite overlain by basal limestone breccia of the Krikov Formation (for details see Rožič, et al., 2017). Some coarser grained calciturbidites (limestone microbreccia) occur within the Krikov Formation.

The studied Middle Jurassic limestone megabreccia occurs solely on the westernmost cliffs of the Mt Mrzli vrh where the section was logged (N46°12'43", E13°41'49"). The contact with the underlying Krikov Formation is erosional. The Ponikve Breccia Member is 44 m thick and composed of a single graded bed with m-sized boulders, with cm-sized clasts at the topmost part of the bed (Fig. 4).

It is overlain by approximately 15 m thick radiolarite of the Tolmin Formation and 4 m of the Biancone-type limestone. The overlying Lower

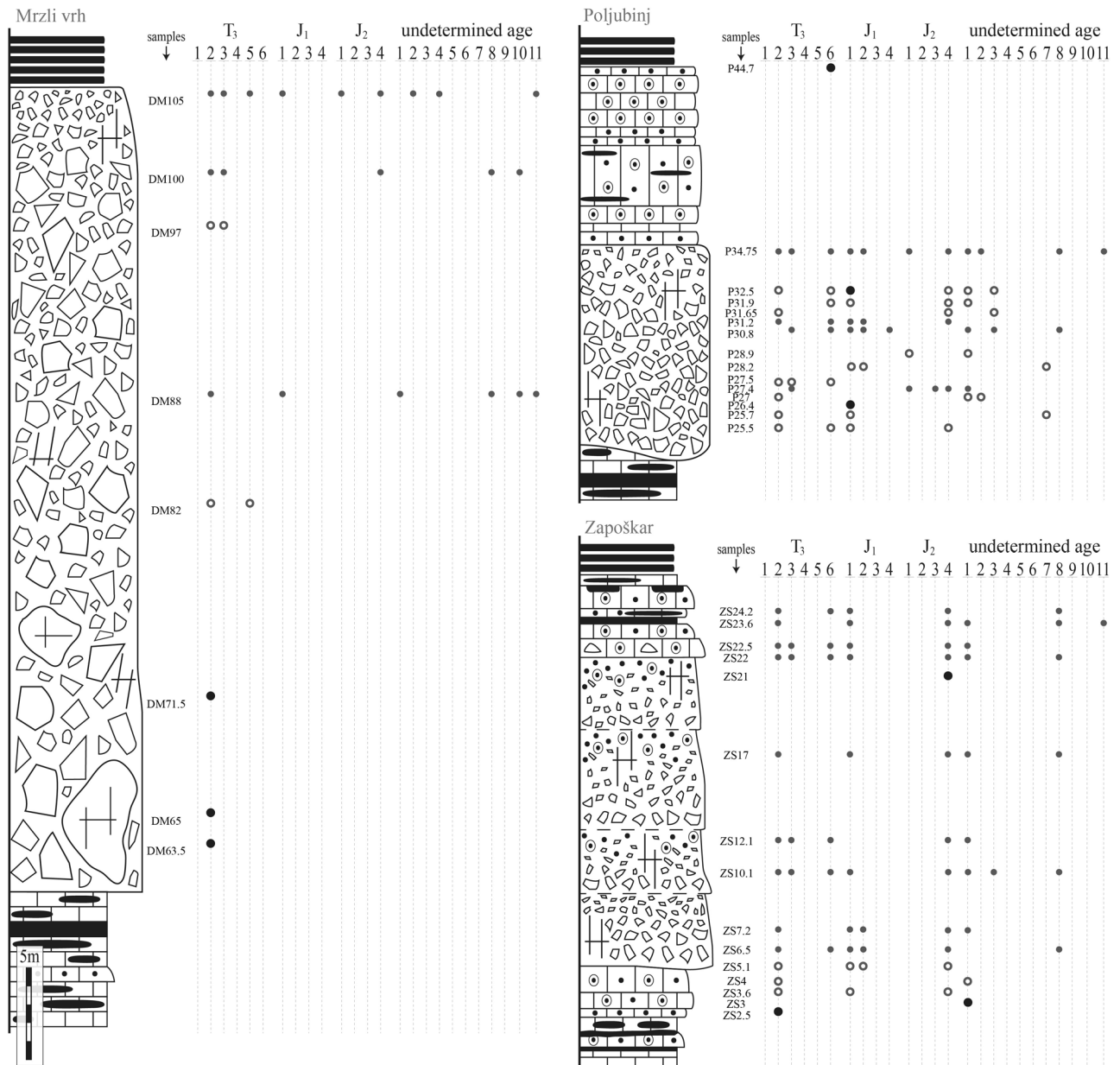


Fig. 4. Detailed stratigraphic logs of the Mrzli Vrh, Poljubinj, and Zapoškar sections with positions of specific lithoclast types (for legend see Fig. 7).

Flyschoid formation is dominated by coarse grained resedimented limestones and forms an angular unconformity with underlying sedimentary rocks. Consequently, all Middle and Upper Jurassic beds are laterally eroded (towards east) and basal limestone breccias of the Lower Flyschoid formation directly overlie the Krikov Formation. In the mapped area, south of two prominent E–W trending faults, the Lower Flyschoid formation lies directly on the massive dolomite, and these faults are proposed to be reactivated paleofaults (for details see Rožič, 2005).

Poljubinj section

The Poljubinj section is located 1.5 km SE of the town of Tolmin, near the Poljubinj Vil-

lage on the NW slopes of Mt. Kuk (N46°10'43", E13°45'28"). Here, the overall succession shows more continuous and “classical” basinal succession, which is displaced along several NW–SE and W–E oriented faults (Fig. 3).

The Ponikve Breccia Member lies on top of the Perbla Formation (maybe even above a few basal beds of the Tolmin Formation). It is 11 m thick and contains dm-sized clasts (Fig. 4). It is followed by 9 m of thin- to medium-bedded ooidal calcarenites (calciturbidites) and further up by radiolarite of the Tolmin Formation (Rožič & Popit, 2006). The base of the latter was dated with radiolarians to the UAZ8 (middle Callovian to lower Oxfordian) (Goričan et al., 2012).

Ponikve Klippe: Idrija pri Bači, Podbrdo, and Lovriš sections

This area is located further to the SE (6 km from the town of Tolmin) on the NE slopes of the Šenviška planota plateau (Fig. 3). The area structurally belongs to the Ponikve Klippe, the only SB succession preserved south of the South-Alpine thrust-front in all of western Slovenia (Busser, 1986; Placer, 1999). The contact with the underlying Trnovo Nappe of the External Dinarides is a thrust that is displaced by NW-SE strike-slip faults.

The SB succession in the Ponikve Klippe is in an overturned position and shows quite typical SB development. The Ponikve Breccia Member forms a continuous belt along the southern slopes of the Šentviška planota plateau facing the Idrija River Valley. Three sections were logged within this belt. In the Idrija pri Bači section (N46°08'26", E13°47'07") on the NW end of the belt, the Ponikve Breccia Member is 80 m thick and seemingly composed of a single breccia bed composed of m-sized boulders (Fig. 5). Towards the SE lies the Podbrdo section, described as the type-section above. The Lovriš section was logged on the SE end of the facies belt (N46°07'55", E13°48'14"). The single limestone megabreccia bed was logged for 75 m, though the breccia unit may be even thicker, because the lower boundary is covered. This bed contains large limestone boulders that often exceed 10 m in diameter (Fig. 5).

The described lateral changes in thickness and grain size of the member indicate that the topmost (thickest and coarsest) megabreccia bed is channelized into the underlying strata, often completely eroding preceding limestone breccia beds, which are preserved only in the Podbrdo section. The upper and lower boundaries of the Ponikve breccia are the same as in the type-locality section.

Zapoškar section

The Zapoškar section is located 3.5 km north of town of Cerkno in the Zapoška grapa gorge that cuts the southern slopes of Mt. Porezen (N46°09'47", E13°58'27"). The facies belt is continuous and displaced solely by a minor NW-SE trending fault (Fig. 6). In the Zapoškar section, the succession of the Lower resedimented limestones of the Tolmin Formation is 25 m thick and composed of calcarenites and limestone breccia beds (Fig. 4). The latter are up to several meters thick and positioned in the central part of this succession and can be assigned also as the Ponikve Breccia Member. It lies on the siliceous lime-

stone of the Lower Member of the Tolmin Formation and is overlain by radiolarite of the Upper Member of the Tolmin Formation. Laterally, the Ponikve Breccia Member pinches out completely, and the two hemipelagic members of the Tolmin Formation are in direct contact.

Škofja Loka: Podpurflca and Trnje sections

The investigated area is constrained to a narrow N-S extending belt of the SB outcrops, which starts approximately 1.5 km west of Škofja Loka's old town and extends for several km towards the north. The area is characterized by a rather complicated tectonic structure (Fig. 6). In a relatively small area three nappes (thrust sheets) are recognized. The lowermost is the Trnovo Nappe composed of the DCP succession ranging from Upper Triassic Dachstein Limestone down to the Palaeozoic basement rocks, whereas the upper two consist of the SB successions.

In the middle thrust-sheet, the Carnian to mid-Cretaceous SB successions are found. It is composed of two distinctly diverse successions that exhibit major differences in the Jurassic part of the succession. The thrust sheet starts with shale/marlstone-dominated Amficlina beds which in the uppermost part contain an interval of thin-bedded micritic limestone several tens of meters thick, which is known in older literature as Škofja Loka limestone (Ramovš, 1994). Upwards, it is followed by Norian-Rhaetian Bača Dolomite dominated by bedded dolomite with chert nodules, but in the Norian part thick dolomite-chert breccia beds are present and accompanied by synsedimentary faults (Oprčkal et al., 2012). Upwards, through the cherty interval it passes into the Krikov Formation (named Vancovec limestone in Demšar, 2016) and the thin (10 m) Perbla Formation (here we notice that in the field it is often impossible to distinguish between the micritic limestones of the Krikov Formation and those from Amficlina beds).

The Ponikve Breccia Member is slightly channelized and reaches approximately 50 m in thickness (Fig. 7). It was logged in a Podpurflca section along the road between the villages of Podpurflca and Gabrovo (N46°09'31", E14°17'24"). It is composed (often indistinctly) of amalgamated beds of limestone (mega)breccia and subordinate calcarenite beds. Bed thicknesses vary from tens-of-centimetres to almost 10 m. The upper part of the member was additionally logged in a supplementary section located along the main road between Škofja Loka and Cerkno (N46°09'12", E14°17'25"). The Ponikve Breccia

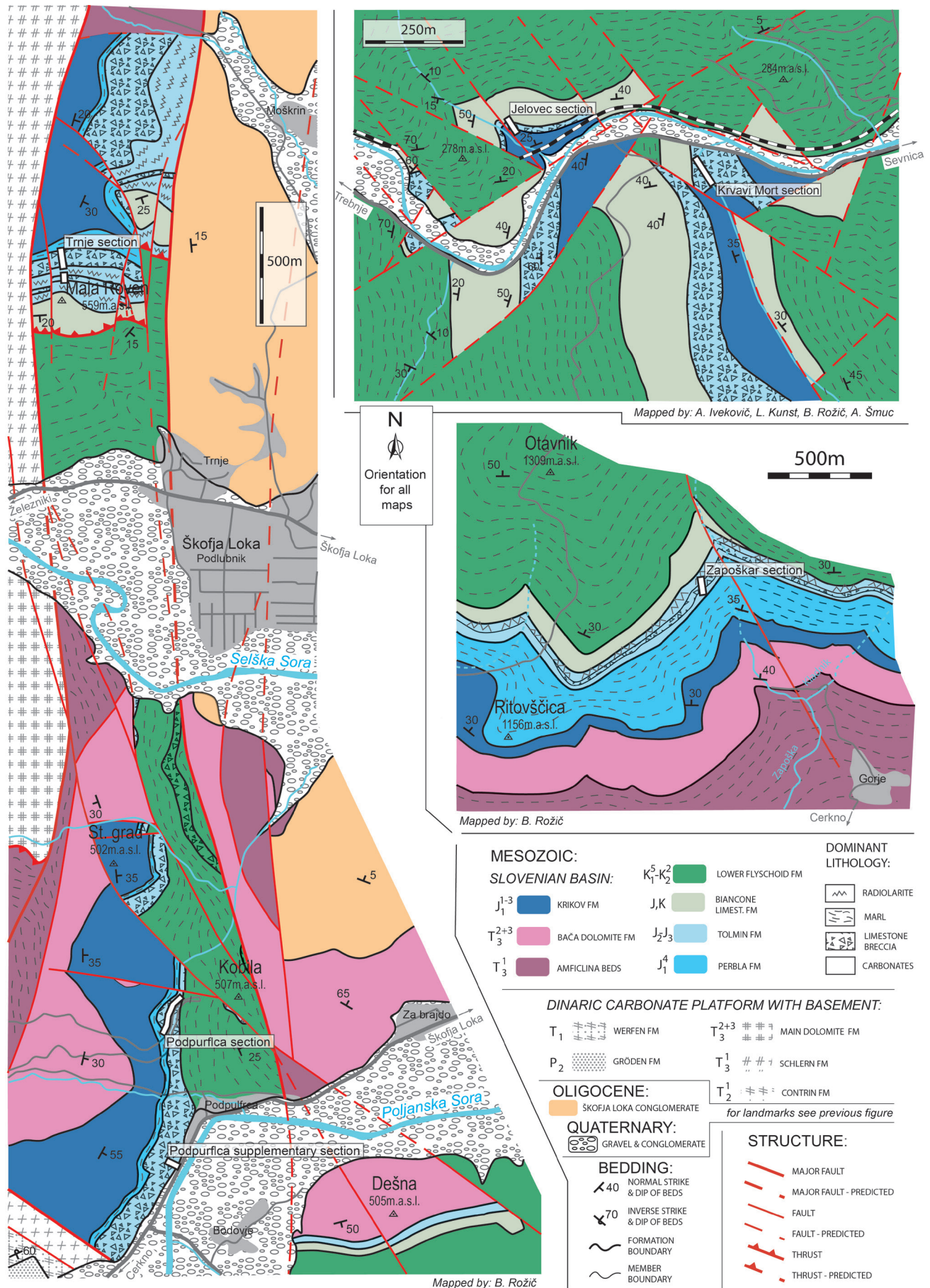


Fig. 6. Geological maps of the Škofja Loka, Zapoškar and Mirna River areas with locations of the studied sections.

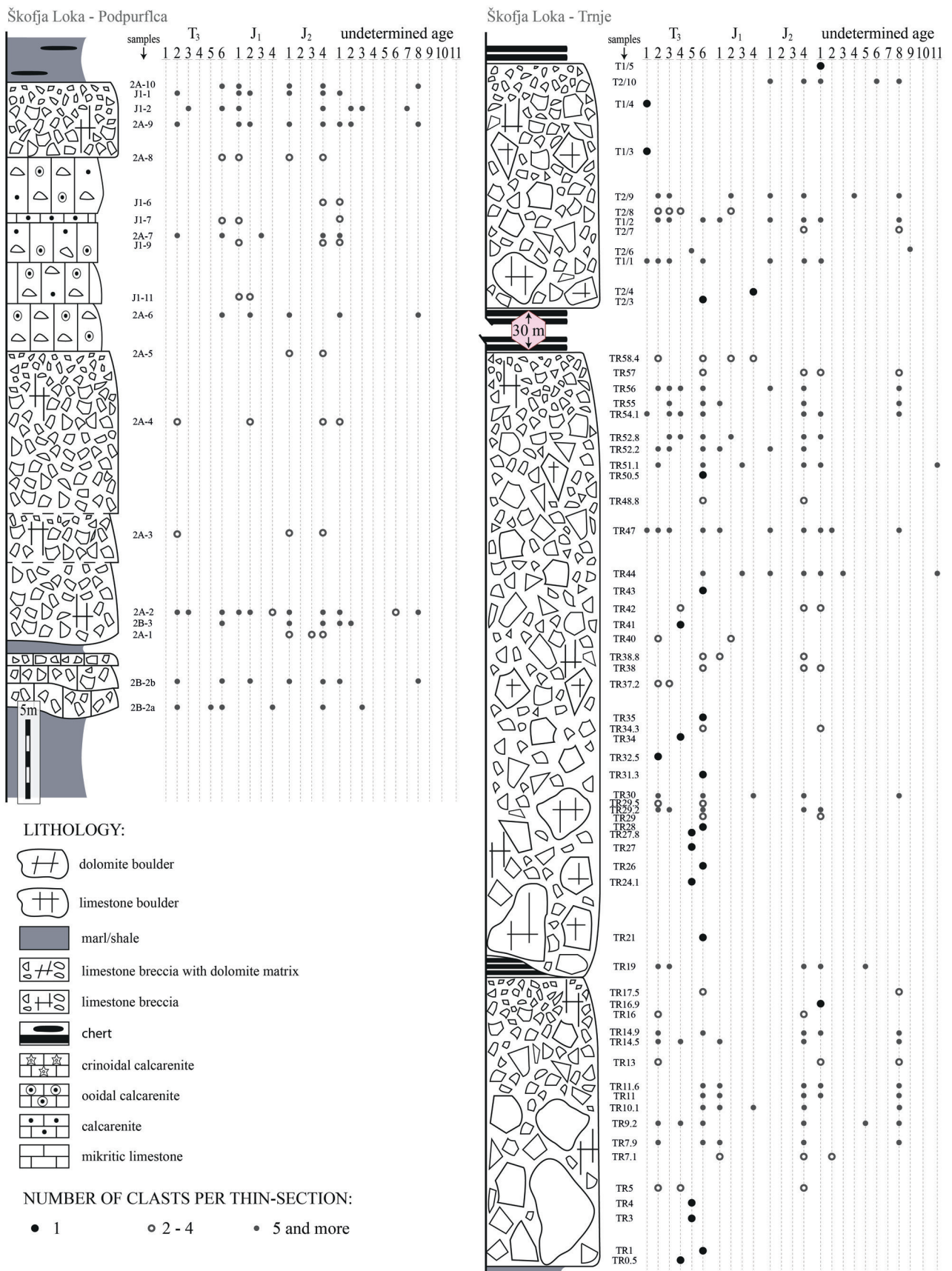


Fig. 7. Detailed stratigraphic logs of the Škofja Loka area: Podpurflica and Trnje sections with positions of specific lithoclast types.

Member is unconformably overlain by the mid-Cretaceous Lower Flyschoid formation. The upper member of the Tolmin Formation, as well as the Biancone-type limestone, were eroded in this area.

In the same thrust-sheet a specific, fault-isolated succession is found on the Dešna hill in the southern part of the mapped area (Figs. 1 and 6). The major part of the hill is composed of Bača Dolomite rich in dolomite breccia. It is overlain, after a long stratigraphic gap, by a thin interval of alternating radiolarite and marlstones (Upper member of the Tolmin Formation). These are overlain by Biancone-type limestone followed by the Lower Flyschoid formation.

In the structurally highest thrust sheet, located north of the Selška Sora River and Trnje Village, the succession is more continuous. Here the Ponikve Breccia Member overlies the Perbla Formation and reaches almost 60 m in thickness (Fig. 7). It is composed of two thick beds (20 and 38 m), separated by a laterally discontinuous interval of reddish radiolarite (alternatively it could be a large chert lithoclast) up to 2 m thick. Both breccia beds show normal grading in the uppermost parts. The Ponikve Breccia Member is followed by a succession of red and green radiolarite some 30 m thick. Upwards, however, another 20 m-thick graded limestone megabreccia bed occurs, whose composition resembles the main interval. Both limestone megabreccia intervals were logged in the Trnje section on the northern slopes of the Mala Roven hill (N46°10'57", E14°17'03"). Upsection, another 20 m of red-violet radiolarite is found, which is followed by 40 m of the Biancone-type limestone. The contact between the Biancone Limestone and the south-lying Lower Flyschoid formation is a north-dipping thrust fault.

Thrust structures are further dissected by a dense network of generally N–S striking normal faults that occasionally redirect towards a NW–SE strike. In this setting, the eastern blocks (closer to the Ljubljana Field) were downthrown. The structure may have originated in the transtensional wedge between two regional NW–SE oriented faults (Rožič et al., 2015). In the mapped area the greatest downward movements were along the contact with the southwestern fault (seen in SW edge of mapped area in Fig. 6), which caused a further tilting of tectonic blocks (including beds as well as thrust planes). The described southward tilting is responsible also for the atypical, slightly south-dipping thrust plane between the Trnovo Nappe (DCP succession) and the middle thrust-sheet (SB succession with Podpulfra section).

Mirna River Valley: Jelovec and Krvavi mort sections

The studied area is situated in the Mirna River Valley, between the small villages of Garbrje and Jelovec, approximately 6 km SW of the town of Sevnica (Fig. 6). The area is dominated by a Lower Flyschoid formation. This shale-rich formation was previously mapped as Ladinian beds, but during mapping nanoplankton as well as foraminifers (in calciturbidites) were found and determined the mid-Cretaceous age of this formation (Iveković, 2008). Jurassic beds outcrop in the central part of the valley in tectonic blocks separated by SWW–NEE and NW–SE striking faults. The Jurassic succession begins with the Krikov Formation, which is dominated by micritic limestones but contains few calciturbidite (graded calcarenite) beds. It is unconformably overlain by a Ponikve Breccia Member

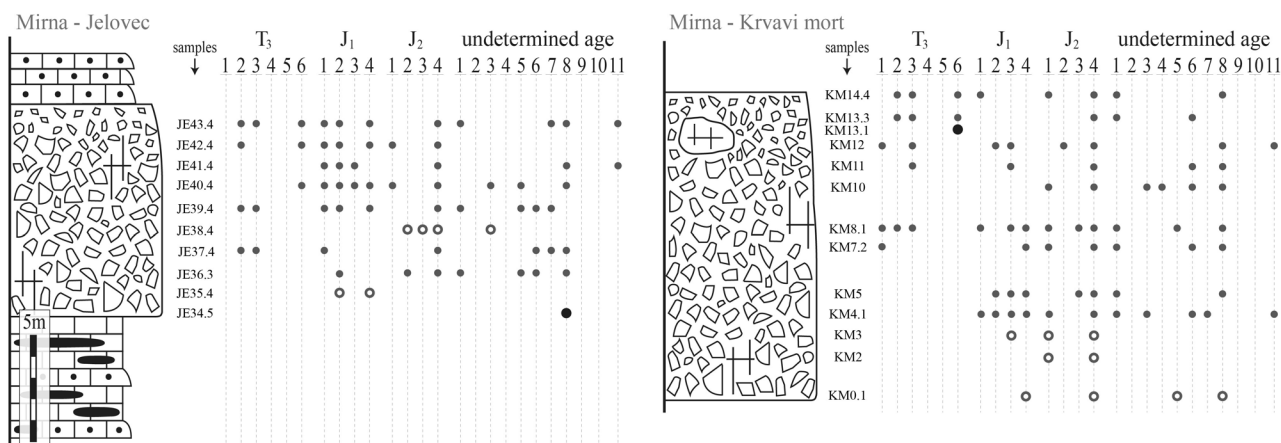


Fig. 8. Detailed stratigraphic logs of the Mirna River area: Jelovec and Krvavi Mort sections with positions of specific lithoclast types (for legend see Fig. 7).

that is composed of a single limestone megabreccia bed. In the Jelovec section, logged in a gorge near the eastern entrance of the Lepi Dob railway tunnel, north of the Trebnje–Sevnica regional road (N45°59'23", E15°13'43"), the breccia bed is 10 m thick and graded (Fig. 8). The supplementary Krvavi Mort section was logged in the Krvavi Mort gorge south of the Trebnje–Sevnica regional road (N45°59'19", E15°14'07"). In this section, the breccia bed is thicker (at least 14 m) with large clasts occurring also in the upper part of the bed. Upsection, the breccia is overlain with sharp contact (logged in the Jelovec section) by an interval of medium-bedded, graded calcarenites (calciturbidites) 8 m thick, which have not yielded age-diagnostic fossils. According to the composition, which is the same as the Upper resedimented limestones of the Tolmin Formation, these calcarenites could already be Late Jurassic in age. Above, the 35 m thick Biancone-type limestone outcrops. In the area studied herein, the interval between the Krikov Formation and the Biancone limestone therefore lacks the hemipelagic sediments of the Perbla and Tolmin formations, which are usually present in other sections. However, radiolarite was reported a few kilometres east by Ogorelec and Dozet (1997).

Microfacies of the Ponikve Breccia Member

The dominant lithology in the Ponikve breccia member is a limestone breccia, whereas in some sections calcarenites also occur. In this paper we focus on the clast- and matrix-analysis of the breccia beds (see below). Calcarenites are often graded grainstone/packstone composed of ooids, peloids, intraclasts, basinal clasts (mud-chips) and bioclasts, i.e. predominantly echinoderms. Other fossils are benthic foraminifers, bivalve, brachiopod and ostracod shells, gastropods, and bryozoans. With fining composition changes into packstone composed of pellets to peloids and bioclasts, predominantly echinoderms, calcified radiolarians, and rare benthic foraminifers (for details see Rožič & Popit, 2006; Rožič, 2009; Rožič et al., 2018).

Composition of the limestone breccia matrix

Apart from the Mt. Mrzli Vrh section, the composition of the breccia matrix is generally uniform in all studied sections. It is mostly packstone, locally grainstone, composed of grains that are believed to be generally contemporaneous with sedimentation. The matrix is locally dolomitized.

The grain composition is variable within and between different sections. However, except for the Mt. Mrzli vrh section, coarse micritized ooids and small- to medium-sized radial ooids with peloids and bioclasts in their cores (foraminifers, gastropods, crinoids, ostracods, bivalves, etc.) are always present and often dominant. The packstone/grainstone exhibit bimodal distribution in the size of the grains (Fig. 9a). Other grains, such as intraclasts, peloids (pellets), aggregate grains (lumps) and diverse bioclasts are also present (Fig. 9b). The most common bioclasts are echinoderm fragments and foraminifers, among which the trocholinids dominate over textularids and lagenids. Fragments of thin-shelled bivalves are locally present. Other molluscs (bivalves, gastropods, and brachiopods) are very rare. Other rare bioclasts are corals, calcimicrobes, bryozoans, and microbially encrusted, completely recrystallized clasts (presumably recrystallization-prone bioclasts, such as chaetetids).

Alongside the aforementioned grain types, oncoids were also observed. They are abundant in the lower part of the Podbrdo section and were documented in the Mirna Valley area (Krvavi Mort section), as well as in the Škofja Loka area (Podpulfrca section). The cores of the oncoids are either micritic or contain bioclasts, such as gastropods, bivalves, fragments of encrusting foraminifers, or calcimicrobes.

In contrast to breccias in other sections, the matrix of breccias in the Mt. Mrzli vrh section is a fine-grained packstone with fragmented thin-shelled bivalves and other bioclasts, among which echinoderms and sponge spicules prevail. Pellets, phosphate, and glauconite grains occur sporadically, whereas micritized ooids are present, but very rare.

Both at the Ponikve Klippe and at Mrzli vrh the matrix of the limestone megabreccia is mostly dolomitized. Locally the dolomitization affects the micritic lithoclasts as well. The primary texture and composition of the matrix are preserved only in the pebbly calcarenites of the lower part (from the 15th to the 20th metre-mark) of the Podbrdo section (Ponikve Klippe) and partially in the uppermost part of the limestone megabreccia bed in the Mrzli vrh section.

In addition to the above-mentioned allochems, the breccia matrix and calcarenites in all sections also contain sand-sized lithoclasts. Their composition is identical to the composition of the larger clasts described in Table 1. Calcarenites overlying the limestone megabreccia in the Podbrdo and Jelovec sections show a distinct increase in

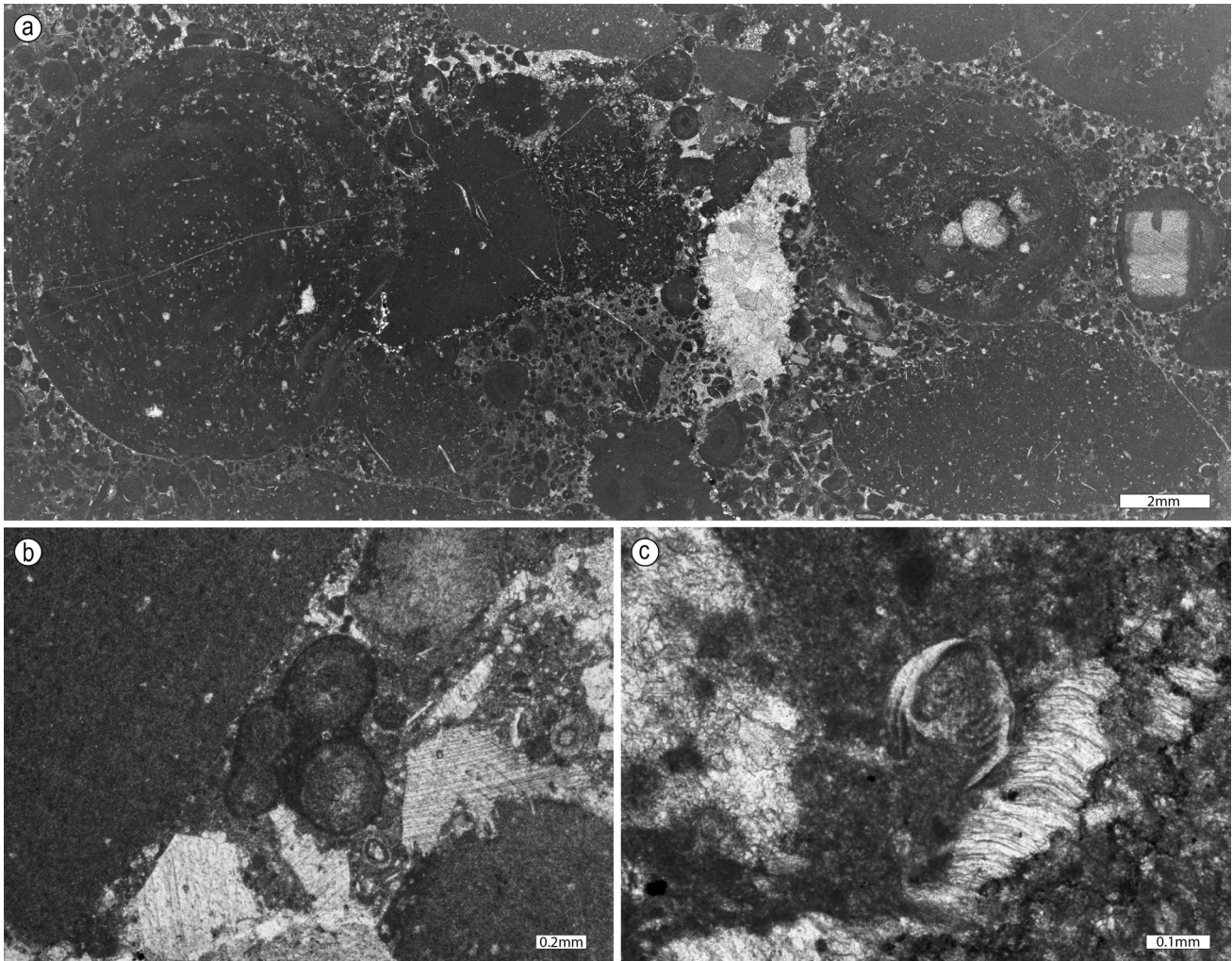


Fig. 9. Matrix of the Ponikve breccia: a) predominant grains are ooids, in some beds large oncoids occur (sample pp21.5), b) other matrix grains are pellets, aggregate grains, and bioclasts such as echinoderms, filaments, etc (sample KM4.1), c) age diagnostic *Protopenneroplis striata* Weynschenk occurs as isolated grain within the matrix (sample KM8.1).

crinoid abundance. This turnover in composition is most apparent in the Jelovec section, in which the overlying beds could already be of Late Jurassic age.

Age of the Ponikve Breccia Member

Some age-diagnostic foraminifers are present in both the matrix of limestone megabreccia and in the calcarenites (packstone/grainstone). They are well preserved, predominantly isolated, or rarely occurring in the cores of radial ooids. *Protopenneroplis striata* Weynschenk (Fig. 9c) is the most omnipresent, with *Andersenolina palastiniensis* Henson and *Mesoendothyra croatica* Gušić also important for biostratigraphy. In the

Podbrdo section, *Mesoendothyra croatica* Gušić was found less than a metre above the limestone megabreccia unit in calciturbidite interstratified in the overlying hemipelagites of the Tolmin Formation. The age-range of the limestone megabreccia studied is thus Bajocian–lower Bathonian (cf. Velić, 2007).

In previous studies, a sample of radiolarite which was taken 2.4 m above the Lower resedimented limestones of the Poljubinj section yielded age diagnostic radiolarian assemblages characteristic for a UAZ 8 (middle Callovian–early Oxfordian) (Goričan et al., 2012). In the Lovriš section a sample of radiolarite was taken 13 m above the limestone megabreccia unit and yield-

Fig. 10. T1 (a-c), T2 (d,e), and T3 (f, g) type lithoclasts: a) bioclastic wacke/packstone with echinoderms, foraminifera, filaments and unrecognisable bioclastic debris (sample LK2-54.5), b) slightly dolomitized bioclastic wackestone with echinoderms, filaments, ammonites and unrecognisable fossil debris (could belong to LJ4 clast type) (sample 338), c) Stromatolite structure within bioclastic wackestone (sample LK2-71.7), d) pelletal bioclastic packstone with Duostominidae foraminifera (sample 325), e) partly washed (corroded) matrix of the packstone with pellets, intraclasts, bivalve shell and foraminifera (*Triasina hantkeni*, *Aulotortus* sp.) (sample M65), f) pelletal intra/bioclastic grainstone with Duostominidae foraminifera (sample 337), g) intra/bioclastic grainstone with *Galeanella tollmanni* foraminifera and rare ooids.

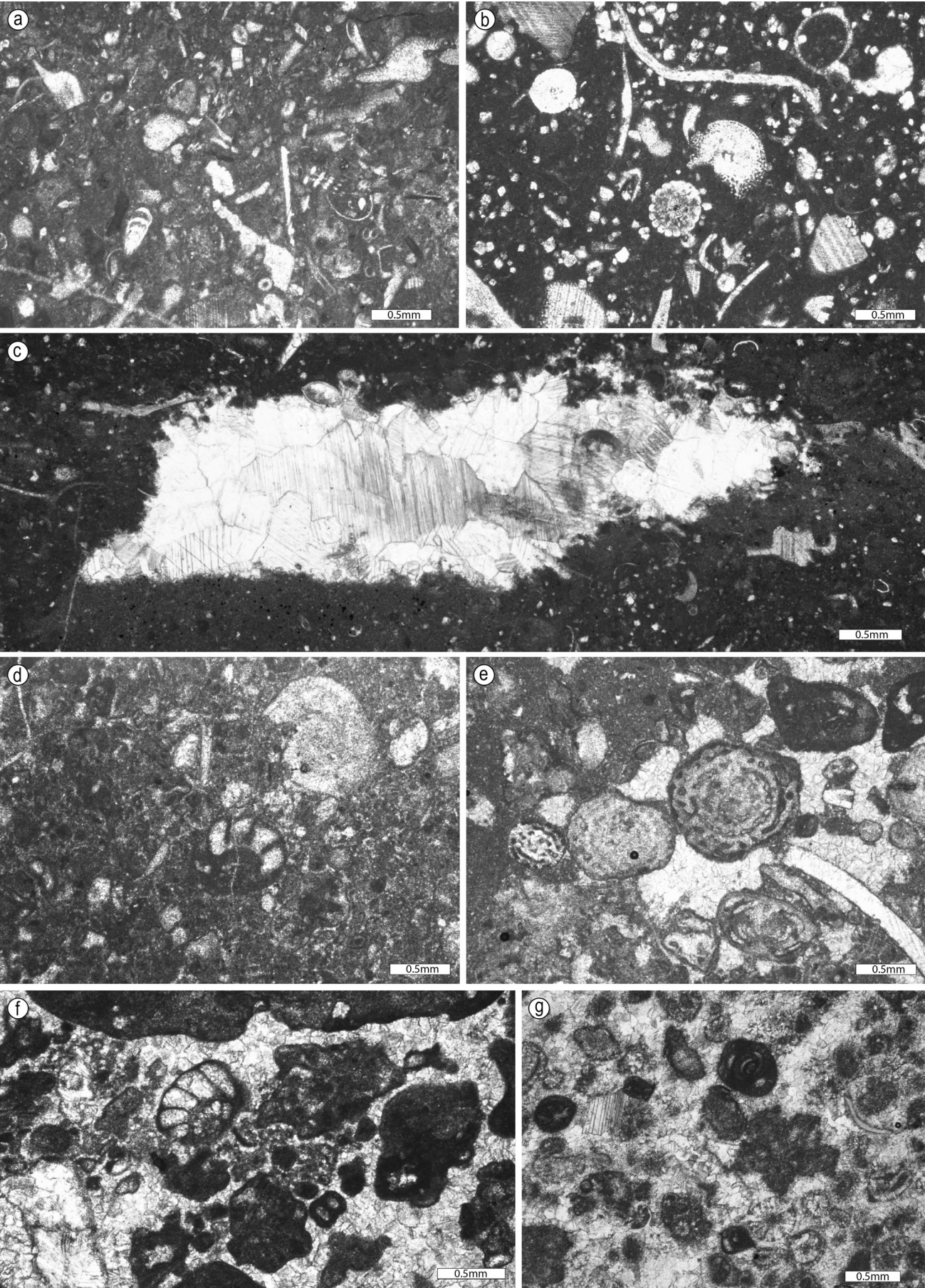


Fig. 10

ed UAZ 9–10 (middle to late Oxfordian to early Kimmeridgian) assemblage (Rožič et al., 2014a). Further basin-ward, the Lower resedimented limestone of the Tolmin Formation (which represents a distal equivalent of the limestone megabreccias presented herein) occur as calciturbiditic beds between radiolarite. Cherts just above the two lowermost calciturbiditic beds were dated to UAZ 4 (upper Bajocian). Cherts close to the uppermost beds were dated to the UAZ 8–10 (middle Callovian–early Kimmeridgian) (Goričan et al., 2012).

Compiling the available data, we conclude that major resedimentation events occurred within a relatively short interval between the Bajocian and early Bathonian. However, it is possible that some large-scale collapses occurred also later during the Middle Jurassic. This is evident particularly in the Trnje section, in which a thick radiolarite interval is interstratified between two limestone breccia megabeds.

Clast analysis

Clasts from breccias of the Ponikve Breccia Member are divided into 25 microfacies types (Table 1). As mentioned above, the composition of clasts in calcarenites corresponds to the clasts in breccias. The age of 14 microfacies types was determined. Six microfacies types are Late Triassic in age, and for most, we could narrow the age to the Norian–Rhaetian. Four microfacies types were assigned to the Early Jurassic, and four to the Middle Jurassic. The exact age for clasts belonging to the remaining 11 microfacies types could not be determined. Below we provide some basic descriptions; for further details see Table 1.

The first microfacies type (T1) from the Upper Triassic clasts is a bioclastic wackestone, which also contains deep-water fauna (Figs. 10a–c). The second microfacies type (T2) is a pelletal bioclastic packstone (often partly washed) with abundant foraminifers (Figs. 10d, e). The third microfacies type (T3) is a grainstone similar in composition to the previous microfacies type, but contains large amount of intraclasts, and in some clasts also cortoids (Figs. 10f, g). Microfacies types T2 and T3 are believed to originate in sand shoals and in transition to the lagoon, but they may also come from the reef area (they are often

observed as sediment fills between reef frames of boundstone clasts). The fourth microfacies type (T4) is a bioclastic rudstone with bioclasts made of reef-building organisms (Figs. 11a–c), and a similar fifth microfacies (T5) also contains reef lithoclasts (Figs. 11d–f). These two microfacies types could represent forereef sediments, or an inter-reef breccia. The last Triassic microfacies type (T6) is a typical reef boundstone with corals and calcisponges (stromatoporoids) as the main framebuilders (Fig. 12).

The first Lower Jurassic microfacies type (LJ1) is a grainstone similar to the third Triassic microfacies type (T3) but contains less bioclasts and additional ooids and aggregate grains. Grains of this microfacies type generally show less recrystallization (Figs. 13a–d). The second microfacies type (LJ2) is an ooidal grainstone, which in some clasts passes into a microfacies of the previous group (Figs. 13d–f). Both microfacies types (LJ1 and LJ2) are believed to originate from sand shoals, the first one closer to the transition with the lagoon. The third microfacies type (LJ3) is a crinoid-dominated grainstone (Figs. 14a, b), which in some clasts passes into a bioclastic wackestone (microfacies type LJ4) composed of diverse bioclasts revealing open-marine conditions (Figs. 14c–f). This clast microfacies type is similar in composition to Triassic bioclastic limestone (T1) but generally contains more sponge spicules.

Middle Jurassic clasts are divided into 4 microfacies types. First is an ooidal packstone/wackestone (MJ1) with a variable amount of ooids (Figs. 15a, b). Namely, in some packstone clasts ooids are dominant, while in others only sporadic ooids are found in a wackestone composed of pelagic fossils. Lithoclasts showing a transition from both end-members are present. The next two microfacies types are found only in the Mirna sections. The first of these two (MJ2) is a crinoidal limestone rich in lithoclasts (otherwise similar to LJ3) (Fig. 15c). The same is characteristic for the next microfacies type (MJ3), which in composition closely resembles older bioclastic limestones (T1 and LJ4 microfacies types) but also contains quite an abundance of lithoclasts (Figs. 15d, e). The last Middle Jurassic clast microfacies type (MJ4) is a mudstone/wackestone

Fig. 11. T4 (a–c), T5 (d–f) type lithoclasts: a) rudstone composed of diverse bioclasts (often encrusted by microbial laminae) deriving from the reef area (sample pp50.2), b) Calcisponge (left) and a microbial grain (right) as large grains of the bioclastic rudstone (sample pp50.2), c) foraminifera (*Duostominidae* and *Galeanella tollmanni*) and other reef debris as smaller grains of the bioclastic rudstone (sample pp52.0), d) reefal litho/bioclastic rudstone additionally contain lithoclasts (sample LK2 72.2), e) peloidal packstone lithoclasts with *Galeanella tollmanni* and bivalve fragments (sample LK2 57.2), f) a coral fragment (sample pp 57.6).

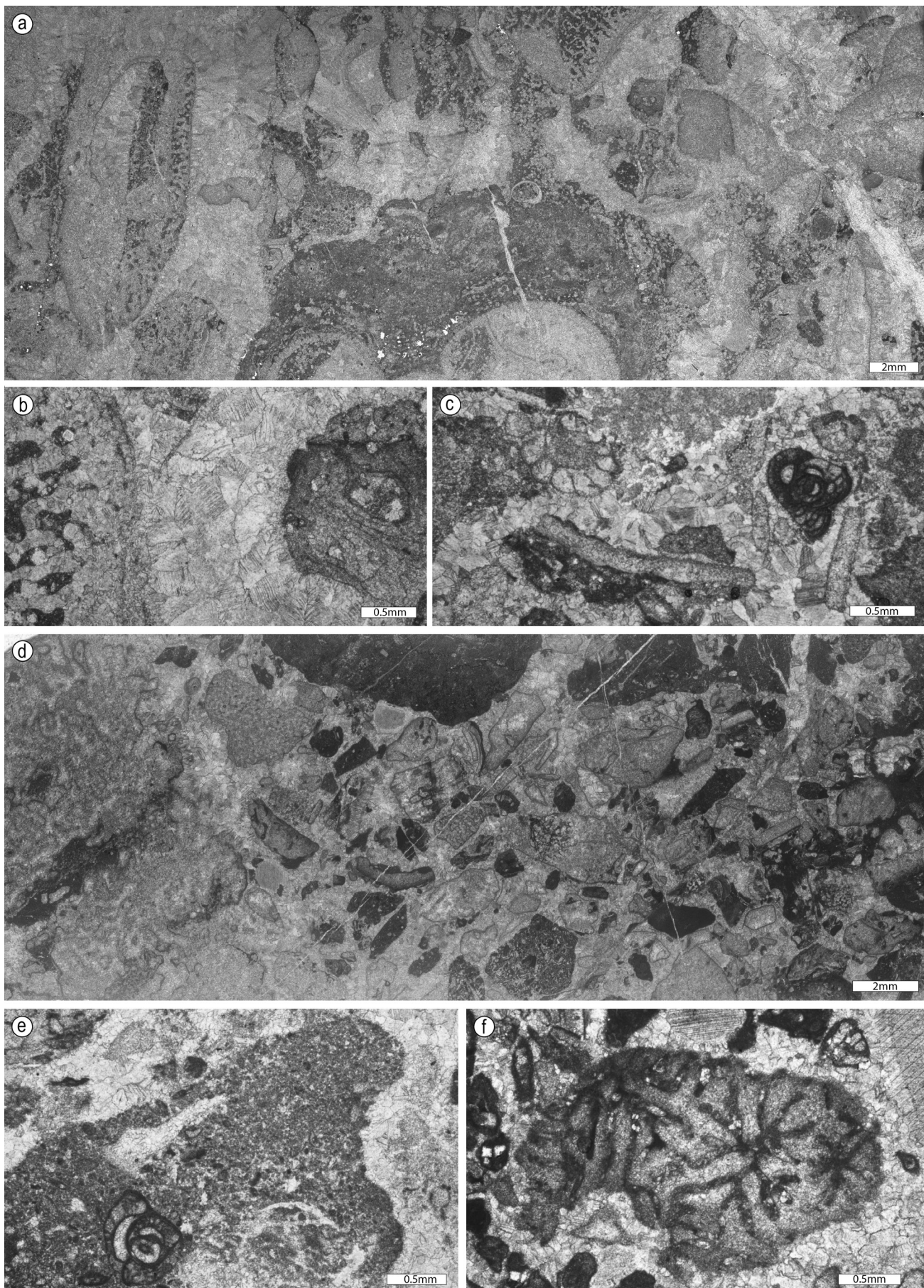


Fig. 11

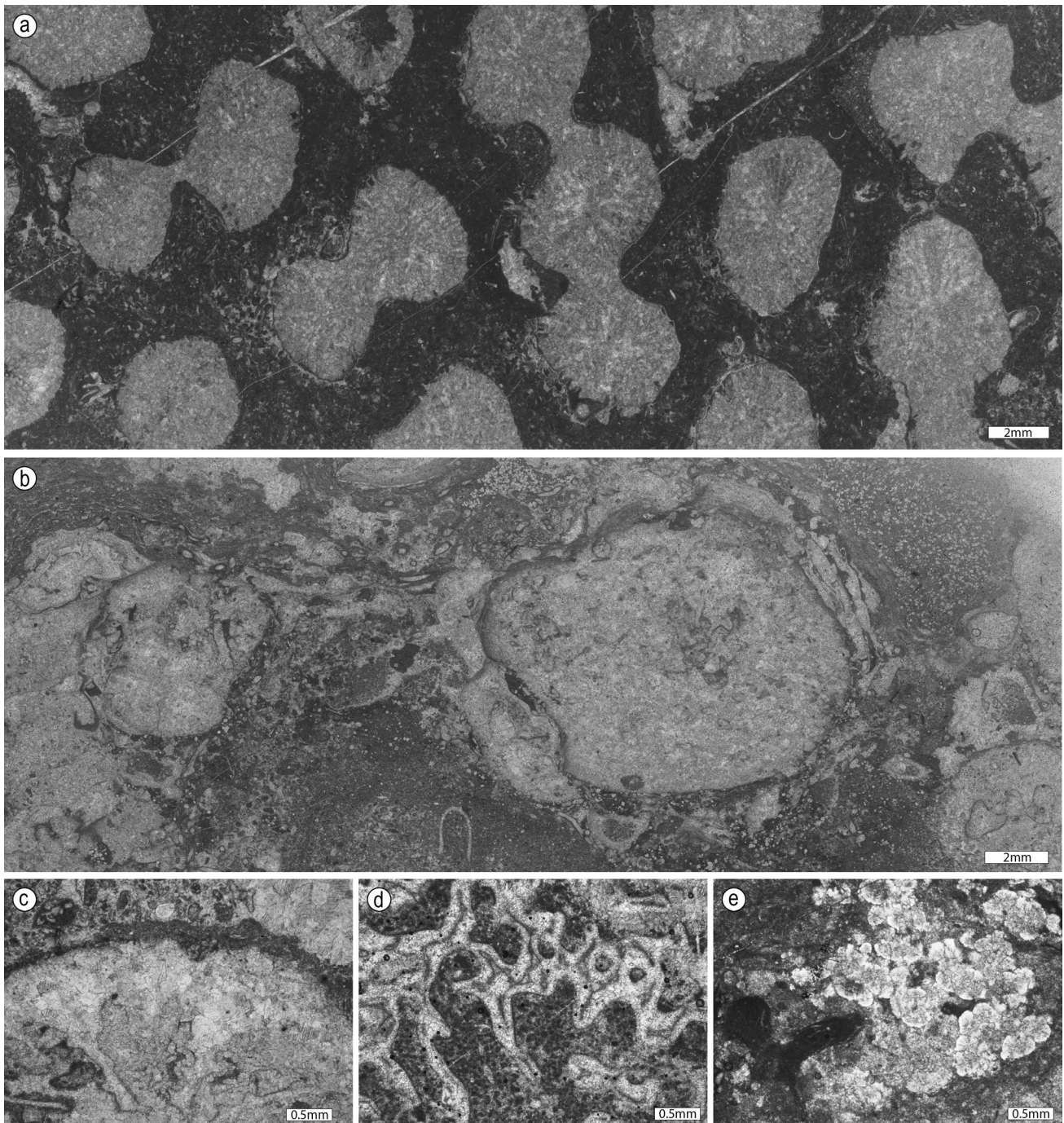


Fig. 12. T6 type lithoclasts: a) coral boundstone with pelletal packstone with corrosive voids infilling a space between corallites (sample 315D), b) Recrystallized frame building calcisponges with encrustations of microbialites, foraminifera and serpulids (sample pp37), c) coral with microbial crust and peletal/bioclastic grainstone matrix between corallites (sample pp57.3), d) calcisponge with voids filled with peletal packstone (sample JE42.2), e) *Baccanella* sp sp and microbial mound (sample LK2 4.8).

with pelagic fossils (Fig. 15f). Herein we note that age of this clast group was assigned due to the presence of planktonic foraminifers (cf. Caron & Homewood 1983; Tappan & Loeblich 1988; Darling et al. 1997). These foraminifers, however, do not occur in all clasts and large amount of these clasts could also be older.

The age of 11 microfacies types could not be univocally determined. The first such microfacies type (UD1) is common in almost all sections. It

is a pelletal packstone that probably originated from a great variety of environments (Fig. 16a). Namely, in some clasts fenestrae were observed, while in others we noticed sponge spicules and thin-shelled bivalves (filaments) indicating open marine conditions. These clasts are likely of variable age. Similar microfacies was observed within the reef-frame of the boundstone clasts (T6) and furthermore, from one such clast we retrieved upper Norian (Sevatian) to lower Rhaetian

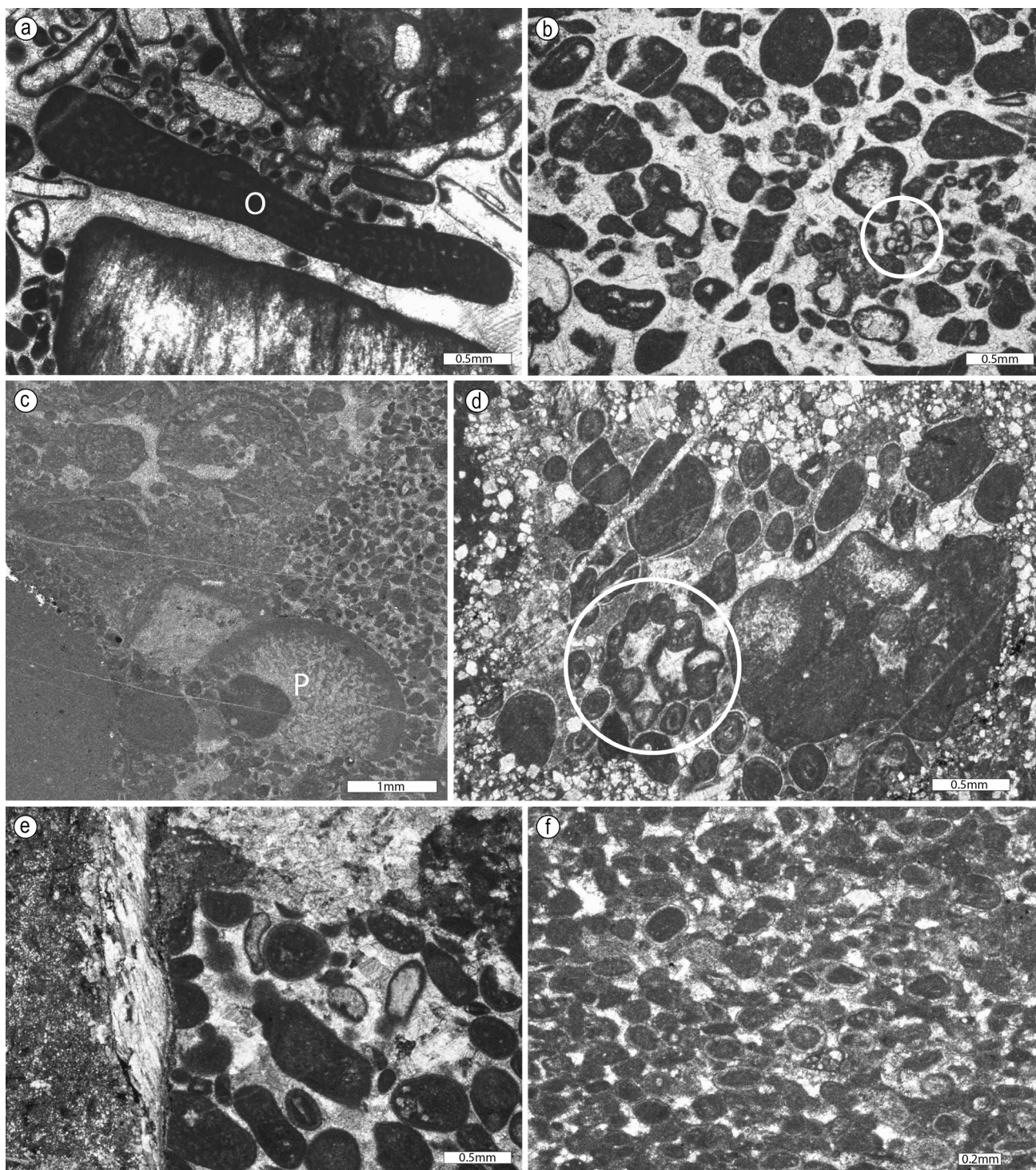


Fig. 13. LJ1 (a-d), and LJ2 (d-f) type lithoclasts: a) grainstone with pellets, intraclasts, micrite rimmed bioclasts (cortoids) and foraminifer *Orbitopsella* sp. (O) (sample 327), b) grainstone with intraclasts, peloids, aggregate grains (lumps), and *Siphovalvolina* sp. (encircled) (sample JE34.4), c) partly washed packstone lithoclasts with intraclasts, pellets, and fragments of calcareous algae and coral *Phacelophyllia termieri* (P); mudstone clast (lower left) and ooidal matrix (sample pp19.6), d) transitional LJ1-LJ2 lithoclast in dolomitized matrix with intraclasts, ooid-dominated and foraminifera *Reophax* sp. foraminifera, which agglutinated ooids (encircled) (sample pp5.2), e) grainstone with ooids, peloids, intraclasts and bioclasts, and chert clast (UD11) to the left (crossed polars) (sample KM12), f) partly washed packstone with ooids and pellets as dominant grains (sample pp5.2).

conodonts. On the other hand, they can contain coarse laminas rich in ooids and intraclasts that are typical for first two Lower Jurassic microfacies types (LJ1, and LJ2). The next microfacies type (UD2) is a wackestone with coarse intraclasts (also some ooids and pellets), which origi-

nated in a quiet environment probably adjacent to the high-energy conditions (Fig. 16b). The third microfacies type (UD3) is a fine-grained and well-sorted packstone with pellets and bioclasts (Fig. 16c). It probably represents clasts of eroded calciturbidites. The next three microfacies

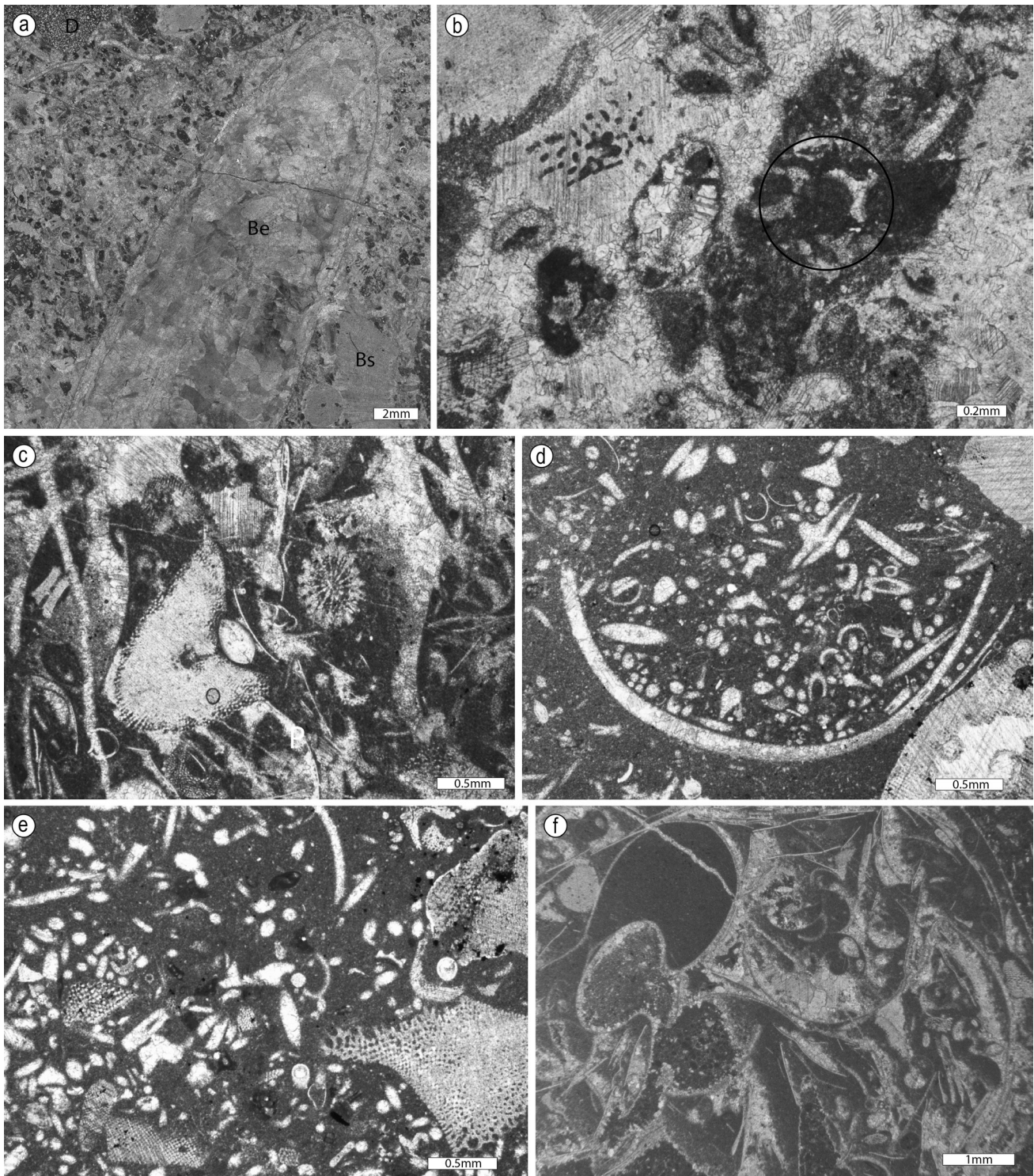


Fig. 14. LJ3 (a, b), and LJ4 (c-f) type lithoclasts: a) crinoidal grainstone with intraclasts, a dolomitized lithoclast (D), belemnite (Be) and bivalve shell (Bs) (sample pp21.05), b) crinoidal grainstone with wackestone litho/intraclasts, and foraminifer *Involutina liassica* (encircled) (sample KM4.1), c) packstone with echinoderms (crinoids), filaments and ostracods (sample JE37.4), d) wackestone with bivalve shell, sponge spicules, echinoderms and ostracods (sample LK2-74.2), e) wackestone with echinoderms, sponge spicules and foraminifera (sample LK2-74.2), f) floatstone with ammonites, filaments and crinoids (sample KM10).

types represent sediments from an open-shelf or slope environment. The first of these (UD4) is a wackestone composed of crinoids and ophthalmidiid foraminifers and small pellets (Fig. 16d). Next is a spiculite crinoidal packstone (UD5) (Fig. 16e), and last is a filament packstone/grain-

stone (UD6) (Fig. 16f). The next microfacies type (UD7) is a packstone with coarse grained pellets that presumably originated from a lagoon (Fig. 16g). The Last four microfacies types do not bear certain information on sedimentary environments and age. First of these (UD8) is an almost

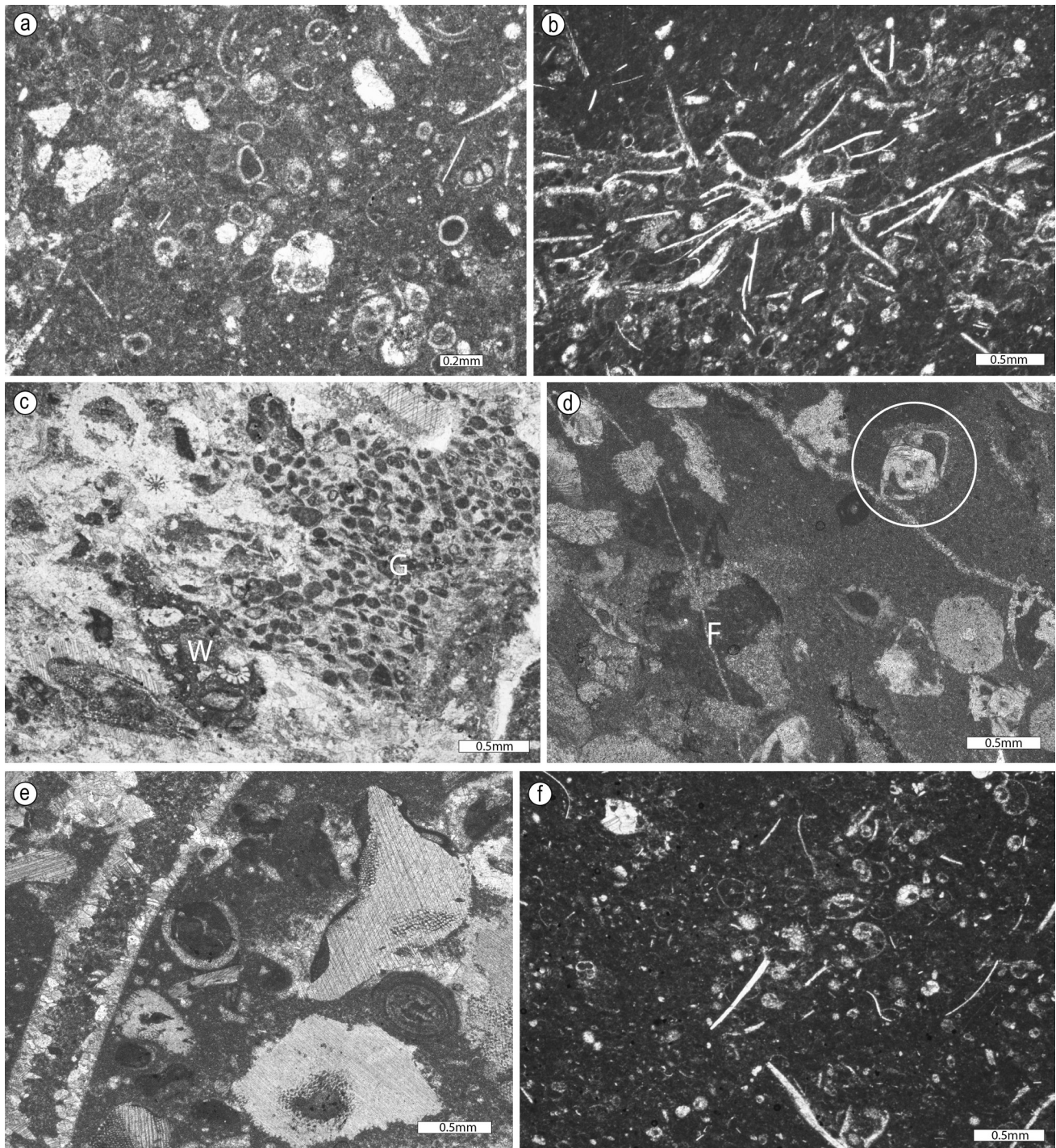


Fig. 15. MJ1 (a, b), MJ2 (c), MJ3 (d, e) and MJ4 (f) type lithoclasts: a) wackestone with superficial ooids, benthic and plankton foraminifer, filaments and unrecognisable bioclasts (sample pp5.3), b) lamina with abundant filaments and peloids (sample KM3), c) grainstone composed of echinoderms (crinoids) and pelletal/ooidal grainstone (G) and bio/intraclastic wackestone (W) lithoclasts (sample KM5), d) wackestone with crinoids, fenestral mudstone (F) lithoclast, unrecognisable bioslasts and benthic foraminifera with determined *Protopennerolis striata* (sample KM8), e) wackestone dominated by crinoids and ooids with fracture filled with dog-tooth rim cement and matrix of the breccia (sample KM5), f) hemipelagic wackestone with calcified radiolarian, filaments, plankton foraminifer and other bioclasts (sample KM0.1).

pure mudstone. In some clasts, pelagic fossils indicate open-marine conditions. Next is a recrystallized limestone (UD9), which sporadically shows ghosts of large fossils such as bivalves and ammonites (Fig. 16h). In the Ponikve Klippe and Mrzli vrh sections dolomitization is present and

some clasts are completely replaced by dolomite (UD10). Last microfacies type (UD11) are chert clasts. In some cases, they most certainly represent replacement cherts, as they show relicts of the primary packstone, grainstone, and boundstone texture.

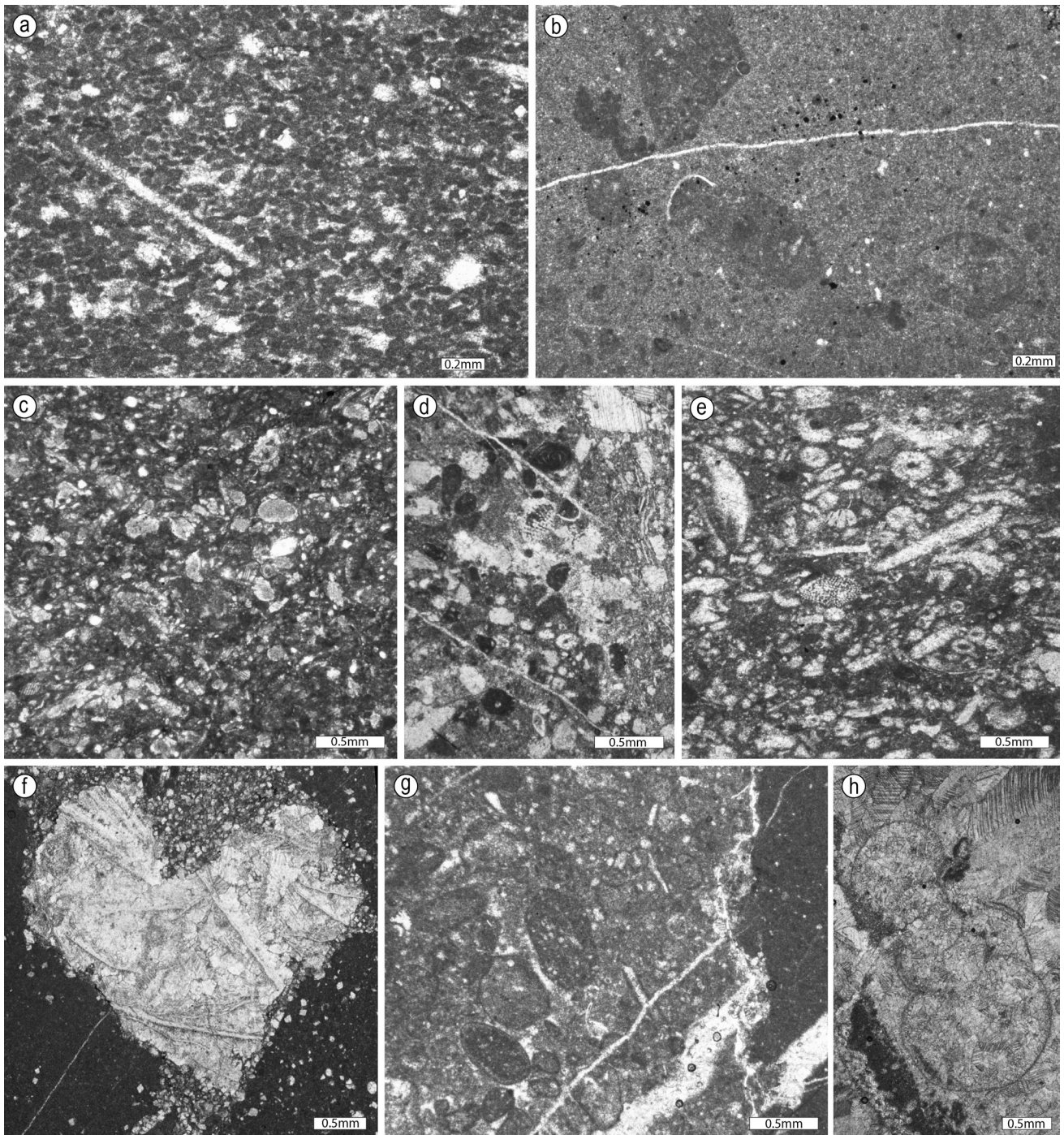


Fig. 16. age-undetermined (UD) lithoclasts: a) pelletal packstone with subordinate bioclasts (UD1) (sample pp18.0), b) intraclastic wackestone with ostracodes (UD2) (sample JE40.4), c) well sorted bioclastic/pelletal packstone (UD3) (sample KM0.1), d) wackestone composed predominantly of echinoderms (crinoids) and ophthalmitid foraminifera (UD4) (sample M105), e) packstone dominated with sponge spicules, and subordinate crinoids, other unrecognisable bioclasts and peloids (UD 5) (sample KM8.1), f) heart-shaped lithoclasts of the filament grainstone (UD6) (sample pp5.5), g) packstone with anemuran pellets, intraclasts, pellets and micritized ooids and bioclasts (UD7) and mudstone (UD8) lithoclasts to the right (sample JE43.4), h) recrystallized floatstone (UD9) with ammonite (sample T2/5).

Table 1. Detailed description of composition, biostratigraphy, and sedimentary environment of microfacies types (abbreviations: M – mudstone, W – wackestone, P – packstone, G – grainstone, R – rudstone, F – floatstone, B – boundstone, D – dolostone, SMF – standard microfacies).

AGE	CLAST TYPE	DESCRIPTION
Upper Triassic	T1 Bioclastic W	<i>Composition:</i> medium-grained grains prevail; echinoderms (crinoid ossicles, echinoid spines), fragmented large bivalves (exceptionally even cm-sized), thin-shelled bivalves, foraminifers (miliolids, lagenids, and nodosarids), ostracods, ammonites, rare bryozoans and peloids. Large intra/bioclasts can have crusts made from calcimicrobes and foraminifers). It can contain laminae of crinoidal G (wash-out sediment; T1/4) and stromatolites (LK2-71.7). <i>Age:</i> upper Carnian – Rhaetian (PODBRDO: foraminifers <i>Lenticulina</i> sp., <i>Decapalina</i> sp., <i>Miliolipora cuvillieri</i> Brönnimann & Zaninetti, LOVRIS: foraminifers <i>Parvalamella friedli</i> (Kristan-Tollmann), <i>Aulotortus sinuosus</i> Weynschenk, <i>Aulotortus tumidus</i> (Kristan-Tollmann)). <i>SMF and environment:</i> SMF 8 – open shelf.
	T2 Pelletal bioclastic P	<i>Composition:</i> structure is fine-grained P that can be partly washed. Some laminae are G or W containing the same type of grains: pellets (peloids) and bioclasts, predominantly diverse foraminifers. Other grains are intraclasts, echinoderms, ostracods (can be abundant in some clasts – pp4.6), bivalves, gastropods; dasycladacean algae, <i>?Thaumatoporella</i> . Transition to G (type T3) was observed within the same clast (JE39.4, DM97, TR37.2). This facies is locally bioturbated and contains large scale dissolution voids filled with crusts of bladed cements (DM63.5, DM71.5), geopetally filled stromatolites (325), rare oncoids (DM97) and isolated corals (TR32.5). <i>Age:</i> Norian-Rhaetian (PODBRDO: foraminifers <i>Galeanella tollmanni</i> (Kristan), <i>Miliolipora cuvillieri</i> Brönnimann & Zaninetti, Duostominidae, LOVRIS: foraminifers <i>Galeanella tollmanni</i> (Kristan), <i>Decapalina schaeferae</i> (Zaninetti et al.), <i>Alpinophragmium perforatum</i> Flügel, MRZLI VRH: foraminifers, <i>Auloconus permodiscoides</i> (Oberhauser), <i>Parvalamella friedli</i> (Kristan-Tollmann), <i>Aulotortus sinuosus</i> Weynschenk, <i>Aulotortus tumidus</i> (Kristan-Tollmann), <i>Galeanella tollmanni</i> (Kristan), Duostominidae, <i>Duotaxis birmanica</i> Brönnimann, Whittaker & Zaninetti, <i>Triasina hantkeni</i> Majzon, <i>Agathamina austroalpina</i> Kristan & Tollmann, Duostominidae <i>Duotaxis</i> sp., <i>Ophthalmidium</i> sp. and <i>Variostoma helicta</i> (Tappan), and microproblematica <i>Thaumatoporella pavovesiculifera</i> Raineri). Clasts containing <i>Triasina hantkeni</i> Majzon reveal Rhaetian age. ŠKOFJA LOKA-PODPURFLCA: Duostominidae., ŠKOFJA LOKA-TRNJE: <i>Duotaxis</i> sp., MIRNA: foraminifers <i>Aulotortus</i> sp. and <i>Trochammina almtalensis</i> Koehn-Zaninetti). <i>SMF and environment:</i> between SMF18-for and SMF 16; lagoon or sheltered areas within the reef.
	T3 Intra/bioclastic pelletal G	<i>Composition:</i> medium- to coarse-grained G, locally partly washed P; predominant grains are intraclasts, pellets and diverse bioclasts: fragmented bivalves (often in form of cortoids), foraminifers (miliolids, textularids, ...), echinoderms, rare gastropods, brachiopods, and grains composed of calcimicrobes (can form cores of few-mm large intraclasts), oncoids was also detected (337). One clast consists of pellets, abundant foraminifers (predominantly <i>Galeanella</i> sp.), frequent small radial ooids, and an oncoid (LK2-41.8). <i>Age:</i> Middle to Upper Triassic, predominantly Norian-Rhaetian (PODBRDO: foraminifers: <i>?Duostominidae</i> , <i>Trochammina alpina</i> Kristan-Tollmann, <i>Trochammina jaunensis</i> Brönnimann & Page, <i>Aulotortus sinuosus</i> Weynschenk; LOVRIS: foraminifer <i>Galeanella tollmanni</i> (Kristan), MRZLI VRH: foraminifers <i>Auloconus permodiscoides</i> (Oberhauser), <i>Parvalamella friedli</i> (Kristan-Tollmann), <i>Triasina hantkeni</i> Majzon). Clasts containing <i>Triasina hantkeni</i> reveal Rhaetian age. ŠKOFJA LOKA-TRNJE: foraminifers <i>Galeanella tollmanni</i> (Kristan), <i>Alpinophragmium perforatum</i> Flügel, Duostominidae ŠKOFJA LOKA-PODPURFLCA: foraminifer <i>Endoteba</i> ex gr. <i>controversa</i> Vachard & Razgallah, MIRNA: foraminifer <i>Galeanella tollmanni</i> (Kristan). <i>SMF and environment:</i> SMF 11, sand shoals at the platform margin.
	T4 Bioclastic R	<i>Composition:</i> structure passes from R to locally coarse-grained G: predominant grains are bioclasts: large grains are fragments of frame-builders: calcisponges, corals and calcimicrobes; other smaller bioclasts are echinoderms, foraminifers, fragmented bivalve shells, <i>Tubiphytes</i> , rare gastropods and dasycladacean algae. Other grains are intraclasts and pellets. Large grains can have microbial encrustations. Bioclasts in some clasts can be altered to cortoids. <i>Age:</i> Norian-Rhaetian (PODBRDO: foraminifers: <i>Galeanella tollmanni</i> (Kristan), Duostominidae, <i>Reophax</i> sp., <i>Aulotortus sinuosus</i> Weynschenk and <i>Decapalina schaeferae</i> (Zaninetti, Altiner, Dager & Ducret); sponge: <i>?Cryptocoelia</i> sp.; coral: <i>Astraeomorpha pratzi</i> Volz; MIRNA: foraminifers <i>Galeanella tollmanni</i> (Kristan), Duostominidae). <i>SMF and environment:</i> SMF11, SMF5 reworked reefal material within or on either side of the reef.
	T5 reefal litho/bioclastic F/R	<i>Composition:</i> There are two main constituents. The first are bioclasts of frame-building organisms up to a few mm in size, such as corals and calcisponges. Subordinate encrusters are calcimicrobes and foraminifers. The second main constituent are lithoclasts of A) reefal limestones, including sponge/coral B with the interstices filled with intra/bioclastic pelletal P/G or with sparite; these clasts resemble microfacies T6, B) pelletal intra/bioclastic P/G (resembling clasts of microfacies types T2 and/or T3), C) pelletal P (resembling clasts of microfacies type UD1), and less frequent D) coarse bioclastic limestone with fragmented bioclasts and intraclasts with echinoderms (resembling clasts of microfacies type T1). The space between large clasts is filled by coarse-crystalline cements (fibrous and dog-tooth rim cements, and drusy mosaic cements), less frequently by micrite. In the area of Škofja Loka (Trnje section) matrix contains echinoderms and sponge spicules. <i>Age:</i> Norian-Rhaetian (PODBRDO: foraminifers: <i>Galeanella tollmanni</i> (Kristan), <i>Reophax rudis</i> (Brady); Duostominidae; sponge <i>?Battaglia minor</i> Senowbari-Daryan & Shaefer, MRZLI VRH: foraminifer <i>Decapalina schaeferae</i> (Zaninetti, Altiner, Dager & Ducret); ŠKOFJA LOKA-TRNJE: foraminifers <i>Decapalina schaeferae</i> (Zaninetti, Altiner, Dager & Ducret), <i>Miliolipora cuvillieri</i> Brönnimann & Zaninetti, <i>Galeanella</i> sp., <i>Endotriada</i> sp.). <i>SMF and environment:</i> SMF 6 fore- or intra-reef breccias.
	T6 B	<i>Composition:</i> The frame is built by corals (mostly faceolid) and sponges (stromatoporoids, inozoan, subordinate chaetetid calcisponges), often encrusted by calcimicrobes and foraminifers, serpulids, in some clasts also by <i>Thaumatoporella</i> sp. <i>Baccanella</i> sp. was spotted. Frame-builders tend to be strongly recrystallized. Intergranular space is filled with coarse-crystalline cements (mostly fibrous rim and drusy mosaic or bladed cements), or intra/bioclastic pelletal P/G (closely resembling microfacies types T2 and T3, described above). Sediment can contain birds-eye fenestrae. Some clasts are strongly dolomitized, and some also silicified (TR44). <i>Age:</i> Norian-Rhaetian (PODBRDO: foraminifers: <i>Galeanella tollmanni</i> (Kristan), Duostominidae; <i>Decapalina schaeferae</i> (Zaninetti, Altiner, Dager & Ducret), <i>Miliolipora cuvillieri</i> Brönnimann & Zaninetti; LOVRIS: foraminifers <i>Endotriada tyrrenica</i> Vachard, Martini, Rettori & Zaninetti, <i>Endotriada</i> sp., <i>Miliolipora</i> sp., ŠKOFJA LOKA-TRNJE: <i>Galeanella</i> sp., MIRNA: foraminifer <i>Alpinophragmium perforatum</i> Flügel, and microproblematica <i>Bacinella irregularis</i> Radojčić). <i>SMF and environment:</i> SMF7; marginal reefs.

AGE	CLAST TYPE	DESCRIPTION
Lower Jurassic	LJ1 Intra/ bioclastic pelletal G with aggregate grains and ooids	<i>Composition:</i> medium to coarse-grained G, subordinate partly washed P; in composition similar to microfacies type T3, but contains less fossils with the addition of aggregate grains (lumps) and ooids, whereas intraclasts tend to be irregularly shaped; some grains have micritic margins or encrustations. Oncoids were also detected. In one clast they form laminae of oncoidal R that separate microfacies LJ1 from ooidal G (LJ2). Oncoidal cores are formed of <i>?Thaumatoporella</i> and calcimicrobes (JE41.4). Foraminifers are mostly textulariids. Some clasts contain laminae with large gastropods. In clasts with abundant aggregate grains, bivalves, crinoids, calcimicrobic grains, <i>?Thaumatoporella</i> , and cortoids were spotted (JE43.4). A clast containing a dasycladacean fragment was also documented, (pp19,7) and another with abundant cortoids and large bioclasts: bivalves, brachiopods, gastropods, dasycladacean algae, ammonite, and a foraminifer <i>Orbitopsella</i> sp. (327). <i>Age:</i> Lower Jurassic (PODBRDO: coral <i>Phacelophyllia termieri</i> Beauvais; IDRIJA PRI BAČI: foraminifers <i>?Lituosepta recoarensis</i> Cati, <i>Orbitopsella</i> sp., MRZLI VRH: foraminifer <i>?Siphovalvolina</i> sp., ZAPOŠKAR: <i>Duotaxis metula</i> Kristan, ŠKOFJA LOKA-PODPURFLCA: <i>?Siphovalvolina</i> sp., MIRNA: corals <i>Rhabdophyllia phaceloidea</i> Beauvais, <i>Thecactinastreaa krimensis</i> Turnšek, <i>Funginella domeriensis</i> Beauvais, foraminifers <i>Involutina liassica</i> Jones, <i>?Siphovalvolina</i> sp.). In one clast in Podpurfica section, a Middle Jurassic foraminifer <i>Nautiloculina</i> was determined. <i>SMF and environment:</i> SMF 15 to SMF 17; platform margin sand shoals.
	LJ2 Ooidal G	<i>Composition:</i> predominant grains are medium-sized, radial ooids, mostly with micritic cores, very subordinate bioclasts. Other grains are intraclasts, peloids, and bioclasts: echinoderms, fragmented mollusks and foraminifers (ophthalmidiid foraminifers, and <i>Reophax</i> sp.). In one clast a chaetid grain was noted (2A-6). Some clasts are partly washed P and have bimodal grain-size distribution with large ooids and bioclasts (mostly crinoids) and small peloids (pellets). Some clasts are composed of fine-grained radial ooids and peloids/pellets (KM5). In one clast this facies passes into oncoidal R (JE41.4) that contains foraminifer <i>Siphovalvolina</i> sp. In one clast this facies passes to bioclastic limestone (J2). <i>Age:</i> Lower Jurassic (MIRNA: <i>Involutina liassica</i> Jones, <i>Siphovalvolina</i> sp.). <i>SMF and environment:</i> SMF 15; platform margin sand shoals.
	LJ3 Crinoidal G	<i>Composition:</i> G, also subordinate P that can contain lithoclasts and fossils some mm in size. Predominant grains are crinoids (echinoderms), angular intraclasts, and sometimes pellets. Crinoids can contain micritic encrustations. Other grains are foraminifers (textulariids, lagenids, ophthalmidiid), bivalves (often fragmented), gastropods, ostracods. Grains some few mm in size are lithoclasts of bioclastic W (in facies similar to clast-type T1 and LJ4) and belemnites. In some clasts crinoids strongly predominate or even represent all the grains. These clasts can be often partly silicified. <i>Age:</i> Lower Jurassic (MIRNA: <i>Involutina liassica</i> Jones). <i>SMF and environment:</i> SMF 12-CRIN; open shelf/platform slope accumulation of crinoidal debris.
	LJ4 Bioclastic W	<i>Composition:</i> grains are mainly medium-sized. Predominant grains are sponge spicules, echinoderms and ostracods. Other bioclasts are amonites, filaments, foraminifers (ophthalmidiids, lagenids, nodosarids, textularids). P and F textures also occurs. These clasts closely resemble type T1 and MJ3, but generally contain more sponge spicules. Without diagnostic fossils it is usually impossible to distinguish the three types. In clasts where it passes to ooidal G (JE35.4) it also contains medium-sized ooids with radial inner and tangential outer cortex (equal to those of ooidal G). Ooids were observed also in one sample (KM5) from the Mirna Valley. This microfacies can also pass to crinoidal G (T2/4). <i>Age:</i> Lower Jurassic (ŠKOFJA LOKA-PODPURFLCA: <i>Involutina farinacciae</i> Brönnimann & Koehn-Zaninetti, MIRNA: <i>Involutina liassica</i> Jones). <i>SMF and environment:</i> SMF 8 – open shelf.
Middle Jurassic	MJ1 Ooidal P/W	<i>Composition:</i> fine- to medium-sized tangential and/or radial ooids, peloids (pellets), intraclasts and echinoderms. Other bioclasts are bivalve fragments, foraminifers (lagenids, textularids), ostracods. Some clasts contain quite abundant thin-shelled bivalves (filaments), sponge spicules, calcispheres and/or radiolarians. Ammonites were detected. In the Mirna section, filament-rich clasts also contain planktic foraminifera (KM3.0) and clasts dominant by pellets and subordinate ooids (KM7.2). This microfacies locally passes into bioclastic M/W (microfacies UD5) within the same clast. Specific sub-type of this clasts group (pp14) is composed of alternating laminae of M and P/W with coarse-grained micritized ooids and subordinate intraclasts and echinoderms. Ooid cores are micritic or bioclastic (gastropods, ostracods). Oncoids also appear. <i>Age:</i> ?Middle Jurassic (ŠKOFJA LOKA-PODPURFLCA: planktic foraminifers). <i>SMF and environment:</i> ?SMF15; structural inversion where grains typical of high-energy conditions are re-sedimented to low-energy, probably deeper water environment.
	MJ2 Lithoclastic crinoidal G	<i>Composition:</i> coarse-grained G composed of echinoderms (mostly crinoids), micritic (intra)clasts, fragmented brachiopods and bivalves, and foraminifers (ophthalmidiid foraminifers, lagenids, nodosarids, fragments of sessile foraminifers). Common are also lithoclasts: A) pelletal/intraclastic/ooidal G and P, B) W with radiolarians and filaments, C) fenestral M, D) spiculitic W, and E) bio/intraclastic W. <i>Age:</i> Middle Jurassic (MIRNA: <i>Protopenneroplis</i> sp.). <i>SMF and environment:</i> SMF 8 – open shelf, but close to source of lithoclasts.
	MJ3 Litho/ bioclastic W	<i>Composition:</i> grains are medium- to coarse-grained W with microsparite matrix. Predominant grains are echinoderms (crinoids as well as orchin spines) and foraminifers (ophthalmidiid foraminifers, lagenids, nodosarids). Other grains are micritic (intra)clasts, fragmented bivalves and brachiopod, ooids and ammonites also occur. These clasts closely resemble microfacies types T1 and J2 but contain more lagenid foraminifers and lithoclasts: A) pelletal ooidal G and P, B) W with radiolarians and filaments, and C) fenestral M. Matrix is microsparite. Without diagnostic fossils it is usually impossible to distinguish the three types. <i>Age:</i> Middle Jurassic (MIRNA: <i>Protopenneroplis striata</i> Weynschenck). <i>SMF and environment:</i> SMF 8 – open shelf.
	MJ4 Bioclastic (hemipelagic) M/W	<i>Composition:</i> predominantly fine-grained W, sometimes with very rare grains (M). Grains are bioclasts, mostly thin-shelled bivalves, ostracods, and calcispheres and/or calcified radiolarians. Rare are lagenid foraminifers, small echinoderms, sponge spicules and other (unrecognisable) small debris. Amonites and gastropods were detected within such clast in the Mirna section (KM0.1, KM4.1), and planktic foraminifers (KM3.0). Tiny pellets are locally visible within matrix. Bioturbation and in one clast (LK2-57) also stromatolites were noticed. These clasts tend to be dolomitized. <i>Age:</i> ?; at least part of clasts are Middle Jurassic (MIRNA: <i>Protoglobigerina</i> sp.). <i>SMF and environment:</i> SMF3 pelagic limestone of the deep-water sedimentary environment (?mud-chips).

AGE	CLAST TYPE	DESCRIPTION
Undetermined	UD1 Pelletal P	<i>Composition:</i> fine-grained P that can be partly washed and bioturbated. Predominant grains are pellets. Other are bioclasts, such as small foraminifera, calcispheres, and ostracods. Matrix is mostly microsparite. Some clasts contain sponge spicules and other filaments (KM13.4; KM14.4), the latter representing transitional facies to filament P/G (microfacies UD6). Rare clasts of this group can contain small fenestrae (pp18, KM8.1, JE39.4). When laminated, some coarse laminae contain intraclasts and ooids and probably represent transitional facies to ooidal G (JE43.4). <i>Age:</i> Large clast from the top of the Lovriš section yielded late Norian to early Rhaetian conodonts <i>Norigondolella steinbergensis</i> (Mosher) and <i>Zieglerioconus rhaeticus</i> Kozur and Mock, but this clast group is almost certainly also of Jurassic age, as in some clasts it contains laminae of ooidal limestone (for this reason we keep it among undetermined clasts). <i>SMF and environment:</i> SMF16 (21) or SMF2; low-energy environment, either restricted lagoon (with subaerial exposure) or open shelf.
	UD2 Intraclastic W	<i>Composition:</i> W with medium-sized intraclasts and pellets, micritized ooids were also detected. Some clasts contain ostracods, unrecognisable bioclastic debris, fenestrae, and large dissolution voids filled by blocky calcite (LK2-17.5; LK2-18.8). <i>Age:</i> ? <i>SMF and environment:</i> ?SMF; structural inversion, where grains typical for high-energy conditions are re-sedimented to a low-energy environment (either lagoon or deeper water).
	UD3 Bioclastic pelletal P	<i>Composition:</i> fine-grained P, composed of bioclasts, such as echinoderms, fragmented bivalves (including filaments), ostracods, calcispheres, foraminifers. Half the grains are pellets. Elongated grains are parallel-oriented. <i>Age:</i> ? <i>SMF and environment:</i> ?SMF4, presumably re-sedimented limestone (calciturbidite).
	UD4 Crinoidal foraminiferal W	<i>Composition:</i> W that laterally pass to partly washed P. It is dominated by echinoderms, ophthalmidiid foraminifers (textularids and lagenids also occur) and small pellets. Rare grains are fragmented bivalves, brachiopods, ostracods and ooids. A subtype of this microfacies occurring in the Lovriš section is P, dominated by echinoderms and pellets. This subtype also contains rare foraminifers. (LK2-8.6, LK 2.8 and LK 12.5) <i>Age:</i> ? <i>SMF and environment:</i> SMF 12-CRIN; open shelf/platform slope accumulation of crinoidal debris.
	UD5 Spiculite crinoidal P	<i>Composition:</i> fine-grained, bioturbated P, composed of sponge spicules and echinoderms. Other grains are foraminifers, ostracods, radiolarians, and pellets. Matrix can be recrystallized to microsparite. Some spicules are calcedonic. <i>Age:</i> ? <i>SMF and environment:</i> SMF 12-CRIN and SMF 2 open shelf/platform slope/basin floor.
	UD6 Filament P/G	<i>Composition:</i> The first subtype is G, composed of accumulated filaments (thin-shelled bivalves) and very rare echinoderm fragments. Cement is drusy-mosaic cement (pp; 5.5; pp11.4). The second subtype is P, which is dominated by filaments, but can also contain echinoderms, peloids, foraminifers, and ammonites. Filaments can have thick rims of fibrous cements, mostly concentrated at one side of the shells (in clast within KM7.2 sample infiltration matrix postdates the cementation). One clast is densely packed P, where predominant filaments wrap around intraclasts, rare echinoderms and foraminifers (occurs in the Idrija pri Bači section in samples 354A; 354B). <i>Age:</i> ?Jurassic. <i>SMF and environment:</i> SMF 12-S open shelf/platform slope/basin floor accumulation of filaments.
	UD7 Coarse peloidal P	<i>Composition:</i> coarse-grained P, composed of peloids and rare micritized oval bioclasts (presumably dasycladacean algae), and intraclasts. Ostracods and small foraminifers were spotted. A sub-type was spotted (JE43.4): W/P with anemuran pellets, other grains are similar, but bivalve fragments, calcispheres and lagenid foraminifers additionally appear. <i>Age:</i> ? <i>SMF and environment:</i> SMF 16 restricted lagoon.
	UD8 M	<i>Composition:</i> mostly pure M. It locally contains ostracods, foraminifers, or pelagic bioclasts (filaments, radiolarians). The matrix is dense micrite, locally microsparite. Rare fenestrae (geopethally filled cavities) occur in few clasts. Some contain numerous fenestrae (T2/10). <i>Age:</i> ? <i>SMF and environment:</i> SMF23 and 21 or SMF3; restricted low-energy environment (restricted lagoon or anoxic basin).
	UD9 Recrystallized F	<i>Composition:</i> strongly recrystallized F (or pure R) with still recognized large fossils, such as ammonites and bivalves (T2/6). Brachiopods and gastropods also occur in other clasts (LK2-16.5). Cements are dog-teeth rim cements, followed by coarsely crystalline bladed cements, and calcisiltite (crystal silt). A little amount of matrix clings to the fossil shells. It is P, composed of tiny pellets and rare ostracods. <i>Age:</i> ? <i>SMF and environment:</i> ? SMF 8 deep-water environment.
	UD10 D	<i>Composition:</i> coarsely crystalline D. The primary texture is locally partly preserved. It is bioclastic M/W (microfacies type UD5), or B (microfacies type T5). <i>Age:</i> ?, some are probably dolomitized clasts of Norian-Rhaetian B. <i>SMF and environment:</i> ? dolomitization obscured information. Some were presumably reefal, others hemipelagic limestone.
	UD11 chert	<i>Composition:</i> microcrystalline chert, locally with concentrated carbonate crystals (in laminae or in patches). One clast laterally passes into B (microfacies T6), a different one into intra/bioclastic pelletal G (microfacies T3). The primary composition of medium-grained P/G is locally recognizable. Silicification can be strong in B clasts (microfacies T6). <i>Age:</i> ? <i>SMF and environment:</i> mostly replacement chert (contains carbonate and passes into limestone).

Discussion

Facies distribution of the Ponikve Breccia Member and corresponding Lower resedimented limestones of the SB indicates that the south-lying DCP was a source area of the Middle Jurassic resedimented material. Namely, coarse and thick limestone breccia beds occur solely in the southernmost SB outcrops (structurally lowest nappe), become finer and thinner (in the form of calciturbiditic calcarenites) in the central part of the basin (central nappe), and are completely absent in the northern part of the SB (structurally highest nappe) (Figs. 17 and 18). Additional proof pointing to the source area is provided by the abundance of ooids within the breccia matrix and inside calciturbidites. As the DCP is the only known post-Aalenian active platform in this part of the Adria microplate (review in Vlahović et al., 2005), the DCP is considered the only possible source of these resediments.

The clast- and matrix-analysis of the Limestone Breccia member therefore enables the reconstruction of the non-outcropping DCP margin from three distinct time periods. The Upper Triassic (Norian–Rhaetian) and Lower Jurassic reconstructions are based solely on the records retrieved from the clast analysis. For the Middle Jurassic reconstruction, the data from matrix- and clast analysis was combined, which considered the age of the matrix to be contemporaneous with the sedimentation event of the breccia beds.

The Upper Triassic: a reef-rimmed epeiric platform

Epeiric platforms covering the tropical margins of the Neotethys Ocean generally consisted of a wide tidal flat, a shallow lagoon, and a platform margin rimmed by reefs (Mandl, 2000; Bernecker, 2005). The tidal flat is stratigraphically represented by the Hauptdolomit (Glavni dolomit/Dolomia Principale/“Main Dolomite”), gradually passing into the bedded Dachstein limestone (Mandl, 2000; Bernecker, 2005; Kovács et al., 2011). Characteristic for these beds is the so-called Lofer cycle, comprising a thin breccia member, a laminated mudstone (intertidal stromatolite), and a biogenic wackestone and/or floatstone with large megalodontid bivalves, gastropods, and locally corals (Fisher, 1964; Ogorelec & Rothe, 1993; Satterley, 1996; Ogorelec & Buser, 1996; Haas, 2004; Samankassou & Enos, 2019). The marginal peri-reef belt has been recorded by Piller (1981), Wurm (1982), Haas et al. (2010), Gale et al. (2012), and Martindale et al. (2013), among others. The massive reef lime-

stone is composed of interreef breccias and small patches of coral-sponge-solenoporacean algae reefs. Molluscs, benthic foraminifers, and dasy-cladacean algae are among the diverse bioclasts within sand-grained detritus (Wurm, 1982; Gale et al., 2013). The slope is characterised by calciturbidites composed of grains derived from the top of the platform and its margin (Rožič et al., 2009; Gale, 2010; Gale et al., 2014). In the interior of the platform small basins of the Kössen type, characterised by depositions of marlstone and limestone and a diminished diversity of benthic fauna came into existence during the Rhaetian. Patch reefs developed at the rims or within these basins. Their composition is comparable to the composition of the marginal Dachstein-type reefs (Schäfer & Senowbari-Daryan, 1981; Kuss, 1983; Bernecker, 2005). In the inner parts of the platform, significantly more restricted basins already formed in the Norian. These basins are characterised by reduced oxygen levels, abnormal salinities and/or eutrophic conditions. Along their margins, small bioherms composed of terbellid worms encrusted in microbialite were present. (Cirilli et al., 1999; Iannace & Zamparelli, 2002).

Norian–Rhaetian Hauptdolomit and Dachstein limestone of the northern External Dinarides have been most intensively studied by Ogorelec and Rothe (1993). Both formations show characteristics of the internal part of the platform, with well-developed Lofer cycles. In the northern External Dinarides, the Dachstein-type reefs are not preserved (Buser et al., 1982; Turnšek, 1997).

Six microfacies types from clasts (T1–T6) were attributed to the Late Triassic DCP. These clasts can reach the size of boulders. Boundstone with typical Norian–Rhaetian reef-dwelling foraminifers *Galeanella*, *Decapoolina*, *Miliolipora* and *Alpinophragmium* (see Gale, 2012) strongly suggest that the original margin of the DCP was rimmed by Dachstein-type reefs, which later collapsed into the SB together with Lower and Middle Jurassic deposits (Fig. 17). Bioclastic rudstone (T4) and litho/bioclastic floatstone/rudstone are interpreted as reef breccia akin to lithoclastic rudstone Gale et al. (2013). The close affinity with the reef zone is supported by the abundance of framebuilders and reef-dwelling microbiota (e.g. *Decapoolina*, *Miliolipora*, *Galeanella*). Bioclastic wackestone (T1), pelletal bioclastic packstone (T2), intra/bioclastic pelletal grainstone, and possibly also part of pelletal packstone (UD1) were also found in clasts within the litho/bioclastic floatstone/rudstone (T5), some also in

boundstone (T6), and thus also likely deposited close to the margin of the platform. This is again supported by the presence of some microfossils. Bioclastic wackestone (T1) might originate in the open-shelf/slope area.

The Lower Jurassic: a lagoon, rimmed by sand shoals

Like the Upper Triassic, the outcropping Lower Jurassic successions from the northern External Dinarides show facies associations characteristic for the inner platform developments. General Lower Jurassic successions from the northern Dinarides were described by Dozet and Strohmenger (2000), Črne and Goričan (2008), Miler and Pavšič (2008), Dozet (2009), Ogorelec (2011), and Gale and Kelemen (2017), among others. An unpublished thesis of Buser (1965) also provides a regional overview of Jurassic successions from southern Slovenia. Lower Jurassic successions from other parts of the Dinarides were (among others) described by Dragičević and Velić (2002), Tišljarić et al. (2002), Bucković (2006), Črne and Goričan (2008), Čadjenović et al. (2008), and Martinuš et al. (2012).

Despite the biocalcification crisis at the Triassic/Jurassic boundary (e.g. Kiessling et al. 2007), a carbonate platform continued to exist (Fig. 17). During the Hettangian, carbonate deposition continued under peritidal conditions. Characteristically, laminae are not wrinkled, but planar and smooth. During the Sinemurian and Pliensbachian, the topography of the platform gradually evolved from the epeiric, flat-topped platform into a platform, internally differentiated into lagoon, marginal shoals, and ephemeral emergent areas (Buser & Debeljak, 1996; Gale and Kelemen, 2017). This, together with the recovery and evolution of biota after the Triassic/Jurassic boundary extinction, results in distinct differences in microfacies. A transgressive trend towards more subtidal conditions was noted in central Slovenia, where most of the Sinemurian part of the succession is represented by mudstone and wackestone, subordinately peloidal and ooidal limestone. Oolithic and bioclastic-oolithic grainstone become predominant by the upper Sinemurian, and the facies association also includes mudstone, peloid wackestone, bivalve floatstone and rudstone, and peloid grainstone. In the Pliensbachian, these facies are joined by common oncoid and bioclast floatstone and rudstone, and lithotid floatstone and rudstone (Gale and Kelemen, 2017). Buser and Debeljak (1996) envisioned the platform margin as dominated by

ooidal and crinoidal shoals, and slope covered by breccias.

The Ponikve Breccia Member contains an abundance of clasts that have been attributed to the Lower Jurassic, either based on foraminifers or their microfacies. The clast microfacies types LJ2 (ooidal grainstone) and LJ1 (intra/bioclastic pelletal grainstone) probably originate from the ooidal shoals and a more agitated part of the internal lagoon, respectively.

In contrast, the crinoidal grainstone (LJ3) and the bioclastic wackestone (LJ4) clasts derive from a deeper water sedimentary environment. Lower Jurassic crinoid/sponge spicule rich limestones are characteristic for diverse environments, such as the drowned platforms of the Eastern Alps and the Trandanubian Range (Böhm et al. 1999; Gawlick et al. 2009; Haas et al. 2014), but they also occur in slope settings (Scheibner and Reijmer, 1999; Blomeier and Reijmer, 2002; Merino-Tomé et al., 2012; Della Porta et al., 2014). Here we emphasise that such facies are also typical for the Sedlo Formation, which originated on the JCP margin that experienced tectonic differentiation and accelerated subsidence already in the Pliensbachian (Šmuc, 2005; Šmuc and Goričan, 2005; Praprotnik Kastelic et al., 2013; Rožič et al., 2014b; Valand et al., 2019). This subsidence of the JCP margin correlates to the initiation of a second rifting phase of the Alpine Tethys that is well recognized also in the rest of the Southern Alps (Berra et al., 2009; Masini et al., 2013) and led to the creation of a North Adriatic Basin located west of the DCP (Masetti et al., 2012). This extension must have influenced the northern DCP margin and potentially led to the partial reorganization of the DCP architecture. Namely, it could have created a fault dissected, step-like margin and slope, which would be reflected in a shift from the carbonate platform to the carbonate ramp architecture of the northernmost part of the DCP. Such depositional setting provided open marine conditions favourable for the creation of the described facies-types. Alternatively, the crinoidal limestone could also represent Toarcian facies originating from the drowned platform margin. During this stage, the succession of the DCP is characterised by thin-bedded micritic limestone and crinoidal-ooidal limestone, recording transgression which roughly coincides with the OAE (Vlahović et al., 2005; Črne and Goričan, 2008; Dozet, 2009; Sabatino et al., 2013).

We note that coeval with Lithotid evolution the re-establishment of marginal reefs is locally documented for the late Lower Jurassic (Leinfelder

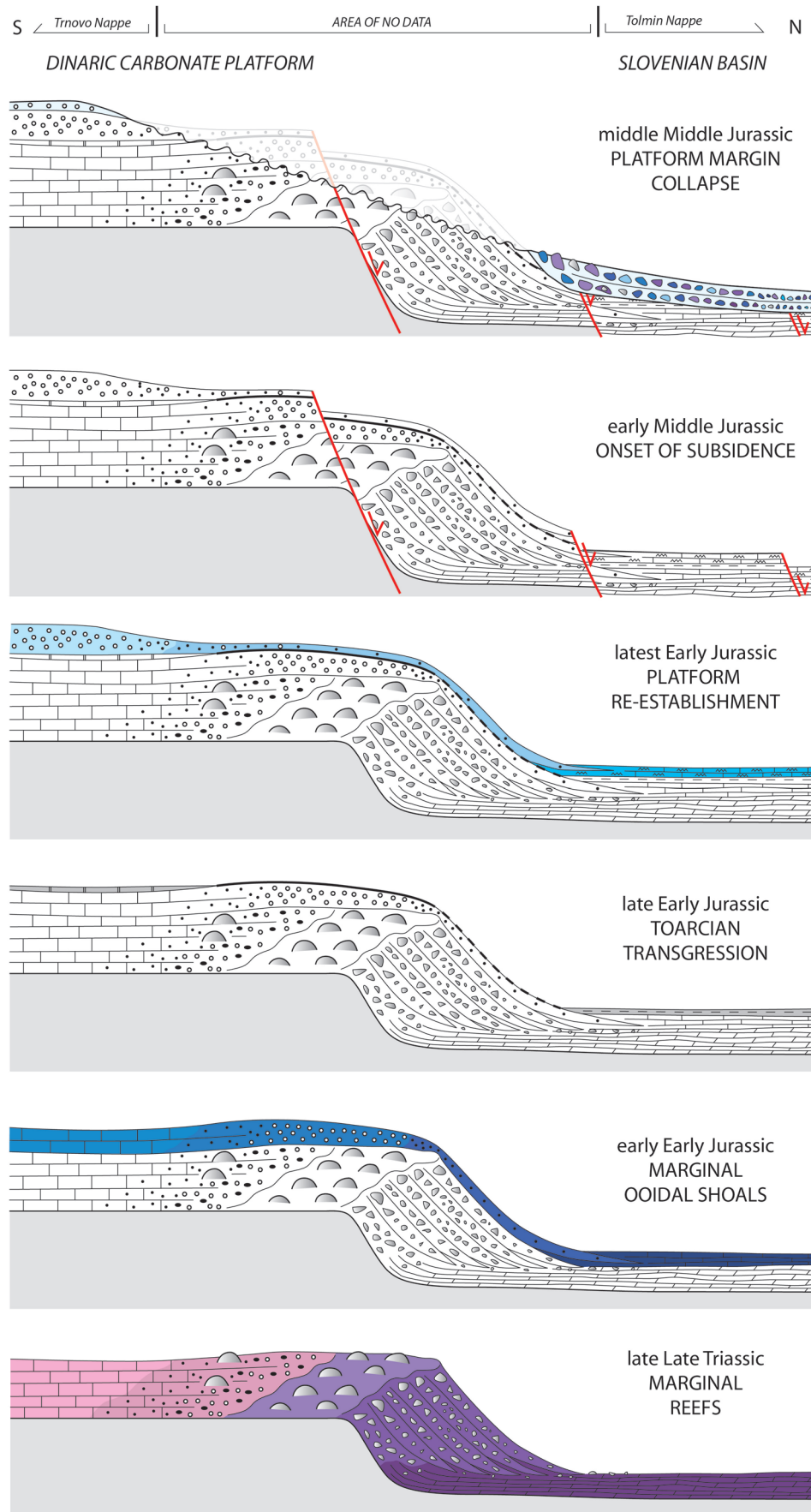


Fig. 17. Reconstruction of the Dinaric Carbonate Platform's northern margin from late Late Triassic (Norian–Rhaetian) reefs, through early Early Jurassic ooidal sand shoals, Toarcian transgression and re-establishment of the carbonate production up to the early- and mid-Middle Jurassic onset of extensional/transensional tectonics, which led to the collapse of the platform margin and deposition of the Ponikve breccia Member of the Tolmin Formation in the Slovenian basin.

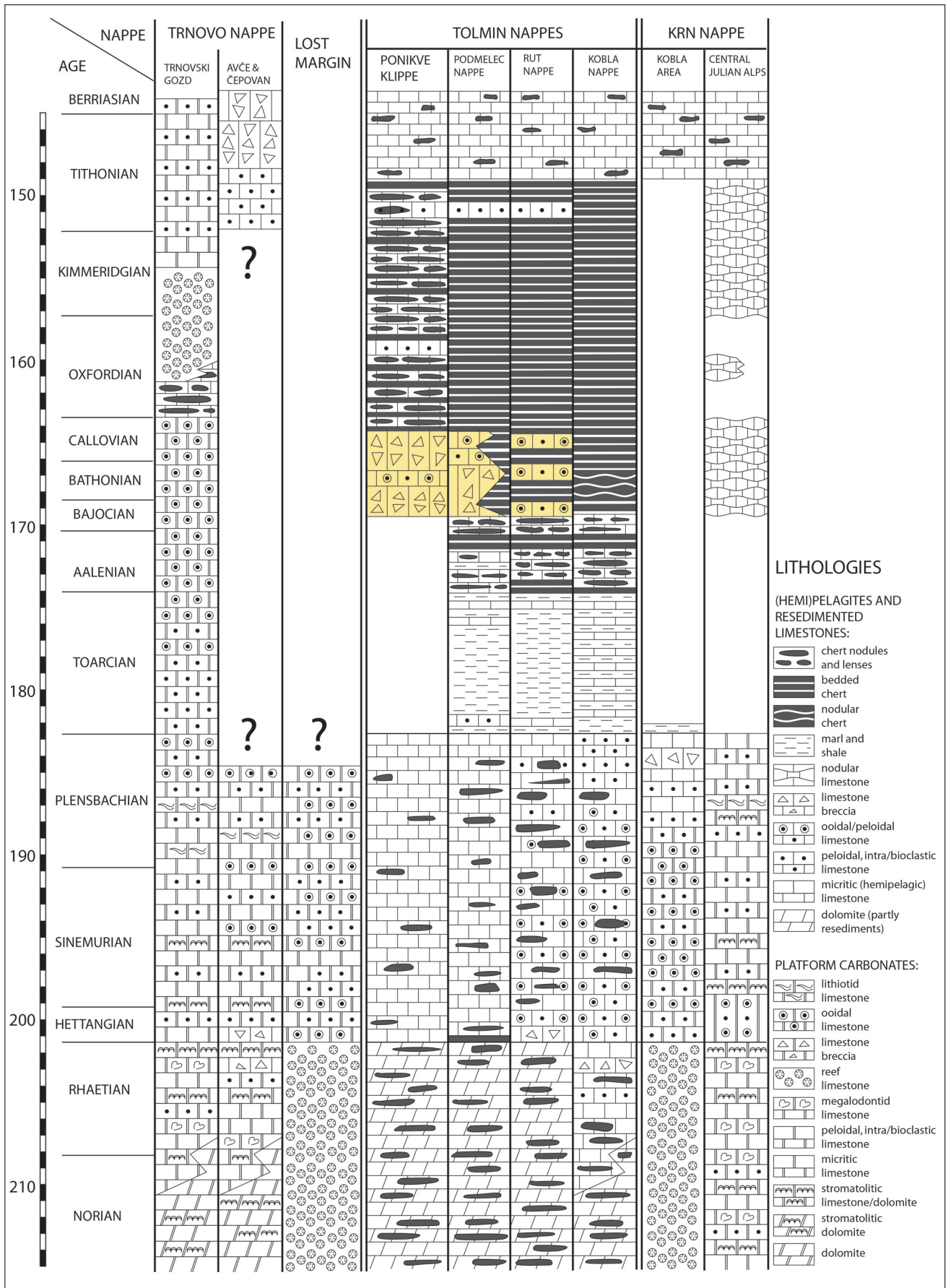


Fig. 18. Stratigraphic columns of the Dinaric Carbonate Platform, Slovenian Basin, and Julian Carbonate Platform with reconstructed (lost) margin of the Dinaric Carbonate Platform. Facies distribution of the Middle Jurassic resedimented limestones (including the Ponikve Breccia) indicate that the south-lying Dinaric Carbonate Platform was a carbonate material source area (compiled from Buser, 1986, 1996, Turnšek, 2007; Šmuc, 2005, Rožič, 2006, 2009; Rožič et al., 2014b; Kovač, 2016; time scale after Cohen et al., 2013; updated).

et al., 2002; Scheibner & Reijmer, 1999; Merino –Tomé et al., 2012; Della Porta et al., 2014). Local occurrence of coral patch reefs is known also from the Pliensbachian of the northern DCP (Turnšek & Košir 2000; Turnšek et al. 2003) with coral species corresponding to those determined in some Lower Jurassic grainstone lithoclasts (type LJ1; Podpurflca and Mirna sections). However, we do not support the existence of barrier reefs on the DCP because: A) Lower Jurassic age was not determined for the boundstone (or related) clasts and B) all other (better preserved) platform margins from the Southern Alps (Clari and Masetti, 2002; Masetti et al., 2012; Francheschi et al., 2013) as well as the DCP are dominated by ooidal sand shoals (Tišljjar et al., 2002; Črne & Goričan, 2008; Čadjenović et al., 2008).

Platform-basin transition zone prior to Middle Jurassic collapses

Breccia beds originated in the toe-of-slope and proximal basin plain environments. They sedimented as the result of debris flows and were a product of large-scale collapses of the DCP margin (for details see Rožič et al., 2019). Already within some sections presented herein, breccia beds are associated with turbidites, and towards the inner parts of the SB they pass completely into calciturbiditic layers (named Lower resedimented limestones) which occur within siliceous pelagites of the Tolmin Formation (Rožič, 2009; Goričan et al., 2012; Rožič et al., 2019).

The abundance of ooids and associated shallow-water grains (peloids, intraclasts, aggregate grains, oncoids and some bioclasts) in the matrix of the breccia and associated calciturbidites indicates that the gravity flows began at the DCP margin. Following the Toarcian deepening, the shallow water sedimentation gradually re-established on the margin and crinoid-rich ooidal limestones that pass upwards into pure ooidal limestone were deposited (Fig. 17) (Buser, 1996; Črne & Goričan, 2008; Miler & Pavšič 2008; Buser & Dozet 2009; Ogorelec 2011; Dozet & Ogorelec 2012).

In addition, the breccia matrix contains deeper-water bioclasts, most typically thin-shelled bivalves, whereas crinoids are also considered as predominantly deeper-water grains (see also below the discussion on Middle Jurassic lithoclasts). This indicates the incorporation of deeper-water (outer shelf/slope and basin) sediments into the debris-flows. In the Mrzli vrh section, ooids and associated shallow-water grains are almost entirely absent, while other grains (thin-shelled bi-

valves, crinoids, sponge spicules, phosphate, and glauconite) point to initiation of this debris flow from the distal deep slope/open shelf area.

Important information on the architecture of the platform-basin transitional area comes from lithoclasts that we have determined to be Middle Jurassic, and therefore contemporaneous with the sedimentation event. Ooidal packstone/wackestone clasts (MJ1) originate from the outer shelf close to the sand shoals. This is indicated by the co-occurrence of ooids and pelagic deeper-marine fauna. Such deposits are known from the Middle Jurassic successions on Mt. Matajur and Mt. Kobariški stol (Šmuc, 2012; Udovč, 2019; Rožič et al., 2022).

Bio/lithoclastic limestones of the MJ2 and MJ3 lithoclasts were proposed to have deposited basin-wards on a step-like slope (Fig. 17). Such paleotopography must have been produced by active faulting, as indicated by the abundance and diversity of lithoclasts, which occur inside these microfacies types (MJ2 and MJ3 lithoclasts types). These “lithoclasts inside lithoclasts” are of shallow-, as well as of deeper-water origin and could be pre-Middle Jurassic or generally contemporaneous with sedimentation of MJ2 and MJ3 lithoclasts types. It seems that their erosion may have been enhanced by the formation of escarpments.

The last type of Middle Jurassic lithoclasts is a hemipelagic limestone (MJ4). These lithoclasts originated with the debris-flow erosion of the contemporaneous, semi consolidated, hemipelagic (lower slope/basin) sediments and are therefore interpreted as “mud-chips”.

Information from lithoclasts of undetermined age

The majority of the lithoclasts of undetermined age was sedimented in deeper-marine environments. Pelletal packstone (UD1) and intraclastic wackestone (UD2) most probably deposited on the outer shelf. At least some of the UD1 clasts are Late Triassic in age, while some could be Jurassic. They were probably located between the typical marginal facies and slope environments similar to ooidal packstone/wackestone (MJ1). Crinoidal foraminiferal wackestone (UD4) and spiculite crinoidal packstone (UD5) correspond to similar crinoid rich clasts, which are typical for the outer shelf/slope environments in different time slices (T1, LJ3, LJ4, MJ2, MJ3).

Filament packstone/grainstone (UD6), mudstone (UD8), and bioclastic pelletal packstone (UD3) mostly originate from the erosion of slope

and basin sediments, the first two being hemipelagic, and the last resedimented limestones. Due to the absence of plankton foraminifers, they are considered Aalenian in age or older. Such facies are common in Lower Jurassic and Upper Triassic pelagites (Cousin 1981; Rožič 2009; Rožič et al. 2009, 2013; Gale et al., 2012, 2014). Therefore, debris flows of the Ponikve Breccia did not solely erode the contemporaneous basinal sediments (MJ4), but also older hemipelagic strata. This is also evident from the stratigraphic position of the breccia megabeds that overlie the older basinal successions with a stratigraphic gap (mostly overlying the Hettangian–Pliensbachian Krikov Formation). We already mentioned the basinal succession of the Dešna Hill in the Škofja Loka area, where (Bajocian or younger) radiolarite of the Tolmin Formation directly overlie the Norian–Rhaetian Bača Dolomite (Fig. 5 in Rožič et al., 2019). During the sedimentation of the Ponikve Breccia megabeds this area was bypassed and was very likely deeply eroded by debris flows.

Although shallow-water clasts predominantly originate from the margins of the DCP, some clasts indicate at least minor erosion of the platform interior. Such are coarse peloidal packstones (UD7), pelletal bioclastic packstones (T2), and partially also pelletal packstones (UD1). Due to diagenetic changes, such as recrystallization (UD9), dolomitization (UD10), and silicification (UD11), the origin of the last three lithoclast types is difficult to determine.

The Middle Jurassic collapse of the Dinaric Carbonate Platform margin

The Ponikve breccia originated with major collapses of the entire northern margin of the DCP (Fig. 17). This is evident from: A) breccia megabeds occur in an almost continuous belt from the westernmost outcrops of the SB near Tolmin, through the Škofja Loka area in central Slovenia, to the easternmost occurrences in the Mirna Valley, B) the extraordinary nature of the resedimentation events, with the large-scale debris-flow deposits representing a great contrast to the underlying and overlying successions characterized by basin–plain (hemi)pelagites, and C) clasts indicate deep erosion of the carbonate platform margin cutting down to the Upper Triassic reef limestone. The compilation of available biostratigraphic data indicates that a major part of these events happened in a relatively short time interval in the Bajocian and early Bathonian. Some large-scale resedimentation events post-dated the main collapse events also

later (in the late Middle Jurassic). This is evident from the Trnje section in which a rather thick radiolarite succession is interstratified between breccia megabeds.

We associate the formation of the breccia megabeds with the regional tectonic activity (Rožič et al., 2019). The initiation of these events coincides with the major mid-Middle Jurassic reorganisation of oceanic domains surrounding the Adria microplate (de Graciansky et al. 2011; Masini et al. 2013; Schmid et al. 2020). Alpine Tethys (Piemont–Ligurian ocean) that was positioned to the west/northwest, moved from the syn-rift to the post-rift phase (oceanisation) during the Middle Jurassic (Chiari et al. 2000; Bill et al. 2001; Manatschal & Müntener 2009; de Graciansky et al. 2011; Ribes et al., 2019, 2020; Le Breton et al., 2021). Towards the east, the Neotethys domain experienced the initiation of the intraoceanic subduction dated as Aalenian to Oxfordian (Borojević Šoštarić et al. 2014; Schmid et al. 2020 and references therein). This was followed by the obduction of ophiolites onto the Adria margin, but the exact timing of the start of the obduction is still debated and varies from mid-Middle Jurassic (Gawlick et al. 2016; 2017a,b,c; 2018; Gawlick and Missoni, 2019, Bragin & Djerić, 2020), the latest Middle Jurassic (Bortolotti et al., 2013) to the Late Jurassic (Mikes et al. 2008; Schmid et al. 2008, 2020; Gallhofer et al. 2017).

Paleogeographically, the transitional zone between the DCP and the SB was located between the Piemont–Ligurian and the Neotethys oceans. For this reason, it must have been highly influenced by the described tectonic perturbations. The exact nature of the tectonic deformations at the transition zone is obscured by the Cenozoic South–Alpine tectonic overprint. However, an accelerated subsidence is documented in the deep-marine successions across the Southern Alps, including the SB (Bertotti et al. 1993; Martire 1996; Martire et al. 2006; Šmuc 2005; Chiari et al. 2007; Rožič 2009; Šmuc & Rožič 2010; Goričan et al. 2012). Subsidence north of the DCP must have (re)activated normal faults along its northern margin, thus increasing the depth of the SB, enhancing the relief, and consequently produced collapses of the platform northern margin.

Comparison of the lithoclast distribution between sections yields no significant variability. This indicates a rather uniform lateral erosion along the DCP–SB transition zone. The same is also valid for the vertical distribution of lithoclasts in most of the sections. This is expected because most of the logged successions probably

belong to the same, single breccia megabed. In the Ponikva-Podbrdo section, which consists of several amalgamated beds, a vertical decrease in Jurassic lithoclasts is visible. This may indicate the progressive downcutting erosion of the gravity-flow events, but it could also be attributed to the size of lithoclasts. We noticed that boulder-sized lithoclasts, which characterize the thickest bed of the Podbrdo section (and also other Ponikve Klippe sections) are predominantly Upper Triassic. This could result in the described distribution. Note that in the upper parts of the Podbrdo and Idrija pri Bači sections, which lack the bolder-sized clasts, Jurassic lithoclasts reappear in greater number.

Backstepping of the Dinaric Carbonate Platform margin

The tectonic subsidence (either forced by extension, transtension, or flexural bending) was not limited solely to the slope between the DCP and the SB, but also influenced the wider transition zone. As discussed in the previous chapter, Middle Jurassic lithoclasts from the breccia point to segmentation of the slope/platform margin and the establishment of a step-like paleotopography. Furthermore, the subsidence of the DCP margin is directly evident from its northern-most outcrops. In western Slovenia, these outcrops are characterized by Upper Triassic and Lower Jurassic (pre-Toarcian) inner platform (lagoon/intertidal) carbonates. In the Idrija Valley, Upper Cretaceous deep-marine (allodapic) limestones of the Volče Limestone Formation directly overlie them (Buser, 1986). This leaves the time of the subsidence wide open. Similar conditions are known from the Soča Valley (Ogorelec et al., 1976; Buser, 1986), but the most recent geological study of the Dobler Hydropower area showed that the Lower Jurassic platform limestones are directly overlain by uppermost Jurassic or lowermost Cretaceous deeper marine sediments, i.e. limestone breccia with a calpionellid-rich micritic matrix (Kovač, 2016). This narrows the drowning of this area to the Middle to Late Jurassic period. Similar conditions are described from eastern Slovenia, where Upper Triassic and often Lower Jurassic inner platform carbonates are overlain by latest Jurassic–Berriasian Biancone-type limestone (Babić 1973, 1979; Aničić & Dozet, 2000; Aničić et al, 2004; Buser, 2010; Poljak, 2017; Rehakova & Rožič, 2019). At Mt. Gorjanci the Lower Jurassic, so-called Krka Limestone is overlain by the siliceous pelagites that are dated to Bajocian–Tithonian (Rižnar, 2006; Skobe et al., 2013; Poljak,

2017). This data from eastern Slovenia indicates that the first prominent subsidence of the DCP margin occurred between the late Early Jurassic and the latest Late Jurassic. Considering the succession of Mt. Gorjanci, we can narrow this interval to the late Early Jurassic–middle Middle Jurassic. A connection to the DCP margin collapse discussed herein appears highly probable.

Indications of the (Middle) Jurassic platform margin retreat also appear in the form of the changed position of the Upper Triassic and Upper Jurassic marginal reefs. In this paper (and Rožič et al., 2019), we present evidence for the existence of Upper Triassic reefs on the DCP margin that were located north of the existing platform outcrops. Today, they are covered by South-Alpine nappes (SB successions), or alternatively, could have been largely destroyed by redepositional events described herein. In contrast, Upper Jurassic reefs are well known and were paleontologically studied in detail (Turnšek, 1997). They are generally located south and southwest of the successions described in the previous paragraph (Fig. 1). These reefal limestones are traced from the Trnovski gozd area, through central Slovenia to Bela Krajina and further SE throughout the External Dinarides (Turnšek et al., 1981; Buser, 1978; 1996; Turnšek, 1997; Vlahović et al., 2005).

In western Slovenia, Upper Jurassic reefs are underlain firstly by Middle Jurassic thin-bedded limestone with cherts, followed by Middle Jurassic ooidal limestones which gradually pass into thin layers of Toarcian crinoidal limestone. These formations are characteristic of the DCP margin or open shelf. Downwards, these lithostratigraphic units pass into the abovementioned pre-Toarcian carbonates of the inner platform (lagoon/intertidal environments). From the described succession, we cannot precisely determine the time of the backstepping, but it must have occurred after the Pliensbachian. While the Toarcian deepening can still be attributed to the major eustatic sea-level rise, the following successions clearly indicate a general shift from inner platform to long-lasting open-marine environments.

In eastern Slovenia (Trebnje area), the Late Jurassic reefs and (fore-reef) breccia overlie the deep-marine hemipelagic and resedimented limestones with cherts, which are probably also Late Jurassic in age. Further downward, beneath a prominent stratigraphic gap, Lower Jurassic limestones equivalent to those from Western Slovenia, i.e. Toarcian crinoidal/ooidal limestones and pre-Toarcian lagoon/intertidal limestones

are found (Otoničar, 2015). Also from this succession, an approximately Middle Jurassic platform retreat seems entirely plausible.

Taking into consideration all of the data presented herein, we propose that the collapse of the platform margin and formation of the Ponikve breccia Member is not the main factor behind the backstepping of the DCP margin. More likely, it represents an extraordinary and extensive sedimentary response to the tectonic processes that caused a significant topographic reorganization of the platform–margin–slope–basin transition.

Conclusions

Hemipelagic sediments and subordinate calciturbidites characterize the Jurassic successions of the Slovenian Basin's southern margin. The main and most striking exception are thick limestone breccia beds, which form successions up to 80 meters thick originating from large-scale debris-flows. These are largely dated to the Bajocian and early Bathonian, but some also occurred later in the Middle Jurassic. We define this limestone breccia as a Ponikve Breccia Member of the Tolmin Formation.

Detailed analyses of lithoclasts allowed for a reconstruction of the Dinaric Carbonate Platform's northern margin, which is no longer preserved nor exposed on the surface due to overthrusting. In the Upper Triassic, a reef complex typical of other Dachstein-type platforms characterized the Dinaric Carbonate Platform margin. In the Lower Jurassic, following the Triassic/Jurassic Boundary calcification crisis, the Dinaric Carbonate Platform margin was dominated by ooidal sand shoals. The Dinaric Carbonate Platform inherited a flat-topped architecture in the early Lower Jurassic and possibly longer. Towards the end of the Lower Jurassic the platform margin may have partially subsided.

Following the Toarcian deepening, shallow-marine conditions on the Dinaric Carbonate Platform margin were re-established with ooidal shoals. Towards the basin, a slope dissected by fault-escarpments likely existed.

In the Bajocian, regional tectonic perturbations started to trigger major collapses of the Dinaric Carbonate Platform margin, in turn giving rise to the formation of the Ponikve Breccia. These collapse events changed the architecture of the platform margin and may have brought about the retreat of the Dinaric Carbonate Platform margin. These tectonic- and sedimentary-events may also have been at least partially responsible for the present-day non-existing sur-

face exposure of the Dinaric Carbonate Platform margin carbonates of the Late Triassic and the Early Jurassic age.

Acknowledgments

This research was financially supported by the Slovenian Research Agency (research core funding No. P1-0195[B] and No. P1-0011). We acknowledge and thank the reviewers for their thorough review of the manuscript. We thank Primož Miklavc and Ema Hrovatin for the preparation of thin sections. And we would like to thank Jeff Bickert for his copy edit of the text.

References

- Aničić, B. & Dozet, S. 2000: Younger Paleozoic and Mesozoic rocks in the northern Krško depression borderland, Slovenia (in Slovenian, with extended English abstract). *Geologija*, 43/1: 13–35. <https://doi.org/10.5474/geologija.2000.001>
- Aničić, B., Ogorelec, B. & Dozet, S. 2004: Geološka karta Kozjanskega 1: 25.000 = Geological map of the Kozjansko (Slovenia) 1: 25.000. Geološki zavod Slovenije, Ljubljana.
- Babić, L. 1973: Upper-Tithonian-to-Valanginian basinal sediments west of Bregana (in Croatian, with extended English abstract). *Geološki vjestnik*, 26: 11–27.
- Babić, L. 1979: Limestone with calpionellids on Mt. Rudnica (eastern Slovenia) (in Croatian, with extended English abstract). *Geološki vjestnik*, 31: 13–20.
- Bernecker, M. 2005: Late Triassic reefs from the Northwest and South Tethys: distribution, setting, and biotic composition. *Facies*, 51/1: 442–453.
- Berra, F., Galli, M., Reghellin, F., Torricelli, S. & Fantoni, R. 2009: Stratigraphic evolution of the Triassic-Jurassic succession in the western Southern Alps (Italy): The record of the two-stage rifting on the distal passive margin of Adria. *Basin Research*, 21: 335–353.
- Bertotti, G., Picotti, V., Bernoulli, D. & Castellarin, A. 1993: From rifting to drifting: Tectonic evolution of the Southalpine upper crust from the Triassic to the early Cretaceous. *Sedimentary Geology*, 86/1-2: 53–76.
- Bill, M., O'Dogherty, L., Guex, J., Baumgartner, P. O. & Masson, H. 2001: Radiolarite ages in Alpine-Mediterranean ophiolites: Constraints on the oceanic spreading and the Tethys

- Atlantic connection. *Geological Society of America Bulletin*, 113: 129–143.
- Blomeier, D. P. G. & Reijmer, J. J. G. 2002: Facies Architecture of an Early Jurassic Carbonate Platform Slope (Jbel Bou Dahar, High Atlas, Morocco). *Journal of Sedimentary Research*, 72/4: 462–475. <https://doi.org/10.1306/111501720462>
- Böhm, F., Ebli, O., Krystyn, L., Lobitzer, H., Rakús, M. & Siblik, M. 1999: Fauna, stratigraphy and depositional environment of the Hettangian–Sinemurian (Early Jurassic) of Adnet (Salzburg, Austria). *Abhandlungen der Geologischen Bundesanstalt*, 56: 143–271.
- Borojević Šoštarić, S., Palinkaš, L., Neubauer, F., Cvetković, V., Bernroider, M. & Genser, J. 2014: The origin and age of the metamorphic sole from the Rogozna Mts., Western Vardar Belt: New evidence for the one-ocean model for the Balkan ophiolites. *Lithos*, 192–195: 39–55. <https://doi.org/10.1016/j.lithos.2014.01.011>.
- Bortolotti, V., Chiari, M., Marroni, M., Pandolfi, L., Principi, G. & Saccani, E. 2013: Geodynamic evolution of ophiolites from Albania and Greece (Dinaric–Hellenic belt): One, two, or more oceanic basins? *International Journal of Earth Sciences*, 102: 783–811.
- Bragin, N. & Djerić, N. 2020: Age of the Jurassic hemipelagic sediments from the Ljubiš area (Zlatibor Mt., SW Serbia). *Geologia Croatica*, 73/3: 143–151. <https://doi.org/10.4154/gc.2020.11>
- Bucković, D. 2006: Jurassic section of Gorski Kotar (Western Karst Dinarides, Croatia) facies characteristics, depositional setting and paleogeographic implications. *Acta Geologica Hungarica*, 49/4: 331–354.
- Buser, S. 1965: Stratigrafski razvoj jurskih skladov na južnem Primorskem, Notranjskem in zahodni Dolenjski: disertacija. Univerza v Ljubljani, Ljubljana: 101 f.
- Buser, S. 1978: Razvoj jurskih plasti Trnovskega gozda, Hrušice in Logaške planote. *Rudarsko – metalurški zbornik*, 4: 385–406.
- Buser, S. 1986: Basic Geological Map SFRJ 1:100.000. Explanatory Booklet. Zvezni geološki zavod Jugoslavije, Beograd. 103 p.
- Buser, S. 1989: Development of the Dinaric and Julian carbonate platforms and the intermediate Slovenian basin (NW Yugoslavia). In: Carulli, G. B., Cucchi, F. & Radrizzani, C. P. (eds.): *Evolution of the karstic carbonate platform: Relation with other periadriatic carbonate platforms*. *Memorie della Società Geologica Italiana*, 40: 313–320.
- Buser, S. 1996: Geology of western Slovenia and its paleogeographic evolution. In: Drobne, K., Goričan, Š. & Kotnik, B. (eds.): *The role of Impact Processes in the Geological and Biological Evolution of Planet Earth*. International workshop, ZRC SAZU: 111–123.
- Buser, S. 2010: Geological map of Slovenia 1: 250.000. Geološki zavod Slovenije, Ljubljana.
- Buser, S. & Debeljak, I. 1996: Lower Jurassic beds with bivalves in south Slovenia. *Geologija*, 37/38: 23–62. <https://doi.org/10.5474/geologija.1995.001>
- Buser, S. & Dozet, S. 2009: Jura = Jurassic. In: Pleničar, M., Ogorelec, B. & Novak, M. (eds.): *Geologija Slovenije = The geology of Slovenia*. Geološki zavod Slovenije, Ljubljana: 215–254.
- Buser, S., Ramovš, A. & Turnšek, D. 1982: Triassic Reefs in Slovenia. *Facies*, 6: 15–24.
- Caron, M. & Homewood, P. 1983: Evolution of early planktic foraminifers. *Marine Micropaleontology*, 7: 453–462.
- Chiari, M., Cobianchi, M. & Picotti, V. 2007: Integrated stratigraphy (radiolarians and calcareous nannofossils) of the Middle to Upper Jurassic Alpine radiolarites (Lombardian basin, Italy): Constraints to their genetic interpretation. *Palaeogeography, Palaeoclimatology, Palaeoecology*, 249/3–4: 233–270. <https://doi.org/10.1016/j.palaeo.2007.02.001>
- Chiari, M., Marcucci, M. & Principi, G. 2000: The age of the radiolarian cherts associated with the ophiolites in the Apennines (Italy) and Corsica (France): A revision. *Ofoliti*, 25: 141–146.
- Cirilli, S., Iannace, A., Jadoul, F. & Zamparelli, V. 1999: Microbial-serpulid build-ups in the Norian–Rhaetian of the western Mediterranean area: ecological response of shelf margin communities to stressed environments. *Terra Nova–Oxford*, 11/5: 195–202.
- Clari, P. & Masetti, D. 2002: The Trento Ridge and the Belluno Basin. In: Santantonio, M. (ed.): *General Field Trip Guidebook, VI International Symposium on the Jurassic System*, 12–22 September 2002: 271–315.
- Cohen, K. M., Finney, S. C., Gibbard, P.L. & Fan, J. -X. 2013: updated The ICS International Chronostratigraphic Chart. *Episodes*, 36/3: 199–204.
- Cousin, M. 1981: Les repports Alpes – Dinarides. Les confins de l'Italie et de la Yougoslavie. *Annales de la Société géologique du Nord*, 5/1: 1–521.
- Čadjenović, D., Kilibarda, Z. & Radulović, N. 2008: Late Triassic to Late Jurassic evolution

- of the Adriatic carbonate platform and Budva Basin, southern Montenegro. *Sedimentary Geology*, 204/1-2: 1–17.
- Črne, A. E. & Goričan, Š. 2008: The Dinaric Carbonate Platform margin in the Early Jurassic: A comparison between successions in Slovenia and Montenegro. *Bollettino della Società Geologica Italiana*, 127: 389–405.
- Darling, K. F., Wade, C. M., Kroon, D. & Brown, A. J. L. 1997: Planktic foraminiferal molecular evolution and their polyphyletic origins from benthic taxa. *Marine Micropaleontology*, 30: 251–266.
- De Graciansky, P. C., Roberts, D. G. & Tricart, P. 2011: The Western Alps, from rift to passive margin to orogenic belt: An integrated geoscience overview. Elsevier, Amsterdam: 432 p.
- Della Porta, G., Merino-Tomé, O., Kenter, J. A. M. & Verwer, K. 2014: Lower Jurassic Microbial and Skeletal Carbonate Factories and Platform Geometry (Djebel Bou Dahar, High Atlas, Morocco). In: Verwer, K., Playton, T. E. & Harris, P. M. (eds.): *Deposits, Architecture, and Controls of Carbonate Margin, Slope and Basinal Settings*. SEPM Special Publication, 105: 237–263.
- Demšar, M. 2016: Geological map of the Selca valley 1:25.000. Explanatory Booklet. Geološki Zavod Slovenije, Ljubljana: 71 p.
- Dozet, S., 2009: Lower Jurassic carbonate succession between Predole and Mlačevo, Central Slovenia = Spodnjejursko karbonatno zaporedje med Predolami in Mlačevim, osrednja Slovenija. *RMZ—Materials and geo-environment*, 56/2: 164–193.
- Dozet, S. & Ogorelec, B. 2012: Younger paleozoic, mesozoic and tertiary oolitic and oncolitic beds in Slovenia – An Overview. *Geologija*, 55/2: 181–208. <https://doi.org/10.5474/geologija.2012.012>
- Dozet, S. & Strohmenger, C. 2000: Podbukovje Formation, central Slovenia. *Geologija*, 43/2: 197–212. <https://doi.org/10.5474/geologija.2000.014>
- Dragičević, I. & Velić, I. 2002: The Northeastern Margin of the Adriatic Carbonate Platform. *Geologia Croatica*, 55/2: 185–232.
- Dunham, R. J. 1962: Classifications of carbonate rocks according to depositional texture. In: Ham, E. W. (ed.): *Classification of carbonate rocks: A symposium*. American Association of Petroleum Geologists Memoir, 1: 108–122.
- Embry, A. F. & Klovan, J. E. 1971: A late Devonian reef tract on northeastern Banks Island, N.W.T. *Bulletin of Canadian Petroleum Geology*, 19: 730–781.
- Fisher, A.G. 1964: The Lofer cyclothems of the Alpine Triassic. *Kansas geological Survey Bulletin*, 169: 107–149.
- Flügel, E. 2004: *Microfacies of carbonate rocks: Analysis, interpretation and application*. Springer, Berlin: 976 p.
- Franceschi, M., Massironi, M., Franceschi, P. & Picotti, V. 2013: Study of the Early Jurassic Calcarei Grigi carbonate platform (Southern Alps, Italy) integrating 3D-modeling and geostatistics. *Rend. Online Soc. Geol. It.*, 29: 59–62.
- Gale, L. 2010: Microfacies analysis of the Upper Triassic (Norian) »Bača Dolomite«: Early evolution of the western Slovenian Basin (eastern Southern Alps, western Slovenia). *Geologica Carpathica*, 61: 293–308. <https://doi.org/10.2478/v10096-010-0017-0>
- Gale, L. 2012: Rhaetian foraminiferal assemblage from the dachstein limestone of Mt. Begunjščica (Košuta unit, eastern Southern Alps). *Geologija*, 55/1: 17–44. <https://doi.org/10.5474/geologija.2012.002>
- Gale, L., Kastelic, A. & Rožič, B. 2013: Taphonomic features of Late Triassic foraminifera from Mount Begunjščica, Karavanke Mountains, Slovenia. *Palaios*, 28: 771–792. <https://doi.org/10.2110/palo.2014.102>
- Gale, L. & Kelemen, M. 2017: Early Jurassic foraminiferal assemblages in platform carbonates of Mt. Krim, central Slovenia. *Geologija*, 60/1: 99–115. <https://doi.org/10.5474/geologija.2017.008>
- Gale, L., Kolar-Jurkovšek, T., Šmuc, A. & Rožič, B. 2012: Integrated Rhaetian foraminiferal and conodont biostratigraphy from the Slovenian Basin, Eastern Southern Alps. *Swiss Journal of Geosciences*, 105/3: 435–462.
- Gale, L., Rožič, B., Mencin, E. & Kolar-Jurkovšek, T. 2014: First evidence for Late Norian progradation of Julian Platform towards Slovenian Basin, Eastern Southern Alps. *Rivista Italiana di Paleontologia e Stratigrafia*, 120: 191–214.
- Gale, L., Skaberne, D., Peybernes, C., Martini, R., Čar, J. & Rožič, B. 2016: Carnian reefal blocks in the Slovenian Basin, eastern Southern Alps. *Facies* 62/23. <https://doi.org/10.1007/s10347-016-0474-8>
- Gallhofer, D., von Quadt, A., Schmid, S. M., Guillong, M., Peytheva, I. & Seghedi, I. 2017: Magmatic and tectonic history of Jurassic ophiolites and associated granitoids from the

- South Apuseni Mountains (Romania). *Swiss Journal of Geosciences*, 110: 699–719. <https://doi.org/10.1007/s00015-016-0231-6>
- Gawlick, H.J. & Missoni, S. 2019: Middle-Late Jurassic sedimentary mélangé formation related to ophiolite obduction in the Alpine-Carpathian-Dinaridic Mountain Range. *Gondwana Research*, 74: 144–172.
- Gawlick, H.-J., Djerić, N., Missoni, S., Bragin, N. Y., Lein, R., Sudar, M. & Jovanović, D. 2017a: Age and microfacies of oceanic Upper Triassic radiolarite components from the Middle Jurassic ophiolitic mélangé in the Zlatibor Mountains (Inner Dinarides, Serbia) and their provenance. *Geologica Carpathica*, 68/4: 350–365.
- Gawlick, H.-J., Missoni, S., Schlagintweit, F., Suzuki, H., Frisch, W., Krystyn, L., Blau, J. & Lein, R. 2009: Jurassic Tectonostratigraphy of the Austroalpine domain. *Journal of Alpine Geology*, 50: 1–152.
- Gawlick, H.-J., Missoni, S., Sudar, M., Goričan, Š., Lein, R., Stanzel, A. I. & Jovanović, D. 2017b: Open-marine Hallstatt Limestones reworked in the Jurassic Zlatar Mélangé (SW Serbia): A contribution to understanding the orogenic evolution of the Inner Dinarides. *Facies*, 63/29. <https://doi.org/10.1007/s10347-017-0510-3>
- Gawlick, H.-J., Missoni, S., Suzuki, H., Sudar, M., Lein, R. & Jovanović, D. 2016: Triassic radiolarite and carbonate components from the Jurassic ophiolitic mélangé (Dinaridic Ophiolite Belt). *Swiss Journal of Geosciences*, 109: 473–494.
- Gawlick, H. J., Sudar, M. N., Missoni, S., Suzuki, H., Lein, R., & Jovanović, D. 2017c: Triassic-Jurassic geodynamic history of the Dinaridic Ophiolite Belt (Inner Dinarides, SW Serbia). *Journal of Alpine geology*, 55: 1–167.
- Gerčar, D. 2017: Sedimentologija in stratigrafija jurske apnenčeve blokovne breče na Ponikvanski tektonski krpi = Sedimentology and stratigraphy of Jurassic limestone blocky breccia from Ponikve tectonic klippe. Magistrsko delo, Naravoslovnotehniška Fakulteta, Ljubljana: 60 p.
- Goričan, Š., Pavšič, J. & Rožič, B. 2012: Bajocian to Tithonian age of radiolarian cherts in the Tolmin Basin (NW Slovenia). *Bulletin de la Société géologique de France*, 183: 369–382.
- Haas, J. 2004: Characteristics of peritidal facies and evidences for subaerial exposures in Dachstein-type cyclic platform carbonates in the Transdanubian Range, Hungary. *Facies*, 50: 263–286.
- Haas, J., Götz, A.E. & Pálffy, J. 2010: Late Triassic to Early Jurassic palaeogeography and eustatic history in the NW Tethyan realm: New insights from sedimentary and organic facies of the Csóvár Basin (Hungary). *Palaeogeography, Palaeoclimatology, Palaeoecology*, 291/3-4: 456–468.
- Haas, J., Gawlick, H.J., Kovacs, S., Karamata, S., Sudar, M., Gradinaru, E., Mello, J., Pollak, M., Halamic, J., Tomljenovic, B. & Ogorelec, B. 2006: Jurassic environments in the Circum-Pannonian region. In: *Proceedings XVIIIth Congress of the Carpathian-Balkan Geological Association*. Slovak Academy of Sciences, Bratislava: 201–204.
- Iannace, A. & Zamparelli, V. 2002: Upper Triassic platform margin biofacies and the paleogeography of Southern Apennines. *Palaeogeography, Palaeoclimatology, Palaeoecology*, 179/1-2: 1–18.
- Iveković, A. 2008: Stratigrafsko - sedimentološki razvoj jurskih in krednih kamnin v dolini reke Mirne. Diplomsko delo, Naravoslovnotehniška Fakulteta, Ljubljana: 89 p.
- Kiessling, W., Aberhan, M., Brenneis, B. & Wagner, P. J. 2007: Extinction trajectories of benthic organisms across the Triassic–Jurassic boundary. *Palaeogeography, Palaeoclimatology, Palaeoecology*, 244: 201–222.
- Kovács, S., Sudar, M., Gradinaru, E., Karamata, S., Gawlick, H. J., Haas, J., Péro, C., Gaetani, M., Mello, J., Polák, M., Aljinović, D., Ogorelec, B., Kolar-Jurkovšek, T., Jurkovšek, B. & Buser, S. 2011: Triassic evolution of the tectonostratigraphic units in the Circum-Pannonian region. *Jahrbuch der Geologischen Bundesanstalt*, 151: 199–280.
- Kovač, A. 2016: Biostratigrafija in sedimentologija srednjekrednih in spodnjekrednih plasti v dolini Soče pri HE Doblar = Biostratigraphy and sedimentology of Middle Jurassic to Lower Cretaceous beds in Soča Valley by the HE Doblar. Diplomsko delo, Naravoslovnotehniška fakulteta, Ljubljana: 61 p.
- Kuss, J. 1983: Faziesentwicklung in proximalen Intraplattform-Becken: Sedimentation, Palökologie und Geochemie der Kössener Schichten (Ober-Trias, Nördliche Kalkalpen). *Facies*, 9/1: 61–171.
- Le Breton, E., Brune, S., Ustaszewski, K., Zahirović, S., Seton, M. & Müller, R. D. 2021: Kinematics and extent of the Piemont–Liguria Basin – implications for subduction processes in the Alps. *Solid Earth*, 12/4: 885–913. <https://doi.org/10.5194/se-12-885-2021>

- Leinfelder, R., Schmid, D. U., Nose, M. & Werner, W. 2002: Jurassic Reef Patterns - The Expression of a Changing Globe Phanerozoic Reef Patterns. SEPM Special Publication, 72: 465–520. <https://doi.org/10.2110/pec.02.72.0465>
- Manatschal, G. & Müntener, O. 2009: A type sequence across an ancient magma-poor ocean-continent transition: The example of the western Alpine Tethys ophiolites. *Tectonophysics*, 473/1–2: 4–19. <https://doi.org/10.1016/j.tecto.2008.07.021>.
- Mandl, G. W. 2000: The Alpine sector of the Tethyan shelf – Examples of Triassic to Jurassic sedimentation and deformation from the Northern Calcareous Alps. *Mitteilungen der Österreichischen Mineralogischen Gesellschaft*, 92: 61–77.
- Martindale, R.C., Krystyn, L., Corsetti, F.A., & Bottjer, D.J. 2013: From fore reef to lagoon: evolution of the Upper Triassic Dachstein carbonate platform on the Tennengebirge (Salzburg, Austria). *Palaios*, 28: 755–770.
- Martinuš, M., Bucković, D. & Kukoč, D. 2012: Discontinuity surfaces recorded in shallow-marine platform carbonates: an example from the Early Jurassic of the Velebit Mt.(Croatia). *Facies*, 58/4: 649–669.
- Martire, L. 1996: Stratigraphy, facies and syn-sedimentary tectonics in the Jurassic Rosso Ammonitico Veronese (Altopiano di Asiago, NE Italy). *Facies*, 35: 209–236.
- Martire, L., Clari, P., Lozar, F. & Pavia, G. 2006: The Rosso Ammonitico Veronese (Middle–Upper Jurassic of the Trento Plateau): A proposal of lithostratigraphic ordering and formalization. *Rivista Italiana Paleontologia e Stratigrafia*, 112: 227–250.
- Masetti, D., Fantoni, R., Romano, R., Sartorio, D. & Trevisani, E. 2012: Tectonostratigraphic evolution of the Jurassic extensional basins of the eastern southern Alps and Adriatic foreland based on an integrated study of surface and subsurface data. *American Association of Petroleum Geologists Bulletin*, 96: 2065–2089.
- Masini, E., Manatschal, G. & Mohn, G. 2013: The Alpine Tethys rifted margins: Reconciling old and new ideas to understand the stratigraphic architecture of magma-poor rifted margins. *Sedimentology*, 60: 174–196.
- Merino-Tomé, O., Della Porta, G., Kenter, J. A. M., Verwer, K., Harris, P. M., Adams, E., Playton, T. & Corrochano, D. 2012: Sequence development in an isolated carbonate platform (Lower Jurassic, Djebel Bou Dahar, High Atlas, Morocco): influence of tectonics, eustacy and carbonate production. *Sedimentology*, 59/1: 118–155. <https://doi.org/10.1111/j.1365-3091.2011.01232.x>
- Mikes, T., Christ, D., Petri, R., Dunkl, I., Frei, D., Baldi-Beke, M., Reitner, J., Wemmer, K., Hrvatović, H. & von Eynatten, H. 2008: Provenance of Bosnian Flysch. *Swiss Journal of Geosciences*, 101/31: 31–54. <https://doi.org/10.1007/s00015-008-1291-z>
- Miler, M. & Pavšič, J. 2008: Triassic and Jurassic beds in Krim Mountain area Slovenia. *Geologija*, 51/1: 87–99. <https://doi.org/10.5474/geologija.2008.010>
- Ogorelec, B. 2011: Microfacies of Mesozoic carbonate rocks of Slovenia. *Geologija*, 54: 1–136.
- Ogorelec, B. & Rothe, P. 1993: Mikrofazies, Diagenese und Geochemie des Dachsteinkalkes und Hauptdolomits in Süd-West-Slowenien. *Geologija*, 35: 81–182. <https://doi.org/10.5474/geologija.1992.005>
- Ogorelec, B. & Buser, S. 1996. Dachstein Limestone from Krn in Julian Alps (Slovenia). *Geologija*, 39: 133–157. <https://doi.org/10.5474/geologija.1996.006>
- Ogorelec, B. & Dozet, S. 1997: Upper Triassic, Jurassic and Lower Cretaceous beds in eastern Sava Folds - Section Laze at Boštanj (Slovenia). *RMZ-Materials and geoenvironment*, 44/3–4: 223–235.
- Ogorelec, B., Šribar, L. & Buser, S. 1976: O litologiji in biostratigrafiji Volčanskega apnenca. *Geologija Revija*, 19: 125–151.
- Oprčkal, P., Gale, L., Kolar-Jurkovšek, T. & Rožič, B. 2012: Outcrop-scale evidence for the norian-rhaetian extensional tectonics in the Slovenian basin (Southern Alps). *Geologija*, 55: 45–56.
- Otoničar, B. 2015: Evolucija severovzhodnega obrobja Jadranske karbonatne platforme med zgornjim triasom in zgornjo juro (Dolenjska, JV Slovenija). In: Rožič, B. (ed.): *Razprave, poročila = Treatises, reports, 22. posvetovanje slovenskih geologov = 22nd Meeting of Slovenian Geologists*. Univerza v Ljubljani, Naravoslovnotehniška fakulteta, Oddelek za geologijo, 23: 147–150.
- Piller, W.E. 1981: The Steinplatte reef complex, part of an Upper Triassic carbonate platform near Salzburg, Austria. SEPM Special Publication, 30: 261–290.
- Placer, L. 1999: Contribution to the macrotectonic subdivision of the border region between

- Southern Alps and External Dinarides. *Geologija*, 41: 223–255.
- Placer, L. 2008: Principles of the tectonic subdivision of Slovenia. *Geologija*, 51/2: 205–217. <https://doi.org/10.5474/geologija.2008.021>
- Poljak, M. 2017: Geological Map of the Eastern Part of the Krško Basin 1:25,000. Explanatory Booklet. Geološki Zavod Slovenije, Ljubljana: 108 p.
- Praprotnik Kastelic, J., Kastelic, A., Gale, L., Šmuc, A. & Rožič, B. 2013: Jurske plasti z manganovimi obogatitvami na Begunjščici. In: Rožič, B. (ed.): Razprave, poročila = Treatises, reports. 21. posvetovanje slovenskih geologov, Ljubljana, 2013 = 21st Meeting of Slovenian Geologists. Naravoslovnotehniška fakulteta, Ljubljana: 127–130.
- Ramovš, A. 1994: O starosti škofjeloških ploščastih apnencev z roženci. *Loški razgledi*, 41/1.
- Reháková, D. & Rožič, B. 2019: Calpionellid biostratigraphy and sedimentation of the Biancone limestone from the Rudnica Anticline (Sava Folds, eastern Slovenia). *Geologija*, 62/1: 89–101. <https://doi.org/10.5474/geologija.2019.004>
- Ribes, C., Manatschal, G., Ghienne, J. F., Karner, G. D., Johnson, C. A., Figueredo, P. H., Incerpi, N. & Epin, M. E. 2019: The syn-rift stratigraphic record across a fossil hyper-extended rifted margin: the example of the northwestern Adriatic margin exposed in the Central Alps, *International Journal of Earth Sciences*, 108: 2071–2095. <https://doi.org/10.1007/s00531-019-01750-6>
- Ribes, C., Petri, B., Ghienne, J. F., Manatschal, G., Galster, F., Karner, G. D., Figueredo, P. H., Johnson, C. A. & Karpoff, A. M. 2020: Tectono-sedimentary evolution of a fossil ocean-continent transition: Tasma nappe, central Alps (SE Switzerland), *Geological Society of America Bulletin*, 132: 1427–1446. <https://doi.org/10.1130/B35310.1>
- Rižnar, I. 2006: History of research of the Krško and Veliki trn beds (revision). *Dela SAZU*, IV. Razreda, 47: 79–99.
- Rožič, B. 2005: Albian–Cenomanian resedimented limestone in the Lower Flyschoid formation of the Mt. Mrzli Vrh Area (Tolmin region, NW Slovenia). *Geologija*, 48/2: 193–210. <https://doi.org/10.5474/geologija.2005.017>
- Rožič, B. 2006: Sedimentology, stratigraphy and geochemistry of Jurassic rocks in the western part of the Slovenian Basin. Ph.D. thesis, University of Ljubljana, Ljubljana: 148 p.
- Rožič, B. 2009: Perbla and Tolmin formations: Revised Toarcian to Tithonian stratigraphy of the Tolmin Basin (NW Slovenia) and regional correlations. *Bulletin de la Société géologique de France*, 180: 411–430.
- Rožič, B. 2016: Paleogeographic units. In: Novak, M. & Rman, N. (eds.): Geological atlas of Slovenia. Geološki zavod Slovenije, Ljubljana: 14–15.
- Rožič, B., Gale, L. & Kolar-Jurkovšek, T. 2013: Extent of the Upper Norian–Rhaetian Slatnik formation in the Tolmin nappe, Eastern Southern Alps. *Geologija*, 56/2: 175–186. <https://doi.org/10.5474/geologija.2013.011>
- Rožič, B., Gale, L., Oprčkal, P., Švara, A., Udovč, J., Debevec, G., Popit, T., Vrabc, M. & Šmuc, A. 2015: Stratigrafija in strukturni pomen kamnin Slovenskega bazena pri Škofji Loki. *Geološki zbornik*, 23: 171–175.
- Rožič, B., Gerčar, D., Oprčkal, P., Švara, A., Turnšek, D., Kolar-Jurkovšek, T., Udovč, J., Kunst, L., Fabjan, T., Popit, T. & Gale, L., 2019: Middle Jurassic limestone megabreccia from the southern margin of the Slovenian Basin. *Swiss Journal of Geosciences*, 112/1: 163–180. <https://doi.org/10.1007/s00015-018-0320-9>
- Rožič, B., Goričan, Š., Švara, A. & Šmuc, A. 2014a: The Middle Jurassic to Lower Cretaceous succession of the Ponikve klippe: The Southernmost outcrops of the Slovenian Basin in Western Slovenia. *Rivista Italiana di Paleontologia e Stratigrafia*, 120: 83–102.
- Rožič, B., Kolar-Jurkovšek, T. & Šmuc, A. 2009: Late Triassic sedimentary evolution of Slovenian Basin (eastern Southern Alps): Description and correlation of the Slatnik Formation. *Facies*, 55: 137–155. <https://doi.org/10.1007/s10347-008-0164-2>
- Rožič, B., Kolar-Jurkovšek, T., Žvab Rožič, P. & Gale, L. 2017: Sedimentary record of subsidence pulse at the Triassic/Jurassic boundary interval in the Slovenian Basin (eastern Southern Alps). *Geologica Carpathica*, 68: 543–561. <https://doi.org/10.1515/geoca-2017-0036>
- Rožič, B. & Popit, T. 2006: Resedimented limestones in Middle and Upper Jurassic succession of the Slovenian Basin. *Geologija*, 49/2: 219–234. <https://doi.org/10.5474/geologija.2006.016>
- Rožič, B., Udovč, J., Žvab Rožič, P., Gale, L. & Gerčar, D. 2022: How far to the west was the Slovenian basin extending?. In: Program, Abstracts and Field Trip Guide. Budapest: 97.
- Rožič, B., Venturi, F. & Šmuc, A. 2014b: Ammonites from Mt Kobla (Julian Alps, NW Slovenia) and their significance for precise dating of Pliensbachian tectono-sedimentary

- event. *RMZ - Materials and geoenvironment*, 61/2-3: 191–201.
- Sabatino, N., Vlahović, I., Jenkyns, H. C., Scopelliti, G., Neri, R., Prtoljan, B. & Velić, I. 2013: Carbon-isotope record and palaeoenvironmental changes during the early Toarcian oceanic anoxic event in shallow-marine carbonates of the Adriatic Carbonate Platform in Croatia. *Geological Magazine*, 150/6: 1085–1102.
- Samankassou, E. & Enos, P. 2019: Lateral facies variations in the Triassic Dachstein platform: A challenge for cyclostratigraphy. *The Depositional Record*, 5/3: 469–485.
- Satterley, A.K. 1996: The interpretation of cyclic successions of the Middle and Upper Triassic of the Northern and Southern Alps. *Earth-Science Reviews*, 40/3-4: 181–207.
- Schäfer, P. & Senowbari-Daryan, B. 1981: Facies Development and Paleocologic Zonation of Four Upper Triassic Patch Reefs Northern Calcareous Alps Near Salzburg Austria. *SEPM Special Publication*, 30: 241–259.
- Scherman, B., Rožič, B., Görög, A., Kövér, S. & Fodor, L. 2022: Platform to basin transitions: mapping observations at the Krvavica Mountain, and Čemšeniška Planina, in the Sava Folds Region. In: Rožič, B. & Žvab Rožič, P. (eds): 15th Emile Argand Conference on Alpine Geological Studies: abstract book & fieldtrip guide. Faculty of Natural Sciences and Engineering, Ljubljana: 61.
- Schmid, S. M., Bernoulli, D., Fügenschuh, B., Mañenco, L., Schefer, S., Schuster, R., Tischler, M. & Ustaszewski, K. 2008: The Alpine-Carpathian-Dinaride orogenic system: Correlation and evolution of tectonic units. *Swiss Journal of Geosciences*, 101: 139–183.
- Schmid, S.M., Fügenschuh, B., Kounov, A., Mañenco, L., Nievergelt, P., Oberhänsli, R., Pleuger, J., Schefer, S., Schuster, R., Tomljenović, B., Ustaszewski, K. & van Hinsbergen, D. J. J., 2020. Tectonic units of the Alpine collision zone between Eastern Alps and western Turkey. *Gondwana Research* 78: 308–374. <https://doi.org/10.1016/j.gr.2019.07.005>
- Scheibner, C. & Reijmer, J. G. 1999: Facies patterns within a Lower Jurassic upper slope to inner platform transect (Jbel Bou Dahar, Morocco), *Facies* 41/1: 55–80. <https://doi.org/10.1007/BF02537460>
- Skobe, S., Goričan, Š., Skaberne, D., Verbič, T., Mišič, M. & Zupančič, N. 2013. K-feldspar rich shales from Jurassic bedded cherts in southeastern Slovenia. *Swiss J Geosci* 106: 491–504. <https://doi.org/10.1007/s00015-013-0147-3>
- Šmuc, A. 2005: Jurassic and Cretaceous stratigraphy and sedimentary evolution of the Julian Alps, NW Slovenia. Založba ZRC, Ljubljana: 98 p.
- Šmuc, A. 2012: Middle to Upper Jurassic succession at Mt Kobariški Stol (NW Slovenia) = srednje- do zgornjajursko zaporedje na Kobariškem Stolu (SZ Slovenija). *RMZ - Materials and geoenvironment*, 59: 267–284.
- Šmuc, A. & Goričan, Š. 2005: Jurassic sedimentary evolution of a carbonate platform into a deep-water basin, Mt. Mangart (Slovenian-Italian border). *Rivista Italiana di Paleontologia e Stratigrafia*, 111: 45–70.
- Šmuc, A. & Rožič, B. 2010: The Jurassic Prehodavci Formation of the Julian Alps: Easternmost outcrops of Rosso Ammonitico in the Southern Alps (NW Slovenia). *Swiss Journal of Geosciences*, 103: 241–255.
- Tappan, H. & Loeblich, A. R. 1988: Foraminiferal evolution, diversification, and extinction. *Journal of Paleontology*, 62: 695–714.
- Tišljar, J., Vlahović, I., Velić, I. & Sokač, B. 2002: Carbonate platform megafacies of the Jurassic and Cretaceous deposits of the Karst Dinarides. *Geologia Croatica*, 55: 139–170.
- Turnšek, D. 1997: Mesozoic corals of Slovenia. Založba ZRC, Ljubljana: 512 p.
- Turnšek, D., Buser, S. & Ogorelec, B. 1981: An Upper Jurassic reef complex from Slovenia, Yugoslavia, *SEPM Special Publication*, 3: 361–369.
- Turnšek, D., Buser, S. & Debeljak, I. 2003: Liassic coral patch reef above the »Lithiotid limestone« on Trnovski gozd plateau, west Slovenia. *Razprave = Dissertationes*, 44: 285–331.
- Turnšek, D. & Košir, A. 2000: Early Jurassic corals from Krim Mountain, Slovenia. *Razprave = Dissertationes*, 41: 81–113.
- Udovč, J. 2019: Sedimentologija in stratigrafija jurskih plasti na Matajurju = Sedimentology and stratigraphy of Jurassic succession from Mt. Matajur. Magistrsko delo, Naravoslovnotehniška Fakulteta, Ljubljana: 63 p.
- Valand, N., Rožič, B. & Gale, L. 2019: Jursko zaporedje z apnenčevimi brečami na južnih pobočjih Begunjščice. In: Rožič, B. (ed.): *Razprave, poročila = Treatises, reports*. 24. posvetovanje slovenskih geologov = 24th Meeting of Slovenian Geologists. Naravoslovnotehniška fakulteta, Ljubljana. *Geološki zbornik*, 25: 143–145.

- Velić, I. 2007: Stratigraphy and palaeobiology of Mesozoic benthic foraminifera of the Karst Dinarides (SE Europe). *Geologia Croatica*, 60: 1–113.
- Vlahović, I., Tišljar, J., Velić, I. & Matičec, D. 2005: Evolution of the Adriatic Carbonate Platform: Palaeogeography, main events and depositional dynamics. *Palaeogeography, Palaeoclimatology, Palaeoecology*, 220: 333–360.
- Vrabec, M. & Fodor, L. 2006: Late Cenozoic tectonics of Slovenia: structural styles at the Northeastern corner of the Adriatic microplate. In: Pinter, N., Grenczy, G., Weber, J., Medak, D. & Stein, S. (eds.): *The Adria microplate: GPS geodesy, tectonics and hazards*. Springer, Dordrecht: 151–168.
- Wilson, J. L. 1975: *Carbonate facies in geologic history*. Springer, Berlin: 471 p.
- Wurm, D. 1982: Mikrofazies, Paläontologie und Palökologie der Dachsteinriffkalke (Nor) des Gosaukammes, Österreich. *Facies*, 6/1: 203–295.



Lower Permian (Artinskian) chondrichthyan tooth remains (Petalodontidae) from Dovje (Karavanke Mts., NW Slovenia)

Spodnjepermski (artinskijski) ostanki zob morskih psov (Petalodontidae) iz Dovjega (Karavanke, SZ Slovenija)

Matija KRIŽNAR

Prirodoslovni muzej Slovenije, Prešernova 20, 1000 Ljubljana, Slovenija; e-mail: mkriznar@pms-lj.si

Prejeto / Received 28. 9. 2022; Sprejeto / Accepted 17. 11. 2022; Objavljeno na spletu / Published online 21. 12. 2022

Key words: Petalodontiformes, *Petalodus ohioensis*, Upper Paleozoic, Artinskian, Karavanke Mountains, Slovenia

Ključne besede: Petalodontiformes, *Petalodus ohioensis*, zgornji paleozoik, artinskijski, Karavanke, Slovenija

Abstract

Fossil remains of chondrichthyan tooth bases (roots) were found in Lower Permian beds exposed along the forest road between Dovje and Plavški Rovt. These layers are part of the clastic development of the Trogkofel Group beds. They are composed of an alternation of dark to light-grey shales, siltstone, and sandstone with rare beds of the conglomerate. Within the clastic succession, layers or lenses of dark-grey to black limestones (biosparitic, biomicritic and oolitic) and limestone breccias occur. The limestone consists remains of algae, fusulinids, brachiopods, and mostly crinoids (*Palermocrinus* and *Entrochus*). Detail study has shown that two remains of tooth bases belong to the genus *Petalodus*, one of them to the species *Petalodus ohioensis*. The bases are tongue-shaped and come to a rounded point in the distal (base end) edge. On the surface of the base, the typical oval-shaped foramina are visible. In addition, the osteodentine is visible on the cross-section of one specimen. Teeth of *Petalodus* are often the most common chondrichthyan fossil vertebrate remains reported from the Carboniferous and Permian rocks of the USA, Europe, and Russia. In Slovenia, *Petalodus ohioensis* has been recorded only from Upper Carboniferous beds. The new record of Lower Permian remains contributes to the knowledge of this cosmopolitan but still common genus of Late Paleozoic chondrichthyans.

Izveček

Iz spodnjepermskih plasti med Dovjim in Plavškim Rovtom so bili odkriti fosilni ostanki korenin zob hrustančnic. Najdbe izhajajo iz klastičnih plasti Trogkofelske grupe, kjer se menjavajo temni do svetlo sivi glinavci in peščenjaki ter redke leče konglomeratov. Med plastmi se pojavljajo tudi zaporedja temno sivih in črnih apnencev in apnenčevih breč, ki vsebujejo fosilne ostanke alg, fuzulin, ramenonožcev in večji delež ploščic morskih lilij (rodov *Palermocrinus* in *Entrochus*). Novo odkrita ostanka zob sta dobro ohranjeni korenini, značilni za rod *Petalodus* in smo ju vsaj v enem primeru taksonomsko pripisali vrsti *Petalodus ohioensis*. Oba ostanka korenin imata jeziku podobno obliko, ki se proti koncu zaokroži. Na površini so opazne manjše odprtine (foramni), medtem ko je na enem primerku opazna tudi kostna struktura (osteodentin). Zobje rodu *Petalodus* se pojavljajo v karbonskih in permskih plasteh skoraj povsod po svetu, predvsem v ZDA, Evropi in Rusiji. V Sloveniji so bili dobro ohranjeni zobje vrste *Petalodus ohioensis* najdeni le v zgornjekarbonskih plasteh, medtem ko so novi ostanki iz spodnjega perma prvič predstavljeni tukaj. Nove najdbe iz Slovenije dopolnjujejo paleontološko sliko tega kozmopolitskega rodu poznopaleozojskih hrustančnic.

Table 1. Compiled list of Late Paleozoic chondrichthyan teeth from the South Karavanke (NW Slovenia). Note: All listed specimens were figured in cited publications. *Preliminary identification of the specimen.

Tabela 1. Pregledni seznam poznopaleozojskih ostankov zob hrustančnic iz južnih Karavank (SZ Slovenija). Opomba: vsi primerki so ilustrirani v citirani literaturi. *Preliminarno določeni primerki.

Age (Stage) Starost (obdobje)	Species (number of the specimen) / Vrsta (število primerkov)	Fossil site - locality / Najdišče fosila	Reference (Publication) / Referenca
Lower Permian (Asselian-Artinskian)	<i>Glikmanius cf. occidentalis</i> (1)	Hrušica (north), forest road near Na Visokih	Križnar, 2015 Križnar, 2016
	Petalodontidae gen et. sp. indet. (1)*	Dovžanova soteska	Novak, 2006 Novak, 2019
Upper Carboniferous (Gzhelian)	<i>Petalodus ohioensis</i> (2)	Javorniški Rovt, Spodnja Počivala	Ramovš & Bedič, 1993 Ramovš, 1997 Ramovš, 1998 Peternel, 1995
	<i>Petalodus ohioensis</i> (1)	Forest road Planina pod Golico - Črni vrh	Ramovš, 1997 Ramovš, 1998
	Petalodontidae gen et. sp. indet. (1)	Planina pod Golico, brook southeast of the village	Ramovš, 1998
	Petalodontidae gen et. sp. indet. (1)	Črni vrh	Peternel, 1995

Introduction

The Petalodontiformes are a small intriguing group of late Paleozoic chondrichthyans, ranging from the Carboniferous (Mississippian) to the Permian. Up to now, there are about 17 genera referred to Petalodontiformes, but most are known principally from isolated teeth (Ginter et al. 2010; Lund et al., 2014). *Petalodus* is the longest-known petalodont cosmopolitan genus. The late Paleozoic chondrichthyans (»shark«) record from Slovenia consists of complete or partial remains of petalodont teeth (*Petalodontidae* gen et. sp. ident. and *Petalodus ohioensis*) and one tooth of *Glikmanius cf. occidentalis* (for the references and the list of localities see Table 1).

Geological and Stratigraphical settings

In the Southern Karavanke Mts. the outcrops of Upper Paleozoic (Upper Carboniferous and Lower Permian) fossiliferous shallow marine deposits are scattered between Solčava and Dovje (Fig. 1). The broadest and best exposed Lower Permian beds are present north of Tržič, in the vicinity of famous fossil sites Dovžanova soteska and Jelendol (Novak, 2007; Novak & Skaberne, 2009). In the western part of Southern Karavanke Mts. Lower Permian beds are mainly exposed

in Javorniški Rovt and Pristava, and between Planina pod Golico and Dovje village (Novak & Skaberne, 2009).

The lithostratigraphic subdivision of Lower Permian rocks in the Southern Karavanke mountains is composed of the Grenzland Fm., Zweikofel Fm. and on top the Trogkofel Group (Novak & Skaberne, 2009, 199). In the youngest beds of the Trogkofel Group, carbonate and clastic developments are distinguished. The carbonate part is represented by light-grey, dark-red, and rose-red reef fossiliferous limestones and fore-reef limestone breccias in some parts. The Trogkofel limestone is massive (as reef bioherm) or thick-bedded and rich in fossils. The clastic development of the Trogkofel Group beds is composed of the alternation of dark to light-grey shales, siltstone, and sandstone with rare beds of conglomerate (Novak & Skaberne, 2009). Within the clastic succession, layers or lenses of dark-grey to black limestones (biosparitic, biomicritic and oolitic) and limestone breccias occur, containing rock-forming remains of algae, fusulinids, brachiopods, rare corals, and crinoids (Novak & Skaberne, 2009). The age of the Trogkofel Group (with Trogkofel limestone) in the Southern Karavanke is middle to late Artinskian, with a thickness of a maximum of 400 meters (Novak & Skaberne, 2009).

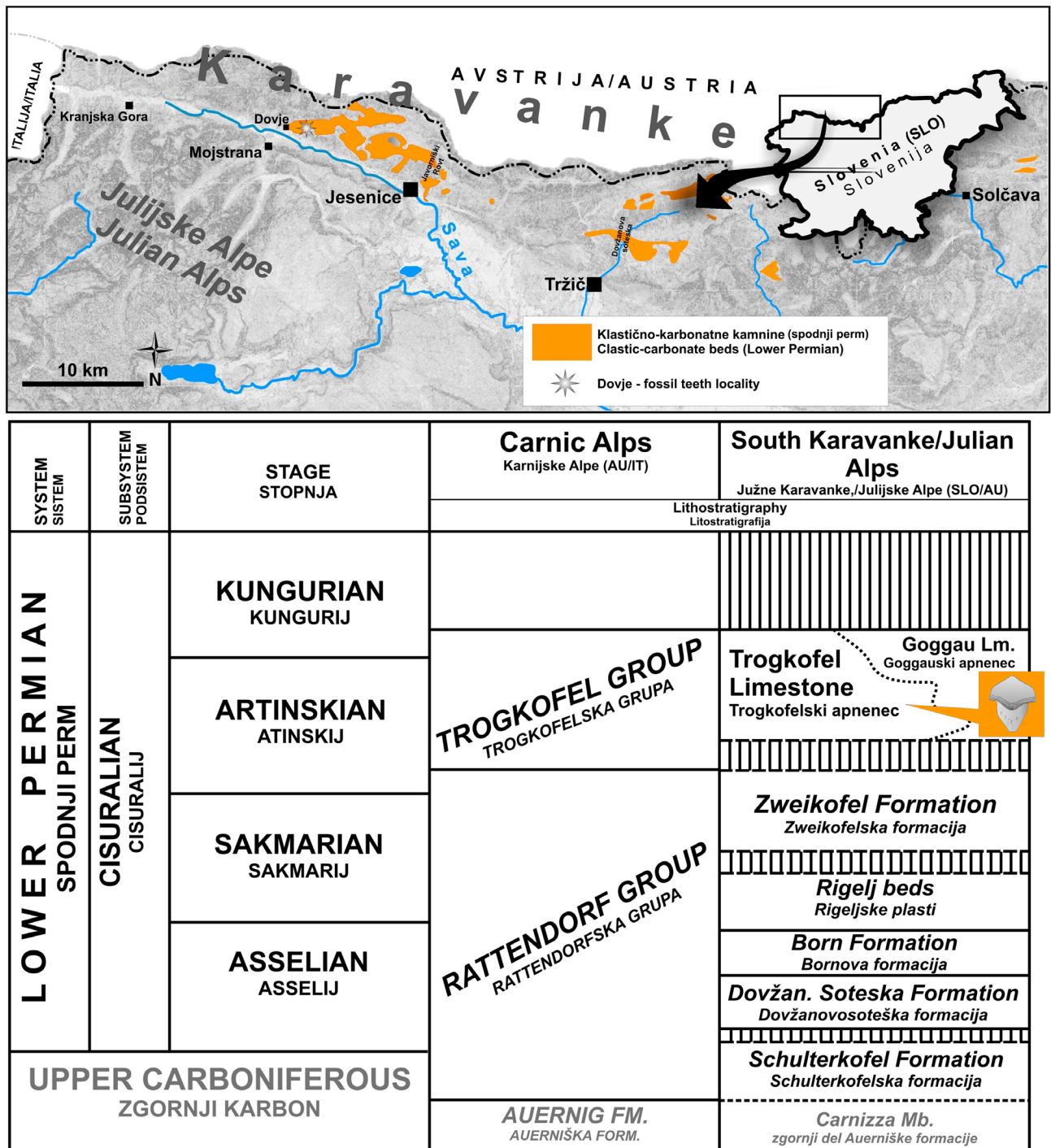


Fig. 1. Index map (top) showing the outcrops of Lower Permian clastic-carbonate beds in the Karavanke (Slovenian part) with the fossil location near Dovje. Summary of the Permian stratigraphy and biostratigraphy (bottom) of the Karavanke Mountains, with the position of fossil chondrichthyan teeth in the Trogkofel Group (adapted from Novak & Skaberne, 2009). Sl. 1. Zemljevid razprostranjenosti klastično-karbonatnih spodnjepersmskih plasti v Karavankah (slovenski del) in pozicija najdišča fosilov pri Dovjem (zgoraj). Poenostavljen stratigrafski stolpec spodnjepersmskih plasti v Karavankah (prirejeno po Novak & Skaberne, 2009).

The outcrop of the newly discovered chondrichthyan tooth fragments is located along the forest road between Dovje and Plavški Rovt (Fig. 2). Layers of dark-grey limestones and an alternation of light-grey shales and siltstone are exposed. All beds are extremely fossiliferous

with numerous disarticulated crinoid remains. The remains of crinoids are mostly fully disarticulated parts (ossicles) of stems (columnals), arms, pinnules, and rarely crinoid crowns (Lach et al. 2013). Crinoid remains were not yet the subject of a thorough paleontological investigation, but

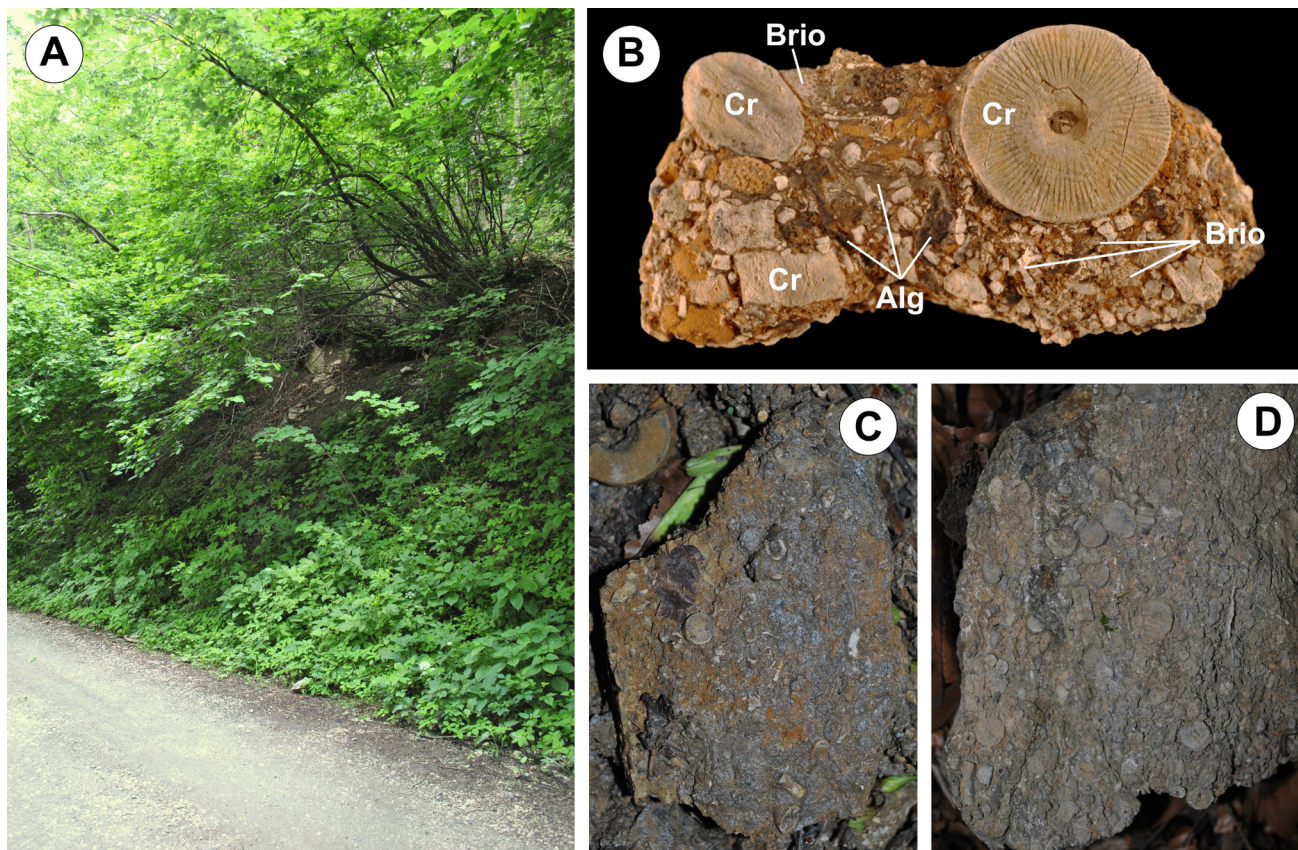


Fig. 2. A: The location of petalodontid teeth remains on a forest road in the vicinity of Dovje (13°58'14", 46°28'1"). B-D: Various remains from crinoid-bryozoan-algae assemblage (biofacies) from the Dovje locality. Not to scale. Abbreviations: Cr - crinoid remains (mostly crinoid columnals); Brio - bryozoans; Alg -algae.

Sl. 2. A: Najdišče petalodontidnih ostankov zob ob gozdni cesti v okolici Dovjega (13°58'14", 46°28'1"). B-D: Različni fosilni ostanki iz krinoidno-briozojnsko-algnih združb iz najdišča pri Dovjem. Ni v merilu. Okrajšave: Cr - krinoidni ostanki (prevladujoče ploščice morskih lilij); Brio - brizozi (mahovnjaki); Alg - alge.

preliminary research shows the presence of the crinoid genera *Palermocrinus* and *Entrochus*, with probably some members of Codiocrinidae (Lach et al., 2013; Ramovš & Sieverts-Doreck 1968). The associated fauna is composed of brachiopods (productids and spiriferids), bivalves, gastropods, foraminifers (fusulinids), algae (*Shamovella-Archaeolithoporella*), and fenestellid bryozoans which are with the crinoids, form the main biotic component in some parts. Similar crinoidal limestone with *Palermocrinus togatus*, with higher carbonate content, is known at Pristava in Javorniški Rovt. The age of the outcrop with new fossil tooth remains is Artinskian (Novak & Skaberne, 2009; Novak M., personal comm.).

Materials and methods

Specimens were discovered by Jure Zupanc around the year 2000 and are stored in his private geological collection. For the specimens described here, we use working identification numbers JZC 001 (Fig. 4) and JZC 002 (Fig. 5). Both specimens were prepared only with minor mechanical tools (needles) and measured with a

metal hand vernier caliper. The specimens were photographed using a Nikon D7200 camera coupled with an AF-S Micro NIKKOR 60mm f/2.8G ED lens. Photos of specimens were additionally edited with the advanced photo editing program Adobe Photoshop Lightroom which enhanced the visibility of some features.

Our description of the tooth base (Fig. 3) follows combined terminology suggested by Dalla Vecchia, (1988), Robb (2003), Harper (2018, 7), and Gai et al. (2021, see their Fig. 2, a1-a3).

Systematic Paleontology

Systematics follows the taxonomic views of Ginter et al. (2010) and Carpenter & Itano (2019).
 Class Chondrichthyes Huxley 1880
 Subclass Euchondrocephali Lund & Grogan 1997
 Order Petalodontiformes Patterson 1965
 Family Petalodontidae Newberry & Worthen 1866
 Genus *Petalodus* Owen 1840
Petalodus ohioensis Safford 1853
 Figure 4

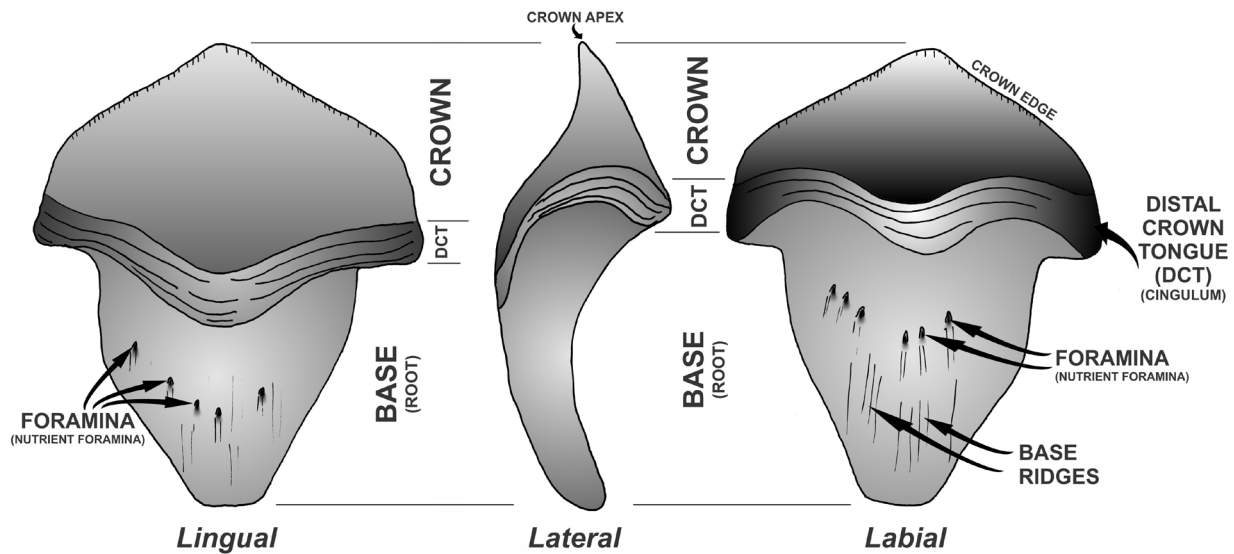


Fig. 3. Anatomical terminology of petalodontid tooth (*Petalodus*). Adapted from Dalla Vecchia, (1988), Robb (2003), and Gai et al. (2021).

Sl. 3. Anatomska terminologija petalodontidnega zoba (*Petalodus*). Prirejeno po Dalla Vecchia, (1988), Robb (2003) in Gai et al. (2021).

Material: One specimen of base of petalodontid tooth (Fig. 4). Specimen (JZC 001) was discovered by Jure Zupanc and is stored in his private geological collection. The specimen represents the complete tooth base (Fig. 4A-C) of a typical petalodont tooth. The tooth crown is missing.

Description: The base is triangular in tongue shape and comes to a rounded point in the distal edge (base end). Transversely the base is oval.

The mesiodistal width is 30 mm, and the total length is 36 mm. The maximal lingual-labial thickness of the tooth base is 6.4 mm. The lingual side of the base is bent to the labial side. On the surface of the lingual side, a few oval-shaped foramina are visible, on faint traces of ridges. On top of the base, the distal crown tongue is poorly preserved and overhangs the base. The labial side of the base has four elongated ridges, with no visible foramina, partially covered with a matrix.



Fig. 4. *Petalodus ohioensis* from Dovje locality. Specimen JZC 001: A - lingual, B - profile, C - labial views. The scale bar equals 10 mm. D - reconstructed position of the base in a tooth.

Sl. 4. *Petalodus ohioensis* iz najdišča pri Dovjem. Primerek JZC 001: A - lingvalni, B - stranski, C - labialni pogledi, merilo je 10 mm. D - rekonstrukcija položaja korenine na zobu.

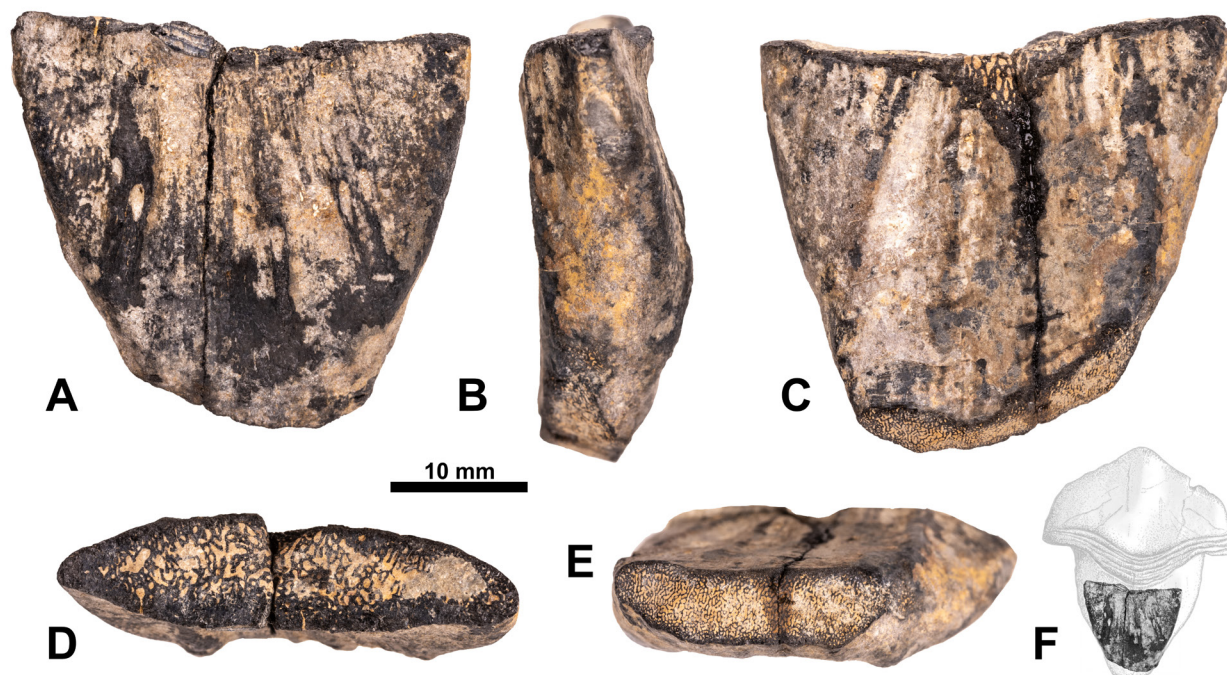


Fig. 5. *Petalodus* cf. *ohioensis* from Dovje locality. Specimen JZC 002: A - lingual, B - profile, C - labial views, D, E - distal surfaces with visible spongy tissue (osteodentine). The scale bar equals 10 mm. F - reconstructed position of the base in a tooth.

Sl. 5. *Petalodus* cf. *ohioensis* iz najdišča pri Dovjem. Primerek JZC 002: A - lingvalni, B - stranski, C - labialni pogled, D, E - distalna površina primerka z vidno kostno strukturo (osteodentin), merilo je 10 mm. F - rekonstrukcija položaja korenine na zobu.

Petalodus cf. *ohioensis* SAFFORD 1853

Figure 5

Material: One specimen of base of petalodontid tooth (Specimen JZC 002) (Fig. 5). The remains represent a fragmentary but typical petalodont tooth base (Fig. 5A-E). The tooth crown is missing.

Description: The base is triangular in shape and it is transversely oval. The mesiodistal width of the preserved base is 33 mm. The maximal lingual-labial thickness of the preserved tooth base is 9.5 mm. Labially the base is more concave and lingually convex. On both sides (lingual and labial) three elongated (vertical) ridges are present. On the lingual side, the oval-shaped foramina are visible on all ridges. On the bordered part (top of the base), a small part of the distal crown tongue is present, with two rows of ridges. On both distal surfaces of the specimen, the spongy tissue is visible. According to Zangerl et al. (1993), this tissue is circumpulpar trabeculine (cavities) and trabecular dentine, or osteodentine by Dalla Vecchia, 1988 and Gai et al., 2021 (Fig. 5D-E).

Discussion and Conclusion

Teeth of *Petalodus* are often the most common chondrichthyan fossil remains reported from the Carboniferous and Permian rocks of the USA, Europe, Russia, and China (Ginter et al. 2010, 141; Dalla Vecchia, 2008; Gai et al. 2021). The remains are mainly isolated teeth. *Petalodus ohioensis* is well known from Upper Carboniferous and Lower Permian beds and it is widespread (Hansen, 1985; Elliott et al, 2004, 277-278; Ginter et al. 2010, 141). The specimen presented here (JZC 001) (Fig. 4), preserved as a tooth base, is typical of *Petalodus ohioensis*. The shape of the tooth base is very similar in shape and dimensions to specimens presented by Brusatte (2007, 3, fig. 2), Harper (2018, 4, fig. 1), Ramovš & Bedič (1993, 149, fig. 1) and Ramovš (1997, 110, fig. 1). All these specimens come from Upper Carboniferous strata and are probably from the anterior part of *Petalodus ohioensis* jaw, based on shape and size of teeth base (Elliott et al, 2004, 277, fig. 5A-B). Even though our second specimen (JZC 002) (Fig. 5) is broken, we attribute it to the genus *Petalodus*. Its shape and dimensions and comparison with other specimens (see Brusatte, 2007; Harper, 2018; Ramovš & Bedič 1993) allow us to classify it as *Petalodus* cf. *ohioensis*.

The new finding increases the petalodont diversity in the Southern Alps, and also sheds new light on the distribution and stratigraphic range of petalodonts in Slovenia and this part of Europe.

Acknowledgments

I would like to thank Jure Zupanc for donating valuable specimens studied in this paper. I would also like to thank dr. Matevž Novak for his helpful comments on the stratigraphy of Permian beds from fossil locality. I am grateful to the anonymous reviewers for their valuable comments and suggestions that helped improve the manuscript.

References

- Brusatte, S.L. 2007: Pennsylvanian (Late Carboniferous) chondrichthyans from the LaSalle Limestone Member (Bond Formation) of Illinois, USA. *Neues Jahrbuch für Geologie und Paläontologie Abhandlungen*, 244/1: 1–8.
- Carpenter, K. & W. M. Itano 2019: Taxonomic validity of *Petalodus ohioensis* (Chondrichthyes, Petalodontidae) based on a cast of the lost holotype. *Geology of the Intermountain West*, 6: 55–60. <https://doi.org/10.31711/giw.v6.pp55-60>
- Dalla Vecchia, F. M. 1988: First record of a petalodont (*Petalodus ohioensis* Safford, 1853) from the Alps. *Gortania - Atti del Museo Friulano di Storia Naturale*, 9: 47–56.
- Dalla Vecchia, F. M. 2008: Vertebrati fossili del Friuli, 450 milioni di anni di evoluzione. *Museo Friulano di Storia Naturale*, Pubblicazione No. 50, Udine: 303 p.
- Elliott, D.K., Irmis, R.B., Hansen, M.C. & Olson, T.J. 2004: Chondrichthyans from the Pennsylvanian (Desmoinesian) Naco Formation of Central Arizona. *Journal of Vertebrate Paleontology*, 24/2: 268–280.
- Gai Z., Bai Z., Lin X., Meng X. & Zhang J. 2021: First Record of *Petalodus* Owen, 1840 (Chondrichthyes, Petalodontidae) in the Lower Permian (Cisuralian) of China. *Acta Geologica Sinica*, 95/4: 1057–1064. <https://doi.org/10.1111/1755-6724.14784>
- Ginter, M., Hampe, O. & Duffin, C.J. 2010: Handbook of Paleichthyology. Chondrichthyes. *Paleozoic Elasmobranchii: Teeth*, vol. 3D. München: 168 p.
- Hansen, M.C. 1985: Systematic relationships of petalodontiform chondrichthyans. In: Dutro, J.T., Jr. & Pfefferkorn, H.W. (eds.): Ninth International Congress on Carboniferous Stratigraphy and Geology, *Compte Rendus*, 5: 523–541.
- Harper, J.A. 2018: Reflections on *Petalodus*, a common late Paleozoic “shark” tooth found in western Pennsylvania’s rocks. *Pennsylvania Geology*, 48: 3–11.
- Huxley, T. 1880: *A Manual of the Anatomy of the Vertebrated Animals*. New York: Nabu Press, 431 p.
- Križnar, M. 2015: Zob paleozojskega morskega psa rodu *Glikmanius* (Chondrichthyes, Ctenacanthidae) iz Karavank (Slovenija) = Upper Paleozoic shark tooth of genus *Glikmanius* (Chondrichthyes, Ctenacanthidae) from Karavanke Mts. (NW Slovenia). *Geologija*, 58/1: 57–62. <https://doi.org/10.5474/geologija.2015.004>
- Križnar, M., Novak, A. & Preisinger, D. 2016: Zob paleozojskega morskega psa iznad Hrušice. *Proteus*, 78/9: 415–419.
- Lach, R., Gale, L., Križnar, M. & Novak, M. 2013: Nagromadzenia enigmatycznych permskich liliowców z Dovje (Karavanki, północna Słowenia). XXII Konferencja Naukowa Sekcji Paleontologicznej Polskiego Towarzystwa Geologicznego, »Aktualizm i antyaktualizm w paleontologii«, 27–30.09. 2013, Tyniec (Poster): 32–33.
- Lund, R. & Grogan, E.D. 1997: Relationships of the Chimaeriformes and the basal radiation of the Chondrichthyes. *Reviews in Fish Biology and Fisheries*, 7/1: 65–123.
- Lund, R., Grogan, E.D. & Fath, M. 2014: On the relationships of the Petalodontiformes (Chondrichthyes). *Paleontological Journal*, 48: 1015–1029.
- Newberry, J.S. & Worthen, A.H. 1866: Descriptions of new species of vertebrates, mainly from the subcarboniferous limestones and coal measures. *Geological Survey of Illinois, Paleontology*, 2: 11–141.
- Novak, M. 2006: Zanimivi fosili in sedimentološke posebnosti Dovžanove soteske. In: Režun, B. (ed.): *Zbornik povzetkov, 2. slovenski geološki kongres*, 26.–28 september Idrija.
- Novak, M., Forke, H. C. & Schönlaub, H. P. 2019: The Pennsylvanian-Permian of the Southern Alps (Carnic Alps/Karavanke Mts.), Austria/Italy/Slovenia - fauna, facies and stratigraphy of a mixed carbonate-siliciclastic shallow marine platform along the northwestern Palaeotethys margin: Field Trip C3. 19th International Congress on the Carboniferous and Permian, Cologne, July 29–August 2, 2019: field guides: 251–302.

- Novak, M. & Skaberne, D. 2009: Zgornji karbon in spodnji perm = Upper Carboniferous and Lower Permian. In: Pleničar, M., Ogorelec, B. & Novak, M. (eds.): *Geologija Slovenije = The Geology of Slovenia*. Geološki zavod Slovenije, Ljubljana: 99–136.
- Owen, R. 1840: *Odontography; or a treatise on the comparative anatomy of the teeth; their physiological relations, mode of development, and microscopic structure in the vertebrate animal*. London, Hippolyte Bailliere: 655 p.
- Patterson, C. 1965: The phylogeny of the chimaeroids. *Philosophical Transactions of the Royal Society of London, Series B*, 249: 101–219.
- Pavšič, J. 1995: Fosili, zanimive okamnine iz Slovenije. Tehniška založba Slovenije: Ljubljana 139 p.
- Peternel, M. 1995: Zobje morskih psov v zgornjem karbonu Karavank. *Jeseniški zbornik (Jeklo in Ljudje)*, 7: 273–276.
- Ramovš, A. 1997: *Petalodus ohioensis* (Chondrichthyes, Upper Carboniferous) from the Karavanke Mountains, Slovenia. *Neues Jahrbuch für Geologie und Paläontologie Monatshefte*, 2: 109–111.
- Ramovš, A. 1998: Two new petalodont teeth (Chondrichthyes, Upper Carboniferous) from the Karavanke Mountains, Slovenia. *Geologija*, 40: 109–112. <https://doi.org/10.5474/geologija.1997.004>
- Ramovš, A. & Bedič, J. 1993: Enkratni petalodontni zobje v karavanških zgornjekarbonskih plasteh. *Proteus*, 56/3: 149–150.
- Ramovš, A. & Sieverts-Doreck, H. 1968: Interessante Mittelperm-Crinoiden in Slowenien, NW Jugoslawien. *Geološki vjesnik*, 21: 191–206.
- Robb, A. J., III. 2003: Notes on the occurrence of some petalodont shark fossils from the Upper Pennsylvanian rocks of northeastern Kansas. *Transactions of the Kansas Academy of Science*, 106/1-2: 71–80. [https://doi.org/10.1660/0022-8443\(2003\)106Š0071:NOTOOSĆ2.0.CO;2](https://doi.org/10.1660/0022-8443(2003)106Š0071:NOTOOSĆ2.0.CO;2)
- Safford, J.M. 1853: Tooth of *Getalodus (Petalodus) ohioensis*. *American Journal of Science*, 2/16: 142.
- Zangerl, R., H. F. Winter & M. C. Hansen 1993: Comparative microscopic dental anatomy in the Petalodontida (Chondrichthyes, Elasmobranchii). *Fieldiana Geology*, 26:1–46.



Statistical approach to interpretation of geochemical data of stream sediment in Pleše mining area

Statistični pristop k interpretaciji geokemičnih podatkov potočnega sedimenta na območju rudišča Pleše

Simona JARC

University of Ljubljana, Faculty of Natural Sciences and Engineering, Department of Geology, Aškerčeva c. 12, SI-1000 Ljubljana, Slovenia; e-mail: simona.jarc@ntf.uni-lj.si

Prejeto / Received 25. 10. 2022; Sprejeto / Accepted 7. 10. 2022; Objavljeno na spletu / Published online 21. 12. 2022

Key words: ANOVA, t-test, correlation, cluster analysis, XRF, mineralization

Ključne besede: ANOVA, t-test, korelacija, klustrska analiza, XRF, mineralizacija

Abstract

The Ba, Pb and Zn ore deposit Pleše near Ljubljana is one of the formerly productive mines. The stream sediments were sampled and analysed by XRF to establish the effect of grain size, mineralization, and downstream location of sampling sites on geochemical composition based on various statistical analyses. Statistical analyses of the geochemical data confirm the impact of mineralization. The parametric t-test, non-parametric Mann-Whitney test and cluster analysis showed only minor differences in the geochemical composition of the samples with different grain sizes (< 0.063 mm and 0.063-2 mm). The parametric and non-parametric correlation coefficients as well as cluster analysis indicate that the contents of Si, Al, K, Rb, and Fe are associated with weathered rock forming minerals such as micas, and clay minerals, whereas Nb and Zr are associated with minerals resistant to weathering. Ca and Mg are associated with carbonates. S, Ba, Sr, Pb, Zn, and Mn indicate local mineralization with sulphates and sulphides. The results of the t-test and analysis of variance, Mann-Whitney tests and Kruskal-Wallis ANOVA of the groups established by the cluster analysis confirm that the contents of Ba, Pb and Sr have a statistically significant influence on the classification of the cluster group - i.e., the influence of sediment mineralization. There are no differences in elemental contents in the sediment samples downstream. The statistical approach to evaluate the geochemical data has proven useful and provides a good basis for further interpretation.

Izvleček

V rudišču Pleše v okolici Ljubljane so v preteklosti pridobivali Ba, Pb in podrejeno Zn. Vpliv velikosti zrn, mineralizacije in lokacije vzorčevanih točk dolvodno na geokemično sestavo sem določala v vzorcih potočnega sedimenta, katerega geokemična sestava je bila določena z metodo XRF. Statistična analiza podatkov geokemične sestave je potrdila mineralizacijo vzorcev potočnega sedimenta. Rezultati parametričnega t-testa, neparametričnega Mann-Whitney-jevega testa in klustrske analize so pokazali, da se geokemični sestavi vzorcev frakcij <0,063 mm in 0,063-2 mm skoraj ne razlikujeta. Tako parametrični kot neparametrični korelacijski koeficienti ter klustrska analiza so pokazali, da prvine Si, Al, K, Rb in Fe kažejo na prisotnost preperelih kamninotvornih mineralov (npr. sljud, glinenih mineralov), Nb in Zr na minerale odporne na preperevanje, Ca in Mg sta značilna za karbonate. S, Ba, Sr, Pb, Zn in Mn kažejo na lokalno mineralizacijo s sulfati in sulfidi. Razlike med skupinami, ugotovljenimi s klustrsko analizo, sem testirala s parametričnim t-testom, analizo variance in Mann-Whitney-jevim testom ter Kruskal-Wallis ANOVO. Na uvrstitev v skupine najbolj vplivajo vsebnosti Ba, Pb in Sr, kar potrjuje vpliv mineralizacije sedimenta. Razlik v geokemični sestavi vzorcev sedimentov dolvodno testi niso zaznali. Statistični pristop k interpretaciji geokemičnih podatkov predstavlja dobro osnovo za nadaljnjo interpretacijo.

Introduction

Nowadays, statistical analyses are very common and useful in many fields of geology (Swan and Sandilands, 1995; Davis, 2002), especially when dealing with geochemical data (e.g., Albanese et al., 2007; Grunsky et al., 2009). A statistical approach can also be useful in determining relationships between the geochemical composition of soils or stream sediments and mineral occurrences (e.g., Candeias et al., 2011; Carvalho et al., 2014; Levitan et al., 2015). There are some former mines and small ore deposits of Pb, Zn, Hg and Fe in the vicinity of Ljubljana (Dervarič et al., 2005). The Pleše Ba, Pb, and Zn ore deposit is one of the formerly productive mines (Mlakar, 2003). Barite, galena, and some sphalerite were mined here for at least 250 years. Between 1729 and 1963, when the mine was opened, more than 100,000 tons of barite, about 10,000 tons of Pb, and some Zn were mined (Žebre, 1955; Fabjančič, 1966; Mlakar, 2003). Today, water seeps and leaks from the formerly productive mine and transports mineralized sediments that may affect the local environment. Stream sediment chemistry is one of the indicators of local geology and also of mining activity (e.g., Hudson-Edwards et al., 1996; Ettlner et al., 2006; Teršič et al., 2018). It can also be used as an indicator of potential contamination from mining materials (Baptista-Salazar et al., 2017; Potra et al., 2017; Gosar et al., 2020; Žibret & Čepelak, 2021; Miler et al., 2022).

Sediments from the stream of the abandoned mine tunnel in the Pleše area were sampled to evaluate their geochemical properties and the influence of grain size (0.063–2 mm and < 0.063 mm) based on statistical analyses. In addition, statistical tests were performed to evaluate the impact of the sampling site on sediment geochemical composition.

Materials and methods

The oldest rocks of the area are the Carboniferous clastites (Buser, 1974; Mlakar, 2003). The Permian rocks of the Val Gardena Formation are followed by Lower Triassic dolomites interbedded with fine clastites, red claystones, oolitic limestone and dolomite lenses. This is followed by Anisian and Cordevolian dolomites, and finally the upper Triassic Main dolomite. Stream and bog sediments with scree are the youngest rocks in the area (Buser et al., 1969; Buser, 1974; Mlakar 2003). The area has a complex tectonic history (Buser, 1974; Premru 1974, 1980; Mlakar, 1987; Placer, 1998; Dozet, 1999; Mlakar, 2003). The Upper Triassic dolomite is overthrust by Pale-

ozoic beds. In addition, several faults of different systems (e.g., cross-alpidic, dinaric, cross-dinaric) are observed. Mineralization with barite, galena and sphalerite occurs in both Paleozoic and Triassic beds (Buser, 1974; Mlakar 2003).

Stream sediment samples were collected at 10 sampling sites at a total distance of 250 m from the abandoned mining tunnel (Fig. 1). The upper 30 cm of the stream sediment was sampled. In the laboratory, all samples were dried at 40 °C. Sample size was reduced by quartering. Samples were sieved through sieves with a 2-mm and a 0.063-mm openings. A total of 15 samples were analysed – 5 samples of fraction 0.063–2 mm (samples designated PO1-2, PO3-2, PO5-2, PO7-2, PO9-2) and 10 samples with grain size of < 0.063 mm (samples designated PO1 to PO10). Geochemical composition was determined using a Thermo Fisher Niton XL3t GOLDD portable X-ray fluorescence (XRF) analyzer at the Department of Geology, Faculty of Natural Sciences and Engineering, University of Ljubljana. The accuracy was checked with several analyses of standard materials and found to be good for elements in question. The only exception is Ba, whose values were not standardised and therefore should be used with caution and only for relative comparison of the analysed samples. Relative percentage difference (%RPD) of duplicate measurements of sample PO1 showed very good precision (< 10 % error) for most elements, with the exception of S (< 12 % error). For further interpretation, the contents of Si, Al, Fe, Mg, Ca, K, S, Mn, Ba, Nb, Pb, Rb, Sr, Zn, and Zr were manipulated. The contents of the other elements were below the detection limit in the majority of the samples or were not of our interest. Statistical analysis was performed using Tibco Statistica software (2017).

Normality of data distribution was checked by comparison of medians, arithmetic and geometric means, by kurtosis and skewness, by visual inspection of histograms, by Kolmogorov-Smirnov and Lilliefors test, and by Shapiro-Wilk test. Because some of the variables aren't normally distributed and because of the small number of samples and for comparison, we applied parametric and non-parametric statistics (Swan and Sandilands, 1995; Davis, 2002). For comparison parametric t-test and non-parametric Mann-Whitney test were performed and correlations (Pearson's product-moment and Spearman rank order correlation coefficients) were calculated. Cluster analyses of the variables and observations were performed using Ward's linkage rule method and the 1-Pearson correlation coefficient and Euclidean distance as a distance measure.

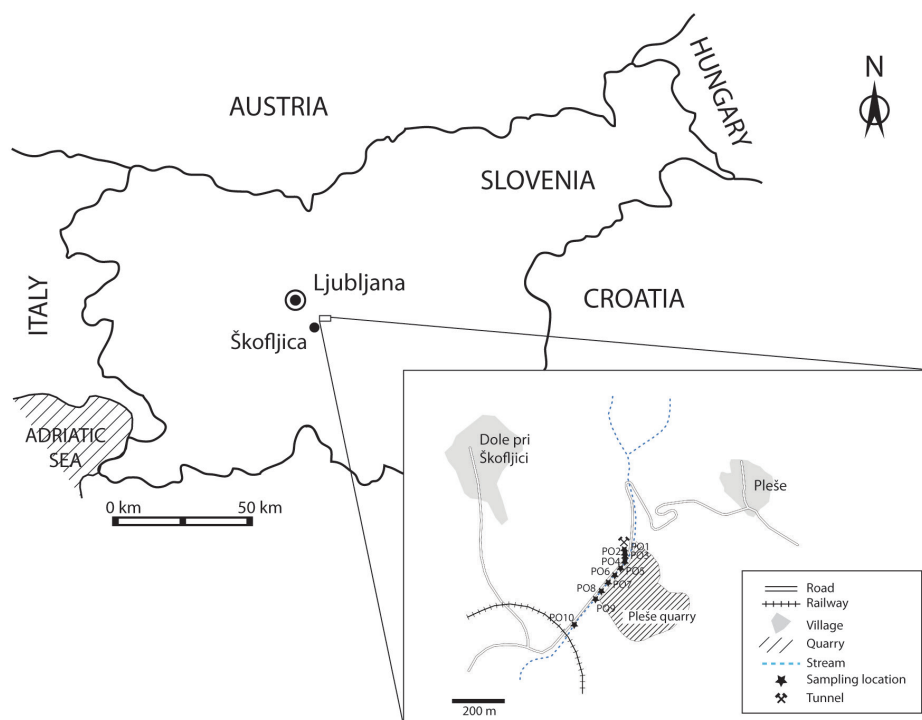


Fig. 1. Map of the area with sampling locations.

Results and Discussion

Ba-Pb-Zn mineralization is clearly evident in the geochemical compositions of the stream sediment samples (Table 1). In some samples, the contents of Ba (the values reported should be used with caution and for relative comparison only), Pb, and Zn exceed the intervention values of 625, 530, and 720 mg/kg, respectively, in soils (Ur. list RS 68/96) and in soils and sediments (VROM, 2000). The contents of Ba and Pb above intervention values were also established by others (Gosar et al., 2014; Miler et al., 2022). For comparison, median values for Ba, Pb and Zn in stream sediments analysed by XRF in Europe are 370, 21 and 71 mg/kg (Salminen et al., 2005).

The presence of silicate and carbonate minerals in sediment samples is also evident (Table 1). The variations in geochemical composition is the result of complex geological composition of the area (Buser, 1974; Mlakar, 2003).

The effect of grain size on the distribution of elements was examined using the parametric t-test and the non-parametric Mann-Whitney test. The parametric t-test revealed statistically significant differences (95 % probability) in the studied fractions (0.063-2 mm and < 0.063 mm) with respect to the content of Mg ($t = -2.53$, $p = 0.025$), Nb ($t = 2.26$, $p = 0.041$), and Zr ($t = 2.35$, $p = 0.036$). The results of the Mann-Whitney test were very similar, with statistically significant differences at the 95 % probability level for the contents of Nb ($Z = 2.02$, $p = 0.043$) and Zr ($Z = 2.88$, $p = 0.004$) in the studied grain size fractions.

The results are also confirmed by box and whisker plots (Fig. 2) - the geochemical composition is very similar in both fractions. Some samples are more mineralized than others, with no clear trend as a function of grain size. Minor differences are observed only in Mg content, which is almost twice as high in the coarse-grained fraction, with a mean of 9.01 % and a median of 9.73 % (in the < 0.063 mm samples, the mean is 5.44 % and the median is 5.98 %). The Mg content can be attributed to the presence of dolomite. Niobium and Zr are more abundant in the fine-grained fraction. For Nb, the mean is 16 mg/kg and the median is 15 mg/kg in the < 0.063 mm fraction, while it is lower in the coarser fraction at 9 mg/kg and 7 mg/kg, respectively. The difference in Zr content is even greater: mean and median are 251 mg/kg and 150 mg/kg in the finer fraction, while 42 mg/kg (mean) and 41 mg/kg (median) in the coarser fraction. Niobium and Zr are bound in weathering resistant minerals.

The small number of samples and the (non-) normality of the distribution clearly affect the differences between mean and median values (Swan & Sandilands, 1995). In the present case, the number of samples (10 vs. 5 samples) also affects the range - the ranges of the fine-grained samples (< 0.063 mm) are generally larger than the ranges of the 0.063-2 mm samples for most elements. The exceptions with wide ranges for S, Ba, Pb, Sr, and Zn in the coarser fraction are probably due to the mineralization of the sediments.

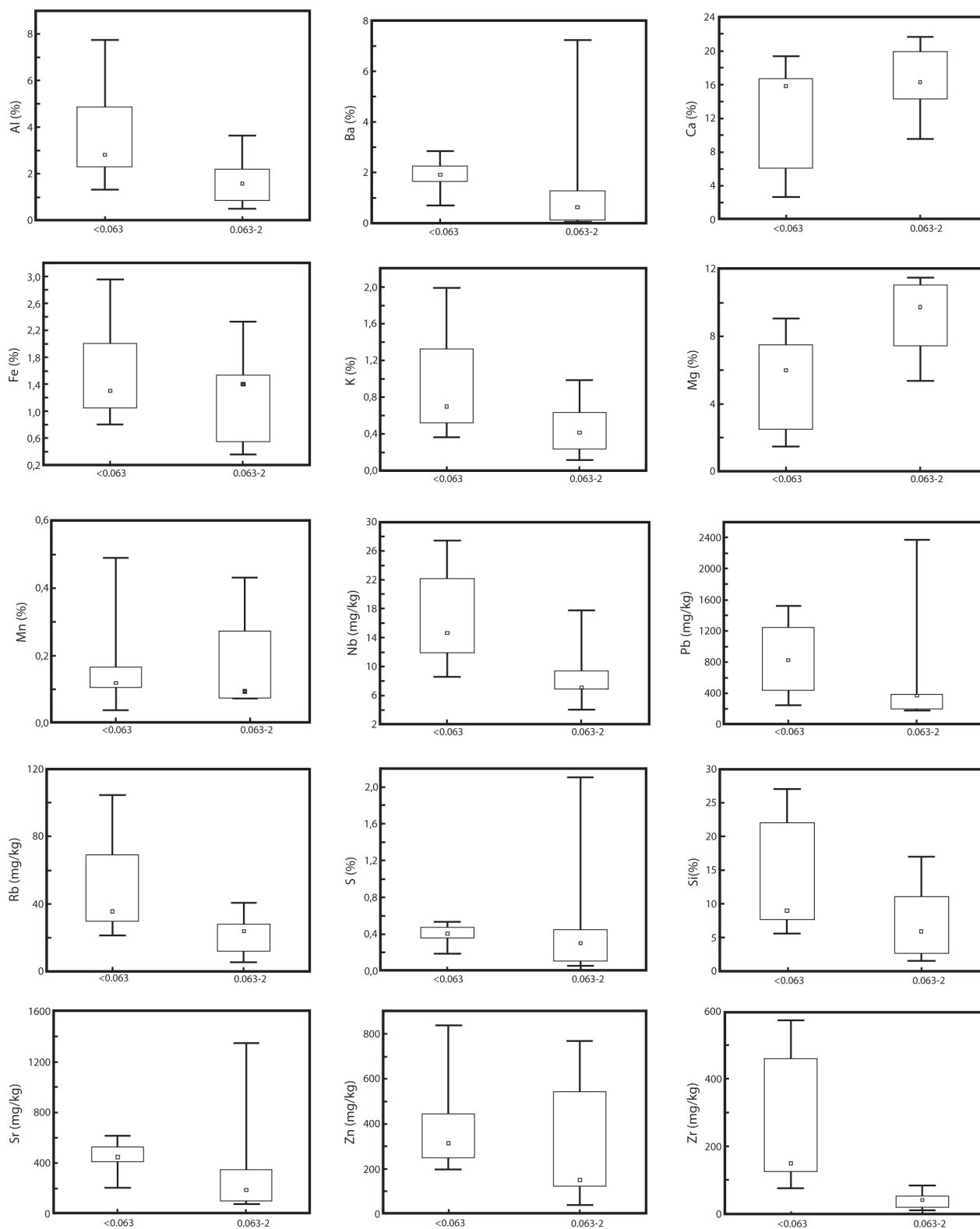


Fig. 2. Medians, interquartile ranges (boxes) with minimum and maximum values (whiskers) of measured elements in finer (<0.063 mm) and coarser (0.063-2 mm) fractions.

The relations between elements have been determined by calculation of correlation coefficients and by cluster analysis. Care should be taken when comparing parametric and non-parametric correlation coefficients calculated using Tibco Statistica software. The software requires

all data to calculate the parametric correlation coefficient. If one or more variable values are missing, the entire observation is excluded from the analysis. As Mn content in sample PO9-2 was not detected by XRF, the entire observation was eliminated from the analysis. Therefore, when

Table 1. Results of geochemical analysis.

Sample	Grain sizes (mm)	Si (%)	Al (%)	Fe (%)	Mg (%)	Ca (%)	K (%)	S (%)	Mn (%)	Ba (%)	Nb (mg/kg)	Pb (mg/kg)	Rb (mg/kg)	Sr (mg/kg)	Zn (mg/kg)	Zr (mg/kg)
PO1	<0.063	26.989	7.750	2.950	1.470	2.680	1.988	0.188	0.128	1.188	27	245	105	302	308	460
PO2	<0.063	22.058	4.882	2.124	2.482	5.475	1.323	0.389	0.106	1.650	22	376	69	409	319	554
PO3	<0.063	24.015	5.296	2.009	2.493	6.104	1.450	0.475	0.159	2.061	24	435	71	459	445	574
PO4	<0.063	10.240	2.920	1.531	5.989	15.450	0.765	0.482	0.188	2.275	15	1454	44	525	664	161
PO5	<0.063	7.665	2.561	1.269	5.967	19.352	0.697	0.465	0.489	2.838	14	1520	37	615	839	138
PO6	<0.063	9.201	3.060	1.341	6.843	15.970	0.700	0.531	0.166	2.564	15	954	34	584	342	138
PO7	<0.063	8.790	2.720	1.124	7.503	16.394	0.595	0.410	0.108	1.928	12	688	32	425	281	126
PO8	<0.063	5.591	1.324	0.967	4.655	15.639	0.456	0.400	0.104	1.908	13	567	26	482	199	124
PO9	<0.063	5.997	1.767	0.803	9.051	18.715	0.363	0.213	0.037	0.703	9	1248	21	206	215	76
PO10	<0.063	8.531	2.299	1.045	7.907	16.742	0.521	0.356	0.071	1.727	12	1193	30	436	250	162
PO1-2	0.063-2	16.970	3.643	2.330	5.356	9.565	0.984	0.056	0.112	0.117	9	177	41	77	150	83
PO3-2	0.063-2	11.080	2.183	1.535	7.438	14.274	0.633	0.300	0.074	0.634	7	371	24	186	769	53
PO5-2	0.063-2	5.910	1.580	1.401	9.726	16.284	0.416	2.106	0.432	7.239	18	2369	28	1350	544	41
PO7-2	0.063-2	2.649	0.853	0.549	11.482	19.940	0.235	0.453	0.071	1.285	7	387	12	347	122	19
PO9-2	0.063-2	1.553	0.510	0.361	11.044	21.651	0.116	0.107		0.055	4	197	5	102	40	11

comparing the two correlation coefficients, some data are “lost” - regardless of whether we omit the entire observation or the variable with the missing data. Consequently, the results may differ to some extent and may also be biased.

First, the coefficients were calculated without the sample PO9-2 data. For most elements, there are almost no differences in the statistically significant correlation coefficients calculated with the parametric Pearson's product-moment correlation coefficient (Table 2) or with non-parametric Spearman rank order correlation coefficient (Table 3). Exceptions are Si-Nb, Fe-Zr, and Mn-Pb, for which parametric correlations were determined to be statistically significant, and Si-Pb, Mn-Nb, Mn-Rb, and Ba-Zn with statistically significant non-parametric correlation coefficients. The results look slightly different if we omit the Mn values (Tables 4 and 5) instead of PO9-2 observation. In this case, the differences are in S-Zn, Ba-Nb, Ba-Zn, Nb-Sr, and Sr-Zn correlations, where non-parametric correlation coefficients are statistically significant, and Pearson's product-moment correlation coefficients aren't. The Pearson's product-moment correlation coefficient is based on the agreement and direction of the linear relationship between two variables, while the non-parametric correlation is based on the ranking of the data values rather than the values themselves (Swan & Sandilands, 1995). Therefore, scatter plots with a distinct trend line may have a low non-parametric correlation even though the parametric correlation is statistically significant because the positive and negative deviations from the line almost cancel each other out. The non-parametric correlation is also less sensitive to extreme values (Swan & Sandilands, 1995). On the other hand, the calculation of Pearson's product-moment correlation coefficient requires a larger number of samples and normality of the distribution. Therefore in presented case, the results of non-parametric correlations are more trustworthy, while parametric Pearson's product-moment correlation coefficient should be used with caution.

The results of cluster analysis of the variables show two main groups (Fig. 3). The first group consists of Si, Al, K, Rb, Fe, Nb, and Zr, while the second group can be divided into two subgroups, with Ca and Mg in one and Zn, Pb, Mn, Sr, Ba, and S in the other subgroup. Cluster analysis confirms the results of correlation coefficients. Namely, members of the groups have in general higher correlation coefficients. The contents of Si, Al, K, Rb, and Fe can be attributed

to secondary minerals (e.g., clay minerals, micas) or oxides (hematite; Mlakar 2003), Nb and Zr to weathering-resistant minerals, and Ca and Mg to carbonates. Ba, Pb, Zn and S indicate local mineralization with sulphates and sulphides, while Sr might be attributed to trace elements in barite (Mlakar, 2003) and Mn in galenite and sphalerite (Drovenik et al., 1980) or to secondary minerals formed with ore mineral weathering (Miler et al., 2022).

When clustering the observations without sample PO9-2 (using Ward's method as a linkage rule and Euclidean distance measurement), three groups are distinguished (Fig. 4): the first group with samples PO1, PO1-2, PO2, PO3, PO3-2, PO7-2; the second group with samples PO6, PO7, PO8, PO9, PO10; and the third group with samples PO4, PO5, and PO5-2. We checked the differences between the groups obtained by cluster analysis using analysis of variance and Kruskal-Wallis

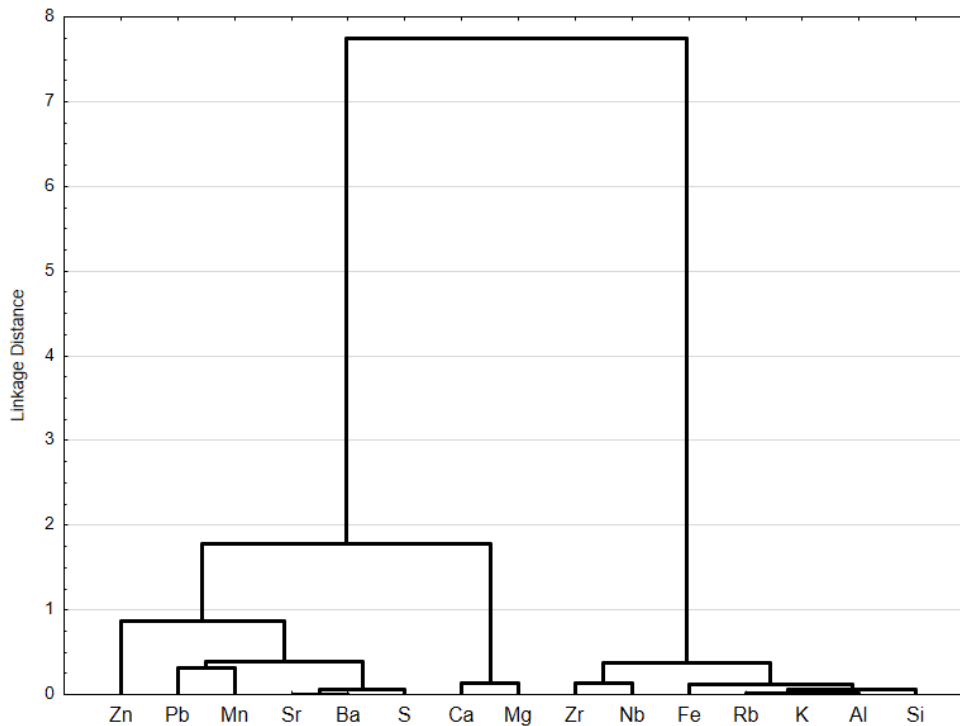


Fig. 3. Cluster analysis of measured elements (calculation is based on Ward's method as a linkage rule and 1-Pearson r as a distance measurement).

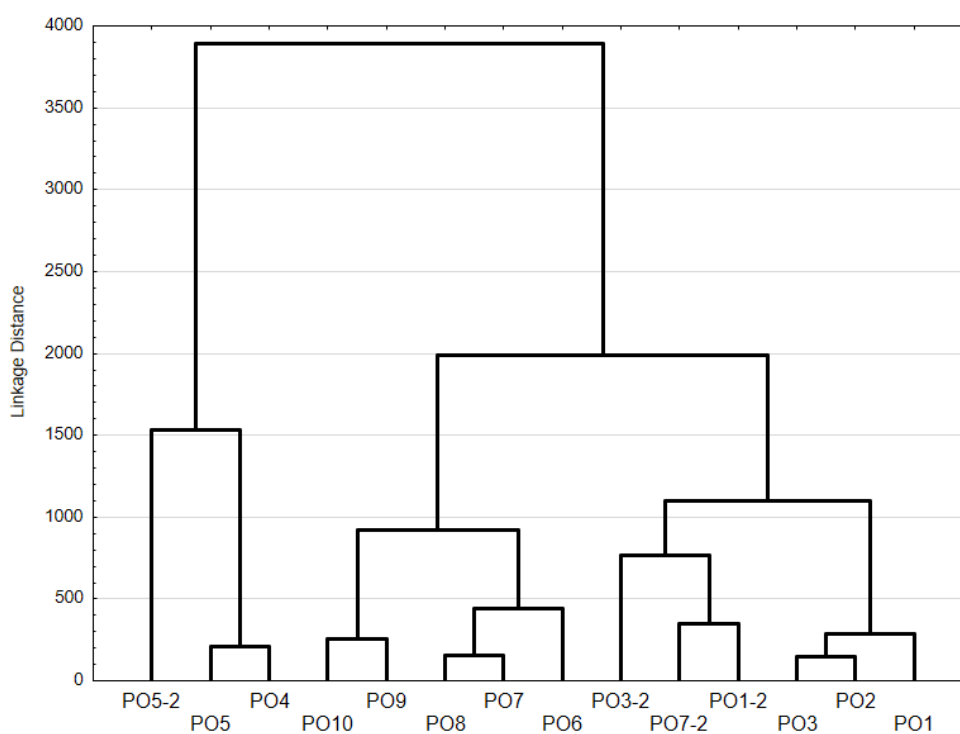


Fig. 4. Cluster analysis of investigated samples without PO9-2 (calculation is based on Ward's method as a linkage rule and Euclidean distances as a distance measurement).

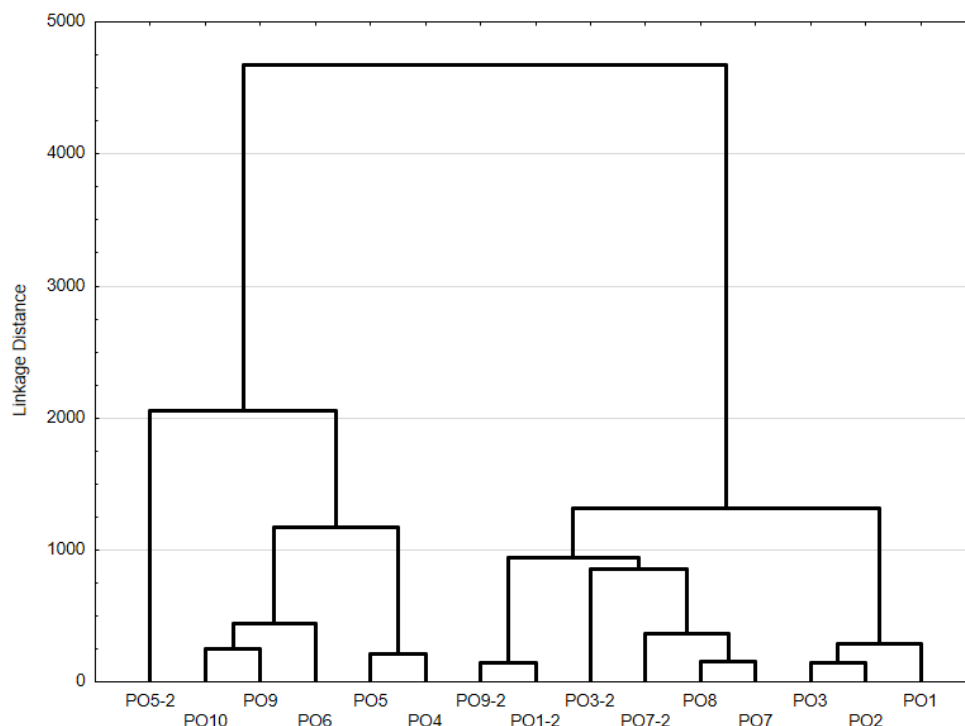


Fig. 5. Cluster analysis of investigated samples without Mn content in all samples (calculation is based on Ward' method as a linkage rule and Euclidean distances as a distance measurement).

Conclusions

ANOVA test. The results show that the content of Pb, Ba, Mn, and Sr (i.e., the mineralization of the sediment) has the greatest influence on the classification into these three individual groups. If we exclude the Mn content from the analysis (it was not detectable in one sample) and manipulate all 15 sediment samples, the result of the cluster analysis looks somewhat different (Fig. 5). Only two groups can be distinguished: PO1, PO2, PO3, PO7, PO8, PO7-2, PO3-2, PO1-2 and PO9-2 form one group, PO4, PO5, PO6, PO9, PO10 and PO5-2 form the second. According to the results of the parametric t-test for independent groups, the contents of Pb and Sr have a significant effect on the grouping. Due to the results of the non-parametric Mann-Whitney test, the contents of Pb, Ba and Sr have a statistically significant influence on the grouping of observations. The statistical analysis clearly shows the different contents of ore minerals of the samples and its effect on the clustering of observations. However, the grain size has no influence on the geochemical composition of the studied samples (< 0.063 mm and 0.063-2 mm; Figs. 4 and 5) as geochemical composition is practically the same in both fractions. Cluster analysis of the samples also shows no significant differences in the geochemical composition regarding the downstream location of sediment samples.

Mineralization with barite, galena and sphalerite in the Pleše area is clearly demonstrated in the geochemical composition of stream sediments. The contents of Ba (the values given should be used with caution and only for relative comparison), Pb and Zn in some samples exceed the intervention values of 625, 530 and 720 mg/kg, respectively (Ur. list RS 68/96; VROM, 2000).

The parametric t-test and the non-parametric Mann-Whitney test showed only minor differences in geochemical composition between samples with different grain sizes, whereas cluster analysis shows no differences. The Mg content is statistically significantly higher in samples of 0.063-2 mm, and the contents of Nb and Zr are higher in < 0.063-mm samples. The number of observations (sediment samples) influence the ranges of the variables as the ranges of fine-grained samples are generally larger than ranges of coarse-grained samples. The diverse composition is the result of the complicated geological composition of the area (Buser, 1974; Mlakar, 2003). Ba, Sr, Pb, Zn, Mn and S indicate local mineralization with sulphide and sulphate minerals and their weathering products.

Pearson's product-moment correlation coefficients, non-parametric Spearman rank order correlation coefficients and cluster analysis indicate that Si, Al, K, Rb, and Fe contents are associated with weathered rock forming minerals such as

mica, and clay minerals, whereas Nb and Zr are associated with weathering-resistant minerals (oxides, silicates). Ca and Mg are characteristics of carbonates and S, Ba, Sr, Pb, Zn and Mn of local mineralization with sulphides and sulphates. The results of the parametric t-test, analysis of variance, and non-parametric Mann-Whitney and Kruskal-Wallis ANOVA tests of the clustered sediment samples confirm that the contents of Ba, Pb and Sr have a statistically significant influence on the clustering of the sediment samples, i.e., the statistical analyses confirm the influence of sediment mineralization. Cluster analysis of the observations also shows no significant differences in the geochemical compositions regarding the downstream sampling position.

Although the number of sediment samples was relatively small, the combination of various statistical tests and analyses shows results that have a geologic basis and significance. The statistical approach to evaluating the geochemical data has proven useful and provides a good basis for assigning elemental data to parent rocks and for identifying potentially contaminated areas.

Acknowledgments

The author gratefully acknowledges financial support from the state budget through the Slovenian Research Agency (Programme No. P1-0195). Special thanks to Ema Hrovatin, Primož Miklavc, Miran Udovč and Gašper M. Volk for preparation of the samples and technical support, and to Prof. Dr. Nina Zupančič for her comments and suggestions.

References

- Albanese, S., De Vivo, B., Lima, A. & Cicchella, D. 2007: Geochemical background and baseline values of toxic elements in stream sediments of Campania region (Italy). *J Geochem Explor*, 93: 21–34. <https://doi.org/10.1016/j.gexplo.2006.07.006>
- Baptista-Salazar, C., Richard, J., Horf, M., Rejc, M., Gosar, M. & Biester, H. 2017: Grain-size dependence of mercury speciation in river suspended matter, sediments and soils in a mercury mining area at varying hydrological conditions. *Appl Geochemistry*, 81: 132–142. <https://doi.org/10.1016/j.apgeochem.2017.04.006>
- Buser, S. 1974: Tolmač lista Ribnica, Osnovna geološka karta SFRJ 1:100.000. Zvezni geološki zavod, Beograd: 60 p.
- Buser, S., Dozet, S., Cajhen, J., Ferjančič, L., Grad, K. et al. 1969: Osnovna geološka karta SFRJ 1: 100.000, list Ribnica. Zvezni geološki zavod, Beograd.
- Candeias, C., Ferreira da Silva, E., Salgueiro, A.R., Pereira, H.G., Reis, A.P., Patinha, C., Matos, J.X. & Ávila, P.H. 2011: The use of multivariate statistical analysis of geochemical data for assessing the spatial distribution of soil contamination by potentially toxic elements in the Aljustrel mining area (Iberian Pyrite Belt, Portugal). *Environ Earth Sci*, 62: 1461–1479. <https://doi.org/10.1007/s12665-010-0631-2>
- Carvalho, P.C.S., Neiva, A.M.R., Silva, M.M.V.G. & Ferreira da Silva, E.A. 2014: Geochemical comparison of waters and stream sediments close to abandoned Sb-Au and As-Au mining areas, northern Portugal. *Chemie der Erde*, 74/2: 267–283. <https://doi.org/10.1016/j.chemer.2013.08.003>
- Davis, J.C. 2002: Statistics and data analysis in geology, 3rd Ed. John Wiley & Sons, New York: 638 p.
- Dervarič, E., Herlec, U., Likar, J. & Bajželj, U. 2005: Rudniki in premogovniki v Sloveniji. Argos, Nazarje: 175 p.
- Dozet, S. 1999: Barite-bearing Pleše Formation, Central Slovenia Camparison of barite-bearing beds and barite occurrences in the Outer Dinarides area (Pleška baritonosna formacija, osrednja Slovenija: Primerjava baritonosnih plasti in baritnih pojavov na območju Zunanjih Dinaridov). *Geologija*, 42/1: 41–68. <https://doi.org/10.5474/geologija.1999.004>
- Drovenik, M., Pleničar, M. & Drovenik, F. 1980: Nastanek rudišč v SR Sloveniji = The origin of Slovenian ore deposits. *Geologija*, 23/1: 1–137.
- Ettler, V., Mihaljevič, M., Šebek, O., Molek, M., Grygar, T. & Zeman, J. 2006: Geochemical and Pb isotopic evidence for sources and dispersal of metal contamination in stream sediments from the mining and smelting district of Příbram, Czech Republic. *Environ Pollut*, 142/3: 409–17. <https://doi.org/10.1016/j.envpol.2005.10.024>
- Fabjančič, M. 1966: About barite occurrences in Slovenia (O baritu na Slovenskem). *Geologija*, 9/1: 505–526. <https://www.geologija-revija.si/index.php/geologija/article/view/234>
- Gosar, M., Šajn, R., Miler, M., Burger, A., & Bavec, Š. 2020: Overview of existing information on important closed (or in closing phase) and abandoned mining waste sites and related

- mines in Slovenia. *Geologija*, 63/2:, 221–250. <https://doi.org/10.5474/geologija.2020.018>
- Gosar, M., Šajn, R., Miler, M., Markič, M. & Čarman, M. 2014: Izdelava popisa zaprtih objektov za ravnanje z odpadki iz rudarskih in drugih dejavnosti izkoriščanja mineralnih surovin: poročilo 3. faze projekta, elaborat, študija. Geološki zavod Slovenije, Ljubljana: 49 p.
- Grunsky, E.C., Drew, L.J. & Sutphin, D.M. 2009: Process recognition in multi-element soil and stream-sediment geochemical data. *Appl Geochem*, 24/8: 1602–1616. <https://doi.org/10.1016/j.apgeochem.2009.04.024>
- Hudson-Edwards, K.A., Macklin, M.G., Curtis, C.D. & Vaughan, D.J. 1996: Processes of Formation and Distribution of Pb-, Zn-, Cd-, and Cu-Bearing Minerals in the Tyne Basin, Northeast England: Implications for Metal-Contaminated River Systems. *Environ Sci Technol*, 30/1: 72–80. <https://doi.org/10.1021/es9500724>
- Levitan, D.M., Zipper, C.E., Donovan, P., Schreiber, M.E., Seal, R.R., Engle, M.A., Chermak, J.A., Bodnar, R.J., Johnson, D.K. & Aylor, J.A. 2015: Statistical analysis of soil geochemical data to identify pathfinders associated with mineral deposits: An example from the Coles Hill uranium deposit, Virginia, USA. *J Geochem Explor*, 154: 238–251. <https://doi.org/10.1016/j.gexplo.2014.12.012>
- Miler M., Bavec, Š. & Gosar, M. 2022: The environmental impact of historical Pb-Zn mining waste deposits in Slovenia. *J Environ Manage*, 308: 114580. <https://doi.org/10.1016/j.jenvman.2022.114580>
- Mlakar, I. 2003: On the problems of Ba, Pb, Zn Pleše ore deposit (Slovenia) = O problematiki Ba, Pb, Zn rudišča Pleše. *Geologija*, 46/2: 185–224. <https://doi.org/10.5474/geologija.2003.018>
- Mlakar, I. 1987: A contribution to the knowledge of the geological structure of Sava Folds and theirsouthern border – Summary = Prispevek k poznavanju geološke zgradbe Posavskih gub in njihovega južnega obrobja. *Geologija*, 29/28: 157–182.
- Placer, L. 1998: Structural meaning of the Sava folds = Strukturni pomen Posavskih gub. *Geologija*, 41/1: 191–221. <https://doi.org/10.5474/geologija.1998.012>
- Potra, A., Dodd, J.W. & Ruhl, L.S. 2017: Distribution of trace elements and Pb isotopes in stream sediments of the Tri-State mining district (Oklahoma, Kansas, and Missouri), USA, *Appl Geochem*, 82: 25–37. <https://doi.org/10.1016/j.apgeochem.2017.05.005>
- Premru, U. 1974: Triadni skladi v zgradbi osrednjega dela Posavskih gub = Trias im geologischen Bau der mittleren Savefalten – Zusammenfassung. *Geologija*, 17: 261–297.
- Premru, U. 1980: Geological structure of Central Slovenia (Summary) = Geološka zgradba osrednje Slovenije. *Geologija*, 23/2: 227–278.
- Salminen, R., Batista, M.J., Bidovec, M., Demetriades, A., De Vivo, B., De Vos, W. et al. 2005: Geochemical atlas of Europe. Part 1, Background information, methodology and maps. Geological Survey of Finland, Espoo: 525 p.
- Swan, A.R.H. & Sandilands, M. 1995: Introduction to Geological Data Analysis. Blackwell Science, Oxford: 446 p.
- Teršič, T., Miler, M., Gaberšek, M. & Gosar, M. 2018: Vsebnosti arzena in nekaterih drugih prvin v potočnih sedimentih in vodah porečja Medije, osrednja Slovenija = Contents of arsenic and some other elements in stream sediments and waters of the Medija drainage basin, central Slovenia. *Geologija*, 61/1: 5–24. <https://doi.org/10.5474/geologija.2018.001>
- TIBCO Software Inc. 2017: Statistica (data analysis software system), version 13. <http://statistica.io>
- Uradni list RS, 1996: Uredba o mejnih, opozorilnih in kritičnih imisijskih vrednostih nevarnih snovi v tleh. Ljubljana, Uradni list, 68: 5773–5774.
- VROM, 2000: Dutch Target and Intervention Values (the New Dutch List), Circular on target values and intervention values for soil remediation. The Ministry of Housing, Spatial Planning and the Environment (VROM). https://esdat.net/Environmental%20Standards/Dutch/annexS_I2000Dutch%20Environmental%20Standards.pdf (Accessed 16 August 2022).
- Žebre, S.: Rudarska dejavnost v območju Posavskih gub. *Rudarsko metalurški zbornik*, 1955,4: 239–255.
- Žibret, G. & Čeplak, B. 2021: Distribution of Pb, Zn and Cd in stream and alluvial sediments in the area with past Zn smelting operations. *Sci Rep.*, 11: 17629. <https://doi.org/10.1038/s41598-021-96989-y>



Depositional environment of the Middle Triassic Strelovec Formation on Mt. Raduha, Kamnik-Savinja Alps, northern Slovenia

Sedimentacijsko okolje srednjetriasne Strelovške formacije na Raduhi v Kamniško-Savinjskih Alpah, severna Slovenija

Primož MIKLAVC¹ & †Bogomir CELARC²

¹University of Ljubljana, Faculty of Natural Sciences and Engineering, Department of Geology, Aškerčeva c.12, SI-1000 Ljubljana, Slovenia; e-mail: primoz.miklavc@ntf.uni-lj.si

²Geological Survey of Slovenia, Dimičeva ulica 14, SI-1000 Ljubljana, Slovenia

Prejeto / Received 14. 11. 2022; Sprejeto / Accepted 12. 12. 2022; Objavljeno na spletu / Published online 21. 12. 2022

Key words: Southern Alps, bituminous limestones, restricted basin, intraformational breccia, Anisian, facies analysis

Ključne besede: Južne Alpe, bituminozen apnenec, zaprti bazen, intraformacijska breča, anizij, faciesna analiza

Abstract

The Raduha section represents a continuation of the research of the Anisian Strelovec Formation in the Kamnik-Savinja Alps. The Strelovec Formation was deposited during the Anisian on a drowned section of the Serla Dolomite carbonate platform in a restricted probably outer ramp environment associated with an intraplateform basin. The base of the section is represented by dolostone breccia containing angular carbonate lithoclasts of shallow-marine origin. This is followed by alternations of laminated and homogenous hemipelagic limestones deposited in a restricted and anoxic environment. Hemipelagic sedimentation was occasionally interrupted by clay input and deposition of sediments from gravity mass flows. Slow filling of the basin lead to a gradual cessation of anoxic conditions and sedimentation of bedded shallow-marine limestones. After shallow water conditions were established, bioclastic dolostone of the Contrin Formation was deposited.

Izveleček

Profil Raduha predstavlja nadaljevanje raziskav anizijske Strelovške formacije v Kamniško-Savinjskih Alpah. V aniziju se je na potopljenem delu karbonatne platforme formiral intraplatformni bazen, v katerem je prišlo do sedimentacije Strelovške formacije na verjetno zunanem delu karbonatne rampe. Profil se prične z dolomitno brečo s klasti spodaj ležeče anizijske karbonatne platforme. Sledi sedimentacija hemipelagičnih plastnatih laminiranih ter homogenih apnencev v hidrodinamično mirnem in anoksičnem okolju. Umirjene pogoje sedimentacije so občasno prekinili gravitacijski tokovi (sinsedimentni zdrsi in turbiditi), ki so vnesli droben klastični material s kopnega. S počasnim zasipavanjem bazenskega okolja pride do postopne prekinitve anoksičnih pogojev ter sedimentacije plastnatih plitvovodnih apnencev, kar nakazuje na popolno zapolnitev intraplatformnega bazena. Sledi sedimentacija bioklastičnega dolomita zgornjeanizijske Contrinske formacije.

Introduction

Kamnik-Savinja Alps are a part of the eastern Southern Alps (Placer, 2008) which were in the Middle Triassic placed at an intertropical northern latitude of 15°18° (Stefani et al., 2010). In the Anisian, the area was subjected to the extensional tectonic phase, probably caused by regional strike-slip tectonics that are charac-

teristic for most of the Southern Alps (e.g., Masetti & Neri, 1980; Doglioni, 1987). This resulted in the formation of blocks with differential subsidence (De Zanche et al., 1993, 1995; Gianolla et al., 1998; Neri & Stefani, 1998). On the uplifted (less subsided) blocks shallow-water platform sedimentation was continuous (Maurer, 2009), whereas different basinal units deposited on in-

tensively subsided blocks (Masetti & Neri, 1980; Farabegoli et al., 1984; Sudiro, 2002; Brack et al., 2007). A similar synsedimentary Middle Triassic tectonics are also typical for the nearby Balaton Highland and Veszprem plateau, located east of the Southern Alps, where the Anisian Felsöors Formation deposited on drowning blocks (Haas & Budai, 1995; Budai & Vörös, 2006).

The first evidence for the Middle Triassic rifting phase in the Kamnik-Savinja Alps are thin- to medium-bedded bituminous limestones of the Velika planina member (Gale et al., 2022) and bedded bituminous carbonates and clastic rocks of the Strelovec Formation (Celarc, 2004). Regardless the similarity of facies and macrofossil biota in the Velika planina Member and Strelovec Formation, the relationship is not yet clear. The Strelovec Formation can be traced over the entire NE part of the Kamnik-Savinja Alps and was first defined as a distinct unit by Celarc (2004). In recent years, excavations in the Strelovec Formation have revealed numerous specimens of macrofossil biota, especially vertebrates. Most of the vertebrate finds are complete and articulated fish fossils (Hitij et al., 2010a; Hitij et al., 2010b; Tintori et al., 2014), while reptilian remains belonging to ichthyosaurs and pachypleurosaur are also locally very common (Hitij et al., 2010a; Hitij et al. 2010b). In addition to vertebrate fossils, the Strelovec Formation is also known for finds of various crustaceans (Gašparič et al., 2019; Laville et al., 2022), including the only horseshoe crab fossil in the Alpine Triassic deposits described by Bicknell et al. (2019), as well as rare echinoderms, bivalves, and plant remains (Hitij et al., 2010b). First detailed sedimentological study of the Strelovec Formation was carried out by Miklavc et al. (2016) in the SW part of the

Robanov kot valley (NE part of Kamnik-Savinja Alps). The studied succession was divided into five lithostratigraphic units probably deposited in a shallow restricted basin under disoxic to anoxic conditions. Due to the depositional conditions and later diagenetic processes, namely dolomitization which occurred at the base and in the upper parts of the succession, no age-diagnostic fossils were found. Based on stratigraphic position above the shallow-water Serla Dolomite and below the shallow-water Contrin Formation, the age of the Strelovec Formation was assigned from Pelsonian to Illyrian (Celarc et al., 2013). Due to highly variable thickness and lithostratigraphy of the formation, additional studies were necessary. To better understand the sedimentary environment and evolution of the Strelovec Formation, a new detailed stratigraphic section was logged, including transitions with the under- and overlying shallow-marine lithostratigraphic units (Serla Dolomite and Contrin Formation).

The aim of this study is to describe and define different lithostratigraphic units of the studied succession, sedimentary processes and depositional environment, and to gain new evidence on the regional evolution of the Anisian basin in the NE part of Kamnik-Savinja Alps.

Geological setting

The studied succession is located on the NW slopes of Mt. Raduha in the NE Kamnik-Savinja Alps (Fig. 1). The succession is exposed along the mountain trail from the Grohat Alpine Meadow (1460 m) towards the top of Mt. Raduha (2062 m).

The Kamnik-Savinja Alps structurally belong to the eastern part of the Southern Alps (Placer, 2008) (Fig. 1). In the Middle Triassic, the area was situated at the SW embayment of the Neotethys

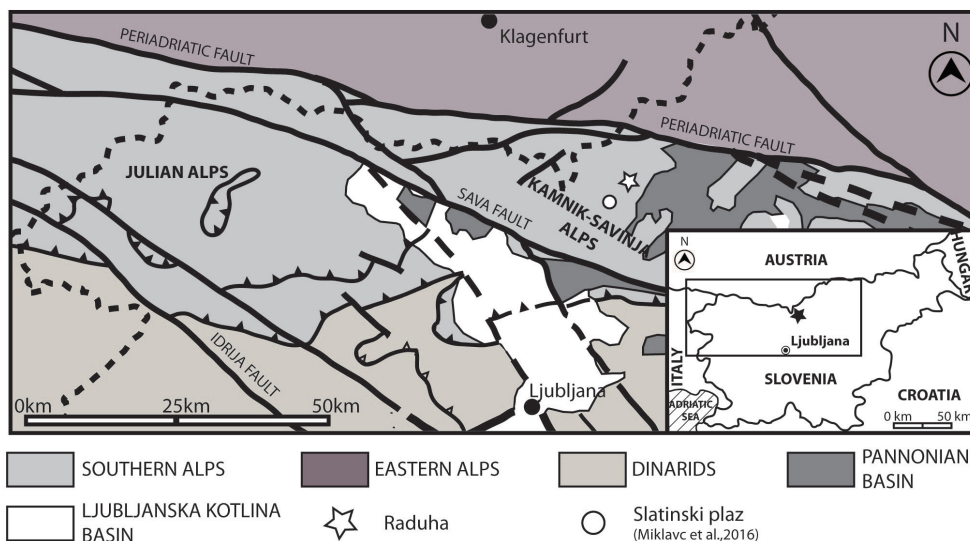


Fig. 1. Structural map of the north-central and north-western Slovenia (simplified after Placer, 2008). The studied section on Mt. Raduha (Kamnik-Savinja Alps) is marked with a star and is located northeast of the previously studied Slatinski plaz section marked by a circle (Miklavc et al., 2016).

Ocean (e.g., Haas et al., 1995; e.g. Stampfli et al., 2002; Schmidt et al., 2008). From the late Permian to the Early Triassic and early Middle Triassic, the eastern part of the Southern Alps belonged to the extensive shallow marine shelf, locally known as the Slovenian Carbonate Platform (Buser, 1989). In the Middle Triassic, during the rifting phase, the uniform platform was dissected into blocks with different subsidence. The earliest evidence for the extension is the Anisian formation of shallow intraplatform basins (Buser, 1989; Bertotti et al., 1993).

The eastern part of the Kamnik-Savinja Alps, where the studied succession is situated, consists of Triassic sedimentary successions (Teller, 1898; Seidl, 1908; Mioć et al., 1983; Celarc 2003, 2004; Celarc et al., 2013) (Fig. 2), which come into tectonic contact with Paleozoic rocks along a steep fault south of Mt. Olševa (Celarc, 2002). Early stratigraphic subdivision of the area was given by Mioć et al. (1983). They stated that the oldest rocks of the investigated area are Lower Triassic carbonates and siliciclastic rocks of the Werfen Formation, followed by Anisian massive crystalline dolomites and Ladinian rocks overlain by a Savinja thrust sheet composed of Upper Triassic massive limestones. Later, Celarc (2003, 2004) proposed a new lithostratigraphic division of Kamnik-Savinja Alps, in which he proved that

the Middle Triassic successions are in a normal contact with the older Werfen Formation, and that the Savinja thrust does not exist (Fig. 2A). Triassic sequence on Mt. Raduha starts with Werfen Formation, which is composed of alternating marlstone, marly limestone, sandstone and oolitic limestone. These rocks are overlain by grey massive, rarely bedded Lower Serla Dolomite (Anisian). Both formations belong to the Slovenian Carbonate Platform (Buser, 1989). During the Middle Triassic tectonic phase, the Anisian carbonate platform was covered by well-bedded carbonates and clastic rocks of the ?Pelsonian to Illyrian Strelovec Formation (Miklavc et al., 2016) (Fig. 2B). After shallow water sedimentation was restored, the Contrin (Illyrian) carbonate platform of massive, rarely bedded limestones and dolomites prograded over the basinal successions (Celarc et al., 2013). Younger Triassic rocks, mainly represented by red nodular limestone (Loibl Formation), pyroclastics and volcanics or carbonate breccia (Uggowitz Formation), thin-bedded limestone (Buchenstein Formation) and massive carbonate (Schlern Formation) are not present on the NW slopes of Mt. Raduha, but outcrop on the SE slopes of Mt. Raduha and on the NW slopes of the Robanov kot valley (Celarc et al., 2013) west of the study area.

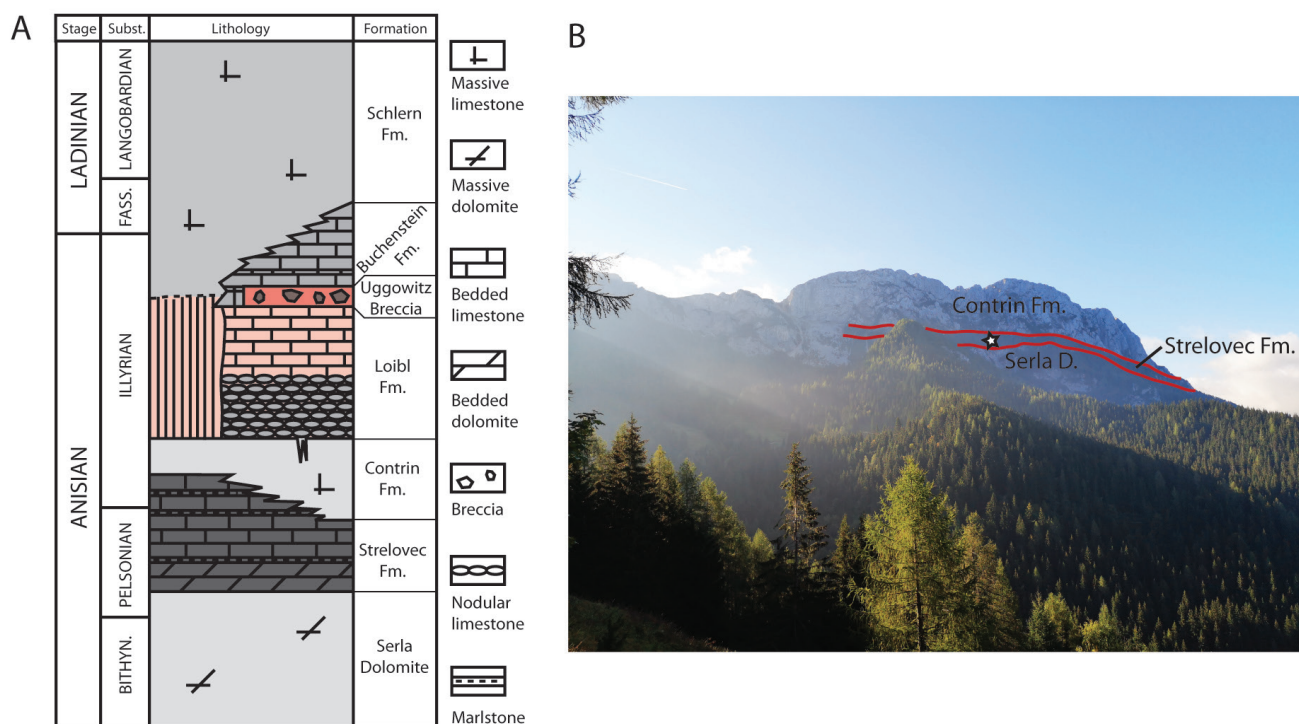


Fig. 2. A) Middle Triassic lithostratigraphic units of NE part of Kamnik-Savinja Alps (Celarc et al., 2013); B) Middle Triassic stratigraphy on NW slopes of Mt. Raduha (Raduha section is marked with a star).

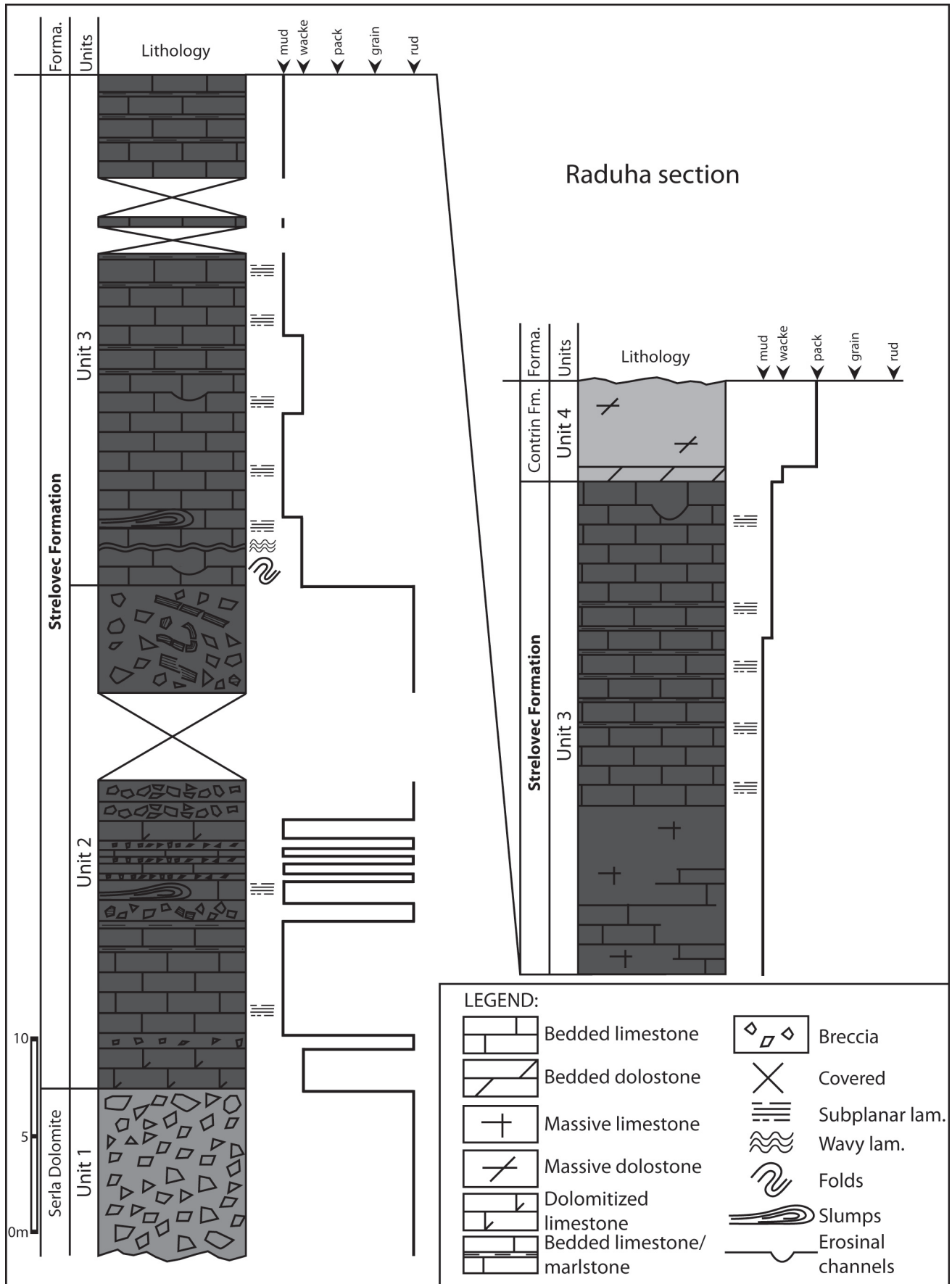


Fig. 3. Lithological and sedimentological characteristics of the Raduha section.

Materials and methods

On the NW slopes of Mt. Raduha, a stratigraphic section of almost perfectly exposed Anisian basinal succession was logged according to the standard sedimentologic procedure. Visual description of the exposed sediments was documented on 1:50 scale graphic log. A total of 25 samples were collected, out of which thin sections for sedimentological analysis were prepared. The latter was conducted on Zeiss Axioplan 2 microscope using plane and polarised light. The thin sections were photographed using a Zeiss Axio-Cam Hrc camera. Limestones and dolomites were classified according to Folk (1959) and Dunham (1962). To better determine and interpret sedimentary textures and structures, eight rock slabs were polished and then scanned using an Epson perfection V750 PRO scanner.

Lithostratigraphic units of Raduha section

The Raduha section ($46^{\circ}24'47,54''$; $14^{\circ}44'20,39''$) (Fig. 3) is 87 m long and is characterised by dark grey and black laminated to medium bedded bi-

tuminous limestones intercalated with marls and, in the lower part of the succession with beds of intraformational breccias. This basin sediments overlay grey massive brecciated dolostones of the Serla Dolomite. The uppermost part of the succession is characterised by a transition from bedded basal limestones to light grey massive dolostones of the Contrin Formation. The section is divided into four distinct lithostratigraphic units.

Lithostratigraphic Unit 1: grey massive dolostone breccia, uppermost Serla Dolomite

The base of the Raduha section is 6,9 m thick and is represented by grey massive dolostone breccia (Fig. 4A) of Unit 1.

Dolostone breccia in the lower part of the unit is composed of lithoclasts of shallow water limestone with microbialite and undetermined sparitic bioclasts (Fig. 6a). The matrix is composed of microsparite. Only locally are clasts cemented with calcite spar. In the upper part of

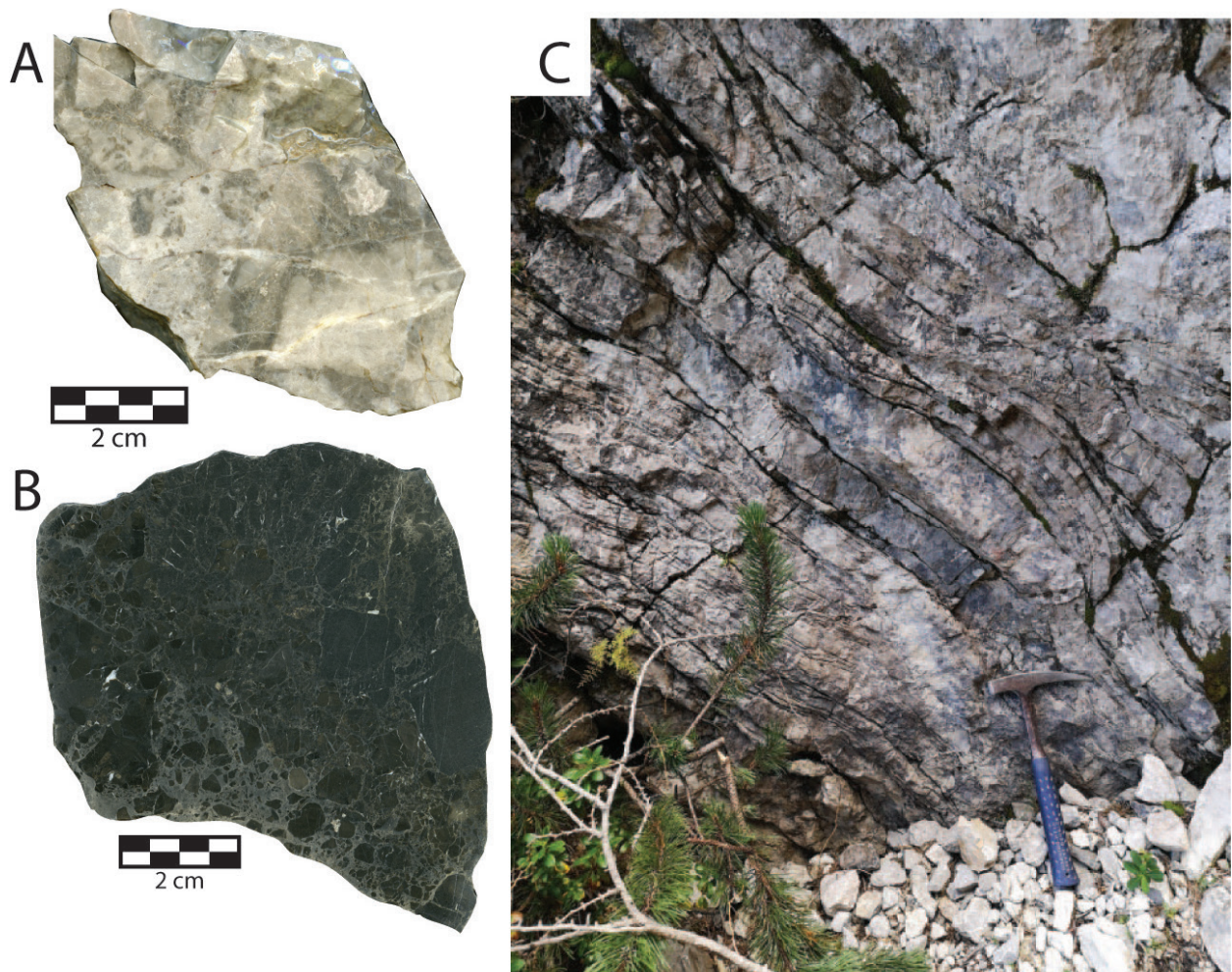


Fig. 4. Lithostratigraphic Units 1 and 2: A) polymictic dolostone breccia of Unit 1; B) polished slab of intraformational breccia of Unit 2; C) thin- to medium bedded limestone of Unit 2 with laterally variable bed thickness (?hummocky cross-stratification).

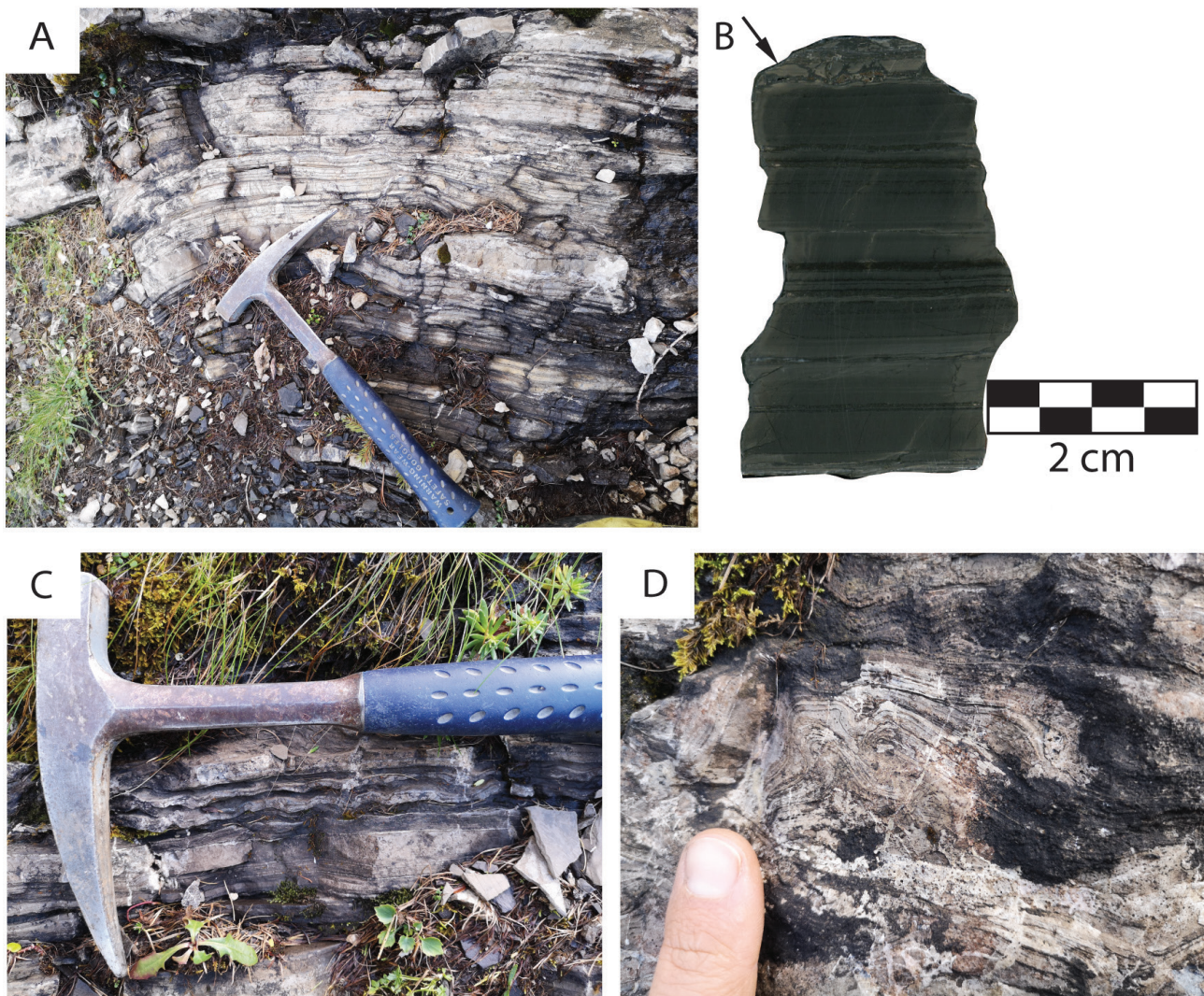


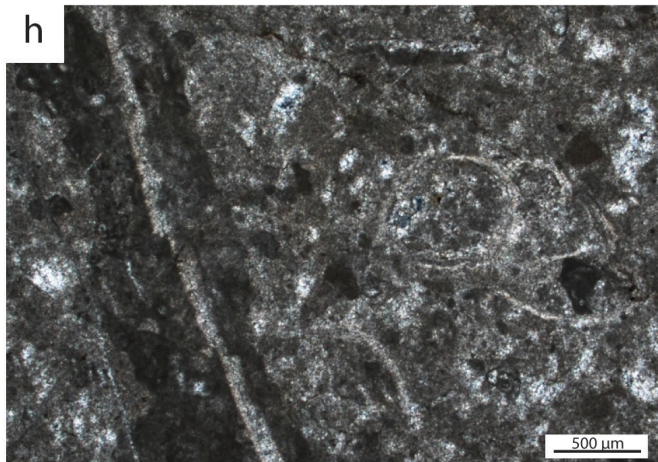
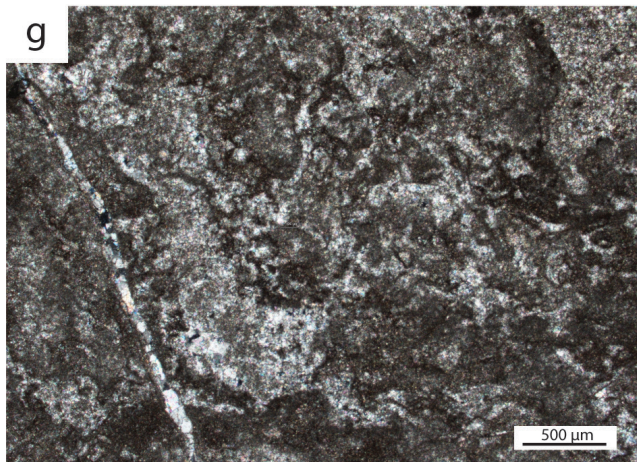
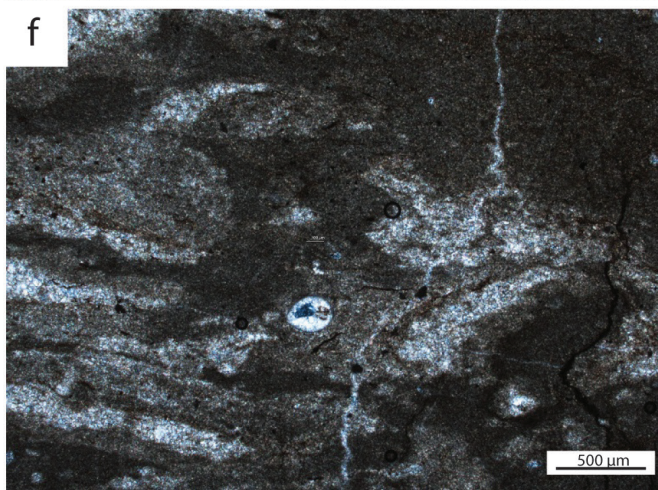
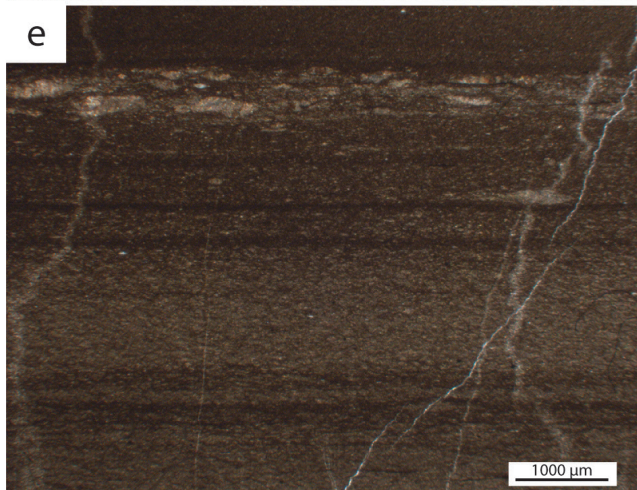
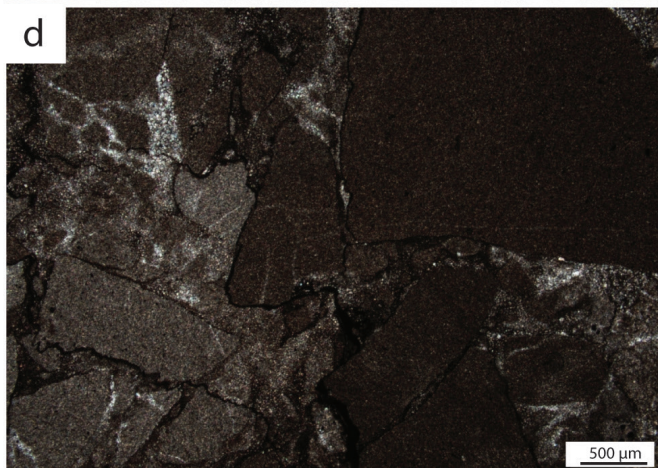
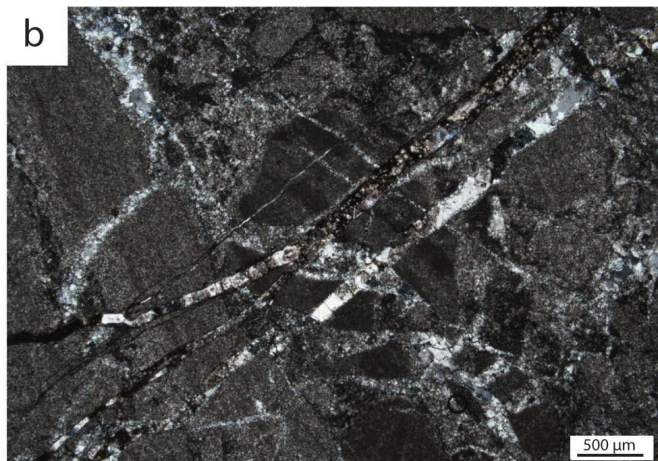
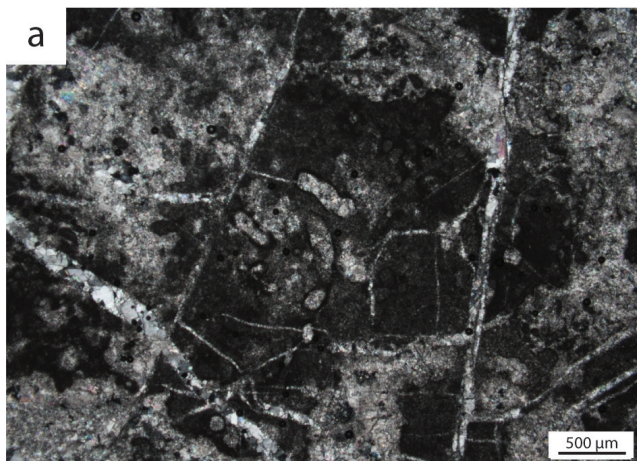
Fig. 5. Lithostratigraphic Unit 3: A) laminated thin- to medium-bedded black limestone; B) polished slab of the laminated limestone. Note rip-up clasts at the top of the sample (arrow); C) wavy bedding probably caused by movement of the semi-consolidated mudstones; D) synsedimentary deformation structures characterised by semi-ductile features.

the unit, clast-supported dolostone breccias are composed of angular granule- to pebble-sized micritic limestone and laminated micritic limestone clasts (Fig. 6b). The majority of clasts are cemented with calcite spar while in parts, microsparite matrix occurs. Strong fracturing of the whole rock and of some individual clasts is common. Some calcite-filled fractures postdate brecciation.

Lithostratigraphic Unit 2: black laminated thin bedded limestone intercalated with breccia, lower part of the Strelovec Formation

Unit 2 with thickness of 26 m overlies Unit 1 with a sharp contact. It is characterised by black laminated to medium bedded limestones which are slightly dolomitized in the first 3 m of the unit. Bed thickness ranges from 1 cm to 15 cm, with the exception of a 30 cm thick layer.

Fig. 6. Microfacies of the Raduha section: a) Unit 1; Polymictic dolostone breccia composed of shallow-water clasts. The clasts are cemented by dolomitized microsparite matrix and calcite spar cement. b) Unit 1; Clast-supported dolostone breccia with mudstone and laminated mudstone clasts. Matrix is in places composed of microsparite, while most of the clast are cemented with calcite spar. Fracturing of individual clasts is common. c) Unit 2; Rare foraminifera *Trochammina* in recrystallised intra-bioclastic wackestone (turbidite layer). Streaks and seams of amorphous organic component are common. d) Unit 2; Grain to matrix-supported intraformational breccia. The dominant clasts are mudstones. Note the tightly packed clasts with boundaries due to pressure solution. Matrix is micrite to microsparite. e) Unit 3; Subplanar laminated mudstone/wackestone. Note the microrhythmic pattern which is indicated with alternation of micrite (dark) and microsparite (light) laminae. In rare microsparite laminae, recrystallized, probably detrital grains, oriented parallel to lamination, can be observed (upper part of the section). f) Unit 3; Bioturbation within bioclastic wackestone with rare ostracods. g) Unit 3; Recrystallized bindstone of microbial origin. h) Unit 4; Peloidal bioclastic wacke-packstone with peloids, bivalve shell fragments (overgrown by microbial mats), foraminifers and intraclasts.



Laterally discontinuous beds of limestones (?hummocky) are characteristic for the lower part of the unit (Fig. 4C). Slumps and synsedimentary folds are also common. Limestone intercalates with up to 120 cm thick beds of black intraformational limestone breccia (Fig. 4B) and layers of dark grey marlstone.

Limestone is thin to medium bedded and occasionally subplanar laminated. Two distinct microfacies types are common for this unit. Peloidal wackestone predominates over recrystallised intra-bioclastic wackestone (Fig. 6c). Peloidal wackestone (grain to matrix ratio of 15:85) is composed of poorly sorted peloids and recrystallised clasts, which are concentrated in bands parallel to stratification, while silicified bioclasts and terrigenous grains of angular quartz are rare. In recrystallised intra-bioclastic wackestone (grain to matrix ratio of 30:70) grains are mainly represented by recrystallized, probably shallow-marine clasts, peloids and intraclasts. Bioclasts of unknown origin are subordinate. Foraminifers are also very rare (Fig. 6c). Streaks and seams of amorphous organic matter parallel to lamination and silicification of small dissolution cavities are also common in this microfacies.

Grain to matrix-supported breccias are intercalated within the limestone in the upper 17 m of the unit. Breccia is polymictic and poorly sorted (Fig. 6d). It is composed of up to 7 cm large, mostly angular to subrounded lithoclasts. Matrix is micrite to microsparite with seams of amorphous organic matter. Some parts of breccia are matrix-free and clasts are cemented with sparry calcite. Sparite-filled fractures indicate fracturing after deposition. Parts of tightly packed clasts with stylolitic contacts are common. The predominant lithoclasts are mudstone, while clasts of bioclastic mudstone and peloidal wackestone also occur.

Lithostratigraphic Unit 3: black laminated thin to medium bedded and massive limestone with intercalated beds of dark grey marlstone and claystone, upper part of the Strelovec Formation

Unit 3 is 50 m thick. In the first 27 m black laminated thin to medium bedded limestone with ranging in thickness from 0,5 cm to 50 cm (thicker beds of 20 cm to 50 cm predominate in the upper part of the unit) (Fig. 5A, B) intercalates with up to 1 cm thick beds of dark grey marlstone and claystone. Limestone in places represents laterally discontinuous beds. Clearly visible erosion

channels also occur. Slumps and synsedimentary folds are common (Fig. 5D) while mudstone rip-up clast are rare (Fig. 5B). The slump structures (Fig. 5D) are mostly few dm in scale and up to one meter thick and show evidence for ductile deformation of semi-consolidated laminated mudstones and brittle deformation of consolidated material (breccia). The next 9 m of the unit are represented by massive black limestone which, especially in the lower part, laterally passes into poorly stratified limestone. Black laminated to thin-bedded limestone intercalated with marlstone forms the last 15 m of the unit 3.

Thin to medium bedded limestone is subplanar laminated mudstone, wackestone and bioclastic mudstone and wackestone. Micritic matrix predominates in the mudstone microfacies types, while the grain to matrix ratio in wackestones is 20:80. Subplanar laminae predominate over rare wavy (Fig. 5C) and wavy discontinuous laminae. Lamination occurs due to alternation between micrite (dark, enriched in organic matter) and microsparite or sparitic laminae, which indicates a micrytmitic pattern of the facies (Fig. 6e). In rare cases normal grading from microsparite to micrite occurs. Grains are mainly represented by various recrystallized grains which are oriented parallel to lamination (Fig. 6e). Poorly sorted peloids, intraclasts and ostracods are rare (Fig. 6f). Pyrite crystals are common while terrigenous angular quartz grains are subordinate. Bioturbation is becoming more common towards the top of the unit (Fig. 6f) while seams and streaks of amorphous organic component are decreasing towards the top of the unit. The uppermost bed of the unit is slightly recrystallized bindstone of microbial origin with rare peloids, foraminifers and bioclasts of unknown origin (Fig. 6g).



Fig. 7. Sharp contact (dashed line) of the Strelovec and the Contrin Formation.

Massive limestone is characterised by a transition from poorly stratified mudstone with traces of subplanar lamination to homogenous mudstone. Micritic matrix predominates. Grains are represented by recrystallized clast of unknown origin and rare terrigenous quartz grains. Traces of bioturbation are very rare, marked by more coarse sparry calcite infillings of cavities.

Lithostratigraphic Unit 4: bedded and grey massive dolostone, Contrin Formation

The lowermost 3 m of Unit 4 were logged. The Contrin Formation begins with brownish-grey slightly wavy bedded dolostone with bed thickness of 30 cm, followed by light grey massive dolostone (Fig. 7).

Medium bedded dolomitic mudstone to wackestone is characterised by wavy and wavy discontinuous micritic laminae. Grains are represented

by peloids, rare unidentifiable recrystallised bioclasts and framboidal pyrite grains.

Massive dolostone is peloidal bioclastic wackestone and packstone. Grains occupy 30-40 % of the area and are represented by peloids, foraminifers, bivalve shell fragments, crinoid fragments, recrystallized bioclasts and rare intraclasts (Fig. 6h).

Depositional environment

Deposition of fine sediments in the Raduha section, that settled from suspension was occasionally interrupted by slumping. In some cases, slumps evolved into debrites and turbidites which is evident from mass-flow breccia (Flügel, 2010) (Fig. 4B) with clasts of deformed and disintegrated individual beds (Miklavc et al., 2016). That these breccias are a product of re-sedimentation within the same basin is also supported by predominantly angular (short transport) organic

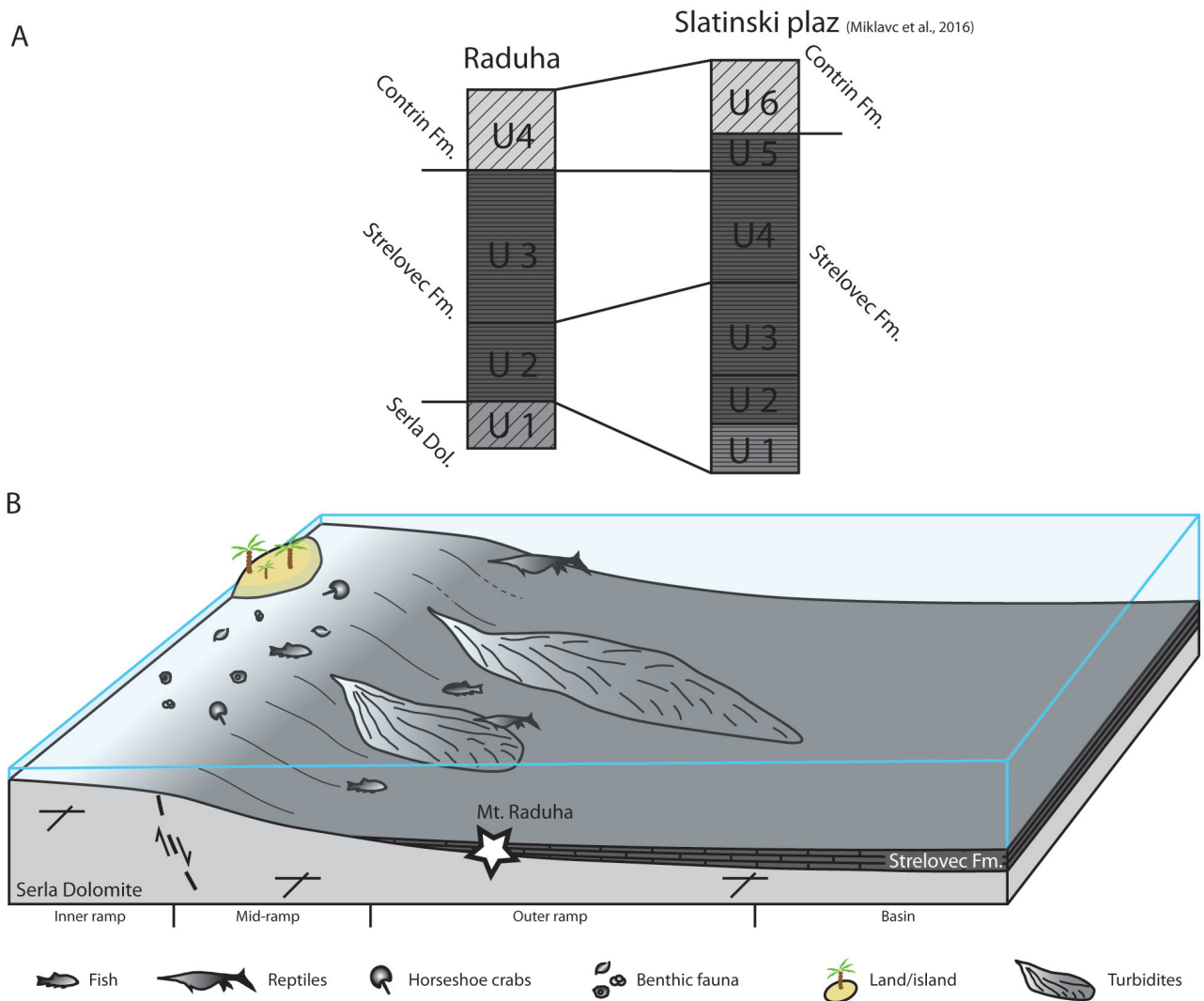


Fig. 8. A) Schematic columns of the Raduha and Slatinski plaz sections (Miklavc et al., 2016) and their correlation between lithostratigraphic units; B) Schematic presentation of the depositional environment of the Strelovec Formation. Relative position of investigated succession on Mt. Raduha is marked with a star.

rich mudstone clasts, with the same facies and texture as underlying beds, within organic-rich mud matrix.

In most cases of laminated mudstone, which is dominant in the lower part of the section (Fig. 5A, B), lamination is subplanar and is mostly homogeneous. Some laminae show grading. Wavy and wavy discontinuous laminations are rare. In some cases, the channels are cut into the underlying beds indicating erosional base surface. Erosional surface is also characteristic for rare laminae containing up to 5 mm in diameter large mudstone rip-up clasts (Fig. 5B). Within homogeneous laminae recrystallised platform-derived grains occur and are oriented parallel to lamination. These characteristics indicate erosion of semi consolidated base sediments and sedimentation from short-lived events related to low-density, fine-grained muddy distal turbidites (Piper & Stow, 1991; Shanmugam, 2002; Stockar, 2010).

Rhythmic interchange of laminated mudstone and homogeneous mudstone is also very common for this section. The absence of stratification in homogeneous beds could be related to the possible presence of weak oscillating bottom currents during the deposition of hemipelagic limestone (Sander, 1989; Bernasconi, 1991) and in the upper part of the succession could also be interpreted as the result of bioturbation.

Very common features of the finely laminated limestones of the Raduha section are relatively high contents of amorphous organic matter, which occurs in the form of streaks and seams parallel to lamination, presence of framboidal pyrite grains, absence of bioturbation in the basal and middle part of the succession and lack of benthic fauna. These features indicate sedimentation in a restricted reducing, anoxic environment.

Mostly in the Unit 3, bedded limestones are intercalated with marls. The periodic input of fine siliciclastic material could indicate periods of humid climate with strong monsoonal activity (Parrish et al., 1986) which intensified the input of fine-grained material into the basin.

Toward the top of Unit 3 bed thickness increases from few centimeters in the lower part to a few tens of centimeters in the upper part, indicating shallowing of the basin. Higher up in the unit, bioturbation and various bioclasts are common, suggest gradual transition from oxygen-deficient to more oxygenated basin conditions. Deposition of massive grey dolostone with numerous bioclasts, especially foraminifers and fragments

of molluscs indicate deposition in moderate to high-energy well-oxygenated subtidal environment.

In view of the observed microfacies and sedimentary structures, the sedimentary succession was deposited on a deepened part of the Anisian platform in a restricted distal part of the carbonate ramp, often under the influence of eutrophic conditions (Fig. 8B).

Discussion

The results of this study suggest that the depositional system of the Strelavec Formation can plausibly be described with a carbonate ramp model linked to an intraplatform basin formed by disintegration of the Anisian carbonate platform (Serla Dolomite), with facies types characteristic for subtidal mid- to outer ramp environment. Ramps are thought to be formed continuously in tectonic regimes characterised by gentle subsidence (Burchette & Wright, 1992; Duda et al., 2015).

Extensional tectonics and sea-level fluctuations are the most probable controlling factors in the formation of the intraplatform basin. Synsedimentary tectonic activity is indicated by the presence of basal polymictic dolostone breccias with angular shallow-marine lithoclasts originating from the underlying Serla Dolomite. Breccias indicate initiation of the tectonically induced subsidence of the area. However, due to Cenozoic deformations of the area, the reconstruction of the geometry of the intraplatform basin is not possible.

Facies types of the Raduha section indicate sedimentation of the Strelavec Formation in a hydrodynamically mostly quiet depositional environment. Considering the absence of typical storm-related features, such as hummocky cross-stratification, and the presence of slumps, fine-grained muddy distal turbidites, and restricted bottom conditions, the sedimentary succession was more likely deposited on the outer part of the ramp, but deposition on middle part cannot be excluded either. In fact, lateral truncation of beds is illustrated in Fig. 4C as an example of hummocky cross-stratification.

This quiet sedimentation was occasionally interrupted by siliciclastic input and deposition of sediments from gravity mass flows. Very similar conditions are characteristic for the Slatinski plaz section (Miklavc et al., 2016) (correlations between the units of the Raduha and Slatinski plaz sections can be seen in Fig. 8A), although due to the greater thickness of the Strelavec Formation in the Slatinski plaz section, sedimentation

of this section probably occurred on more distal parts of the ramp environment, compared to the Raduha section. The diversified vertebrate fauna found in Strelavec Formation indicates shallow basin environment in close connection to carbonate platform with near-shore areas inhabited with different fishes, pachypleurosaurs, ichtyosaurs, and horseshoe crabs (Hitij et al., 2010; Stockar, 2010; Čerňansky et al., 2018; Bicknell et al., 2019; Gale et al., 2022).

Anoxic conditions, recognisable by dispersed framboidal pyrite and sediment rich in organic matter (Stockar et al., 2013; Huang et al., 2017), are characteristic for the outer ramp environment. The development of poorly oxygenated conditions could be related to transgressive pulses that transported larger amounts of terrestrial organic debris into the basin, which was later consumed by bacteria (Jenkyne, 1980). Temporary basin anoxic conditions in the lower and middle part of the Strelavec Formation are indicated by well-preserved primary sedimentary textures (lamination) and excellent preservation of vertebrate skeletons (Hitij et al., 2010; Miklavc et al., 2016; Bicknell et al., 2019). Both are possible due to the absence of bioturbation and scavenging of macrofaunal biota. The preservation of skeletons could also be possible due to the growth of microbial mats, which prevent early decay after death (Stockar, 2010). In the Raduha section, absence of benthic fauna is a further indicator of anoxic conditions. Towards the middle ramp, transition from anoxic to more oxygenated conditions is suggested, which is evident from the lighter colour and absence of organic matter in the uppermost part of the Slatinski plaz section (Miklavc et al., 2016) and from bioturbation, which is evident in the last few meters of the Unit 3 in the Raduha section. Oxygenation of the uppermost parts of Strelavec Formation is probably related with shallowing of the basin (Miklavc et al., 2016). Beds of grey to dark marlstone and claystone indicate periods of increased input of silticlastic material into the basin. These periods could be related to Anisian pulse of humid climate (Parrish et al., 1986; Stefani et al., 2010) and tectonic evolution of the area. During humid period in an otherwise arid and dry Anisian climate, there was also an increase in the vegetation of the land areas, as evident from the fossil plant remains within the Strelavec Formation (Hitij et al., 2010).

Conclusions

The depositional system of the Raduha section can be described as a carbonate ramp. The subtidal facies types were deposited in a restricted, mostly hydrodynamically quiet and probably distal parts of the carbonate ramp, occasionally disturbed by episodic storm deposits and tectonically induced depositional events (slumps, turbidites), partly under anoxic conditions.

After Anisian extensional tectonics, the dolostone breccia of Unit 1 was deposited on the submerged part of the shallow-water carbonate platform, represented by the Serla Dolomite. The Strelavec Formation begins with Unit 2, characterised by mudstone and wackestone deposited from fine-grained muddy turbidites. This exchange of hemipelagic mudstone and turbidite-derived wackestone was occasionally interrupted by slumps, that formed beds of intraformational breccias, and rare clay-rich interlayers. In Unit 3, hemipelagic sedimentation continues with fewer turbidite intercalations and more clay input. This indicates that the area was more tectonically active during deposition of Unit 2 than during Unit 3, where there was a greater amount of gravitational mass-flow deposition. The increased input of fine clastic component in Unit 3 indicates probably more humid climate than in Unit 2. After deposition of Unit 3, the basin was successively filled, as reflected by the deposition of mudstones under more oxygenated conditions and the progradation of shallow-marine bioclastic dolostones from Contrin Formation.

This paper supports the previous interpretation by Miklavc et al. (2016) that the Strelavec Formation in the NE part of the Kamnik-Savinja Alps deposited in the distal parts of the ramp environment. However, some outcrops still need to be investigated to gain a better insight into the evolution of the carbonate ramp environment of the intraplatform basin.

Acknowledgments

This work was financially supported by project IGCP 710: Western Tethys meets Eastern Tethys (Anisian Strelavec Formation in Kamnik-Savinja Alps) and the research program P1-0195 (Geo-environment and Geomaterials) and is dedicated to the memory of co-author and mentor Bogomir Celarc, who led the way in studying Triassic stratigraphy of Kamnik-Savinja Alps. We would also like to thank two reviewers for thorough and constructive remarks that improve the original version of the manuscript.

References

- Bertotti, G., Picotti, V., Bernoulli, D. & Castellarin, A. 1993: From rifting to drifting: tectonic evolution of the South-Alpine upper crust from the Triassic to the Early Cretaceous. *Sedimentary Geology*, 86: 53–76. [https://doi.org/10.1016/0037-0738\(93\)90133-P](https://doi.org/10.1016/0037-0738(93)90133-P)
- Bicknell, R. D.C., Žalohar, J., Miklavc, P., Celarc, B., Križnar, M. & Hitij, T. 2019: A new limulid genus from strelovec Formation (Middle Triassic, Anisian) of northern Slovenia. *Geological Magazine*, 156/12: 2017–2030. <https://doi.org/10.1017/S0016756819000323>
- Brack, P., Rieber, H., Mundil, R., Blendinger, W. & Maurer, F. 2007: Geometry and chronology of growth and drowning of Middle Triassic carbonate platforms (Cerneria and Bivera/Clapsavon) in the Southern Alps (northern Italy). *Swiss Journal of Geosciences*, 100: 327–347. <https://doi.org/10.1007/s00015-007-1229-x>
- Bernasconi, S. M. 1991: Geochemical and microbial controls on dolomite formation and organic matter production/preservation in anoxic environments a case study from Middle Triassic Grenzbitumenzone, Southern alps (Ticino, Switzerland). Ph.D. Thesis, Swiss Federal Institute of Technology Zurich: 196 p.
- Burchette, T.P. & Wright, V.P. 1992: Carbonate ramp depositional systems. *Sedimentary Geology*, 79: 3–57. [https://doi.org/10.1016/0037-0738\(92\)90003-A](https://doi.org/10.1016/0037-0738(92)90003-A)
- Budai, T. & Vörös, A. 2006: Middle Triassic platform and basin evolution of the Southern Bakony mountains (Transdanubian Range, Hungary). *Rivista Italiana di Paleontologia e Stratigrafia*, 112/3: 359–371.
- Buser, S. 1989: Development of the Dinaric and Julian carbonate platforms and of the Intermediate Slovenian basin (NW Yugoslavia). *Mem. Soc. Geol. It.*, 40: 313–320.
- Celarc, B. 2002: Tectonic contact between Paleozoic and Triassic rocks south of Podolševa (Slovenia). *Geologija*, 45/2: 341–346. <https://doi.org/10.5474/geologija.2002.030>
- Celarc, B. 2003: Preliminarni rezultati geološkega kartiranja severovzhodnega dela Kamniško-Savinjskih Alp. *Geološki zbornik*, 17. posvetovanje slovenskih geologov. Oddelek za geologijo, Ljubljana: 25–27.
- Celarc, B. 2004: Geological structure of the northwestern part of the Kamnik Savinja Alps. Ph.D. Thesis, University of Ljubljana: 137 p.
- Celarc, B., Goričan, Š. & Kolar-Jurkovšek, T. 2013: Middle Triassic carbonate-platform breakup and formation of small-scale half-grabens (Julian and Kamnik–Savinja Alps, Slovenia). *Facies*, 59/3: 583–610. <https://doi.org/10.1007/s10347-012-0326-0>
- Čerňansky, A., Klein, N., Soták, J., Olšavský, M., Šurka, J. & Herich, P. 2018: A Middle Triassic pachypleurosaur (Diapsida: Eosauropterygia) from a restricted carbonate ramp in the Western Carpathians (Gutenstein Formation, Fatric unit): paleogeographic implications. *Geologica Carpathica*, 69/1: 3–16. <https://doi.org/10.1515/geoca-2018-0001>
- De Zanche, V., Gianolla, P., Mietto, P., Siorpaes, C. & Vail, P. R. 1993: Triassic Sequence Stratigraphy in the Dolomites (Italy). *Mem. Sci. Geol.*, 45: 1–27.
- De Zanche, V., Gianolla, P., Manfrin, S., Mietto, P. & Roghi, G. 1995: A middle Triassic back-stepping carbonate platform in the Dolomites (Italy): Sequence stratigraphy and Biochronostratigraphy. *Memorie di Scienze Geologiche*, 47: 135–155.
- Dogliani, C. & Bosellini, A. 1987: Eoalpine and mesoalpine tectonics in the Southern Alps. *Geologische Rundschau*, 76: 735–754. <https://doi.org/10.1007/BF01821061>
- Duda, J.P., Zhu, M. & Reitner, J. 2015: Depositional dynamics of a bituminous carbonate facies in a tectonically induced intra-platform basin: the Shibantan Member (Dengying Formation, ediacaran Period). *Carbonate Evaporites*, 31: 87–99. <https://doi.org/10.1007/s13146-015-0243-8>
- Dunham, R.J. 1962: Classification of carbonate rocks according to depositional texture. In: Ham, W.E. (ed.): *Classification of carbonate rocks*. AAPG Memoirs, 1: 108–121.
- Farabegoli, E., Levanti, D., Perri, M. C. & Veneri, P. 1984: M. Bivera Formation: an atypical Middle Triassic »Rosso Ammonitico« facies from Southern Alps (Italy). *Giornale di Geologia*, ser. 3, 46/2: 33–46.
- Flügel, E. 2010: *Mikrofacies of carbonate rocks: analysis, interpretation and application*. Springer: New York: 984 p.
- Folk, R.L. 1962: Spectral Subdivision of Limestone Types. In: Ham, W.E. (ed.): *Classification of Carbonate Rocks Symposium*. AAPG, Memoir 1, 62–84, Tulsa.
- Gale, L., Hitij, T., Vičič, B., Križnar, M., Žalohar, J., Celarc, B. & Vrabec, M. 2022: A sedimentological description of the Middle Triassic vertebrate-bearing limestone from Velika

- planina, the Kamnik-Savinja Alps, Slovenia. *Geologia Croatica*, 75/1: 101–113. <https://doi.org/10.4154/gc.2022.06>
- Gianolla, P., De Zanche, V. & Mietto, P. 1998: Triassic Sequence Stratigraphy in the Southern Alps (Northern Italy): Definition of Sequences and Basin Evolution. *Mesozoic and Cenozoic Sequence Stratigraphy of European Basins*, SEPM Special Publication, 60: 719–747.
- Hass, J. & Budai, T. 1995: Upper Permian-Triassic facies zones in the Transdanubian Range. *Rivista Italiana di Paleontologia e Stratigrafia*, 101/3: 249–266.
- Hitij, T., Žalohar, J., Celarc, B., Križnar, M., Renesto, S. & Tintori, A. 2010a: Scopolia; Kraljestvo Tetide, *Revija Prirodoslovnega muzeja Slovenije*, 5: 197 p.
- Hitij, T., Tintori, A., Žalohar, J., Renesto, S., Celarc, B., Križnar, M. & Kolar-Jurkovšek, T. 2010b: New fossil sites with Triassic vertebrate fauna from the Kamnik-Savinja Alps, Slovenia. In *Proceedings of International Symposium on Triassic and later Marine Vertebrate Faunas*, Beijing: 42–46.
- Hitij, T. 2012: Okostje triasnege pahiplevozavra. *National Geographic Slovenija*, 2: 17.
- Huang, Y., Chen, Z.-Q., Wignall, P.B. & Zhao, L. 2017: Latest Permian to Middle Triassic redox condition variations in ramp settings, South China: Pyrite framboid evidence. *Bulletin of the Geological Society of America*, 129/1-2: 229–243. <https://doi.org/10.1130/B31458.1>
- Jenkyns, H.S. 1980: Cretaceous anoxic events: from continents to oceans. *Journal of the Geological Society*. 137: 171–188. <https://doi.org/10.1144/gsjgs.137.2.0171>
- Laville, T., Hitij, T., Gašparič, R., Žalohar, J., Forel, M.B. & Charbonnier, S. 2022: The Triassic thylacocephalans from Slovenia: implications for their evolution and diversification. In *Proceedings of 8th Symposium on Fossil Decapod Crustaceans*, Zaragoza, 70–71.
- Masetti, M. & Neri, C. 1980: L' Anisico della Val di Fassa (Dolomiti occidentali). *Sedimentologia e Paleogeografia: Ann. Un. Ferrara*, 7: 1–19.
- Miklavc, P., Celarc, B. & Šmuc, A. 2016: Anisian Strelovec Formation in the Robanov kot, Savinja alps (Northern Slovenia). *Geologija*, 59/1: 23–34. <https://doi.org/10.5474/geologija.2016.002>
- Mioč, P. 1983: Osnovna geološka karta SFRJ 1: 100.000. Tolmač za list Ravne na Koroškem. Zvezni geološki zavod, Beograd: 69 p.
- Neri, C. & Stefani, M. 1998: Sintesi cronos-tratigrafica e sequenziale dell'evoluzione permiana superiore e triassica delle Dolomiti. *Mem. Soc. Geol. It.*, 53: 417–463.
- Parrish, J.M., Parrish, J.T. & Ziegler, A.M. 1986: Permian-Triassic paleogeography and paleoclimatology and implications for therapsid distribution. In: Hotton, N., MacLean, P.D., Roth, J.J. & Roth, C.E. (eds.): *The ecology and biology of mammalian-like reptiles*, Smithsonian Inst. Press: 109–131.
- Piper, D. J. W. & Stow, D. A. V. 1991: Fine-grained turbidites. In: Einsele, G. & Seilacher, A. (eds.): *Cyclic and Event Stratification*: 360–376.
- Placer, V. 2008: Principles of the tectonic subdivision of Slovenia. *Geologija*, 51/2: 205–217. <https://doi.org/10.5474/geologija.2008.021>
- Röhl, H.J., Schmid-Röhl, A., Furrer, H., Frimmel, A., Oschmann, W. & Schwark, L. 2001: Microfacies, geochemistry and palaeoecology of the Middle Triassic Grenzbitumenzone from Monte San Giorgio (Canton Ticino, Switzerland). *Geol. Insubr.*, 6/1: 1–13.
- Schmid, S.M., Bernoulli, D., Fügenschuh, B., Matenco, L., Schefer, S., Schuster, R., Tischler, M. & Ustaszewski, K. 2008: The Alpine-Carpathian-Dinaridic orogenic system: correlation and evolution of tectonic units. *Swiss Journal of Geosciences*, 101/1: 139–183. <https://doi.org/10.1007/s00015-008-1247-3>
- Sander P.M. 1989: The pachypleurosaurids (Reptilia: Nothosauria) from the Middle Triassic of Monte San Giorgio (Switzerland) with the description of a new species. *Phil. Trans. Roy. Soc. London*, 325/1230: 561–670. <https://doi.org/10.1130/B31458.1>
- Seidl, F. 1907/1908: Slovenska zemlja. Opis slovenskih pokrajin v prirodnoznanem, statističnem, kulturnem in zgodovinskem oziru. Peti del: Kamniške ali Savinjske Alpe, njih zgradba in lice. Poljuden geološki in krajinski opis. 1. zvezek. Matica Slovenska, Ljubljana.
- Shanmugam, G. 2002: Ten turbidite myths. *Earth-Science Reviews*, 58: 311–341. [https://doi.org/10.1016/S0012-8252\(02\)00065-X](https://doi.org/10.1016/S0012-8252(02)00065-X)
- Stampfli, G. M., Borel, G. D., Marchant, R. & Mosar, J. 2002: Western Alps geological constraints on western Tethyan reconstructions. In: Rosenbraun, G. & Lister, G. S. (eds.): *Reconstruction of the evolution of the Alpine - Himalayan Orogen*. *Journal of the Virtual Explorer*, 7: 75–104.
- Stefani, M., Furin, S. & Gianolla, P. 2010: The changing climate framework and depositional dynamics of Triassic carbonate platforms

- from the Dolomites. *Palaeogeography, Palaeoclimatology, Palaeoecology*, 290: 43–57. <https://doi.org/10.1016/j.palaeo.2010.02.018>
- Stockar, R. 2010: Facies, depositional environment, and palaeoecology of the Middle Triassic Cassina beds (Meride Limestone, Monte San Giorgio, Switzerland). *Swiss J Geosci*, 103: 101–119. <https://doi.org/10.1007/s00015-010-0008-2>
- Stockar, R., Adatte, T., Baumgartner, P.O. & Föllmi, K.B. 2013: Palaeoenvironmental significance of organic facies and stable isotope signatures: the Ladinian san Giorgio Dolomite and Meride Limestone of Monte San Giorgio (Switzerland, WHL UNESCO). *Sedimentology*, 60: 239–269. <https://doi.org/10.1111/sed.12021>
- Teller, F. 1898a: Eisenkappel und Kanker, Zone 20, Col. 11 (Geologische Spezialkarte der k. k. Österreichisch – Ungarischen Monarchie 5453, 1: 75 000). K. k. Geologische Reichsanstalt, Wien.
- Tintori, A., Hitij, T., Jiang, D., Lombardo, C. & Sun, Z. 2014: Triassic actinopterygian fishes: the recovery after the end-Permian crisis. *Integrative Zoology*, 9: 394–411. <https://doi.org/10.1111/1749-4877.12077>
- Sudiro, P. 2002: Carbonate slope deposits of the Contrin formation, Costabella area (Western dolomites, NE Italy). *Mem. Soc. Geol. It.*, 57: 19–28.
- Žalohar, J. & Hitij, T. 2013: Paleontološke raziskave v anizijskih plasteh strelovške formacije pod Vernarjem. *Acta Triglavensia, znanstveno izobraževalni časopis*, 2: 42.

Poročila in ostalo - Reports and More

Poročilo o aktivnostih Slovenskega geološkega društva v letu 2021

Branka BRAČIČ ŽELEZNIK

JPVOKA SNAGA d.o.o., Vodovodna cesta 90, SI-1000 Ljubljana, Slovenija;
e-mail: branka.bracic.zeleznik@vokasnaga.si

Leto 2021, je bilo jubilejno leto Slovenskega geološkega društva, ki je praznovalo 70 let delovanja. 1. junija 1951 je bil ustanovni občni zbor, na katerem so bila sprejeta pravila delovanja Geološkega društva v Ljubljani ter izvoljen redni in nadzorni odbor ter častno razsodišče.

V prvih letih delovanja je bil poudarek na organizaciji predavanj, kjer so se reševali različni geološki problemi, tako praktični kot teoretični. Februarja 1952 je društvo štelo 27 rednih članov. Prvi geološki kongres v Ljubljani pa je društvo organiziralo leta 1954.

Ker se ob obletnicah in svečanih dogodkih radi lepo oblečemo in uredimo, smo tudi Slovenskemu geološkemu društvu ob praznovanju namenili novo grafično podobo. V januarju 2021 smo razpisali natečaj za novo grafično podobo. Prispelo je 14 predlogov izmed katerih smo izbrali predlog Ane Tiane Bauman.



Sl. 1. Zmagovalna ideja natečaja za nov logotip Slovenskega geološkega društva.

Osnovni predlog smo v sodelovanju z oblikovalko Natašo Kastelic, Designa studio razvili do končne oblike.



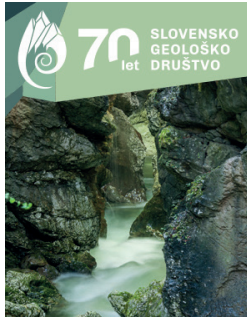
Sl. 2. Logotip, ki vsebuje jubilejno številko

Sl. 3. Nov logotip

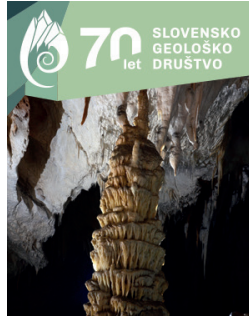
V oblikah logotipa so posamezni geološki elementi:

- Spirala: predstavlja življenje. S spiralo geologi ponazarjamo geološko zgodovino oziroma geološki čas. V njej se skriva pomen rojstva in celotnega razvoja Zemlje. Spirala je tudi pogosta oblika fosilov, ki nam govorijo o življenju v preteklosti. Ti se ohranijo v sedimentnih kamninah, najpogostejših kamninah Slovenije.
- Gorstvo: predstavlja Alpe z osrednjim simbolom Triglava kot enega od najpomembnejših nacionalnih simbolov Slovenije. Oblika ponazarja tudi minerale, glavne gradnike kamnin. Poševni deli različnih odtenkov zelene barve ponazarjajo plasti, ki so zamaknjene ob prelomih (bele črte).
- Jama: prazen prostor z nakazanimi kapniki. Predstavlja enega najbolj tipičnih in poznanih podzemnih elementov krasa. To je tudi eden od najpomembnejših geoloških fenomenov slovenskega ozemlja.
- Voda: osnovni vir življenja je skrita v osnovni obliki logotipa, ki ima obliko kapljice
- Planet Zemlja: osrednji del logotipa je krog, ki je tudi jedro spirale. Gre tudi za potovanje od globin morja (fossil v spirali) do višav gora (Alpe – Triglav).

V počastitev 70 let delovanja Slovenskega geološkega društva smo izdali devet **priložnostnih znamk z geološkimi motivi**, ki pokrivajo različna področja geologije: megalodontna školjka v Dolini Jezera v Lužnici, rudistna školjka Pironaea buseri, Stalagmit z več vrhovi in raznobarvnimi stalaktiti iz Zgornjega Tartarusa v Postojnski jami, Ivanjševski vrelec, Prevrnjena guba na Travniku, kristali vulfenita, korita Mostnice, kombajn za pridobivanje premoga in izkopno čelo vzhodne cevi Karavanškega tunela.



Sl. 4. Korita Mostnice



Sl. 5. Stalaktiti iz Zgornjega Tartarusa.



Sl. 4. Megalodontidna školjka



Sl. 5. Ivanjševski vrelec



Sl. 6. Rudistna školjka



Sl. 7. Prevrnjena guba na Travniku



Sl. 8. Izkopno čelo vzhodne cevi Karavanškega tunela



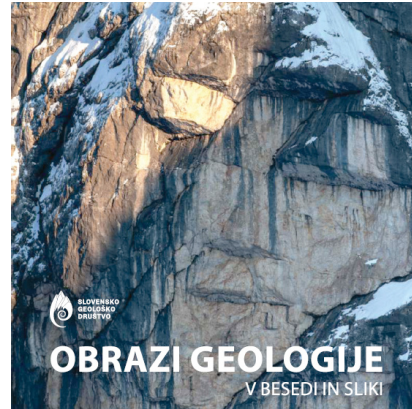
Sl. 9. Kristali vulfenita



Sl. 10. Kombajn za pridobivanje premoga

Vse **znamke** je mogoče, posamezno ali v kompletu naročiti in kupiti (anja.torkar@ntf.uni-lj.si).

V počastitev 70 let delovanja Slovenskega geološkega društva smo izdali knjigo **70 obrazov geologije**. Knjiga je rezultat sodelovanja 102 geologov, ki so prispevali 110 besed, ki jih označujejo kot geologe ali kaj je za njih geologija. Besede poudarijo in pojasnijo številne lepe fotografije, ki bogatijo knjigo. Tudi knjigo lahko naročite in kupite (anja.torkar@ntf.uni-lj.si).



Sl. 11. Vpogled v knjigo Obrazi Geologije

Tudi leto 2021 je bilo v znamenju epidemije koronavirusa, zato smo 1.6.2021 v počastitev 70 let delovanja Slovenskega geološkega društva organizirali dogodek preko zoom portala. Na slavnostnem dogodku smo imeli nagovor povabljenih govornikov, predstavili zgodovino društva, nov logotip, novo številko glasila društva **PRELOM** in priložnostne znamke z geološkimi motivi.



V letu 2021 smo pričeli z organizacijskimi aktivnostmi za 6. slovenski geološki kongres, ki bo od 3. 10. do 5. 10. 2022 v Rogaški Slatini s temo »Vedeti (ne)vidno – vloga geologije v naši družbi«. Sestavili smo organizacijski odbor in znanstveni svet. Izdelan je bil logotip kongresa in postavljena spletna stran (6. slovenski geološki kongres 2022 (geo-zs.si)).

Zelo aktivni so bili člani skupine za **promocijo geologije**. Na področju **Učnih načrtov** so predstavnikom skupine za geografijo in biologijo Zavoda republike Slovenije za šolstvo predstavili osnutke idejne prenovе geoloških vsebin v učnih načrtih.

Napisali so številne **strokovne članke in pripevke** ter sodelovali **na konferencah**.

V septembru so v Idriji izvedli **Dan geologije** za učence 7. razredov OŠ Idrija, OŠ Spodnja Idrija, OŠ Črni vrh nad Idrijo in OŠ Cerčno,

Člani so sodelovali tudi na naravoslovnih dneh. V juniju na naravoslovnem dnevu »**Zakaj geologija?**« za učence 9. razredov OŠ Železniki. V oktobru jih je pot ponovno zanesla v Železnike, kjer so sodelovali na naravoslovnem dnevu za učence 9. razredov OŠ Železniki z naslovom »**Geologija v mestu?**«. V novembru pa je bila v Piranu delavnica »**Minerali in kamnine**« za otroke 6. razreda OŠ Cirila Kosmača Piran.

Za OŠ Stična je bila v septembru v Termah Čatež organizirana delavnica. Člani so sodelovali na Znanstivalu v Ljubljani (Vrt eksperimentov: geološka delavnica **Voda-skrito bogastvo Slovenije**) in Koliščarskem dnevu.

Člani so izvedli tudi vrsto **izobraževanj** v sklopu Programov profesionalnega usposabljanja.

Tudi člani **sekcije za geokemijo** so bili v letu 2021 aktivni in so v preteklem letu nadaljevali z delom začrtanim že v preteklih letih. Raziskovali so vplive antropogenih dejavnosti na okolje v odvisnosti od naravnih geoloških danosti. Težišče je bilo na področju okoljske geokemije potencialno škodljivih snovi, ki je pomembno in hitro razvijajoče se področje geologije oziroma geokemije povsod po svetu. Namen raziskav je preučiti vire, transportne poti ter usodo potencialno škodljivih snovi v geološko različnih, neobremenjenih in onesnaženih okoljih. Glede na epidemiološke razmere v letu 2021 ni bilo predavanj in skupnih dogodkov.

Člani **sedimentološke sekcije** so v letu 2021 izdelali so tabelarni pogled slovenskih formacij za zgornji paleozoik in trias

V letu 2021 smo oživili aktivnosti v povezavi z **geološkimi stolpci**. Pripravili smo idejne zasnove in izvedli kreativno produkcijo sodelovanja študentov pri predmetu Programiranje interaktivnih medijev, Katedre za informacijsko in grafično tehnologijo (Oddelek za tekstilstvo, grafiko in oblikovanje) in predmetu Geologija v šoli (oddelek za geologijo).



Sl. 12. Utrinki z Dneva geologije v Idriji.



Slovensko geološko društvo, kot član Evropske zveze, sodeluje v petih evropskih projektih Obzorje 2020 (Horizon 2020).

V letu 2021 so se nadaljevale aktivnosti na projektu **ENGIE** – Vzpodbujanje deklet za izbiro poklica geoznanstvenice (*Empowering Girls to become the geoscientists of tomorrow*).

Na 25. Posvetovanju slovenskih geologov je bil projekt predstavljen s prispevkom:

Žvab Rožič, P. **ENGIE** - vzpodbujanje deklet za izbiro poklica geoznanstvenice. V: Rožič, B. (ur.): Razprave, poročila = Treatises, reports: 25. posvetovanje slovenskih geologov = 25th Meeting of Slovenian Geologists. 25. posvetovanje slovenskih geologov = 25th Meeting of Slovenian Geologists, Ljubljana, october, 2021. Ljubljana: Univerza v Ljubljani, Naravoslovnotehniška fakulteta, Oddelek za geologijo, Geološki zbornik, 26, str. 157.

V časopisu projekta "ENGIE magazine" je bil objavljen prispevek: Valand, N., Brajkovič, R. & Žvab Rožič, P.: RockCheck app - when the rocks make sense. <https://www.engieproject.eu/2021/02/16/rockcheck-app-when-the-rocks-make-sense/>

Projekt je bil predstavljen na dnevu odprtih vrat na Univerzi v okviru projekta **Noč Moč. 24. 9. 2021**

V letu 2021 smo v okviru projekta **CROWD THERMAL** (Sodelovanje družbe pri razvoju geotermalnih projektov z uporabo alternativnih virov financiranja (*Community-based development schemes for geothermal energy*)) poskušali izpolniti bazo ((Meta-database of geothermal projects for alternative finance), vendar nismo uspeli identificirati primernih projektov, ki bi iskali skupnostno financiranje. Še naprej smo vzdrževali projektno stran v slovenskem jeziku ter preko spletnih kanalov vabili deležnike na dogodke, ki jih je organiziral projekt. 8. oktobra 2021 smo predstavili tematiko projekta s postrom na 25. posvetovanju slovenskih geologov: Rman, Nina. Razvoj geotermalnih projektov z množičnim financiranjem - projekt Crowdthermal. V: Rožič, B. (ur.): Razprave, poročila = Treatises, reports: 25. posvetovanje slovenskih geologov = 25th Meeting of Slovenian Geologists. 25. posvetovanje slovenskih geologov = 25th Meeting of Slovenian Geologists, Ljubljana, october, 2021. Ljubljana: Univerza v Ljubljani, Naravoslovnotehniška fakulteta, Oddelek za geologijo, 2021. Str. 105-106. Geološki zbornik, 26.

V letu 2021 žal ni potekalo nič aktivnosti v sklopu projekta **ROBOMINERS** – Razvoj bio-navdihnjenega robotskega rudarja (*Resilient Bio-Inspired Modular Robotic Miner*), ker je nosilec projekta imel zaradi Covid-19 situacije precej otežene delovne razmere. Poleg tega pa tudi diseminacija samega projekta ni bila toliko aktivna kot v letu 2020 (ni bilo obvestil za javnost oz. press release).

V letu 2021 smo v sklopu projekta **REFLECT** (Redefiniranje lastnosti geotermalnih tekočin v ekstremnih pogojih (*Redefining geothermal fluid properties at extreme conditions to optimize future geothermal energy extraction*)) zbrali podatke iz 48 vrtin, o 27 termalnih vodah, 14 jedrih in 6 tipih geotermalnih vodonosnikov, ki so o bili vključeni v evropski atlas tekočin in predstavljajo pogoje v Sloveniji. Maja 2021 smo se udeležili webinarja 'Geothermal Energy in Turkey'. Pripravili smo seznam deležnikov, katerim smo redno pošiljali obvestila in vabila na projektne spletne dogodke. Vzdrževali smo predstavitev projekta na spletnih straneh SGD in GeoZS.

V okviru SGD deluje Slovenski nacionalni odbor **INQUA (SINQUA)**, ki povezuje raziskovalce kvartarja in skrbi za pretok informacij med slovensko in mednarodno kvartarno znanstveno sfero. Glavni cilj je napredek na področju kvartarnih znanosti, pri čemer si prizadevamo za interdisciplinarno zastopanost članov in večje medsebojno sodelovanje. Vpeti smo v aktivnosti INQUA komisij in fokusnih skupin, sodelujemo pri organizaciji znanstvenih srečanj in delavnic.

V letu 2021 je bilo največ aktivnosti v okviru SINQUA namenjenih organizaciji mednarodnega znanstvenega srečanja »6th Regional Scientific Meeting on Quaternary Geology: Seas, Lakes and Rivers¹«, ki je potekal med 27. in 30. septembrom pod okriljem INQUA ter v sodelovanju s Hrvaškimi nacionalnim odborom INQUA ter drugimi slovenskimi, hrvaškimi in italijanskimi raziskovalnimi ustanovami. Kot vodilni organizatorji smo člani SINQUA organizirali srečanje, ki je potekalo v hibridni obliki: preko spleta ter v živo v Ljubljani v Atriju ZRC SAZU. Tridnevnega srečanja se je udeležilo približno petdeset kvartarnih raziskovalcev iz devetih držav. Prva dva dneva srečanja sta bila posvečena znanstvenim sekcijam ter plenarnim predavanjem, zadnji dan srečanja pa je bil posvečen virtualnim ekskurzijam. Po srečanju je bila izdana knjiga povzetkov²,

¹ Spletna stran srečanja: <https://www.geo-zs.si/rmqg/>

² Knjiga povzetkov: https://www.geo-zs.si/PDF/Monografije/6thRMQG_BookOfAbstracts.pdf

v pripravi pa je tudi posebna številka znanstvene revije »Quaternary«³. Poročili s srečanja sta bili objavljena v »Quaternary Perspectives«⁴ ter v »Geologiji«⁵.

Poleg tega smo v letu 2021 sodelovali tudi v aktivnostih INQUA komisij in fokusnih skupin. Predstavniki SINQUA je sodeloval na spletnih sestankih, volitvah in pri odločanju mednarodnega Sveta INQUA. Kot člani INQUA smo nadaljevali sodelovanje pri oblikovanju skupnih aktivnosti v okviru različnih komisij. Člani SINQUA smo vpeti v aktivnosti komisij CMP (Coastal and Marine Processes), PALCOM (Paleoclimates), SACCOM (Stratigraphy and Chronology) in TERPRO (Terrestrial Processes, Deposits and History).

V okviru CMP komisije smo v 2021 nadaljevali z vodenjem aktivnosti v okviru štiriletnega projekta NEPTUNE⁶, kjer članica SINQUA sodeluje kot ena od vodij projekta. V okviru projekta smo v 2021 vodili sekcijo na vEGU21, organizirali mednarodno dvodnevno spletno konferenco (v sodelovanju z INQUA fokusno skupino SPLOSH), ter preko spleta pripravili letno srečanje projekta. Poleg tega smo v okviru projekta sodelovali pri pripravi posebne številke INQUA znanstvene revije »Quaternary International«, ki bo predvidoma izšla v 1. polovici 2022. V letu 2022 izvajamo serijo šestih mesečnih seminarjev na temo spreminjanja morskih in priobalnih okolij s predavanji uveljavljenih znanstvenikov. V jeseni nameravamo izvesti prvo letno srečanje projekta v živo. V okviru SACCOM komisije smo se v letu 2021 udeležili dveh spletnih srečanj »INQUA-SEQS 2021 Meetings on Middle Plei-

stocene Stratigraphy«. V okviru TERPRO fokusne skupine »Terrestrial Processes Perturbed by Tectonics« smo se v letu 2021 udeležili uvodnega znanstvenega srečanja v okviru projekta EDITH – »From Earthquake Deformation to Seismic Hazard Assessment«, katerega cilj je izmenjava znanja o potresnem ciklu za namene ocene potresne nevarnosti. O aktivnostih v sklopu komisij ter v okviru SINQUA smo poročali v INQUA novičniku »Quaternary Perspectives«.

In še nekaj zanimivosti!

V letu 2021 je imelo Slovensko geološko društvo 82 članov.

V letu 2021 smo izdali glasilo društva PRELOM, ki nadaljuje tradicijo glasila, ki ga je društvo izdajalo pred leti.

Glasilo smo natisnili, dosegljivo pa je tudi na spletni strani društva v pdf datoteki. [Glasilo Slovenskega geološkega društva \(slovenskogeolokodrustvo.si\)](http://www.geolokodrustvo.si)

Načrti za leto 2022?

Veliko energije in časa bo usmerjene v organizacijo in izvedbo **7. slovenskega geološkega kongresa**.

Člani Sekcije za promocijo geološke znanosti bodo nadaljevali z aktivnostmi pri pripravi kataloga profesionalnih posodobitvenih programov in vključevanjem študentov v izvedbo geoloških delavnic.

V letu 2022 se nadaljuje delo na projektih EN-GIE, CROWD THERMAL, REFLECT in ROBO-MINERS.

Članarino za leto 2022 smo povečali, tako je sedaj za člane 20 EUR, za študente pa 10 EUR. Vabljeni, da podaljšate članstvo oziroma postanete član.

Vabim vas, da obiščete spletno stran društva www.geolokodrustvo.si, kjer lahko spremljate aktivnosti društva.

SREČNO!

*Branka Bračič Železnik
(predsednica Slovenskega geološkega društva)*

³ Spletna stran posebne številke: https://www.mdpi.com/journal/quaternary/special_issues/6th_RMQG

⁴ Stran 17 na povezavi <https://www.inqua.org/media/uploads/QP31%20Dec%202021.pdf>

⁵ Poročilo: <https://www.geologija-revija.si/index.php/geologija/article/view/1823/1889>

⁶ Spletna stran projekta: <http://dist.altervista.org/neptune/index.html>

Nova razstava

Dihanje Zemlje - mofete v Slovenskih Goricah

Mojca BEDJANIČ

Zavod Republike Slovenije za varstvo narave, Območna enota Maribor, Pobreška cesta 20, SI-2000 Maribor;
e-mail: mojca.bedjanic@zrsvn.si

Območje Ščavniške doline in Radencev je izjemno zaradi številnih mofet, ki se pojavljajo na nekaj sto kvadratnih metrov velikih površinah. Gre za izjemen in redek naravni pojav izhajanja čistega in hladnega plina CO₂. Zanje je značilen poseben plinski režim s povečano koncentracijo CO₂, ki vpliva na tla, podzemno vodo in organizme, ki so se strukturno in funkcionalno prilagodili na te razmere. Zaradi izjemnosti, redkosti, ohranjenosti in znanstveno – raziskovalne pomembnosti so mofete razglašene za geološke, hidrološke in ekosistemske naravne vrednote.



Sl. 1. Burno izhajanje plina v mokri mofeti Slepica. Foto: Simon Veberič, 3. nagrada na foto natečaju 6. SGK na temo geoprostosti.

Avtorja razstave prof. dr. Dominik Vodnik iz Oddelka za agronomijo Biotehniške fakultete Univerze v Ljubljani in dr. Nina Rman iz Geološkega zavoda Slovenije sta na zanimiv in splošni javnosti razumljiv način predstavila »zgodbo« mofet. Materiale je grafično postavila Staša Čertalič iz GeoZS, fotografski material so prispevali različni avtorji. Strokovno so pri snovanju razstave sodelovali številni strokovnjaki (prof. dr. Hardy Pfan, prof. dr. Helena Grčman, asist. Rok Turniški, Simon Mozetič, dr. Marjana Zajc in Saša Kos), pomembna pa je bila tudi podpora domačinov (Stanislav Žiško, Vlado Šiško, Aljoz Firbas in Mirko Kurbos).

Temačna grajska klet in posneto glasno brbotanje plina skupaj s slikovitimi posnetki pokrajine na velikem TV pomagajo obiskovalcu, da se vživi v potovanje plina. Tega in njegove učinke opisuje vsebina razstave, ki na petih informativnih panojih zajema tematike od nastanka, zgodovine, nevarnosti, plinskega režima in rastlinskega sveta do turizma in industrijske rabe mofet. Razstava je opremljena z interpretacijskimi elementi, med katerimi izstopajo trodimenzionalni batimetrični modeli treh tipičnih mofet ter »brbotajoči« model, ki ponazarja delovanje mofet.

Razstava je zanimiva tako za domačine kot tudi obiskovalce, dviga ozaveščenost o pomenu teh pojavov, ob enem pa predstavlja dodatno ponudbo in turistični popestritev Gradu Negova in širšega območja.



Sl. 2. Razstava »Dihanje Zemlje – mofete v Slovenskih Goricah« v Gradu Negova. Foto: Simon Mozetič

V okviru postavitve razstave sta bila organizirana dva strokovna posveta »Mofete – upravljanje in varovanje naravne dediščine«. Na njem so sodelovali domači in tuji strokovnjaki s področja geologije, biologije in varstva narave, ki so predstavili pojav in pomen mofet kot dela naravne dediščine. Pregledali so tudi trenutno stanje njihovega varovanja. Kot rezultat posveta, ki je

potekal 31. 3. 2022 na gradu Negova in 8. 4. 2022 spletno, so nastale smernice za njihovo upravljanje:

- varstvene usmeritve morajo biti podane za vsako območje posebej, glede na geološke, hidrološke, pedološke in biološke značilnosti.
- spodbujajo se aktivnosti za ozaveščanje in izobraževanju o fenomenu, pomenu njihovega ohranjanja in varovanja; znanstveno-raziskovalne in turistične aktivnosti morajo biti prilagojene varstveni funkciji.
- tla ter rastlinski pokrov morajo na območju mofet ostati intaktni, zato se po potrebi omeji gnojenje, košnjo, prekopavanje, oranje in dostop.

Tako razstava kot tudi spremljajoča posveta pomembno doprinašajo k ozaveščanju o mofetah, njihovi vrednosti ter pomenu njihovega ohranjanja. So dobra popotnica in temelj za nadaljnje aktivnosti v smislu proaktivnega varovanja območja, dodatnega raziskovanja kot tudi k razvoju prepoznavnosti območja izhajajoč iz izjemne geološke naravne dediščine.

Razstava je nastala v okviru operacije »Negovske zgodbe - Implementacija igre pobega v turistično ponudbo gradu Negova«, s katero je vodilni partner Zavod za kulturo, turizem in promocijo Gornja Radgona (Kultprotur) uspešno kandidiral na 5. javnem pozivu LAS Prlekija. Dodatne aktivnosti so potekale v okviru ARRS raziskovalnih programov Podzemne vode in geokemija (P1-0020) ter Agroekositemi (P4-0085) ter podpori donatorjev Radenske ADRIATIC d.o.o. in Sava Turizem d. d. PE Zdravilišča Radenci.

Viri:

<https://www.kultprotur.si/sl/kultprotur/mediateka>

Tea Kolar-Jurkovšek's Pander Medal

During the celebration of the European Conodont Symposium at Utrecht University in September 2022, Dr Tea Kolar-Jurkovšek, scientific advisor at the Geological Survey of Slovenia, was awarded the highest recognition of the Pander Society, the Pander Medal for “a life dedicated” to the study of conodonts.

The Pander Society is an international association of palaeontologists and stratigraphers with a common interest in the study of conodonts, whose main goal is to encourage the exchange of information about conodont research. According to the Pander Society, The Pander Medal, which is the society's highest recognition, acknowledges senior conodont workers who have made truly outstanding contributions to the study of conodonts. After evaluating her many merits, this award was conferred on Dr Tea Kolar-Jurkovšek, one of Slovenia's most prominent palaeontologists.

Tea Kolar-Jurkovšek was born in August 1954 in Litija, Slovenia. After completing her graduate studies at Ljubljana University (1979), she obtained her PhD at the University of Belgrade in 1989. Since then, she has been employed at the Geological Survey of Slovenia as a researcher, serving in various positions as a project and program leader. Tea actively collaborates in other scientific institutions, especially as a member of the IUGS International Commission on Triassic Stratigraphy, where she is part of several working groups.

Her work has focused primarily on Slovenian palaeontology, working on Devonian, Carboniferous, and Permian, and mainly Triassic conodonts in Slovenia as well as in the wider Dinarides area, where she was responsible for long-term programs and bilateral scientific exchanges where she directly contributed to our knowledge of conodonts by solving important taxonomical, geological, and biostratigraphical questions.

In the course of her substantial contributions to and advances in conodont knowledge, which spans over four decades, she has published over 200 contributions, most of them related to work on conodonts. At the same time, Dr Kolar-Jurkovšek developed an international network collaborating with several leading international experts on various fossil groups all over the world. In this context, she has been part of several international projects working on biostratigraphic issues in various countries.

In related work, Dr Kolar-Jurkovšek, together with her husband Dr Bogdan Jurkovšek, stands out with her commitment to transferring some part of her work to the general public, by means of books and public exhibitions. Recently, they have published two books – “Conodonts of Slovenia (2019)” and “Fossils of Slovenia (2021)”, published in Slovenian and English, and both issued by the Geological Survey of Slovenia.

In summary, Tea Kolar-Jurkovšek has been one of the most productive and influential researchers working on conodonts, establishing a working network of researchers and international scientific exchanges that continues to this day. For these reasons, and as she approaches retirement, the international community of conodont researchers recognises her work, awarding her with its highest recognition, the Pander Medal, for a lifetime of achievements in the diverse study of conodont palaeontology. On behalf of the Pander Society, I would like to congratulate her and wish her a long and most productive future in her ongoing and widely recognised conodont studies.

*Dr. Carlos Martínez-Pérez
University of Valencia*



Dr. Tea Kolar-Jurkovšek after receiving the Pander Medal during the European Conodont Symposium, celebrated at the University of Utrecht in September 2022. From left to right: Dr. Carlos Martínez-Pérez (University of Valencia, Spain), Dr. Tea Kolar-Jurkovšek (Geological Survey of Slovenia), and Dr. Emilia Jarochovska (University of Utrecht, Netherlands). Photo: Nicola Vuolo.

Navodila avtorjem

GEOLOGIJA objavlja znanstvene in strokovne članke s področja geologije in sorodnih ved. Revija izhaja dvakrat letno. Članke recenzirajo domači in tuji strokovnjaki z obravnavanega področja. Ob oddaji člankov avtorji lahko predlagajo **tri recenzente**, uredništvo pa si pridruži pravico do izbire recenzentov po lastni presoji. Avtorji morajo članek popraviti v skladu z recenzentskimi pripombami ali utemeljiti zakaj se z njimi ne strinjajo.

Avtorstvo: Za izvirnost podatkov, predvsem pa mnenj, idej, sklepov in citirano literaturo so odgovorni avtorji. Z objavo v GEOLOGIJI se tudi obvežejo, da ne bodo drugje objavili prispevka z isto vsebino.

Avtorji z objavo prispevka v GEOLOGIJI potrjujejo, da se strinjajo, da je njihov prispevek odprto dostopen z izbrano licenco **CC-BY**.

Jezik: Članki naj bodo napisani v angleškem, izjemoma v slovenskem jeziku, vsi pa morajo imeti slovenski in angleški izvleček. Za prevod poskrbijo avtorji prispevkov sami.

Vrste prispevkov:

Izvirni znanstveni članek

Izvirni znanstveni članek je prva objava originalnih raziskovalnih rezultatov v takšni obliki, da se raziskava lahko ponovi, ugotovitve pa preverijo. Praviloma je organiziran po shemi **IMRAD (Introduction, Methods, Results, And Discussion)**.

Pregledni znanstveni članek

Pregledni znanstveni članek je pregled najnovejših del o določenem predmetnem področju, del posameznega raziskovalca ali skupine raziskovalcev z namenom povzemanja, analiziranja, evalvirati ali sintetizirati informacije, ki so že bile publicirane. Prinaša nove sinteze, ki vključujejo tudi rezultate lastnega raziskovanja avtorja.

Strokovni članek

Strokovni članek je predstavitev že znanega, s poudarkom na uporabnosti rezultatov izvirnih raziskav in širjenju znanja.

Diskusija in polemika

Prispevek, v katerem avtor ocenjuje ali komentira neko delo, objavljeno v GEOLOGIJI, ali z avtorjem strokovno polemizira.

Recenzija, prikaz knjige

Prispevek, v katerem avtor predstavlja vsebino nove knjige.

Oblika prispevka: Besedilo pripravite v urejevalniku Microsoft Word. Prispevki naj praviloma ne bodo daljši od 20 strani formata A4, v kar so vštete tudi slike, tabele in table. Le v izjemnih primerih je možno, ob predhodnem dogovoru z uredništvom, tiskati tudi daljše prispevke.

Članek oddajte uredništvu vključno z vsemi slikami, tabelami in tablami v elektronski obliki po naslednjem sistemu:

- Naslov članka (do 12 besed)
- Avtorji (ime in priimek, poštni in elektronski naslov)
- Ključne besede (do 7 besed)
- Izvleček (do 300 besed)
- Besedilo
- Literatura
- Podnaslovi slik in tabel
- Tabele, Slike, Table

Citiranje: V literaturi naj avtorji prispevkov praviloma upoštevajo le objavljene vire. Poročila in rokopise naj navajajo le v izjemnih primerih, z navedbo kje so shranjeni. V seznamu literature naj bodo navedena samo v članku omenjena dela. Citirana dela, ki imajo DOI identifikator (angl. Digital Object Identifier), morajo imeti ta identifikator izpisan na koncu citata. Za citiranje revije uporabljamo standardno okrajšavo naslova revije. Med besedilom prispevka citirajte samo avtorjev priimek, v oklepaju pa navajajte letnico izida navedenega dela in po potrebi tudi stran. Če navajate delo dveh avtorjev, izpišite med tekstom prispevka oba priimka (npr. Pleničar & Buser, 1967), pri treh ali več avtorjih pa napišite samo prvo ime in dodajte et al. z letnico (npr. Mlakar et al., 1992). Citiranje virov z medmrežja v primeru, kjer avtor ni poznan, zapišemo (Internet 1). V seznamu literaturo navajajte po abecednem redu avtorjev.

Imena fosilov (rod in vrsta) naj bodo napisana poševno, imena višjih taksonomskih enot (družina, razred, itn.) pa normalno. Imena avtorjev taksonov naj bodo prav tako napisana normalno, npr. *Clypeaster pyramidalis* Michelin, *Galeanella tollmanni* (Kristan), Echinoidea.

Primeri citiranja članka:

Mali, N., Urbanc, J. & Leis, A. 2007: Tracing of water movement through the unsaturated zone of a coarse gravel aquifer by means of dye and deuterated water. *Environ. geol.*, 51/8: 1401–1412. <https://doi.org/10.1007/s00254-006-0437-4>

Pleničar, M. 1993: *Apricardia pachiniana* Sirna from lower part of Liburnian beds at Divača (Triest-Komen Plateau). *Geologija*, 35: 65–68

Primer citirane knjige:

Flügel, E. 2004: *Mikrofacies of Carbonate Rocks*. Springer Verlag, Berlin: 976 p.

Jurkovšek, B., Toman, M., Ogorelec, B., Šribar, L., Drobne, K., Poljak, M. & Šribar, Lj. 1996: Formacijska geološka karta južnega dela Tržaško-komenske planote – Kredne in paleogenske kamnine 1: 50.000 = Geological map of the southern part of the Trieste-Komen plateau – Cretaceous and Paleogene carbonate rocks. Geološki zavod Slovenije, Ljubljana: 143 p., incl. Pls. 23, 1 geol. map.

Primer citiranja poglavja iz knjige:

Turnšek, D. & Drobne, K. 1998: Paleocene corals from the northern Adriatic platform. In: Hottinger, L. & Drobne, K. (eds.): *Paleogene Shallow Benthos of the Tethys*. Dela SAZU, IV. Razreda, 34/2: 129–154, incl. 10 Pls.

Primer citiranja virov z medmrežja:

Če sta znana avtor in naslov citirane enote zapišemo:

Čarman, M. 2009: Priporočila lastnikom objektov, zgrajenih na nestabilnih območjih. Internet: http://www.geo-zs.si/UserFiles/1/File/Nasveti_lastnikom_objektov_na_nestabilnih_tleh.pdf (17. 1. 2010)

Če avtor ni poznan zapišemo tako:

Internet: <http://www.geo-zs.si/> (22. 10. 2009)

Če se navaja več enot z medmrežja, jim dodamo še številko:

Internet 1: <http://www.geo-zs.si/> (15. 11. 2000)

Internet 2: <http://www.geo-zs.si/> (10. 12. 2009)

Slike, tabele in table: Slike (ilustracije in fotografije), tabele in table morajo biti zaporedno oštevilčene in označene kot sl. 1, sl. 2 itn., oddane v formatu TIFF, JPG, EPS ali PDF z ločljivostjo 300 dpi. Le izjemoma je možno objaviti tudi barvne slike, vendar samo po predhodnem dogovoru z uredništvom. Če avtorji oddajo barvne slike bodo te v barvah objavljene samo v spletni različici članka. Pazite, da bo tudi slika tiskana v sivi tehniki berljiva. Grafični materiali naj bodo usklajeni z zrcalom revije, kar pomeni, da so široki največ 172 mm (ena stran) ali 83 mm (pol strani, en stolpec) in visoki največ 235 mm. Večjih formatov od omenjenega zrcala GEOLOGIJE ne tiskamo na zgib, je pa možno, da večje oziroma daljše slike natisnemo na dveh straneh (skupaj na levi in desni strani) z vmesnim "rezom". V besedilu prispevka morate omeniti vsako sliko po številčnem vrstnem redu. Dovoljenja za objavo slikovnega gradiva iz drugih revij, publikacij in knjig, si pridobijo avtorji sami.

Če je članek napisan v slovenskem jeziku, mora imeti celotno besedilo, ki je na slikah in tabelah tudi v angleškem jeziku. Podnaslovi naj bodo čim krajši.

Korekture: Avtorji prejmejo po elektronski pošti članek v avtorski pregled. Popravijo lahko samo tiskarske napake. Krajši dodatki ali spremembe pri korekturah so možne samo na avtorjeve stroške.

Prispevki so prosto dostopni na spletnem mestu: <http://www.geologija-revija.si/>

Oddaja prispevkov:

Avtorje prosimo, da prispevke oddajo v elektronski obliki na naslov uredništva:

GEOLOGIJA

Geološki zavod Slovenije
Dimičeva ulica 14, SI-1000 Ljubljana
bernarda.bole@geo-zs.si ali urednik@geologija-revija.si

Instructions for authors

Scope of the journal: GEOLOGIJA publishes scientific papers which contribute to understanding of the geology of Slovenia or to general understanding of all fields of geology. Some shorter contributions on technical or conceptual issues are also welcome. Occasionally, a collection of symposia papers is also published.

All submitted manuscripts are peer-reviewed. When submitting paper, authors can suggest **three reviewers**. Note that the editorial office retains the sole right to decide whether or not the suggested reviewers are used. Authors should correct their papers according to the instructions given by the reviewers. Should you disagree with any part of the reviews, please explain why. Revised manuscript will be reconsidered for publication.

Author's declaration: Submission of a paper for publication in GEOLOGIJA implies that the work described has not been published previously, that it is not under consideration for publication elsewhere and that, if accepted, it will not be published elsewhere.

Authors agree that their contributions published in GEOLOGIJA are open access under the licence [CC-BY](#).

Language: Papers should be written in English or Slovene, and should have both English and Slovene abstracts.

Types of papers:

Original scientific paper

In an original scientific paper, original research results are published for the first time and in such a form that the research can be repeated and the results checked. It should be organised according to the IMRAD scheme (**I**ntroduction, **M**ethods, **R**esults, **A**nd **D**iscussion).

Review scientific paper

In a review scientific paper the newest published works on specific research field or works of a single researcher or a group of researchers are presented in order to summarise, analyse, evaluate or synthesise previously published information. However, it should contain new information and/or new interpretations.

Professional paper

Technical papers give information on research results that have already been published and emphasise their applicability.

Discussion paper

A discussion gives an evaluation of another paper, or parts of it, published in GEOLOGIJA or discusses its ideas.

Book review

This is a contribution that presents a content of a new book in the field of geology.

Style guide:

Submitted manuscripts should not exceed 20 pages of A4 format including figures, tables and plates. Only exceptionally and in agreement with the editorial board longer contributions can also be accepted.

Manuscripts submitted to the editorial office should include figures, tables and plates in electronic format organized according to the following scheme:

- *Title (maximum 12 words)*
- *Authors (full name and family name, postal address and e-mail address)*
- *Key words (maximum 7 words)*
- *Abstract (maximum 300 words)*
- *Text*
- *References*
- *Figure and Table Captions*
- *Tables, Figures, Plates*

References: References should be cited in the text as follows: (Flügel, 2004) for a single author, (Pleničar & Buser, 1967) for two authors and (Mlakar et al., 1992) for multiple authors. Pages and figures should be cited as follows: (Pleničar, 1993, p. 67) and (Pleničar, 1993, fig. 1). Anonymous internet resources should be cited as (Internet 1). Only published references should be cited. Manuscripts should be cited only in some special cases in which it also has to be stated where they are kept. Cited reference list should include only publications that are mentioned in the paper. Authors should be listed alphabetically. Journal titles should be given in a standard abbreviated form. A DOI identifier, if there is any, should be placed at the end as shown in the first case below.

Taxonomic names should be in italics, while names of the authors of taxonomic names should be in normal, such as *Clypeaster pyramidalis* Michelin, *Galeanella tollmanni* (Kristan), Echinoidea.

Articles should be listed as follows:

- Mali, N., Urbanc, J. & Leis, A. 2007: Tracing of water movement through the unsaturated zone of a coarse gravel aquifer by means of dye and deuterated water. *Environ. geol.*, 51/8: 1401–1412. <https://doi.org/10.1007/s00254-006-0437-4>
- Pleničar, M. 1993: *Apricardia pachiniana* Sirna from lower part of Liburnian beds at Divača (Triest-Komen Plateau). *Geologija*, 35: 65–68.

Books should be listed as follows:

- Flügel, E. 2004: *Mikrofacies of Carbonate Rocks*. Springer Verlag, Berlin: 976 p.
- Jurkovšek, B., Toman, M., Ogorelec, B., Šribar, L., Drobne, K., Poljak, M. & Šribar, Lj. 1996: *Formacijska geološka karta južnega dela Tržaško-komenske planote – Kredne in paleogenske kamnine 1: 50.000 = Geological map of the southern part of the Trieste-Komen plateau – Cretaceous and Paleogene carbonate rocks*. Geološki zavod Slovenije, Ljubljana: 143 p., incl. Pls. 23, 1 geol. map.

Book chapters should be listed as follows:

- Turnšek, D. & Drobne, K. 1998: Paleocene corals from the northern Adriatic platform. In: Hottinger, L. & Drobne, K. (eds.): *Paleogene Shallow Benthos of the Tethys*. Dela SAZU, IV. Razreda, 34/2: 129–154, incl. 10 Pls.

Internet sources should be listed as follows:

Known author and title:

Čarman, M. 2009: Priporočila lastnikom objektov, zgrajenih na nestabilnih območjih. Internet: http://www.geo-zs.si/UserFiles/1/File/Nasveti_lastnikom_objektov_na_nestabilnih_tleh.pdf (17. 1. 2010)

Unknown authors and title:

Internet: <http://www.geo-zs.si/> (22.10.2009)

When more than one unit from the internet are cited they should be numbered:

Internet 1: <http://www.geo-zs.si/> (15.11. 2000)

Internet 2: <http://www.geo-zs.si/> (10.12. 2009)

Figures, tables and plates: Figures (illustrations and photographs), tables and plates should be numbered consecutively and marked as Fig. 1, Fig. 2 etc., and saved as TIFF, JPG, EPS or PDF files and submitted at 300 dpi. Colour pictures will be published only on the basis of previous agreement with the editorial office. If, together with the article, you submit colour figures then these figures will appear in colour only in the Website version of the article. Be careful that the grey scale printed version is also readable. Graphic materials should be adapted to the journal's format. They should be up to 172 mm (one page) or 83 mm wide (half page, one column), and up to 235 mm high. Larger formats can only be printed as a double-sided illustration (left and right) with a cut in the middle. All graphic materials should be referred to in the text and numbered in the sequence in which they are cited. The approval for using illustrations previously published in other journals or books should be obtained by each author.

When a paper is written in Slovene it has to have the entire text which accompanies illustrations and tables written both in Slovene and English. Figure and table captions should be kept as short as possible.

Proofs: Proofs (in pdf format) will be sent by e-mail to the corresponding author. Corrections are made by the authors. They should correct only typographical errors. Short additions and changes are possible, but they will be charged to the authors.

GEOLOGIJA is an open access journal; all pdfs can be downloaded from the website: <http://www.geologija-revija.si/en/>

Submission: Authors should submit their papers in electronic form to the address of the GEOLOGIJA editorial office:

GEOLOGIJA

Geological Survey of Slovenia
Dimičeva ulica 14, SI-1000 Ljubljana, Slovenia
bernarda.bole@geo-zs.si or urednik@geologija-revija.si

- 129 Bračić Železnik, B. & Rman, N.
Uvodnik
- 131 Peternel, T., Šegina, E., Jež, J., Jemec Auflič, M., Janža, M., Logar, J., Mikoš, M. & Bavec, M.
Review of the research and evolution of landslides in the hinterland of Koroška Bela settlement (NW Slovenia)
- 151 Fifer Bizjak, K. & Vezočnik, R.
Prediction of the peak shear strength of the rock joints with artificial neural networks
- 161 Šegina, E., Jemec Auflič, M., Zupan, M., Jež, J. & Peternel, T.
Composite landslide in the dynamic alpine conditions: a case study of Urbas landslide
- 177 Rožič, B., Gale, L., Oprčkal, P., Švara, A., Popit, T., Kunst, L., †Turnšek, D., Kolar-Jurkovšek, T., Šmuc, A., Ivekovič, A., Udovč, J. & Gerčar, D.
A glimpse of the lost Upper Triassic to Middle Jurassic architecture of the Dinaric Carbonate Platform margin and slope
- 217 Križnar, M.
Lower Permian (Artinskian) chondrichthyan tooth remains (Petalodontidae) from Dovje (Karavanke Mts., NW Slovenia)
- 225 Jarc, S.
Statistical approach to interpretation of geochemical data of stream sediment in Pleše mining area
- 237 Miklavc, P. & †Celarc, B.
Depositional environment of the Middle Triassic Strelovec Formation on Mt. Raduha, Kamnik-Savinja Alps, northern Slovenia